LABUSCHAGNE, L S

EVOLUTION OF THE ORE-FORMING FLUIDS
IN THE ROOIBERG TIN-FIELD

PhD UP 1998

Digitised by the Department of Library Services in support of open access to information, University of Pretoria, 2021

Evolution of the ore-forming fluids in the Rooiberg tin-field

By

Lourens Stefanus Labuschagne

Submitted in partial fulfilment of the requirements for the degree of Doctor of Philosophy in the Faculty of Science, University of Pretoria

Pretoria

January, 1998

Digitised by the Department of Library Services in support of open access to information, University of Pretoria, 2021

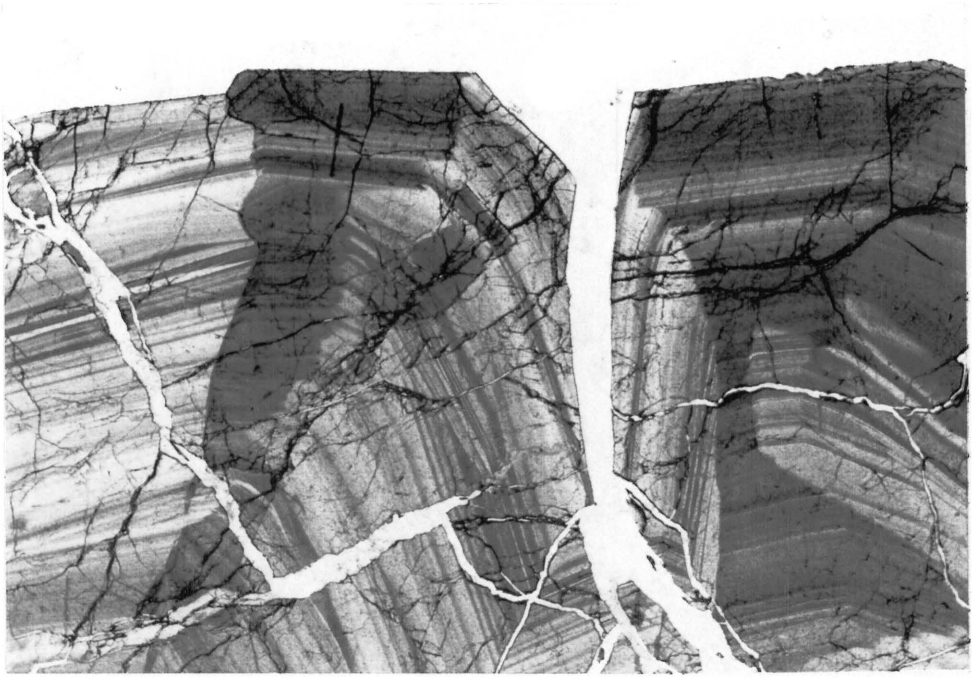

Frontispiece - *Zoned cassiterite (orange to brown) penetrated by ankerite (white) along micro-fractures.*

(Photomicrograph, plane polarised light)

Digitised by the Department of Library Services in support of open access to information, University of Pretoria, 2021

Behind every important mineral there once was a fluid

Hans P. Eugster

Presidential Address: Mineralogical Society of America, 1985.
Published in 1986.

Digitised by the Department of Library Services in support of open access to information, University of Pretoria, 2021

CONTENTS

Abstract.....(i)
Opsomming.....(ii)
1. INTRODUCTION.....1
2. PREVIOUS WORK.....2
3. SCOPE AND AIMS OF THIS STUDY.....10
4. ACKNOWLEDGEMENTS.....11
5. METHODS.....13
5.1 Surface mapping and sampling of the granites.....13
5.2 Underground mapping and sampling of the ore-bodies.....15
5.3 Laboratory techniques.....18
6. GEOLOGICAL SETTING.....24
6.1 The Leeuwpoort Formation of the Pretoria Group.....24
6.2 The Smelterskop Formation of the Pretoria Group.....24
6.3 The Kwaggasnek and Schrikkloof Formations of the Rooiberg Group.....26
6.4 The Stavoren Granophyre of the Rashoop Granophyre Suite.....27
6.5 The Lebowa Granite Suite 27
7. THE GRANITES.....28
7.1 Introduction.....28
7.2 Field distribution.....28
7.3 Petrography and correlation 31
7.4 Geochemical characterisation.....35
7.5 Emplacement history.....44
8. THE GEOCHEMICAL TIN LANDSCAPE AT ROOIBERG.....46
9. THE C, NAD AND A MINES ORE-BODIES.....51
9.1 The Leeuwpoort C Mine.....51
9.2 The Rooiberg NAD Mine.....51
9.3 The Rooiberg A Mine.....51
10. TOURMALINE, ANKERITE AND CASSITERITE.....56
10.1 Tourmaline.....56
10.1.1 Introduction 56
10.1.2 Distribution of tourmaline in the A Mine pockets.....57
10.1.3 Physical and optical properties.....59
10.1.4 Mineral chemistry 62
10.2 Ankerite.....68
10.2.1 Introduction.....68

Digitised by the Department of Library Services in support of open access to information, University of Pretoria, 2021

10.2.2 Distribution.....68
10.2.3 Microscopic investigations.....72
10.2.4 Mineral chemistry.....74
10.3 Cassiterite.....81
10.3.1 A microscopic comparison of A Mine cassiterite-1 and -2.....81
10.3.2 Trace element content.....83
10.3.3 Comparison of the trace element content in cassiterite-1 and -2.....83
10.3.4 Comparison of the trace element content in cassiterites from the A and C Mines.....86
11. EVOLUTION OF THE ORE-FORMING FLUIDS.....88
11.1 Evolution of the ore-forming fluids in the granite.....88
11.1.1 The alternative models.....88
11.1.2 Physical evolution of the ore-forming fluids.....91
11.1.3 Geochemical evolution of ore-forming fluids in the granite.....93
11.1.4 Evolution of tin in the ore-forming fluids.....96
11.2 Migration history.....102
11.2.1 The migration path.....102
11.2.2 Compositional changes 108
11.2.3 Residence time.....109
11.3 Deposition of tourmaline, ankerite and cassiterite.....111
11.3.1 Tourmaline 111
11.3.2 Cassiterite and ankerite.....115
11.4 Polyphase mineralisation.....123
SUMMARY AND CONCLUSIONS.....125
REFERENCES.....127
APPEDIX

Digitised by the Department of Library Services in support of open access to information, University of Pretoria, 2021

Abstract

The evolution of the ore-forming fluids in the Rooiberg tin-field has been reconstructed from their source, through the migration history and to the final site of ore deposition.

The granites in the west and in the east of the Rooiberg Fragment have been mapped, sampled and chemically analysed. Four granite types are present: Nebo, Klipkloof, granophyric and Bobbejaankop Granite. The granites are considered to be high heat producing. The Bobbejaankop Granite is geochemically the most evolved and supplied the ore-forming fluids.

Pb-Pb isotope analyses of ankerite yielded dates of 2181 - 2712 Ma, which are older than 2054 Ma of the Bobbejaankop Granite. These anomalous dates are ascribed to assimilation with extraneous Pb in the arkosite during fluid migration.

A prolonged period of pervasive migration of the fluids took place through the arkosite, and was probably in the order of tens of million years. Feeder channels for the ore-forming fluids only attained importance at the site of ore-deposition when the fluids migrated from the arkosite into them. Alteration of the arkosite on a large scale represents the geochemical footprint of the ore-forming fluids.

Polyphase mineralisation is manifested in at least four ways:

1. Ore deposition first took place in the pockets and subsequently in the lodes, but both types of ore-bodies were formed from the same ore-forming fluids, liberated as a single batch from their source, and residing in the arkosite for a long period of time;
2. Two pulses of ore-forming fluids led to two periods of tourmaline formation during the early stages of pocket mineralisation;
3. Early-formed cassiterite in the pockets was redissolved and redeposited as a later phase of high-grade mineralisation; and
4. A separate pulse of fluids was responsible for late stage development of ankerite in fractures.

Digitised by the Department of Library Services in support of open access to information, University of Pretoria, 2021

Opsomming

Die evolusie van die ertsvormende oplossings in die Rooiberg-tinveld is gerekonstrueer vanaf hulle bron, deur hulle migrasiegeskiedenis, en tot op die finale plek van ertsvoming.

Die graniete in die weste en in die ooste van die Rooiberg Fragment is karteer, bemonster en chemies geanaliseer. Vier graniet-tipes is teenwoordig, te wete Nebo, Klipkloof, granofiriese graniet en Bobbejaankop Graniet. Die graniete word beskou as hoë hitte-produserend. Die Bobbejaankop Graniet is die mees ontwikkelde van die vier en het ook die ertsvormende oplossings verskaf.

Pb-Pb isotoop analises van ankeriet het "ouderdomme" van 2181 - 2712 Ma aan die lig gebring, wat ouer is as 2054 Ma van die Bobbejaankop Graniet. Die anomale ouderdomme word toegekryf aan assimilasie met vreemde Pb gedurende die migrasie van die oplossings.

'n Uitgerekte periode van wydverspreide migrasie van die oplossings deur die arkosiet het plaasgevind en was waarskynlik in die orde van tientalle miljoen jaar. Toevoerkanale vir die ertsvormende oplossings het eers op die plek van ertsvorming van belang geword, nadat die oplossings vanuit die arkosiet na diè kanale gemigreer het. Grootskaalse verandering van die die arkosiet verteenwoordig die geochemiese getuienis van die oplossings.

Meermalige mineralisasie is op ten minste vier maniere gemanisfesteer:

1. Erts is eerste in die sakvormige knolle en daarna in die ertsare afgesit, maar albei hierdie tipes van ertsliggaam is gevorm van dieselfde ertsvormende fluidum wat as 'n enkele stooksel van die bron geskei is en lank in die arkosiet vertoef het;
2. Twee pulse van ertsvormende vloeistof het gelei tot twee periodes van toermalynvorming gedurende die vroeë stadiums van sakvormige mineralisasie;
3. Vroeg gevormde kassiteriet is opgelos en weer gepresipiteer as 'n latere fase van hoëgraadse mineralisasie; en
4. 'n Aparte puls van vloeistof was verantwoordelik vir die vorming van ankeriet in breuk-strukture gedurende 'n laat stadium.

Digitised by the Department of Library Services in support of open access to information, University of Pretoria, 2021

1. INTRODUCTION

The Rooiberg tin-field is situated 120 km NW of Pretoria within sediments and subordinate mafic volcanics collectively referred to as the Rooiberg Fragment. The tin-field embraces the following main past producers: Leeuwpoort C Mine, Rooiberg A Mine (of which the NAD Section is large enough to be referred to as the NAD *Mine* in company reports, some publications and also in this study), Nieuwpoort - Blaauwbank B Mine and Vellefontein, as well as a host of other but very small deposits, some of which were in production for short periods, yielding minor quantities of ore. The "Fragment" is approximately 500 km^2 of which the economic interesting area (the "tin-field") occupies approximately three quarters (Fig. 1). All the main producers used to have outcropping ore-bodies; extensive mining was in fact done by possibly foreign communities a few centuries ago and the "rediscovery" of the ore-bodies, at the beginning of this century, resulted from the investigation of the ancient workings.

Modern mining was carried out almost continuously for nearly a century and historically the Rooiberg tin-field was the largest producer of tin ore in South Africa with a total production of 83 000 tons of tin metal up to 1992 (Misiewicz, 1992). The operating company, Rooiberg Tin Limited, survived the collapse in the tin price of 1985, but sadly, and despite admirable efforts, could not financially withstand the 1989 collapse which led to a gradual but permanent phasing out of mining. By mid 1993, all mining activities were stopped, underground workings were allowed to become flooded, shafts were sealed off, shaft headgears and extraction plants dismantled and the company's assets were put up for sale.

There are basically three types of ore-bodies:

(1) *Emplacement* of minerals along fracture-structures, commonly referred to as bedded lodes, counter-dipping lodes (or counter-dippers) and steep structures, which are sometimes, but wrongly, called "fissures". Ore-bodies of this type are confined to the C, NAD and Vellefontein Mines.

(2) *Replacement* by minerals to form *pockets*, hundreds of which are dispersed through the arkosite at the A Mine; economically the most important ones occur within a conformable 80 metre thick stratigraphic zone, referred to as the "tin-zone".

(3) *Replacement* in the form of *large single bodies*, wedged between steep

Digitised by the Department of Library Services in support of open access to information, University of Pretoria, 2021

dipping fracture-structures, such as the Stewart ore-body at B Mine and the Salvation prospect.

Cassiterite in these ore-bodies is associated with a long list of minerals, of which tourmaline, ankerite and pyrite are the most abundant. More than 80 per cent of the tin ore was won from the first two types of ore-bodies.

The classical granite-derived hydrothermal origin is accepted by most authors, but in the latest comprehensive publication prior to this study, Rozendaal *et al*. (1986) concluded that the metallogenesis is still poorly understood. This may be partly attributed to the fact that studies of particulary the geochemistry of the ore-forming minerals have been neglected after the initial pioneering work of Leube and Stumpfl in 1963. Moreover, isotope determinations, which may provide vital clues regarding the formation of the ore-bodies, have never been done before.

The author seized the opportunity before the mines were permanently closed to carry out underground studies and to collect sample material for this study.

2. PREVIOUS WORK

The previous work clearly illustrates the share, or rather the *lack* of it, which Rooiberg received in the literature of earth sciences, despite the facts that (1) mining was carried out almost continuously over nearly a century, (2) Rooiberg was historically the largest tin producer in South Africa and (3) the ore-bodies, particulary those at the A mine are unequalled in Southern Africa with regard to number, morphology and complexity. The total of no more than twelve publications and four dissertations, *over this whole period*, dealing directly with Rooiberg ore-bodies, compares poorly to that of Zaaiplaats, the number two tin producer. During the ten-year period between 1984 to 1994 alone, the publications and dissertations dealing with Zaaiplaats amounted to at least ten, and these are: Coetzee (1984); Von Gruenewaldt & Strydom (1985); Coetzee (1986); Crocker (1986); Coetzee & Twist (1989); Pollard *et al*. (1989, 1991a, 1991b, 1991c); McNaughton *et al*. (1993). During the same period, only two publications, Rozendaal *et al*. (1986); Misiewicz (1992) and one dissertation, Naude (1993), appeared on the Rooiberg tin-field. Ironically, it was towards the end of the mining operations and after the closure of the

Digitised by the Department of Library Services in support of open access to information, University of Pretoria, 2021

mines that most publications and dissertations appeared. Apart from this study and the work of Naude (1993), two publications by Rozendaal *et al.* appeared during 1995 and more are in preparation (Rozendaal, pers. comm.).

There are two main reasons for this sad state regarding the number of publications. Firstly, staff and students attached to the former Bushveld Research Institute at the University of Pretoria showed an obvious preference for Zaaiplaats over Rooiberg in their studies of the Bushveld tin deposits. The second reason is rooted in the perception held by some mine managers and mine engineers on the usefulness of geological advice and research at operating mines. This is particulary true for Rooiberg during its first fifty years of production when geological work was rarely done, and on an *ad hoc* basis only. This work, incidently, included the services of some eminent geologists such as Dr L Reinecke (1929) and others mentioned below. It was only after Gold Fields of SA took technical and administrative control that this perception started to change for the better. When viewed against the background of some hitherto unpublished events and developments which directly or indirectly influenced geological work, and hence publications, it will become clear that the geological fraternity is only partially responsible for this sad state of affairs. Since this is also, in all probability, the last major work on the Rooiberg tin-field for many years to come, a slightly broader review of the previous work will at the same time document the history and development of geological thought and work over almost a century at Rooiberg.

Immediately after the mining operations were started at the beginning of this century, three important publications by non-resident geologists appeared in quick succession: Recknagel (1908) gave an account of the then newly discovered mineral deposits in the area which were later developed into the A Mine, followed by McDonald (1912; 1913), dealing more specifically with what became the C Mine. McDonald's publication of 1913 is of particular interest and historic value since this is the first documentation of polyphase mineralisation in the tin-field. Considering the limited extent of the underground excavations before 1913, less than five years after mining commenced and the limited scale thereof, McDonald's observations were truly remarkable. With reference to the occurrence of ankerite in the Spruit Lode at C Mine, he states (p. 128) .."there is no reasonable doubt that, *after the*

Digitised by the Department of Library Services in support of open access to information, University of Pretoria, 2021

first mineralisation had been completed, fracturing took place, and... then ... ankerite was deposited". Also on p. 129 ..*"Not only has the mineral.. [ankerite].. been deposited in the open cracks formed by the shattering of a previous ore*, but has also penetrated by replacing other minerals in the ore fragments".

After this early pioneering work, there was a long period during which nothing was published on Rooiberg, and only in 1946 did the next publication appear - also by a non-resident geologist (Boardman, 1946). Much of this is attributed to the fact that over this period, the operating companies saw no merit in employing the services of a resident geologist, despite the complexity of the ore bodies. Because of this complexity, along with the fact that mining was much a hand to mouth operation, and ore had to be found in certain sections of the mines on a day to day basis, miners developed their own pet theories. Acceptance or rejection of these theories generally paralleled the seniority in the ranks of the underground officials! In retrospect, these miners has done pretty well in developing a "feel" for ore, and the author have good reasons to believe that the services of a geologist during this period, would not have altered this culture. At best, such a geologist could have perhaps published more on the ore deposits as they became exposed underground.

It must be emphasised also that the three pioneering publications, despite the limited extent of the workings when they were compiled, contain a very accurate description of the structure, mineralogy and genesis of the ore-bodies. Very little scope was left for publications on the ore-bodies as such, other than an update on their extent as mining proceeded. In fact, the first "modern" account by Leube and Stumpfl (1963), fifty years after the first publications could not fault the observations contained in these very early works. Neither can this study.

Realising the strategic importance of tin (and some other commodities) during and shortly after World War 2, Government, through the Geological Survey, commissioned four of its senior geologists - L.G. Boardman, T.W. Gevers, J.T. Wessels and J. Willemse - to conduct a systematic geological survey, mainly of the surface, of the entire tin-field. Although important contributions were made, e.g. production of the first detailed regional geological maps of the area and the discovery of the Rio Rita lode by Willemse and Wessels, only the

Digitised by the Department of Library Services in support of open access to information, University of Pretoria, 2021

work of Boardman was published in 1946. This was also the first geological work for which the State received financial reimbursement from the private sector, a total of 20-odd thousand pounds (Visser, 1970), mainly as a result of the discovery of the Rio Rita lode.

It was also at approximately this time that some continuity of geological work was maintained through the services of T. Marrack in the 1940s and later by N.A.N Clack in the 1950s, followed by A. Leube. It is rumoured that Marrack was not allowed by the mine management to go underground and he had to concentrate on surface mapping; Clack was for a fact most frustrated and only stayed on because of a contractual agreement. Clack's final report (unpubl.), covering a three year period, is one of bitterness and fierce criticism levelled at mine management. Leube was initially employed by the Geological Survey of South Africa but joined the operating company in 1960. He was stubborn, but at the same time hard-working, and when his efforts started to pay off, management changed their attitude as well. His publication on the structural control in 1960 was the first one to appear after that of Boardman in 1946. Leube, in his capacity as resident geologist and E.F. Stumpfl, an academic, conducted a study of particularly the A and C Mines - the main producers - and published their results in 1963. This work introduced an entirely new approach of geological reasoning at Rooiberg and is one of the most important papers ever published on Rooiberg. For instance, Leube's interpretation of the structural control, particulary at C Mine, laid the foundation for searching for ore at depth. According to the prevailing theories of that time and subscribed to by foremost geologists, tin mineralisation was epithermal and unlikely to be found below ± 100m from surface. In the face of much opposition, Leube instigated the drilling of a deep borehole, the first of approximately 200 drilled up to the time of this study, which not only proved payable ore at C Mine 300m below surface but also established the structural arrangement of the lodes, referred to at the mine as "sandwiching". Leube's interpretation led directly to the discovery of the Agnes lode (named after Leube's daughter) and later to other deep-seated lodes at a time when ore reserves at C Mine were low. Stumpfl's work on the other hand, was the first comprehensive account of the mineralogy, petrology and geochemistry, which directly led to additional geochemical and related studies to account for the economically important "tin-zone".

Digitised by the Department of Library Services in support of open access to information, University of Pretoria, 2021

Leube and Stumpfl also reaffirmed the observations made initially on polyphase mineralisation by McDonald (1913) fifty years earlier and in a brief passage to the mineralisation at A Mine they state (p. 540).."Later fractures that cut mineralized pockets are widespread in A-6 (*A Mine)*. They are filled with a matrix of young carbonate and fine-grained chlorite and clearly indicate that tectonic activity and mineralization in this area are closely inter-related processes extending in *several phases over considerable time*".

During the same year as Leube and Stumpfl's publication, Prof A.P.G. Söhnge expressed quite different thoughts on the origin of tin mineralisation in the Bushveld and promoted an idea of tin in the country rocks as a precursor for economic mineralisation. This suggestion is contained in the Presidential Address which he delivered to the Geological Society of South Africa in 1963. In dealing with "Genetic problems of pipe deposits in South Africa", Söhnge, to a certain extent, echoed the much contested transformation hypothesis to explain the Bushveld Complex, advocated by van Biljon (1949). This idea was not taken too seriously at that time, at least not for the Rooiberg deposits, although Prof J. Willemse, a staunch adherent of a magmatic origin of the Bushveld Complex, expressed the view that serious consideration should be given to a sedimentary origin for the A Mine pockets (Willemse, 1967, pers. comm.).

The author was employed as resident geologist at Rooiberg from 1963 to 1971 and it was during the latter part of this period that he gave impetus to the concept of polyphase mineralisation initially recognised by McDonald (1913). Towards the end of the 1960s, when the concept of polyphase mineralisation at the A and B Mines became entrenched, it was, as far as other tin mines are concerned, only recognised beyond doubt in the Cornish mines (Garnett, 1965; 1966a; 1966b) and at the Shakh-Shagaila tin deposit in Central Kazakhstan. In the latter deposit, Lebedev (1967) gives evidence for .. " multistage ore deposition ... caused by pulsations in tectonic movements; mineralization of the fractures formed in each of the stages differed qualitatively from mineralization of the previous stage" (p. 85). Polyphase mineralisation at that point in time was, however, the most comprehensively studied and documented in the Cornish mines, as amply described by Garnett (*op cit*), and was subsequently incorporated in other publications as well, e.g. the fourth edition of the Handbook of South-West England published by the British

Digitised by the Department of Library Services in support of open access to information, University of Pretoria, 2021

Geological Survey (Edmonds *et al.*, 1975).

During the same period, the author became acutely aware that polyphase mineralisation may indeed be present at other tin mines in South Africa, but has escaped detection (Labuschagne, 1970b, p. 2) - a view shared by Garnett (pers. comm.) who also enthusiastically promoted it for other tin mines outside South Africa. In retrospect, Garnett's notion seems to be well founded. The list of tin deposits showing polyphase mineralisation has grown since 1970 and those added include Herberton, Australia (Georgees, 1974), Pelapah Kanan, Malaysia (Taylor, 1978) and Chorolque, Southern Bolivia (Lehmann, 1990).

Polyphase mineralisation has both practical and academic implications. On the practical side, the development of the 19N Section of the A Mine, which for a number of years "has been the economic back-bone of the Rooiberg Mines" (Stear, 1976, p. 56), was based on geological plans which show the distribution of the economically high grade second phase tin mineralisation. Regarding the Cornish Mines, Taylor (1978, p. 146) states that.. "Major tin veins are usually multiphase and have formed as a result of continued reopening and deposition of successive phases of mineralisation. Since not all phases will contain valuable minerals it becomes of prime importance to know their distribution and character". As far as the academic implications are concerned, it may provide valuable clues regarding the history of events during the emplacement of the granite, the generation of the ore-forming fluids from the granite and the subsequent migration of these fluids through the country rock and feeder channels. Investigations by Clark *et al.* (1976) and Clark & Robertson (1978) of the Argentina-Bolivian-Peru tin-belt suggested at *least five main episodes of tin mineralisation* ranging from Ordovician-Silurian to Mid-Pliocene. Taylor (1978, p. 39) speculated that this situation could well reflect a contribution from a persistent tin anomaly, which has been tapped periodically and which may reflect crustal contributions from the adjacent Brazilian shield. While the events at Rooiberg were certainly not as dramatic as these, the author kept an open view that polyphase mineralisation may well be related to more subtle pulses of the granitic source, particularly since mineralisation took place over a prolonged period of time.

During the 1970s and the early 1980s, four dissertations on various aspects

Digitised by the Department of Library Services in support of open access to information, University of Pretoria, 2021

of Rooiberg were submitted: Labuschagne (1970a), Stear (1976), Dinsdale (1982) and Phillips (1982). Only that of Stear (1977a and b) was published. Much original work, particulary on the sedimentology and structure was done by Stear and the new stratigraphic names accepted by The South African Committee for Stratigraphy (SACS) were proposed by him. To date, the studies of Phillips are the most comprehensive accessible account of the C Mine, and he clearly showed the economic importance of cymoid loops.

Söhnge's contention of a sedimentary origin for tin was reviewed by Hunter in 1976. He (Hunter, 1976) concluded that there is no evidence that the sediments were originally stanniferous as a result of a sedimentary process but suggested (p. 242) that .." serious consideration should be given to a possible exhalative origin for deposits such as those in the Rooiberg and Nylstroom fields, particulary as volcanics are interbedded with the sedimentary succession".

When considering an exhalative origin as an alternative, the work of Plimer (1980) should be taken into account. Plimer evaluated numerous tin and tungsten deposits world-wide and suggested that the origin of some of these should be reconsidered since they may be exhalative in origin when associated with mafic volcanics. From his studies he concluded that while basaltic rocks have extremely low Sn and W contents, the presence of these elements indicates an elevated geothermal gradient. Consequently, the mafic volcanism provided the energy for fluids to circulate through and leach Sn and W from large volumes of sediments. Precipitation of Sn and W phases at the sediment-seawater interface would therefore be coeval with or associated with mafic volcanism. He also noted the close association between these deep water sequences and intrusions of S-type granites which indicates genetic relationships between exhalative and granitic mineralisation. Anatexis of sequences containing exhalative Sn and W deposits which may be uneconomic would provide a mechanism for reconcentration and finally an economic deposit associated with granite may result.

Stear (1977a), however, indicated that the arkosite was deposited in a braided stream environment and the lower portion of the overlying Blaauwbank Shale Member was deposited by fluvial channel processes; only the upper portion may be interpreted as marginal marine. The deep water sequence commonly associated

Digitised by the Department of Library Services in support of open access to information, University of Pretoria, 2021

with exhalative Sn deposits as proposed by Plimer (*op cit*) i.e. pelites, carbonate and chert is absent. Also, the stratigraphic position of the andesitic lavas, being near the top of the Smelterskop Formation, cannot be reconciled with coeval volcanism and precipitation of Sn in deep water sediments.

Rozendaal *et al.* (1986) gave an eloquent review of the Rooiberg tin deposits and also suggested lines for future research. This publication, which is in many ways an excellent review of the Rooiberg tin deposits, has been compiled from information available as at 31 March 1986 (p. 1326). Nothing is said about polyphase mineralisation, and it is assumed that the authors (tacitly) dismissed the presence thereof in the Rooiberg tin-field at that time. While Rozendaal *et al.* (1986) recognised a hydrothermal origin of the tin deposits they pointed out that several observed associations are inconsistent with the classic epigenetic granite-related model. They suggested that alternative models should be considered, taking into account the concept of a possible Bushveld tin province and quoted the exhalative origin as proposed Hunter (1976) as an alternative model.

Misiewicz (1992) reviewed the application of resource management at Rooiberg and his publication also contains excellent case studies of the importance of sound geological reasoning when developing and mining the complex ore bodies.

Naude (1993) researched the mineralisation of the NAD Mine which led to a M.Sc. dissertation and made some important contributions regarding the mineralogy and related geochemistry of the NAD Mine.

Finally, two publications by Rozendaal *et al.* appeared during 1995. In the first of these (Rozendaal *et al.* 1995a), they dealt specifically with the tin-zone. In the second one (Rozendaal *et al.* 1995b), the authors outlined three successive phases of mineralisation which they relate to multiple pulses of hydrothermal fluids. Thus the concept of polyphase mineralisation, originally recognised by McDonald in 1913 and later strongly advocated by the author, finally received recognition by Rozendaal *et al.* in 1995.

The enormous volume of unpublished company reports, which accumulated over many years, stands in marked contrast to the few publications. As can be

Digitised by the Department of Library Services in support of open access to information, University of Pretoria, 2021

expected, the overwhelming majority of these deals with geology related to local mining and as such are of little use, particulary to the reader who is unfamiliar with Rooiberg. Nevertheless, they do contain a wealth of information, which, if synthesized, may lead to useful publications. More than half of these reports were generated during the last two decades and it was during this period that geological work advanced to such an extent that it became almost indispensable to mine planning, both on the short and certainly on the long term. At one stage, eleven geologists were employed simultaneously by the company and geological team work became organized through a well managed Geological Department.

Some of the more important achievements during the latter two decades, based on geological advice, include the development of the northern part of C Mine and the revival of the NAD workings. The northern part of the C Mine was developed as a result of an elaborate drilling programme directed by P.D.F Vickers. Figures on ore reserves have not been made available to the author, but it appears from mine plans that this northern part contains huge reserves. The NAD Mine also became an important producer.

The permanent closure of the mines will adversely effect future research on the Rooiberg deposits, since the underground workings, being sealed off, are totally inaccessible. Moreover, a depressed tin price is not likely to stimulate exploration and, as a result, further geological research of these deposits will also suffer.

3. SCOPE AND AIMS OF THIS STUDY

The scope and aims of this study are two-fold. Firstly, while virtually all the workers who have published on the origin of the Rooiberg tin deposits subscribe, in one way or the other, to a granitic origin for the ore-forming fluids, more specifically the tin-bearing fluids, proof of this is lacking. The only work done on the granite to date is regional mapping west of Rooiberg by Iannello (1970), some mapping (on a very small scale) by Crocker (1976) and as far as geochemistry is concerned, no more than 13 samples have been collected by Phillips (1982) along a road traverse near the C Mine and analysed. Five analyses were obtained by Iannello (1970) in the west. In addition, no thorough petrographic comparison of the granites east and west

Digitised by the Department of Library Services in support of open access to information, University of Pretoria, 2021

of the Rooiberg tin-field has been done to date.

In this study, the Bushveld granite will be evaluated as the possible primary source for the tin mineralisation at Rooiberg. This necessitates that the granites east and west of the Rooiberg tin-field are studied over a wide spectrum ranging from the form of emplacement, magmatic differentiation, geochemical specialisation and the concentration of the ore-forming fluids. Closely associated with this is the migration history of the ore-forming fluids from their primary source to the final site of deposition. Possible alternatives for a primary source of the tin other than the granite will also be evaluated.

Secondly, the concept of polyphase mineralisation at the A and B Mines was developed on the basis of macroscopic evidence alone. Without mineralogical, geochemical or isotopic support, the author, who was the chief advocate for this concept, admits that some observations made underground can be interpreted as the result of either poly- or mono-phase mineralising episodes. In this study, the two main minerals, tourmaline and ankerite as well as cassiterite will be studied in detail, ranging from the microscopic description, mineral geochemistry and isotope systematics. This work should allow substantiated conclusions to be drawn regarding mono- and polyphase mineralisation.

The ultimate aim is to reconstruct the evolution of the ore-forming fluids from their primary source, through their migration history to the final site of deposition.

4. ACKNOWLEDGEMENTS

This study was carried out during three main periods which entailed underground and field work, analytical work and interpretation and compilation of the results. Without the assistance of numerous persons and some organisations, this would not have been possible.

Underground and field work. An informal arrangement with the Office of the Consulting Mine Engineer of Gold Fields of SA and the Mine Manager at Rooiberg allowed the author underground access to the dormant and producing mines.

Digitised by the Department of Library Services in support of open access to information, University of Pretoria, 2021

The Senior Geologist at Rooiberg, Mr Julian Misiewicz, rendered immense support by organising logistics to ensure the safety of the author and his assistant in dormant underground workings. Julian is also thanked for guiding the author underground from time to time as well as for the many stimulating discussions on the Rooiberg deposits. Mr P Malose accompanied the author underground at all times and carried more than his fair share of the load of samples to surface.

Permission by land owners Mr Botha, Dr Naude and Mr Cavaleros to use private 4X4 tracks along the slopes of the Boschoffsberg is appreciated. Mr Cavaleros also availed his farm manager and a vehicle for a short period which speeded up the field programme considerably.

Analytical work and ancillary tasks. The majority of the analyses were carried out at the laboratories of the Council for Geoscience and the author is indebted to the following persons: Dr D de Bruin and Miss W Havenga for the microprobe analyses; Mr J H Elsenbroek and Mmes C Cloete and A Schoeman for XRF analyses; Dr R Edge and Messrs J Trojak, H Sello, M Matlou and P Malose for wet chemical, AAS, IRS and selective ion electrode analyses and Mr B Ivanfy for HPLC analyses. The neutron activation analyses were done at the Schonland Research Centre by Dr R Hart and Mr A Damarupurshad. The XRD determinations were done by Dr D Bühmann and Mrs M Atanasova. Sample preparation was carried out by Messrs S Mabena and R Pludik and thin sectioning and polishing by Messrs M Lekotoko and A Digkomo. Assistance with technical photography was given by Messrs N Mabuela and M Köhler; the photographs of the hand specimens were taken by Martin Köhler. Isotope analyses of Pb were done by Dr F Walraven.

Interpretation and compilation of the results. Dr Walraven's interest in this study extended beyond isotope analyses and many fruitful discussions related to isotope systematics are appreciated. Dr de Bruin kindly calculated the atomic proportions in tourmaline from the chemical analyses. Mr Paul Ernst Wipplinger checked the calculations of element concentrations in the fluids. Mr R Holdsworth prepared a geochemical contour map of tin in the Rooiberg area. Information provided by correspondence with Prof Richard J Reeder of the State University of New York at Stony Brook regarding ankerite is acknowledged.

Digitised by the Department of Library Services in support of open access to information, University of Pretoria, 2021

This study was commenced while the author was employed by the Council for Geoscience and permission by the Director, Dr C Frick, to carry out a large part of the field work and to make liberal use of the analytical services of the laboratories of the Council is much appreciated. Some of the analyses were done after the author resigned from the Council. Thanks are also due to the Department of Mineral and Energy Affairs for bursary assistance and study leave during the first year of this study.

The author is greatly indebted to his promoter, Professor C P Snyman, for his interest throughout this study and for constructive criticism.

Finally, thanks are due to my wife, Laurette, who accompanied me during many weekends to the field and for her patience and understanding during the last four years.

5. METHODS

5.1 Surface mapping and sampling of the granites

Two areas occupied by granites, located west and east of the Rooiberg tin-field, were selected for this study. The areal extent of these areas was governed by the availability of outcrops, and 100 and 220 square km in the west and east respectively were finally incorporated. The localities of these two areas in relation to the Rooiberg Fragment and the Rooiberg tin-field are shown in Fig. 1.

In the west, particulary along the steep slopes of the western side of the Boschoffsberg, the outcrops of fresh granite are abundant and the area is ideal for mapping and sampling. However, because of the ruggedness of the terrain, most of the area is accessible by foot only. In the east, outcrops are scarce and the granite is seldom fresh. This necessitated the selection of a larger area to obtain enough samples. Although the area is flat, well serviced by tracks and easily accessible, mapping is difficult due to the scarcity of outcrops. Eventually, 68 field stations were set up in the west, or an average of one station per 1,5 square km and 57 in the east, or an average of one station per 4 square km. The stations were coordinated using the Global Positioning System (GPS) and the positions were plotted directly

Digitised by the Department of Library Services in support of open access to information, University of Pretoria, 2021

onto available geological maps. Several hours were spent at each station to examine as much of the outcrops in the vicinity as deemed necessary, to check the existing geological maps, to make whatever modifications were required and to document the rock type(s). At each station, one sample was collected for a permanent record, another for the preparation of thin sections and at least 10 kg of the least weathered chips were bagged for chemical and isotope analyses. The sample number, rock type and coordinates of each station are given in Table I of the Appendix.

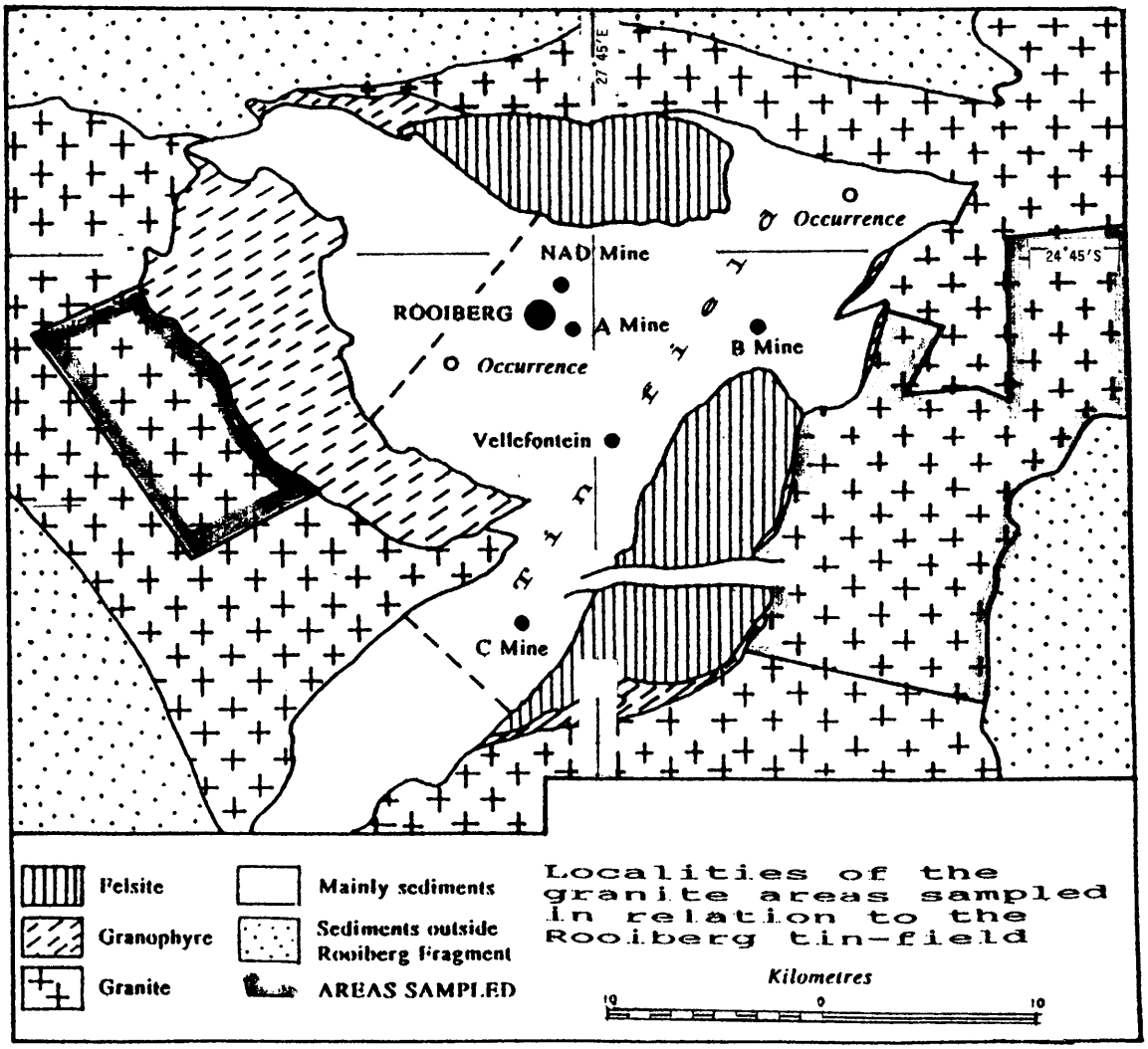

Fig. 1 - Localities of the granite areas mapped and sampled in the west and in the east of the Rooiberg tin-field. Also shown are the past producers (circles filled) and two tin occurrences (open circles).

Digitised by the Department of Library Services in support of open access to information, University of Pretoria, 2021

It was clear at the outset that apart from systematic sampling, fairly reliable geological maps of the granites in the two areas would be needed if any meaningful conclusions were to be drawn. In the west, the relevant portion of the map by Iannello (1970) was checked in the field and found to be very reliable; minor modifications were made to this map and the granite types were renamed. In the east, the available geological maps were found to be totally unsuitable and, for the purpose of the study, a map was compiled showing the distribution of the granite types, but not necessarily their mutual relationships.

5.2 Underground mapping and sampling of the ore-bodies

During May to August, 1992, shortly before the A, NAD and C Mines were permanently closed and sealed, comprehensive sampling and a limited amount of underground mapping were carried out in the accessible parts of the A and NAD Mines and the northern part of C Mine. The smaller producers, Vellefontein and B Mine were already flooded at that time and hence totally inaccessible. The author also retrieved maps from the files of the mine office prepared by him during his employment at Rooiberg, particulary those related to polyphase mineralisation.

A total of 350 samples were collected underground, their localities determined by using survey stations ("pegs") or mine plans, and their mineral content and relationship to the ore-bodies or country rock recorded. The number and the localities of the samples were governed by accessibility, representation on a mine scale as wide as possible, suspected mono- or poly-phase mineralisation (in the A Mine) and adequate representation of the major minerals. The main areas sampled underground are shown in Figs. 2 and 3 and the number of samples taken from ore-bodies in these main areas are as follows:

A Mine		**NAD Mine**		**C Mine**	
Section	*Samples*	*Lode*	*Samples*	*Lode*	*Samples*
M18	17	C Lode	26	A Lode	4
Jewel Box	28	AMS Lode	1	Hosking	5
Q22-Magazine	93	Cotton Lode	5	Gap Lower	35
19N	37	Union Lode	9	New Lode	3
U30	14	Bonus Lode	14	Gap Lode	23
		U Lode	16	CA Lode	14
		Ross-Watt	5	Fault Lode Fr.	1
Total A	***189***	***Total NAD***	***76***	***Total C***	***85***

Digitised by the Department of Library Services in support of open access to information, University of Pretoria, 2021

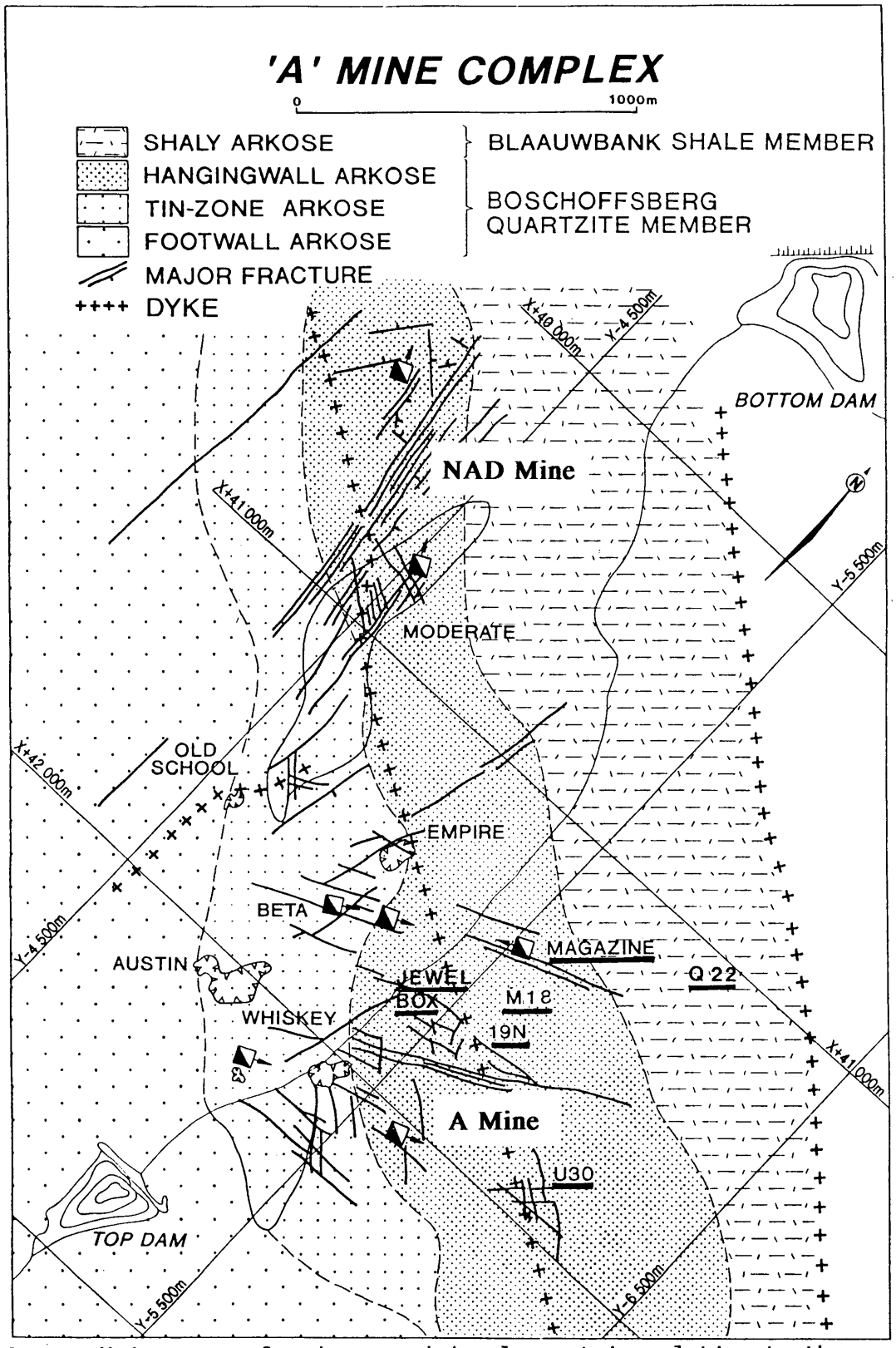

Fig. 2 - Main areas of underground development in relation to the surface geology at the A Mine Complex, comprising the A Mine proper and the NAD Mine. Only the development along major fracture-structures is shown and not the very extensive development along minor fractures, which exposed the pockets. The sections of the A Mine proper sampled are underscored. (After Misiewicz, 1992)

Digitised by the Department of Library Services in support of open access to information, University of Pretoria, 2021

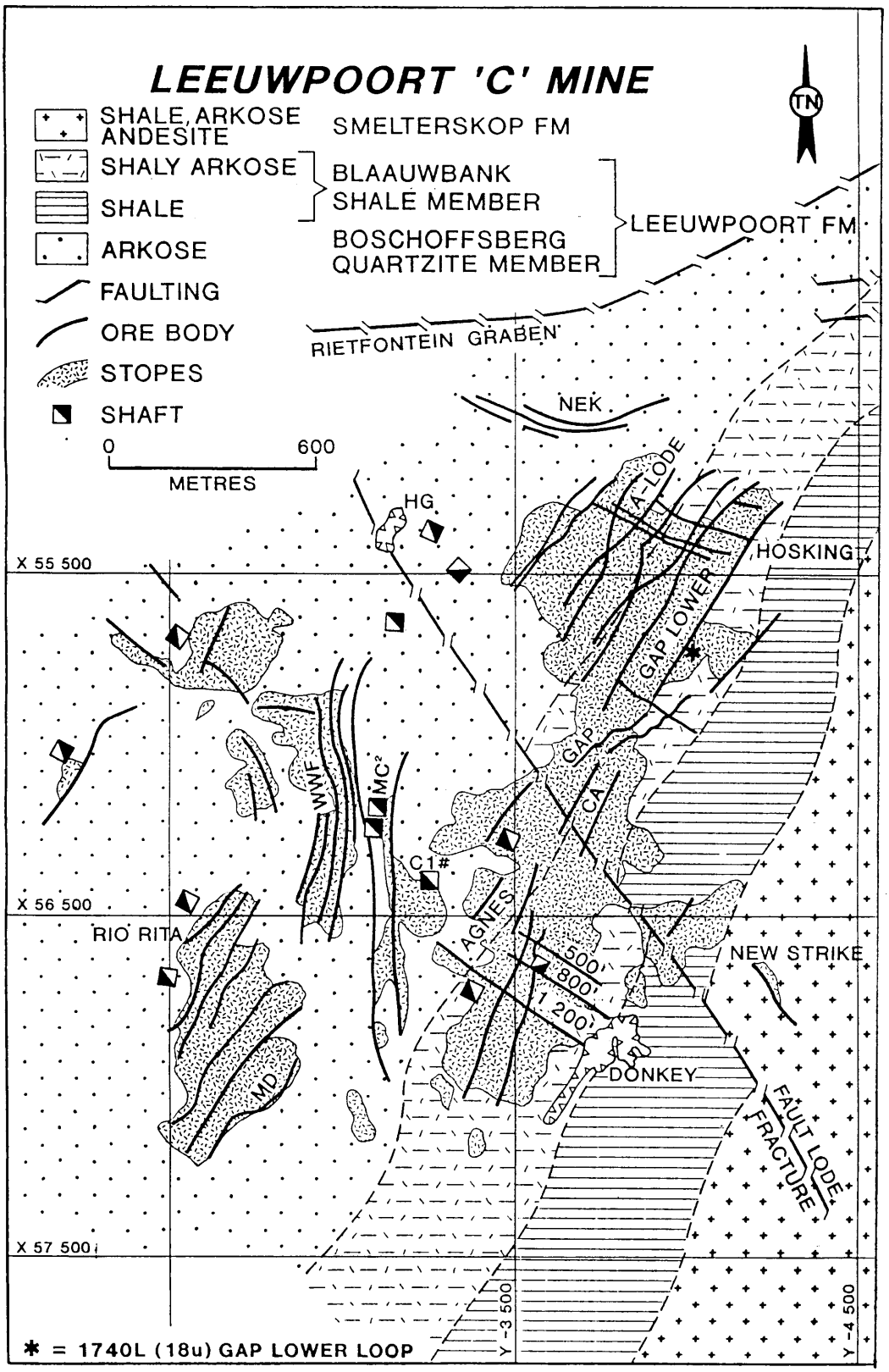

Fig. 3 - Main areas of underground development in relation to the surface geology at the C Mine. Sampling was carried out in the northern part of the mine only, that is north of the Fault Lode Fracture.
(After Misiewicz, 1992)

Digitised by the Department of Library Services in support of open access to information, University of Pretoria, 2021

The names of the stratigraphic units in Figures 2 and 3 are those which were used by the mine personnel; the coordinates are local mine coordinates. The localities of, and main minerals present in the samples are given in Table II of the Appendix.

5.3 Laboratory techniques

The types of analyses done by various laboratories for the various rocks and minerals are summarised in Table 1. Most of the analyses were done in the laboratories of the Council for Geoscience at Pretoria and a limited number of specialised analyses was done at the Schonland Research Centre for Nuclear Physics at the University of the Witwatersrand. Duplicate samples were done for some trace elements by different methods in the same laboratory. In the case of tin, analyses were also done by a commercial laboratory. Some of the Rooiberg tourmalines collected for this study were analysed by Anglo American Research Laboratories for a different project, and these results were made available to the author.

Granitoids. All 125 samples were analysed by X-Ray Fluorescence Spectrometry using the method of Norrish & Hutton (1969) for the major elements and that of Feather & Willis (1976) for trace elements. The volatiles H_2O^+, H_2O^-, CO_2 and S were determined by means of Infra Red Spectrometry. Li and B were determined by Atomic Absorption Spectrometry and F was done by Selective Ion Electrode analyses. Rare earth element determinations were done by means of High Pressure Liquid Chromatography.

Since the granite samples are usually coarse-grained with individual grains up to 1 cm in the coarsest samples, the validity of analyses of a split portion of the crushed and pulverised sample, in particular for the trace elements with levels of concentration below 10 ppm, was tested as follows: One of the coarsest grained samples was split into 10 equal portions after initial crushing to ± 1 cm chips. One of these split portions was analysed in 10 consecutive runs and each of the 10 portions was analysed once for the same trace elements. The results were compared and the following conclusions were made:

Digitised by the Department of Library Services in support of open access to information, University of Pretoria, 2021

Table 1 - Summary of various analytical methods used for various rock types or minerals by various laboratories

Rock/ mineral	Micro-scopic	Council for Geoscience Laboratory								*Schon-land	Commercial Laboratories	
		XRF (Major)	XRF (Trace)	AAS	IRS	Ion	HPLC	Micro probe	Pb-Pb Isotope	INAA	ICP	Micro probe
Granitoids	124	125	125	125	125	125	52				30	
Ankerite	37		20		32			48(192)	59		20	
Tourmaline (Rooiberg)	74							10(65)				6(188)
Tourmaline (Other localities	2							1(8)				1(25)
Cassiterite (Rooiberg)	50									32		
Cassiterite (Other localities)	10									4		

XRF = X-Ray Flourescence Spectrometry
AAS = Atomic Absorbtion Spectrometry
IRS = Infra Red Spectrometry
Ion = Selective Ion Electrode analysis
HPLC = High Pressure Liqiud Chromatography

Microprobe = Electron Microprobe analysis
Pb-Pb Isotope = Radiogenic Pb isotopes
INAA = Instrumental Neutron Activation Analysis
ICP = Inductively Coupled Plasma analysis

*Schonland = Schonland Research Centre for Nuclear Physics (Univ. Wits)

Note: 1. Numbers in Table refer to number of samples analysed and numbers in brackets to total number analysis done
2. Names of analysts appear in the Tables in the Appendix

Digitised by the Department of Library Services in support of open access to information, University of Pretoria, 2021

1. The deviation in Ta values is too high and these values are not used in further discussions in this study.

2. The standard deviations of Ni, U and W, when expressed as a percentage, also appear high but these are related to the low level of concentration of these elements; the actual standard deviations are in fact less than 1 ppm and the analyses are acceptable.

3. The standard deviations (expressed as per cent) of the remaining trace elements are generally below 10% and are very much the same for each of the elements, indicating that the sampling procedure in the field and subsequent sample preparation for analyses are valid.

Since tin values are critical for this study and since the levels of concentration are generally low (<10 ppm in most cases), tin was treated as a special case. The analyses by XRF were done separately after proper calibration against suitable International Standards (GA, GS-N & GSS-6) and much longer counting times were used to increase the accuracy and to lower the detection limit to 2 ppm. Samples done by XRF were also analysed by AAS in the laboratories of the Council for Geoscience and by ICP in a commercial laboratory. The correlation between the AAS and ICP results is good and the "accepted value" for the wet chemistry compare to the XRF values as follows:

Wet chem *Sn ppm*	**XRF**	**Wet chem** *Sn ppm*	**XRF**
4	3	5	4
4	10*	4	11*
6	6	4	7*
3	3	4	4
3	4	3	3
3	4	5	4
12	12	3	2
3	2	5	5
5	5	4	9*
2	3	4	5

Four samples indicated by * have relatively high XRF values and it is suspected that during the sample preparation for the wet chemistry, problems existed when the samples were brought into solution. This suspicion is based on other results obtained (not detailed here) from the two laboratories using both solid material and prepared solutions. Nevertheless, a correlation coefficient of 0,6 between the wet chemistry and XRF for all the results is reasonable and if the samples marked * are ignored, where a problem of solution may have been present, a near perfect correlation coefficient 0,95 is obtained.

After consulting the analytical staff of the laboratories at the Council for Geoscience, is was decided to use the XRF values of tin throughout this study for the following reasons:

Digitised by the Department of Library Services in support of open access to information, University of Pretoria, 2021

1. Suspected problems to bring the samples into solution are eliminated.
2. The procedures for the XRF analyses have been modified for this study to ensure the highest degree of accuracy.
3. Standards used for the XRF analyses are suitable to cover the low level of Sn concentrations.
4. The correlation coefficients, whether 0,6 or 0,95, are good.

The major and trace element analyses of all the granitoid samples and the REE analyses of selected samples are given in Table III in the Appendix.

Ankerite. Of the 350 samples collected underground, 110 contain ankerite from trace to major amounts. Of these, 48 were selected for chemical analyses based on the availability of enough ankerite, sample representation in the respective mines and suspected mono- and polyphase of ankerite mineralisation.

After its "surgical" removal from the sample by means of diamond saw cutting, the ankerite was hand-crushed to approximately minus 3 mm and screened. Individual grains of pure ankerite were hand-picked from the plus 1 mm fraction with the aid of the binocular microscope and extreme care was taken to avoid ankerite grains containing minute inclusions or intergrowths of other minerals. Depending on the purity of the ankerite and the initial amount available, between 5 and 40 g clean ankerite could be separated from the sample and was pulverised in an agate mill.

Because of difficulties encountered in fusing discs on account of the high CO_2 content, the major element analyses could not be carried out by XRF and these had to be done by means of the electron microprobe. Two grains were selected from the minus 1 mm fraction of each sample and two point analyses were done on each of the two grains, one at the edge and the other near the centre of the grain. The arithmetic mean of these four analyses is taken to represent the composition of that particular sample. The disadvantage of not using XRF is that only a very small portion of the sample is analysed by the microprobe (10 micron defocussed beam) which may not be representative. However, this is offset by doing two analyses on two grains from each sample and by the fact that 12 samples were selected from each of the four groups (C,N,P and F), discussed in the chapter on ankerite. The advantage of using the microprobe over XRF or wet chemistry, on the other hand, is apparent in cases of chemical zoning.

Digitised by the Department of Library Services in support of open access to information, University of Pretoria, 2021

The volatiles, H_2O^+, H_2O^-, CO_2 and S, were analysed in 32 samples by IRS and the results were added to those obtained by the microprobe. The totals obtained in this way vary between 97,52 and 101,33 % with an arithmetic mean of 100,13 and standard deviation of 0,96. For the calculations of the stoichiometric formulae and the mole percentages, these totals were normalised to 100% and the analyses recalculated accordingly, placing equal reliance on both microprobe and IRS results.

Minor quantities of SiO_2 and Al_2O_3 were detected in the ankerite; sodium and potassium were not determined. One ankerite sample was dissolved in 6N hot HCl for 20 minutes and the residue, after centrifuging, analysed by XRD. The presence of quartz and sericite was detected, but the amount of impurities is estimated to be no more than 0,2% and less than 0,05% in the majority of the samples.

For the trace element analyses by XRF, only 20 of the 48 samples had enough material for a ± 20 g powder briquette. An XRF scan for all the elements heavier than boron indicated that the following elements are contained as traces in ankerite: Cu, Ni, Sc, Sr, V, Y and Zn and quantitative analyses for these were done on a sequential XRF spectrometer. The presence of Sn is reflected in a few analyses but is regarded as due to minute cassiterite inclusions not seen during the hand cleaning of the ankerite.

An additional 12 samples of the original 48 selected, were analysed by ICP for trace elements. Finally, eight samples of those done by XRF were also analysed by this method, as a control on the quality on both means of analyses, by the two laboratories. The analytical results are given in Tables IV a - d of the Appendix.

For the Pb-Pb isotope determinations, 59 samples containing ankerite were selected, using the same criteria as for the selection of the samples for the chemical analyses. The samples were hand crushed and clean, fresh ankerite grains were hand-picked and pulverised in an agate mortar. Approximately 150 mg powder was dissolved with warm 6N HCl and because of the ease of solubility, all the sample was dissolved after 20-30 minutes. In a few samples, an extremely small quantity of undissolved sample, originating from minute impurities, were centrifuged off. After evaporating the solution, the

Digitised by the Department of Library Services in support of open access to information, University of Pretoria, 2021

residue was dissolved in 0,8N HBr, passed through an anion exchange resin and the Pb fraction eluted with 6N HCl. The separated fraction was further purified electrolytically and the final yield loaded onto a rhenium filament and covered with silica gel. Runs were carried out on a Finnigan MAT 261 multicollector mass spectrometer and mass fractionation corrections done. The data were regressed using the GEODATE software package developed by Eglington and Harmer (1989). The Pb-Pb isotope results are given in Tables V a-d of the Appendix.

Tourmaline. A total of 16 samples from the A and NAD Mines were selected for tourmaline analyses. The tourmaline grains are too small to permit hand picking of individual grains until a sufficient amount was collected, and electron microprobing of grains in polished thin sections had to be done. The main advantage of using the microprobe, is that because all the tourmalines are optically zoned, several analyses could be carried out on each grain at several positions ranging from the core to the rim. At least two grains of each sample were analysed. The disadvantage of using the microprobe is that boron and trace elements cannot be analysed for, and the analyses are only partial on account of the substantial boron component. Approximately 250 individual analysis were done on the Rooiberg tourmalines and 33 on a tourmaline in a pegmatite from another locality. Only the results of the analyses of which the probed position in relation to the zoning is absolutely certain, i.e. grains orientated perpendicular to the c-axis (or nearly so), are given in Table VI of the Appendix.

Cassiterite. Thirty two cassiterite samples from the A, NAD and C Mines and four from other localities were crushed and clean cassiterite grains hand-picked for trace element analyses (including some REE) by means of Instrumental Neutron Activation Analysis. The samples from the A Mine contained cassiterite from both suspected cassiterite-1 and -2 mineralising phases. The method used at the Schonland Research Centre is described by Erasmus *et al*. (1977) and entails that the samples are irradiated with an neutron flux in the Safari I reactor at Pelindaba. Counting was done with a gamma ray detector at intervals determined by the decay periods of the elements analysed for. The analytical results are given in Table VII of the Appendix.

Digitised by the Department of Library Services in support of open access to information, University of Pretoria, 2021

6. GEOLOGICAL SETTING

The Rooiberg tin-field is located in the north-eastern part of a roughly triangular block of sediments and subordinate volcanics of the Transvaal Supergroup referred to as the Rooiberg Fragment. These rocks are conformably overlain by rhyolite (commonly called felsite) and were intruded along the flanks by granophyre and granites (Fig. 4).

Except for the granites, all these rock types have received considerable attention (Recknagel, 1908; Boardman, 1946; Leube and Stumpfl, 1963; Labuschagne, 1970a; Iannello, 1971; Stear, 1977a; Phillips, 1982; Rozendaal *et al.*, 1986; Walraven, 1987; Richards and Eriksson, 1988; Eriksson *et al.*, 1988 & 1991; Du Plessis and Walraven, 1990; Rozendaal *et al.* 1995a & b; Schweitzer *et al.* 1995) but it is necessary to highlight a few salient features. The granites are dealt with in detail since the work done to date is not adequate and since they are evaluated as the possible source for the ore-forming fluids.

6.1 The Leeuwpoort Formation of the Pretoria Group

The largest part of the Rooiberg Fragment is occupied by a 1 400 m thick succession of upward-fining, multi-coloured "quartzite" to which the name "arkosite" was given to accommodate the high feldspar content. The arkosite becomes more argillaceous towards the top and grades into shaly arkose and finally shale. The shaly arkose and shale attain a thickness of ± 280 m. SACS (1980) has accepted the terms Boschoffsberg Quartzite and Blaauwbank Shale Members, as proposed by Stear (1977a), as a lower and upper subdivision of the Leeuwpoort Formation.

6.2 The Smelterskop Formation of the Pretoria Group

A ± 300 m thick succession of alternating feldspathic quartzite and tuffaceous shale with interbedded andesitic lavas overlies the Leeuwpoort Formation. In places, a disconformable relationship between the Smelterskop and Leeuwpoort Formations is recognised. The outcrop pattern of the rocks of the Smelterskop Formation delineates the two limbs of an open anticline (Fig. 4).

Digitised by the Department of Library Services in support of open access to information, University of Pretoria, 2021

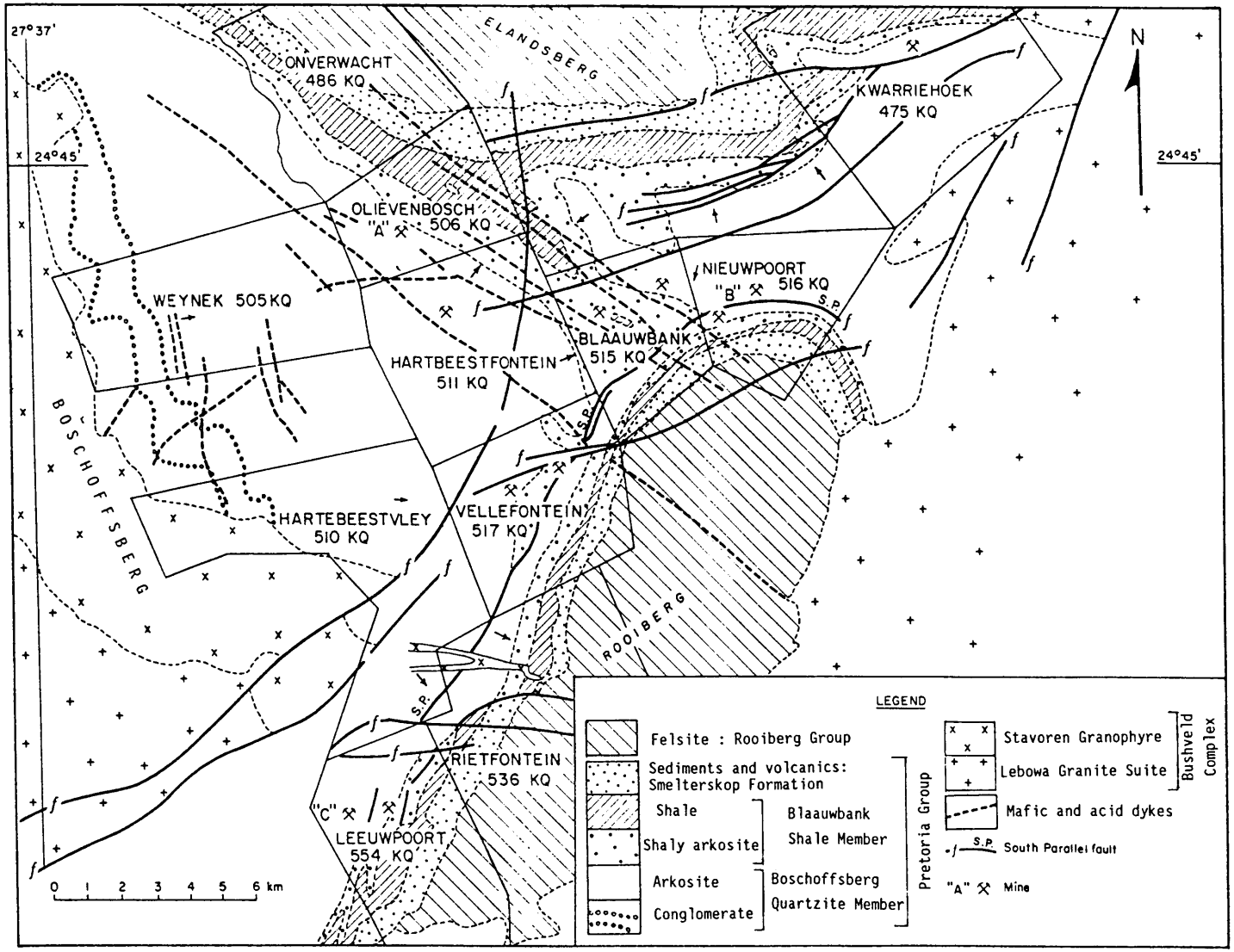

Fig. 4 - General geology of the Rooiberg Fragment.
(After Labuschagne, 1970a)

Digitised by the Department of Library Services in support of open access to information, University of Pretoria, 2021

Issues which are still debated and are as yet not clarified include:

1. The anomalous thickness of the Boschoffsberg Quartzite Member, compared to other quartzite units of the Transvaal Supergroup.
2. The high feldspar content (up to 80 % modal composition) of the arkosite.
3. The stratigraphic position and correlates of the Leeuwpoort and Smelterskop Formations.

The author originally held the view that the feldspar in the arkosite was deposited as a primary constituent (Labuschagne, 1970a) but at present concurs with the recent views of Rozendaal *et al.* (1995b) that at least some of the feldspar was due to subsequent feldspathisation. Rozendaal *et al.* (1995b) indicated that the upper 500 - 600 m of the sedimentary sequence were reconstituted by pervasive sodic, potassic and sericitic (increased Al_2O_3) alteration.

As far as the stratigraphic position is concerned, the debate centres on whether the Rooiberg Fragment represents a protobasin formed during early Transvaal sedimentation or whether it is an uplifted portion, now forming a detached roof pendant. Cognizance must be taken of the disconformable relationship which is present in places between the Leeuwpoort and Smelterskop Formations, and it can be speculated that the Leeuwpoort Formation has been deposited in a protobasin, whereas the Smelterskop Formation may have only been deposited towards the closing stages of Transvaal sedimentation.

6.3 The Kwaggasnek and Schrikkloof Formations of the Rooiberg Group

Rhyolites (felsites) of the Rooiberg Group cap the Elandsberg and the Rooiberg proper in the north and the east of the Rooiberg Fragment respectively. The rhyolites were more resistant to weathering than the sediments, so that they form these two mountains. (The name *Rooiberg* has been derived from the predominantly brick-red colour of the rhyolites).

The author mapped 64 square km of the Elandsberg as part of an earlier study and reported four different mappable felsic units (Labuschagne, 1970a). The rhyolites of the Rooiberg Group have subsequently received a fair amount of

Digitised by the Department of Library Services in support of open access to information, University of Pretoria, 2021

attention and at present those which comprise the Elandsberg are correlated with the Kwaggasnek Formation and those of the Rooiberg proper are correlated with the Schrikkloof Formation in the Loskop Dam area (Schweitzer *et al.* 1995).

Absolute age determinations commonly give unreliable results, probably due to hydrothermal alteration by fluids emanating from the granites and causing isotopic disturbances. However, some sample suites gave ages of 2070 Ma for the Rooiberg Group (Harmer and Farrow, 1995), subsequently confirmed by the 2061 ± 2 Ma and 2062 ± 2 Ma single zircon evaporation dates (Walraven, 1997). These dates are acceptable on the basis of field relations elsewhere in the Bushveld Complex. Accordingly, onset of Rooiberg volcanism preceded the magmatism of the Rustenburg Layered Suite, but some radiometric ages indicate that part of the Rooiberg volcanism might have been temporally synchronous with the Rustenburg Layered Suite (Hatton and Schweitzer, 1995).

6.4 The Stavoren Granophyre of the Rashoop Granophyre Suite

The main body of the Stavoren Granophyre is located west of the Rooiberg Fragment between the basal portion of the Boschoffsberg Quartzite Member and the granites further west and south. Thinner bodies of granophyre are also present north and east of the Rooiberg Fragment between the rocks of the Rooiberg Fragment and the granites. The main body caps the Boschoffsberg itself, which owes its topographic relief to the fact that the granophyre is more resistant to weathering than the arkosite and the granites. A clearly intrusive relationship is recognised between the granophyre and arkosite: Thin but persistent conglomerate bands near the base of the Boschoffsberg Quartzite Member terminates abruptly against a tongue of granophyre. The contact between the arkosite and granophyre is sharp and metasomatic alteration of the arkosite is evident over a thickness of a few metres along the contact.
Walraven (1987) considered that the Rashoop Granophyre Suite belongs to a phase of shallow magmatic intrusion and volcanism which preceded the main intrusive phase (Rustenburg Layered Suite) of the Bushveld Complex.

6.5 The Lebowa Granite Suite

The rocks of the Rooiberg Fragment, the granophyre and the rhyolites have been

Digitised by the Department of Library Services in support of open access to information, University of Pretoria, 2021

intruded by granites and four types - Nebo, Klipkloof, granophyric and Bobbejaankop - have been recognised and are discussed in the next chapter.

7. THE GRANITES

7.1 Introduction

Iannello (1970) mapped large areas of the granites west and east of Rooiberg. While his mapping in the west is very good, his work in the east could not be used for this study, mainly because of the fact that he did not recognise that these were in fact the same granites as in the west. Crocker (1976) mapped large tracts of ground on a regional scale which included the granites east of Rooiberg. While his work may be perfectly acceptable on a regional scale, it is inadequate for the scale required in this study.

Both Iannello and Crocker introduced new names for most of the granite types. Those assigned by Iannello to granites west of Rooiberg differ from their apparent counterparts in the east and vice versa. This confusion is further aggravated by the fact that the names assigned by Crocker to some granites differ from those given by Iannello for the same granites. Consequently, additional mapping of the granites was deemed necessary.

Despite the fact that, with one or two exceptions, all authors who have published on the Rooiberg tin-field, subscribe in one way or another to a primary granitic source for the ore-forming fluids (Leube and Stumpfl, 1963; Labuschagne, 1970a and b; Lenthall, 1972; Hunter, 1973; Stear 1977a and b; Dinsdale, 1982), no one, with the exception of perhaps Ollila (1981), used geochemical data to substantiate this. The available geochemical data on the granites are, in fact, so limited that they are almost meaningless to validate any conclusions regarding a granitic source for the ore-forming fluids. Only five analyses were done by Iannello (1970), 13 by Phillips (1982) and a few by Fourie (1968) but these are certainly not representative of the granites as a whole. Moreover, the number of elements analysed for by these authors were also limited.

7.2 Field distribution

The distribution of the granite types in the areas west and east of Rooiberg, as demarcated in Fig. 1, is shown in Figs. 5 and 6.

Digitised by the Department of Library Services in support of open access to information, University of Pretoria, 2021

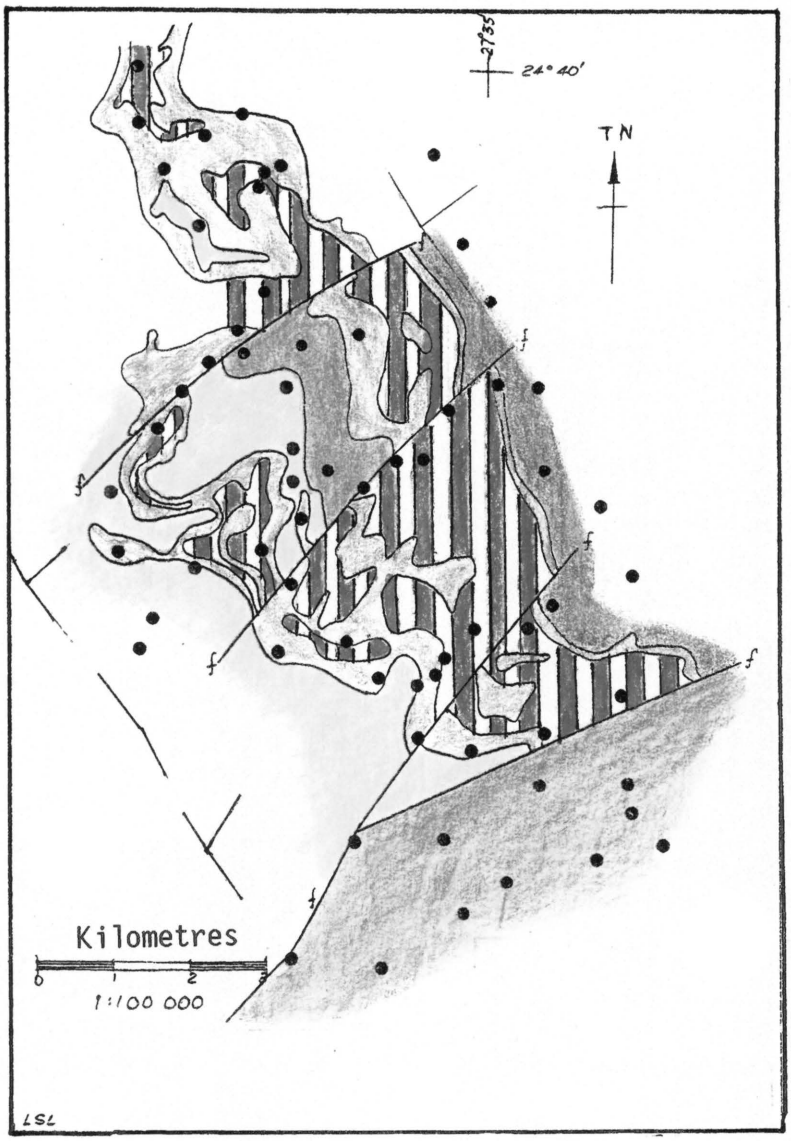

LEGEND

Karoo sediments

Bobbejaankop Granite
Granophyric granite
Klipkloof Granite
Nebo Granite
] Lebowa Granite Suite

Granophyre, felsite, sediments

Dots = Field stations
Faint broken lines = farm boundaries

Fig 5 - Geological map of the granites west of Rooiberg. Adopted from Iannello (1970) with modifications by the author.

Digitised by the Department of Library Services in support of open access to information, University of Pretoria, 2021

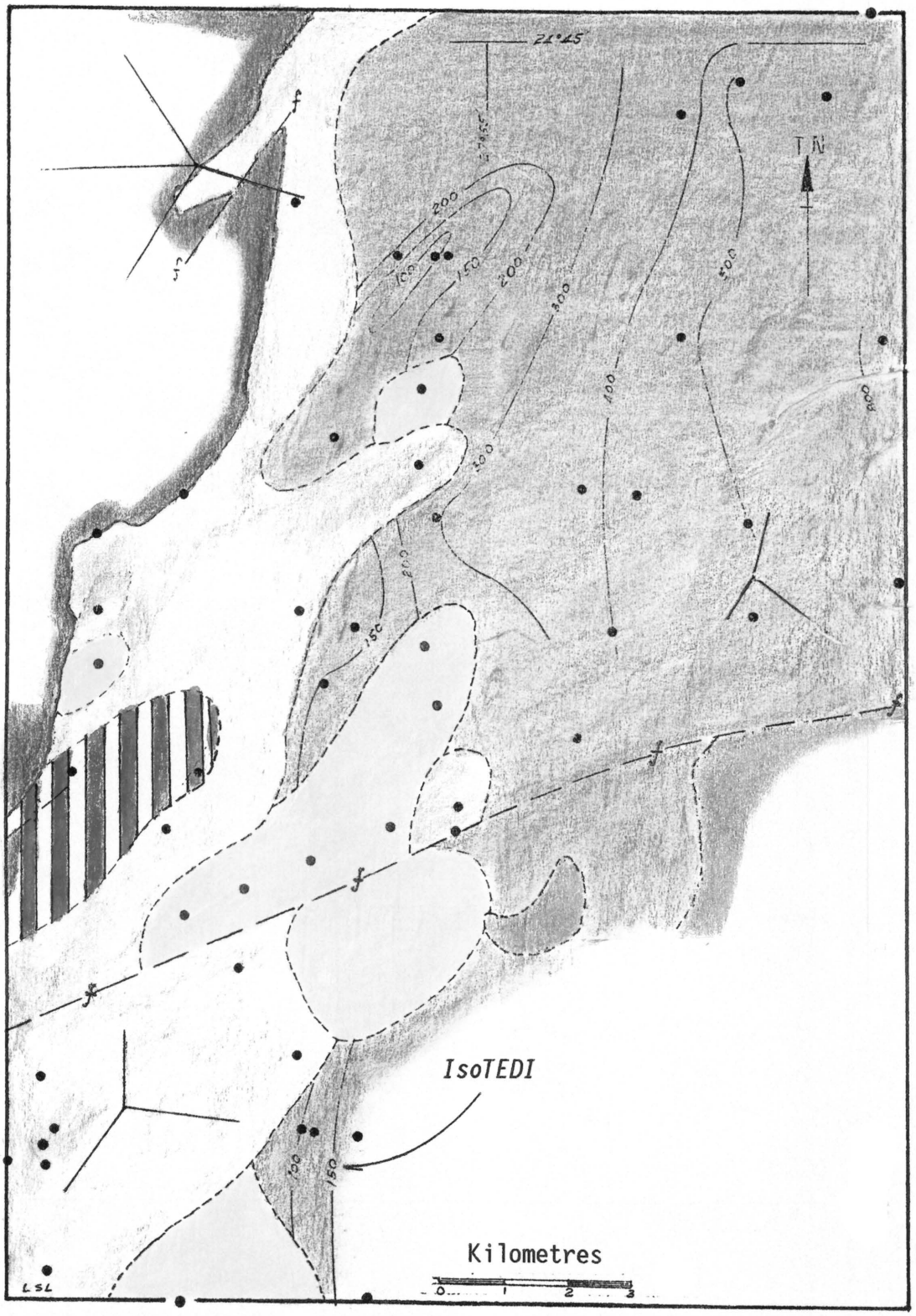

LEGEND - Same as Fig. 5 - p. 29

Fig. 6 - Map showing the distribution of the granites east of Rooiberg.

Digitised by the Department of Library Services in support of open access to information, University of Pretoria, 2021

The designation Nebo and Bobbejaankop Granite was done soon after the field work commenced but correlation with the Klipkloof Granite was done only after all the relevant information such as petrography, analytical data, etc. became available.

Fig. 5, showing the distribution of the granites in the west, is based largely on Iannello's map (1970). Relatively minor modifications to this map were required: The distribution of the Klipkloof Granite was added, the positions of some geological contacts shifted according to what is believed to be faults and the map as a whole was somewhat simplified.

In the east, the existing maps were found to be totally unsuitable and Fig. 6 was compiled to show the distribution of the granite types only. The IsoTEDIs -- lines drawn through points having a similar **T**race **E**lement **D**ifferentiation **I**ndex or TEDI -- were added later. The term TEDI has been coined by Walraven (1986) and is calculated as (BaxSr)/Rb. This serves as a useful index to assess the degree of magmatic differentiation.

7.3 Petrography and correlation

The *Nebo Granite* is the predominant granite in the area adjoining the Rooiberg tin-field. It is coarse-grained, mostly pink-red but also grey, and consists of equigranular quartz, feldspars and mafic minerals. The feldspars are orthoclase, plagioclase, perthite and antiperthite. The mafic minerals are mainly biotite, amphibole or both; chlorite is present as an alteration product of biotite.

The name *Klipkloof Granite* was assigned to a granite which, during the field programme, was simply named type DE. In both study areas, this granite occurs between the granophyric granite and Nebo Granite. Correlation of this granite with the Klipkloof Granite at the type locality is based on the following:

(1) Porphyritic character. In the study area, the granite is medium- to coarse-grained and porphyritic. SACS (1980) characterised the Klipkloof Granite as medium- to fine-grained in the type area. In the Groblersdal area, however, Kleemann and Twist (1989) recognised a medium- to coarse-grained variety as well as "other types of Klipkloof Granite" including a porphyritic variety.

Digitised by the Department of Library Services in support of open access to information, University of Pretoria, 2021

(2) Mineralogy. Biotite is the only mafic mineral present which contrasts with the Nebo Granite which contains amphibole in addition to biotite. Kleemann and Twist (1989) recognised the similarities in the mineralogy between the Nebo and Klipkloof Granites except for amphibole which they have found to be absent in the Klipkloof Granite.

(3) Geochemistry. The analytical data indicate that the Klipkloof Granite in the Rooiberg area is magmatically more differentiated than the Nebo Granite. Kleemann and Twist (1989) argued that while the Klipkloof Granite in the Groblersdal area is not a simple magmatic differentiate of the Nebo Granite, these two granites nevertheless form closely related suites and they showed that the Klipkloof Granite is magmatically more differentiated.

In the west, a *granophyric granite* occurs extensively below the main body of Stavoren Granophyre and in the east it is confined to an area between the rhyolites of the Rooiberg Group and the Nebo Granite. The ubiquitous granophyric intergrowths between quartz and feldspar are in many places so well developed that there is texturally little difference from the Stavoren Granophyre (Figs. 7 and 8). Chemically, however, the difference is pronounced as shown by the variation diagram (Fig. 9).

Granophyric textures in the *Lease Granite* in the Zaaiplaats area are common but not always present (Coetzee, 1986). Pegmatites are associated with the granophyric granite at Rooiberg and a thin pegmatite is as a rule developed along the contact with the Rashoop Granophyre (Iannello, 1970). At Zaaiplaats the contact between the Lease Granite and the granophyre is commonly marked by a coarse quartz-feldspar pegmatite (Von Gruenewaldt & Strydom, 1985). Correlation of the granophyric granite with the Lease Granite appears feasible and fits chronologically as well. In this study, however, it is preferred not to correlate the granophyric granite with the Lease Granite and it is simply referred to as *granophyric granite.*

The *Bobbejaankop Granite* is well developed in the western study area where it occupies a position directly below the Stavoren Granophyre, but a thin band of the granophyric granite is always present between the two. In the eastern study area it is poorly represented on surface and was in fact only recognised at three field stations.

Digitised by the Department of Library Services in support of open access to information, University of Pretoria, 2021

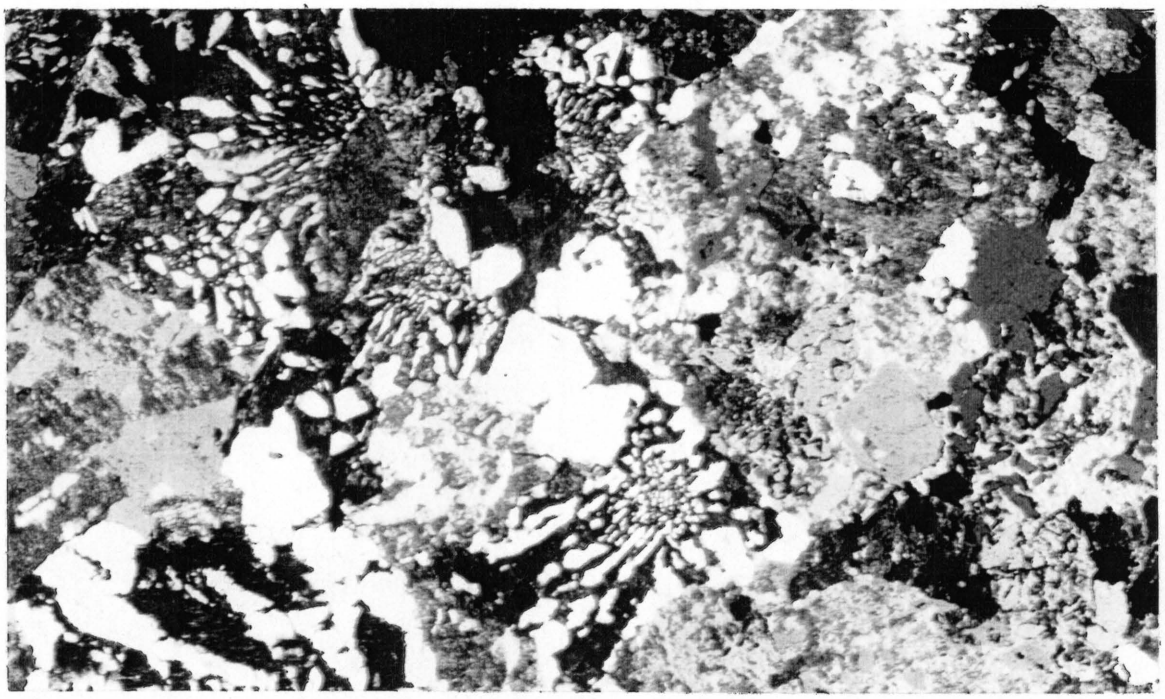

Fig. 7 - Granophyric texture in Stavoren Granophyre.
+N 30X Sample 501LO

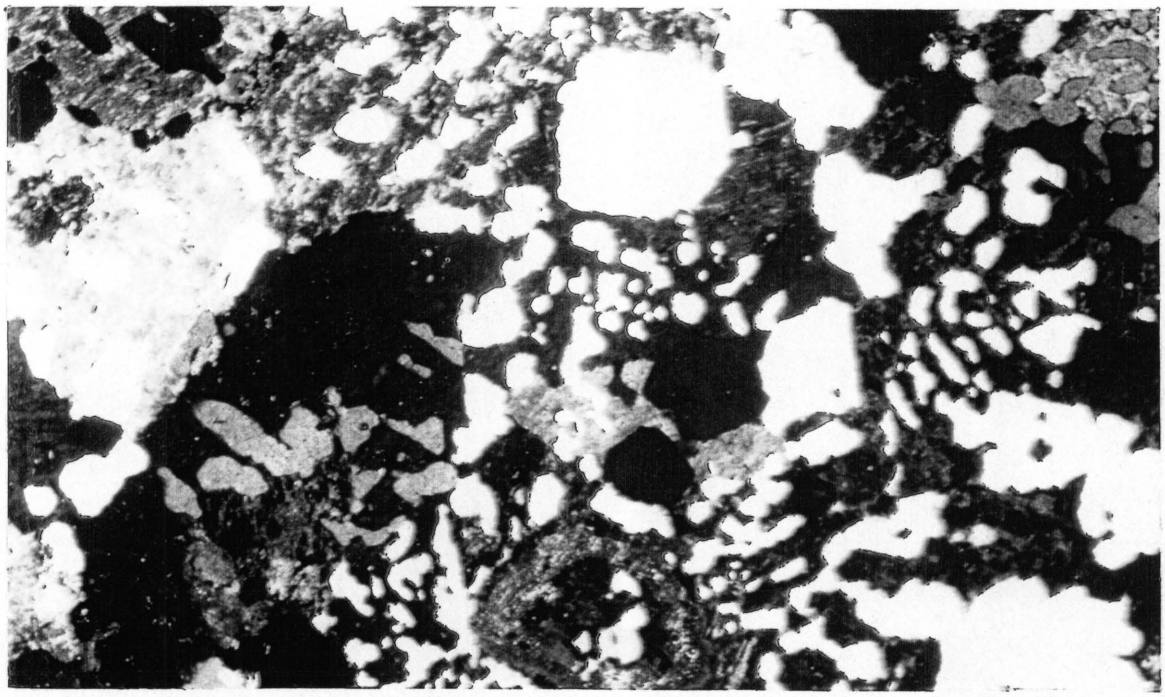

Fig. 8 - Granophyric texture in granophyric granite.
The texture is coarser than that in the Stavoren Granophyre and is less radiating with respect to early formed feldspar.

+N 30X Sample 522LO

Digitised by the Department of Library Services in support of open access to information, University of Pretoria, 2021

The Bobbejaankop Granite is readily recognised in hand-specimen by its intense red to brick-red colour. It consists of quartz, orthoclase, plagioclase, perthite and antiperthite and biotite. Muscovite is present in some areas.

The granites at 14 field stations could *not be classed* in any of the above types. Of these, the granites at five are highly altered, at three the granites are too oxidised and at six the granites could not be classified although they were quite fresh. This latter group represents less than 5% of the total samples. The oxidised samples are all from the eastern study area where weathering is generally deep, but they probably belong to the Nebo Granite. The altered samples are from both areas; the two from the west are located close to a major fault but the three in the east do not seem to be affected by a common structural or lithological control.

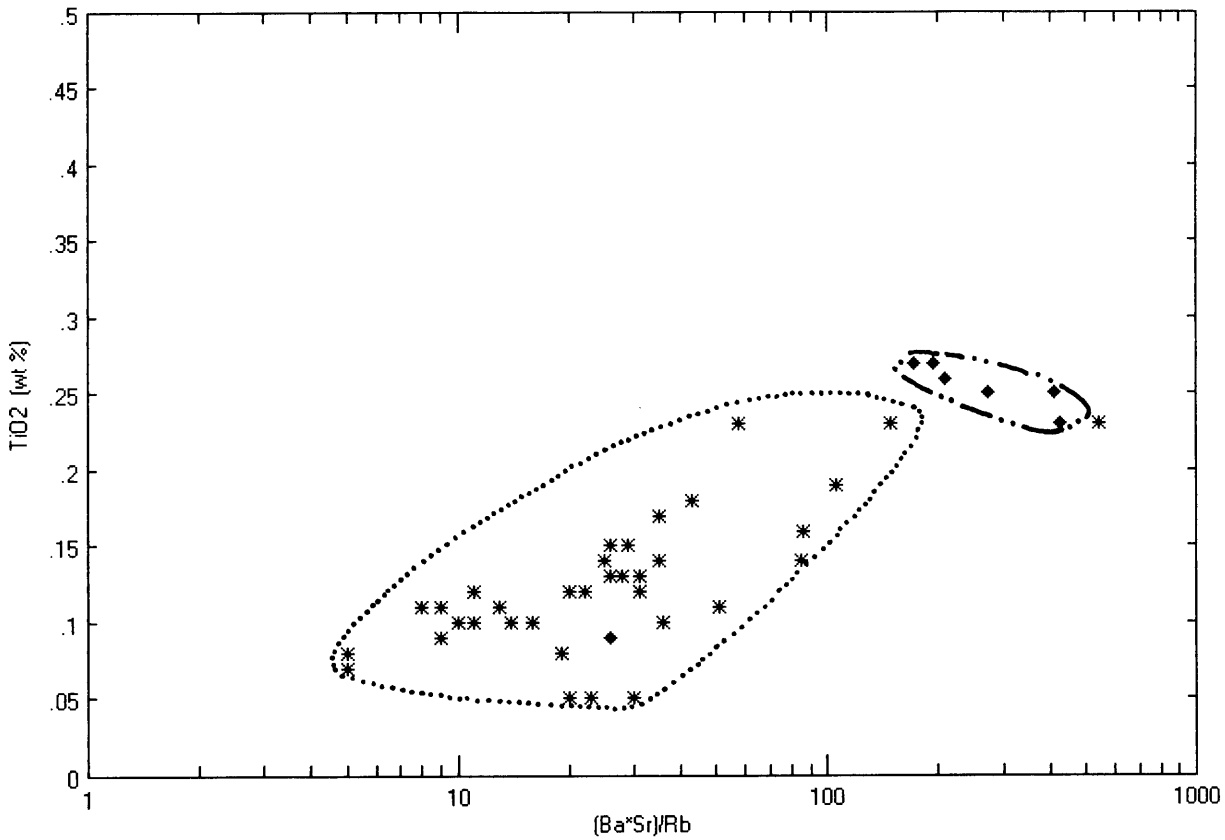

Fig. 9 - Variation diagram of (BaXSr)/Rb v TiO_2 of Stavoren Granophyre (diamond) and granophyric granite (asterisk). The Stavoren Granophyre is geochemically less evolved than the granophyric granite.

Digitised by the Department of Library Services in support of open access to information, University of Pretoria, 2021

7.4 Geochemical characterisation

The hand-specimens, petrography and geochemistry indicate that there is neither a visual nor a chemical difference between individual granite types from the west and the east of the Rooiberg tin-field and the analytical data (Table III - Appendix) from these two areas may thus be pooled.

Major element variation. The greatest relative variations in the major elements are in decreasing order: TiO_2 - FeO - MgO - Fe_2O_3 - CaO - P_2O_5. The Fe_2O_3 and FeO contents (Fe^{3+} and Fe^{2+}), particulary their relative abundances, are influenced by oxygen fugacity and these two are not considered in the discussions on variations caused by magmatic differentiation. This leaves TiO_2, MgO, CaO and P_2O_5 to gauge the geochemical variation in the granite types.

The trace elements Ba, Sr and Rb are useful indicators to assess the degree of magmatic differentiation in the Bushveld granites (Walraven, 1986; Kleemann and Twist, 1989; McCarthy and Hasty, 1976 and others). In turn, these three elements and TEDI - (BaxSr)/Rb - can also be used to assess the variation in the major elements as a result of magmatic differentiation.

TiO_2. The variation diagrams are given by Figs. 10 and 11. The fields of the four granite types overlap but the general trend is from the least differentiated Nebo Granite (high TiO_2 and TEDI) to the most differentiated Bobbejaankop Granite (low TiO_2 and TEDI).

CaO. A medium-strong trend is recognised in the variation diagrams between CaO and Sr (Fig. 12) and a weak trend between CaO and Rb (not shown). The magmatic differentiation is similar to that expressed by the variation diagrams of TiO_2 v TEDI.

P_2O_5. A medium-strong trend is recognised between the granites with a decrease in the P_2O_5 content with increasing differentiation (not shown) which conforms with the general differentiation trend as above.

MgO. No trend is recognised *between* the granites but of significance is the variation in MgO *within* the granites. In the case of the Nebo Granite, no

Digitised by the Department of Library Services in support of open access to information, University of Pretoria, 2021

trend exists (Fig. 13) whereas a weak trend is discerned in the Bobbejaankop Granite (Fig. 14). The trends in the Klipkloof Granite and the granophyric granite (not shown) are slightly weaker than that of the Bobbejaankop Granite.

The variation of the TiO_2, CaO and P_2O_5 contents against the trace elements indicate a magmatic differentiation trend of

Nebo -> Klipkloof -> granophyric -> Bobbejaankop Granite

Mineralogy. The decrease in TiO_2 with increasing magmatic differentiation may be due to the fact that more TiO_2 is accommodated by biotite (and amphibole) in the geochemically lesser evolved granites. The Ab/An ratios of the plagioclase were not determined, but it is assumed that the more Ca-rich varieties are confined to the lesser evolved granites. Strontium is probably accommodated in the plagioclase and Rb in the orthoclase, as Sr and TiO_2 decrease as Rb increases.

Apatite is the main mineral to accommodate P_2O_5 and a decrease of this mineral with increasing magmatic differentiation is inferred.

Trace element variation (excluding REE).

Regression analysis of the trace elements shows that the highest correlation coefficients occur between Ba, Sr and Rb - the same elements used in TEDI in the variation diagrams of the major elements above. The TEDI was used to determine the behaviour of the trace elements in (1) all granites and (2) the Bobbejaankop Granite only and the results are summarised in Table 2.

Apart from Ba, Sr and Rb, only Ga and Nb show a strong trend due to magmatic differentiation. Another three, namely Sn, Th and V have a weak but recognisable trend.

For clarity, only the fields occupied by the data points of the Nebo and Bobbejaankop Granites are shown in Figs. 15 and 16. A magmatic differentiation trend from Nebo -> Bobbejaankop Granite is recognised with the data points of the Klipkloof Granite and the granophyric granite occupying positions somewhere between these two. The arithmetic averages (Table 3) aided in establishing the overall trend.

Digitised by the Department of Library Services in support of open access to information, University of Pretoria, 2021

Table 2 - Summary of the trends of TEDI vs various trace elements in all the granite types and in the Bobbejaankop Granite

	All Granites		**Bobbejaankop Granite**	
TEDI	*Trend:*	*Increase/ Decrease with increasing magmatic differentiation*	*Trend:*	*Increase/ Decrease with increasing magmatic differentiation*
Ba	(Strong)	(Decrease)	(Medium)	(Decrease)
B	No	-	Weak	Increase
Cr	No	-	Medium	Decrease
Cu	No	-	No	-
F	No	-	Medium	Increase
Ga	Strong *	Increase	Medium	Increase
Li	No	-	No	-
Mo	No	-	No	-
Nb	Strong *	Increase	Weak	Increase
Ni	No	-	Medium	Increase
Pb	No	-	No	-
Rb	(Strong)	(Increase)	(Weak)	(Increase)
Sc	No	-	No	-
Sn	Weak	Increase	No	-
Sr	(Strong)	(Decrease)	(Strong)	(Decrease)
Th	Weak	Increase	Weak	Increase
U	No	-	Weak	Increase
V	Weak	Decrease	No	-
W	No	-	Weak	Decrease
Y	No	-	Medium	Increase
Zn	No	-	Weak	Decrease
Zr	No	-	No	-

* Shown as Figures 15 and 16

Table 3 - Arithmetic average of Ga, Nb, Rb and Sr in the granite types

	Arithmetic average			
Granite	*Ga*	*Nb*	*Rb*	*Sr*
Nebo	23,9	25,2	206	40,2
Klipkloof	25,7	30,8	238	18,1
Granophyric	26,2	37,9	270	16,4
Bobbejaankop	26,1	41,1	298	11,2

Digitised by the Department of Library Services in support of open access to information, University of Pretoria, 2021

Except for a small discrepancy in the Ga values in the granophyric granite and Bobbejaankop Granite, which are in any case close to each other, the magmatic differentiation trend is the same as established with the major elements and is

Nebo -> Klipkloof -> granophyric -> Bobbejaankop Granite

Table 2 indicates that the trend in the distribution for the majority of the trace elements is more strongly developed *in* the more evolved Bobbejaankop Granite than *between* the four granites. Elements which became concentrated during the final stages of magmatic differentiation in the Bobbejaankop Granite are B, F, Nb, Ni, Rb, Th, U, and Y. A decrease occurs in Cr, Sr, W and Zn. It should be noted that Sn does not show a trend.

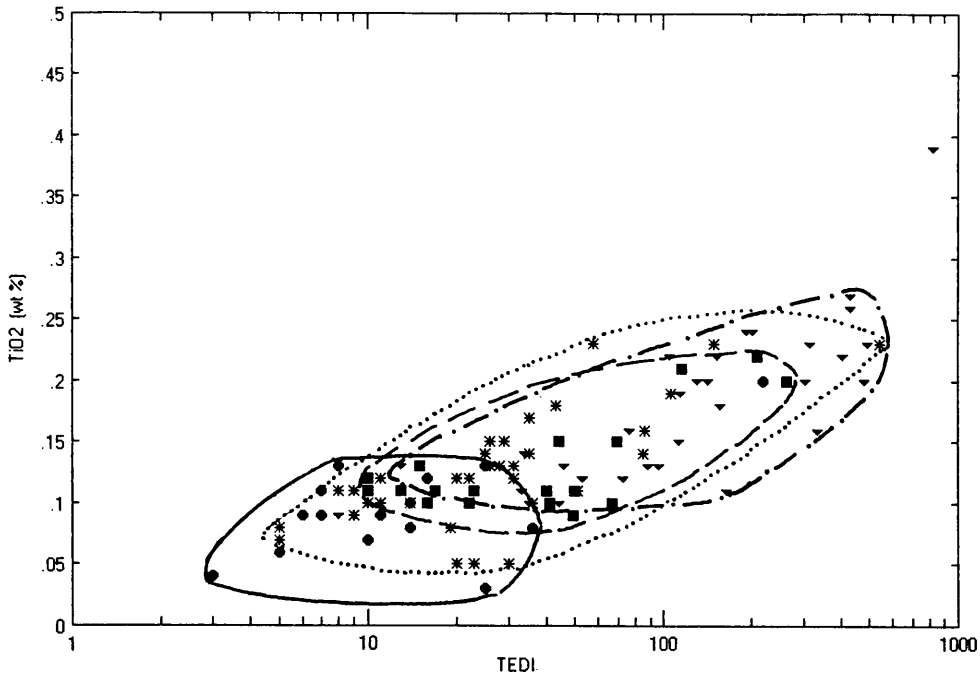

Fig. 10 - Variation diagram of TEDI v TiO2. Nebo Granite (triangle - dot-dash line), Klipkloof Granite (square - broken line), granophyric granite (asterisk - dotted line) and Bobbejaankop Granite (circle - solid line). Low values of TEDI are indicative of a higher degree of differentiation.

Digitised by the Department of Library Services in support of open access to information, University of Pretoria, 2021

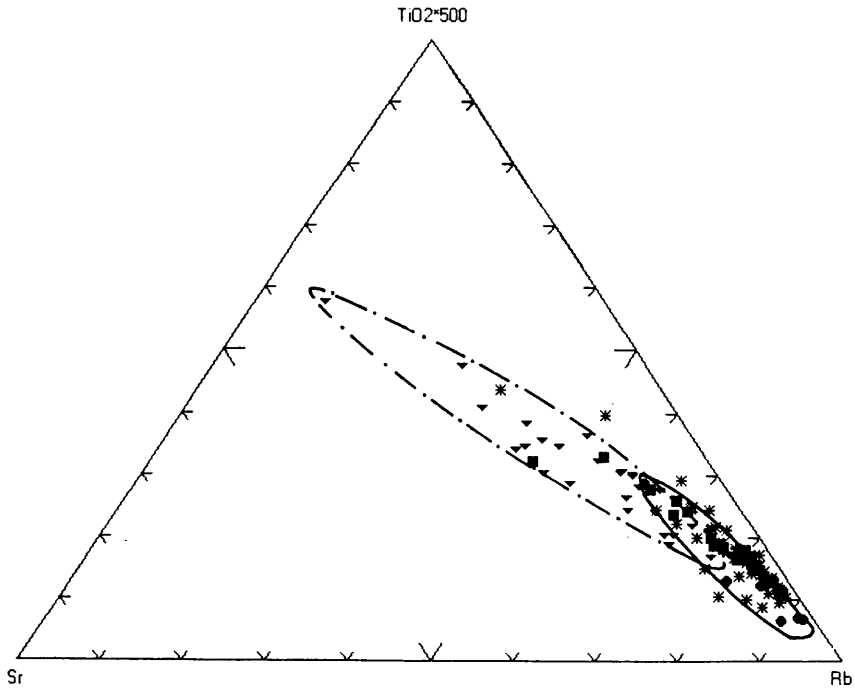

Fig. 11 - Ternary diagram: TiO2 (%X500) - Sr (ppm) - Rb (ppm). Symbols as in Fig. 10. For clarity only the fields of Nebo Granite (dot- dash-line) and Bobbejaankop Granite (solid line) are shown. Higher Rb and lower Sr and TiO_2 values indicate that the Bobbejaankop Granite is the most diffentiated of the four granite types.

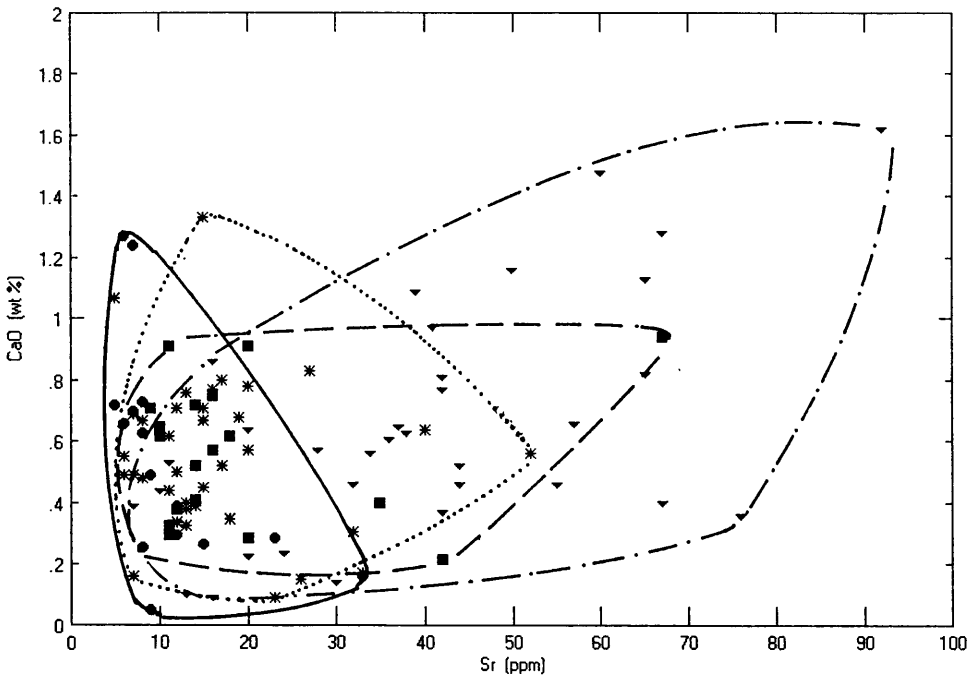

Fig. 12 - Variation diagram of Sr v CaO. Symbols and lines as in Fig. 10. A medium-strong differentiation trend is recognised with the Bobbejaankop Granite containing the lowest Sr values.

Digitised by the Department of Library Services in support of open access to information, University of Pretoria, 2021

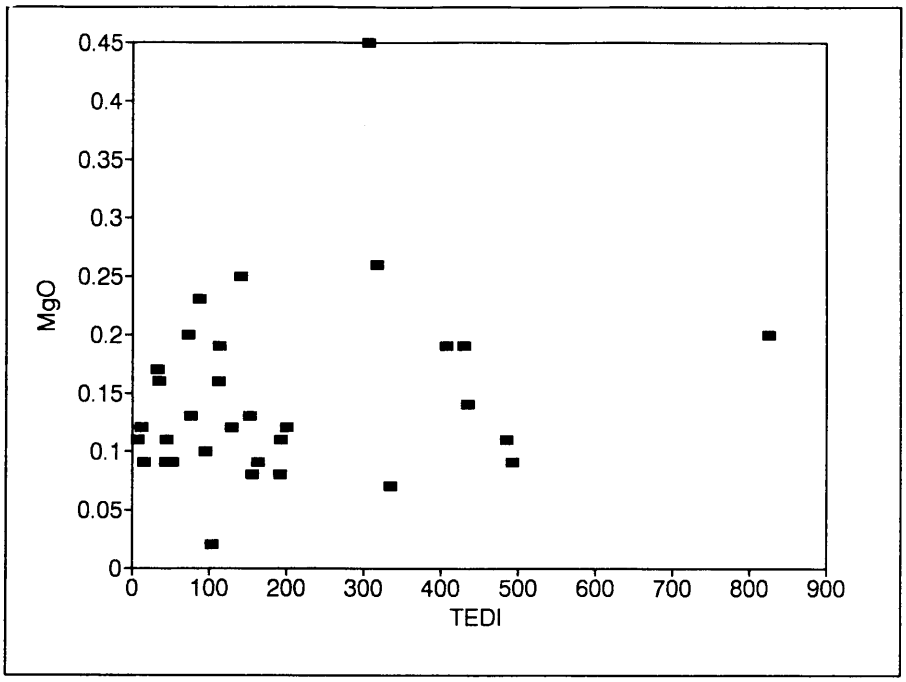

Fig. 13 - Variation diagram of TEDI v MgO for the Nebo Granite. No trend is recognised indicating that the Mg content was not affected during emplacement of the Nebo Granite.

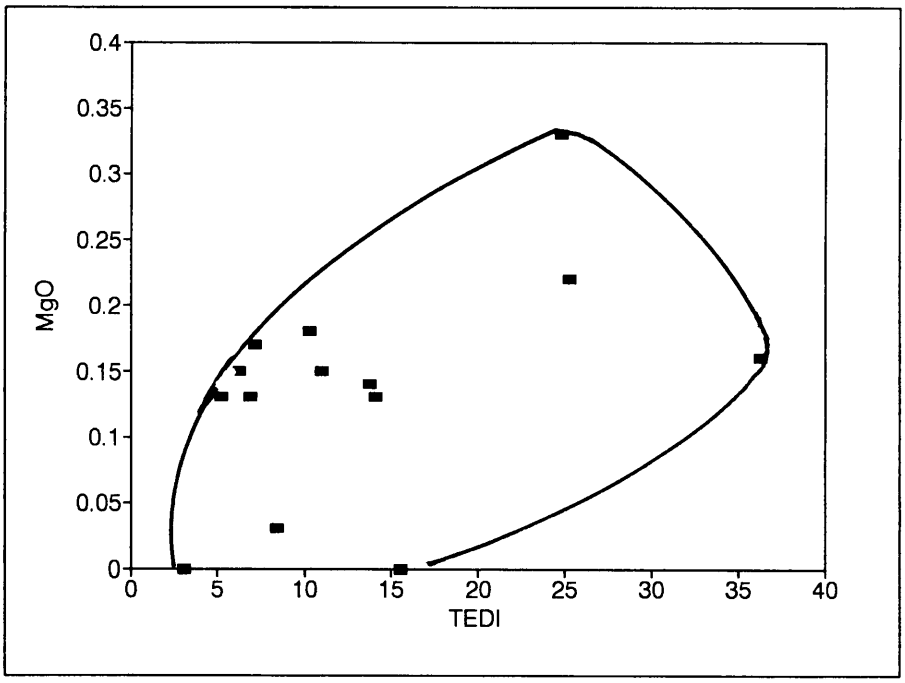

Fig. 14 - Variation diagram of TEDI v MgO for the Bobbejaankop Granite. A weak trend indicates that the Mg content was affected during emplacement of the Bobbejaankop Granite

Digitised by the Department of Library Services in support of open access to information, University of Pretoria, 2021

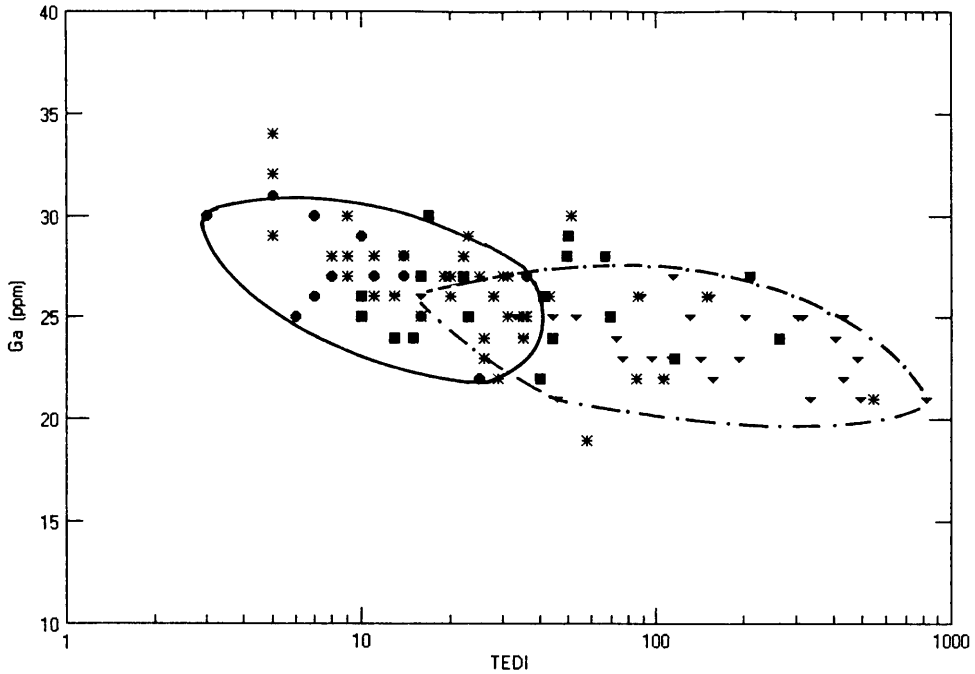

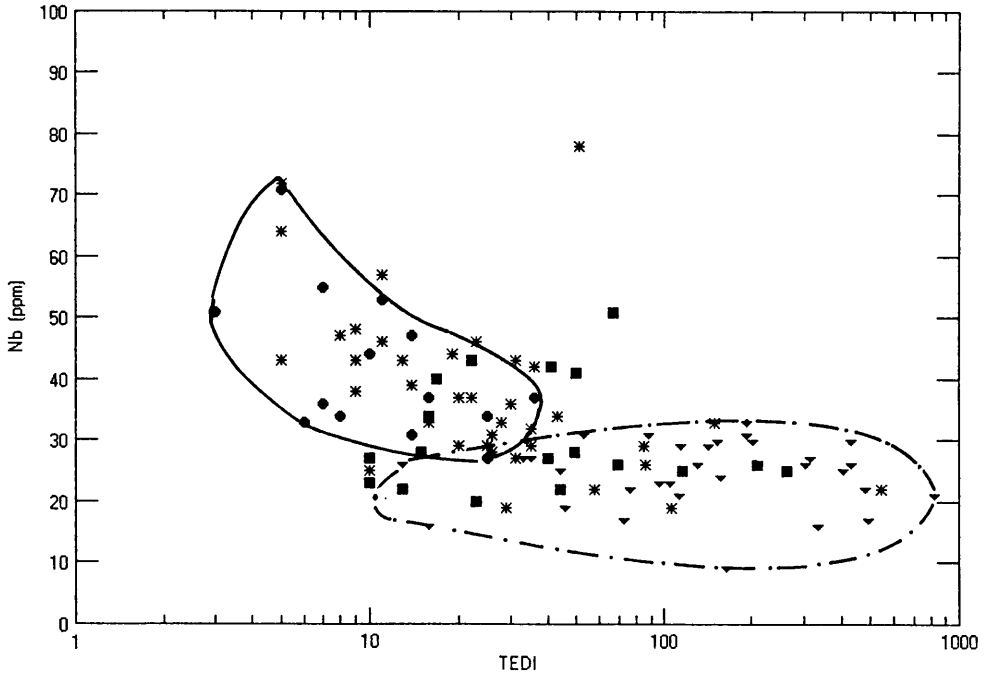

Figs. 15 (above) and 16 (below) - Variation diagrams of TEDI v Ga and TEDI v Nb. Symbols and lines as in Fig. 10. For clarity only the fields of the Nebo Granite (dot-dash line) and Bobbejaankop Granite (solid line) are shown. Both Ga and Nb values increase with decreasing TEDI.

Digitised by the Department of Library Services in support of open access to information, University of Pretoria, 2021

Rare Earth Element variation. The REE results of 48 samples were averaged for each of the granite types and normalised using C1 chondrite and primitive mantle analytical data of Sun and McDonough (1989). The chondrite and primitive mantle normalised data show exactly the same trend and only the distribution of the chondrite normalised data is given in Figs. 17 and 18. (Artificial Ho values were calculated by averaging the Dy and Er values since the analytical method used does not discriminate between Ho and Y and a combined value only of these two is given).

Significant variations recognised are (1) increasing negative Eu anomaly from Nebo -> Bobbejaankop Granite and (2) a relative enrichment in the HREE (heavy rare earth elements) in the Bobbejaankop Granite. Decreasing Eu values (increase in the negative Eu anomaly) are due to either magmatic differentiation or a breakdown of feldspars (Alderton *et al.*, 1980). Petrographically very little sericite was observed and this latter cause can be ruled out. Enrichment in HREE is characteristic of extremely differentiated granites (Hannah and Stein, 1990) and the Bobbejaankop Granite represents, along with its position in the Eu anomaly, the most differentiated and possibly also a geochemically extremely evolved granite.

The positions of the Klipkloof Granite and granophyric granite in the Eu anomaly are very close to each other, but the Klipkloof Granite appears to be marginally more evolved than the granophyric granite. The Nebo Granite is the least evolved. The magmatic differentiation trend indicated by the REE conforms to that indicated by the major and trace elements, except in the case of the Klipkloof Granite and the granophyric granite of which the REE distribution is very similar.

Discussion. Kleemann and Twist (1989) and Coetzee and Twist (1989) do not endorse such a simple evolution of the granites by magmatic differentiation in other parts of the Bushveld. Kleemann and Twist (1989) suggested that the Klipkloof Granite in the Groblersdal area is not merely a magmatic fractionate of the Nebo Granite and concluded that while there is enough evidence to indicate that these two granites are closely related comagmatic suites, the Klipkloof Granite underwent alteration, presumably in reaction with its own exsolved fluids.

Digitised by the Department of Library Services in support of open access to information, University of Pretoria, 2021

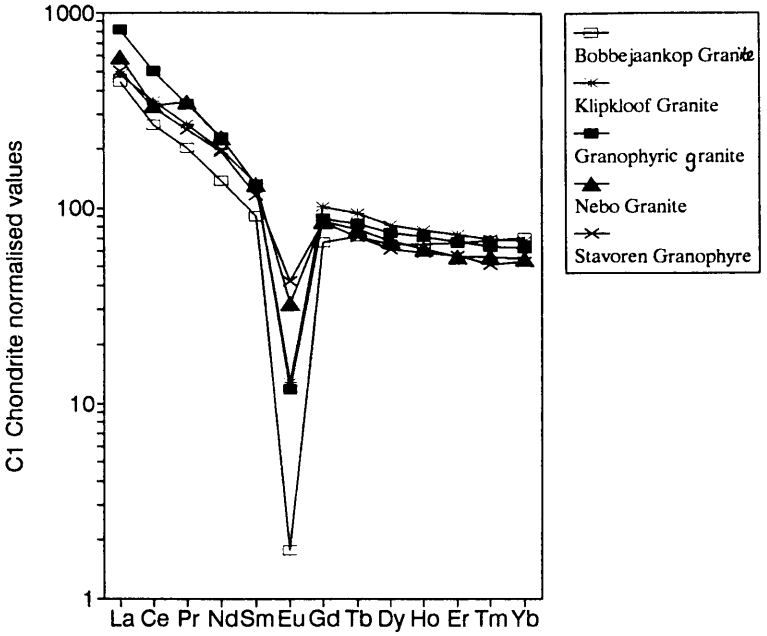

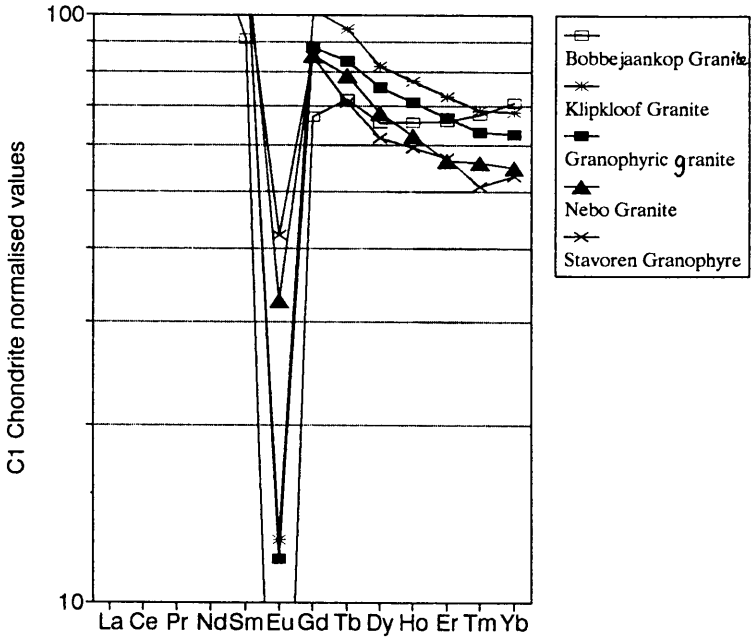

Figs. 17 (above) and 18 (below). C1 Chondrite normalised REE values of granophyre and granites. Fig. 18 is an enlargement of Fig. 17 between values 10 and 100 to show the trends in the Eu-anomaly and the heavy REE.

Digitised by the Department of Library Services in support of open access to information, University of Pretoria, 2021

Coetzee and Twist (1989) proposed that the Bobbejaankop Granite at Zaaiplaats did not crystallise from a distinct magma but represents altered roof facies of the typical Nebo Granite. They produced evidence that hydrothermal fluid interaction transformed parts of the Nebo Granite to form the Bobbejaankop Granite. However, to ascribe this as the sole mechanism responsible for the transformation from the Nebo Granite to Bobbejaankop Granite is unjustified as certain element ratios are characteristic of magmatic differentiation (Table 4).

Table 4 - TEDI and TiO_2 contents of Nebo and Bobbejaankop Granites at Rooiberg and other areas of the Bushveld Complex

Locality - Granite	**TEDI BaxSr/Rb**	**TiO_2**
Rooiberg - Bobbejaankop	13	0,09
Groblersdal - Bobbejaankop	8	0,10
Zaaiplaats - Bobbejaankop (Unmineralised)	6	0,08
Zaaiplaats - Bobbejaankop (Mineralised)	6	0,07
Rooiberg - Nebo	191	0,18
Groblersdal - Nebo	1147	0,34
Zaaiplaats - Nebo	Not available	Not available

(Based on data from Kleemann and Twist (1989); Coetzee and Twist (1989) and this study).

The TEDI of the Nebo Granites is at least ten times and the TiO_2 content twice as high as that of the Bobbejaankop Granites. This suggests a common cause for the similarities in element content of the Bobbejaankop Granite in the Rooiberg, Groblersdal and Zaaiplaats areas. In the Rooiberg area, the change in the element content is ascribed solely to magmatic differentiation. It is therefore not accepted that hydrothermal alteration alone could have caused such dramatic geochemical changes in the major, trace and rare element contents (Figs 17 and 18) in the transition of Nebo Granite to Bobbejaankop Granite, and these changes resemble those expected from magmatic differentiation.

7.5 Emplacement history

The variation diagrams (Figs. 10, 11, 12, 15, 16, 17 and 18) reveal progressive geochemical evolution from Nebo -> Bobbejaankop Granite. In none

Digitised by the Department of Library Services in support of open access to information, University of Pretoria, 2021

of these diagrams is any suggestion of a break in the trend which could have been caused by a renewed influx of magma. It is concluded that the granites in the Rooiberg area evolved from a single parent magma and that geochemical differences between the granites are the result of simple magmatic differentiation. The emplacement history of the granites, based on the geochemical evidence and field relationships, is proposed as follows:

The parent granitic magma from which the granites evolved intruded as a sheet of which the thickness is estimated to be approximately 3 km by analogy to other localities in the Bushveld (Kleemann and Twist, 1989).

The Nebo Granite, geochemically the least evolved, crystallised over large areas and completely engulfed the Rooiberg Fragment. IsoTEDIs in the study area in the east (Fig. 6) indicate that on the presently exposed surface, crystallisation apparently proceeded towards the west in the direction of the Rooiberg Fragment, or upwards if the present dip of the granite sheet is to the west.

The Klipkloof and granophyric granite magmas were evolved from the Nebo Granite magma by fractional crystallisation and accumulated near the roof of the Nebo Granite. Both in the east and the west, the Klipkloof Granite partly occupies a position between the Nebo Granite and the granophyric granite, and in turn the granophyric granite occurs between the Klipkloof Granite and sedimentary rocks of the Rooiberg Fragment.

Finally, the Bobbejaankop Granite magma, geochemically the most evolved, was separated and became entrapped within a shell of granophyric granite. Geochemical evolution resulted in an increase of the F and Cl contents of the entrapped Bobbejaankop Granite magma which caused a decrease in the viscosity and depressed the liquidus and solidus temperatures which in turn prevented quenching (Manning and Pichavant, 1983; Webster and Holloway, 1990). Moreover, the cooling rate of the Bobbejaankop Granite magma was decreased by the fact that it was entrapped within a shell of hot granophyric granite.

Sections across the granites in the west (not shown) suggest that the Bobbejaankop Granite thins out towards the north-west and south-east and attains a maximum thickness in the central part. Unfortunately, Iannello

Digitised by the Department of Library Services in support of open access to information, University of Pretoria, 2021

(1970) did not recognise the Bobbejaankop Granite and it is thus not possible to ascertain the form of emplacement of this granite over larger areas. Nevertheless, it is believed to be in the form of a series of lens-shaped bodies since this fits the geochemical distribution patterns of tin on surface, discussed in the next chapter. Chains of lenticular granite bodies are common phenomena (Pitcher, 1979) and it is proposed that the overall large-scale structure of the Bobbejaankop Granite is a series of lenticular bodies (scallops) of approximately equal size.

This also explains the relatively small outcrop areas of Bobbejaankop Granite in the east: The present erosion surface only exposed the apex, at a higher stratigraphic level, of an inferred lenticular body.

8. THE GEOCHEMICAL TIN LANDSCAPE AT ROOIBERG

Geochemical tin anomalies in the Rooiberg tin-field, based on the Regional Geochemical Programme of the Council for Geoscience (Labuschagne *et al.*, 1993), and carried out on a sample density of 1/km^2, are indicated in Fig. 19. Eight major and several minor anomalies are identified and those relevant to this study are listed in Table 5.

Table 5 - Regional geochemical anomalies relevant to this study and their localities.

Anomaly	Mine/occurrence/farm	Remarks
I	A Mine complex	Past major producer
II	A Mine complex	Past major producer
III	Blaauwbank Mine	Past small producer
IV	B Mine	Past medium-sized producer
V	Golden Kopje	Known occurrence
VI	Vellefontein	Past medium-sized producer
VII	Rietfontein	Known occurrence
VIII	C Mine	Past major producer
a	Kwarriehoek	Known occurrence
b	Nieuwpoort/Hartbeestpoort	Known occurrence
c	Kwaggafontein	Past very small producer
d	Morgenzon	Known occurrence
e	Rooykrans 533 KQ	Unknown occurrence
f	Vaalwater	Known occurrence

Digitised by the Department of Library Services in support of open access to information, University of Pretoria, 2021

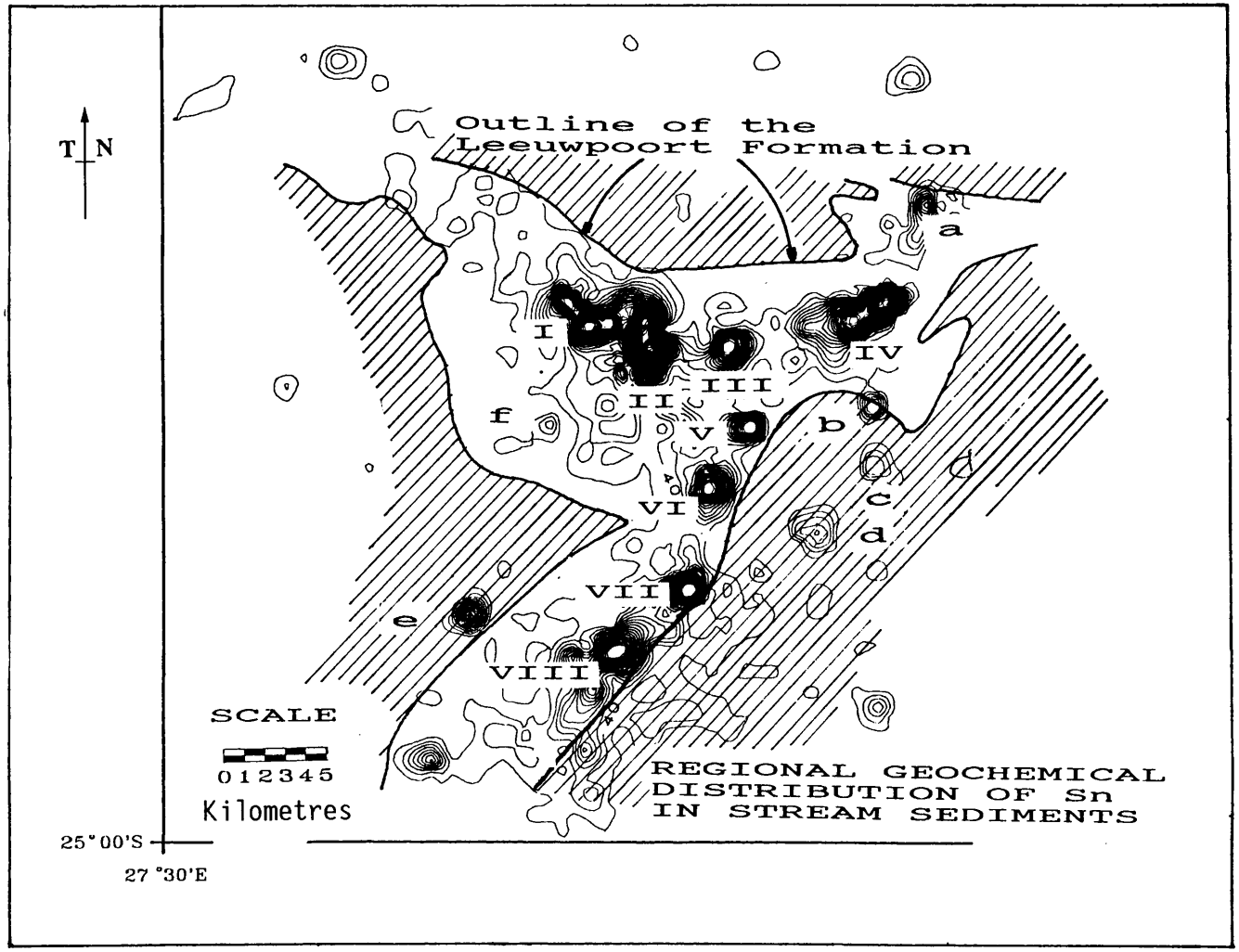

Fig. 19 - Geochemical anomalies in the Rooiberg tin-field.
I - VIII = Major anomalies; a - f = Minor anomalies.
Hatched area = Smelterskop Formation, Rooiberg Group, Stavoren Granophyre and Lebowa Granite Suite.
Blank area inside hatching = Leeuwpoort Formation

Digitised by the Department of Library Services in support of open access to information, University of Pretoria, 2021

Anomaly b was explored only recently but had been discovered prior to the Regional Geochemical Programme. To date, it is the only known occurrence where tin is present in the sediments of the Smelterskop Formation. For many years, geologists held the view that tin mineralisation only occurred stratigraphically below the Blaauwbank Shale Member on account of its impervious nature to the ore-forming fluids (Rozendaal *et al.*, 1995a). As a result, no serious attention has been given to the possibility of economically mineralised ore-bodies in the Smelterskop Formation.

Ironically, anomaly f is very weak but it was in this area that cassiterite was first recognised in the sand of the Vaalwater Spruit, and this triggered mining at the beginning of this century (Labuschagne, 1970a). The mineralisation in the Vaalwater and Weynek area which is closely related to anomaly f, comprises mainly quartz and tourmaline - both high temperature minerals - with only trace amounts of cassiterite. This, along with the fact that the mineralisation occurs stratigraphically low down in the arkosite, and hence closer to the granite source, may imply that the temperature of the ore-forming fluids was too high for economic concentrations of cassiterite and other associated gangue minerals to form.

It is most probable that contamination from past mining operations enhanced the intensity of the anomalies in some areas, but this is not considered too serious. The tin ore-bodies in the mining areas used to crop out and geochemical anomalies are therefore to be expected, irrespective of how much any contamination may have contributed towards the anomaly. Anomalies located over non-producing areas e.g. V and VII, where contamination can be virtually ruled out, are considered to be natural.

The regional distribution of the anomalies emphasizes three important aspects:

1. The Leeuwpoort Formation as a whole contains higher tin values than the adjacent Smelterskop Formation and the granitoids (Fig. 19)
2. The anomalies are confined to the top of the arkosite i.e along the eastern and northern extremities of the outcrop area of the open, north-east plunging anticline formed by the Leeuwpoort Formation.
3. The pattern of the geochemical anomalies clearly indicates that tin mineralisation is located over discrete and separate foci of mineralisation.

Digitised by the Department of Library Services in support of open access to information, University of Pretoria, 2021

All the past producing mines are situated over such foci and several known occurrences which did not produce on account of too low ore grades and/or limited ore tonnages are also represented by these foci (Table 5).

Discussion. The fact that economic tin mineralisation, particulary at the A Mine, only occurs near the top of the arkosite in the so-called tin-zone has been known to geologists since the mid 1950s or more or less from the period that some continuity was achieved with the employment of permanent geological staff. In the 1950s it was known as "mud-seam related mineralisation"; in the 1960s as the "calcareous or orthoclase-rich" horizon and from the 1970s the term "tin-zone" became a household word.

Several attempts have been made to define the top and bottom of the tin zone and to establish the factors which controlled economic mineralisation (Leube and Stumpfl, 1963; Haikney, 1986; Rozendaal *et al.*, 1986, 1995 a & b). While the limits of the tin-zone can be defined reasonably accurately, the factors which controlled economic ore deposition within this zone are as yet not fully understood and mostly speculative. In the most recent publications dealing specifically with the tin zone, Rozendaal *et al.* (1995 a & b) used petrological and geochemical data and distinguished between a highly albitised footwall, a sericitic tin zone and a potassium-rich hanging wall. These geochemical differences are, however, the result of hydrothermal alteration and have not exercised primary control over tin deposition. Factors which according to them retarded the ascent of the ore-forming fluids, and resulted in ore deposition, are equilibration of fluid and lithostatic pressure, limited fracture evolution and/or impermeable rocks such as shaly arkosite. They also considered that a lowering of fluid temperature and oxygen fugacity (*sic*), as well as compositional changes (of the ore-forming fluids) due to wall rock alteration enhanced tin deposition.

Of particular significance is the lateral spacing between the anomalies or foci of mineralisation. The average distance between the foci of ten pairs is 5 km. The low standard deviation of 1,05 km implies that this spacing is regular and the fact that ten pairs were used in the measurements further implies that this regular spacing is not merely coincidental. Three possibilities which could have accounted for this regular spacing are considered.

Digitised by the Department of Library Services in support of open access to information, University of Pretoria, 2021

(a) The factors which, according to Rozendaal *et al.* (op cit), could have controlled tin deposition were only effective at these foci. These include fluid temperature, oxygen fugacity and compositional changes, as mentioned above, but it is difficult to reconcile the influence of these with the regular lateral spacings.

(b) Rozendaal *et al.* (1995 a & b) suggested that the tin-zone is not confined to the A Mine complex only, but extends from A Mine through Vellefontein (anomaly VI) southwards to C Mine (anomaly VIII) and is in actual fact a semi-continuous stratiform horizon with minor breaks. They emphasized that the role of pre-existing steep fractures, acting as fluid conduits, is imperative in creating a plumbing system to allow formation of exo-granitic deposits. They also stated that areas of intense fracturing are spatially synonymous with mining sites.

To a certain extent, the geochemical pattern of the geochemical anomalies supports this view of disconnected sections of the tin-zone, but it also clearly indicates that tin mineralisation is located over discrete and separate foci of mineralisation with *considerably larger breaks between the foci* than envisaged by these authors.

(c) Based on the field mapping, the Bobbejaankop Granite appears to have finally solidified as a scalloped lenticular body enclosed by older granites. Release of the ore-forming fluids took place through localised fractures of limited extent which developed at the apices in the lenticular body. The ore-forming fluids migrated from the Bobbejaankop Granite via these localised fractures into the arkosite and then diffused through the arkosite to the site of ore deposition. It is suggested that these scallops were about the 5 km in diameter, and that the dimensions were determined by the relative competence of the partly consolidated granites in question. Each focus of mineralisation is regarded to correspond to such an apex in the scallops in the Bobbejaankop Granite.

Rozendaal *et al.* (1995b) proposed that the major feeder channels dealt with in (b) above were developed at the cupolas of what they called "Granite 2" - a younger fractionated phase of "Granite 1". Except for the major feeder channels, their proposal is basically the same as that presented here. The

Digitised by the Department of Library Services in support of open access to information, University of Pretoria, 2021

Bobbejaankop Granite could represent their "Granite 2", and the Nebo Granite their "Granite 1", while the apices in the Bobbejaankop Granite could correspond with their cupolas.

9. THE C, NAD AND A MINES ORE-BODIES

The style of mineralisation has been described comprehensively by Leube and Stumpfl (1963), Labuschagne (1970a), Stear (1977a), Dinsdale (1982), Phillips (1982), Rozendaal *et al*. 1986, Naude (1993) and others, and only a brief review is necessary. However, aspects of the mineralisation at the A Mine are described in more detail since polyphase mineralisation is suspected in some areas.

9.1 The Leeuwpoort C Mine

The mineralisation is essentially open-space filling of low-angle bedding plane or steeply dipping fracture-structures generally referred to as lodes and fissures, respectively. Pocket-type mineralisation, the predominant style of mineralisation at the A Mine, is rare and was considered a novelty rather than a source of tin ore. Where both lodes and pockets are present, the lodes cut through the pockets and are distinctly younger (Phillips, 1982).

9.2 The Rooiberg NAD Mine

The ore-bodies are basically the same as those in the C Mine, except that more non-bedded lodes than bedding-plane lodes are present. A relatively large number of pockets are also present, particulary in the upper levels of the mine. Where both pockets and lodes are present, the mutual relationship indicates an earlier stage of formation for the pockets.

9.3 The Rooiberg A Mine

Literally thousands of pockets, formed by a process of replacement, are dispersed throughout the upper part of the arkosite at the A Mine. About ten steeply dipping, well developed, mineralised fractures are also present. In its typical development, a pocket consists of a tourmaline ring surrounding cassiterite, pyrite, ankerite, quartz and minor quantities of other oxides and

Digitised by the Department of Library Services in support of open access to information, University of Pretoria, 2021

sulphides (Chapter 10). A 2 - 5 cm wide whitish ring in the pink or red arkosite surrounds some of the pockets. The origin of this ring, sometimes referred to as a halo, is discussed in Chapter 10.

Steeply dipping, thin and *unmineralised* fractures of limited extent are always associated with the pockets and invariably cut through their central part. These fractures form a regular pattern comprising three sets which intersect each other at 60°. On account of their close association with the pockets, they are regarded as the local feeder channels for the ore-forming fluids (Leube and Stumpfl, 1963; Dinsdale 1982 and others). In fact, mining at the A Mine in ancient and modern times was not by way of conventional stoping methods, but by driving along these fractures, the pockets were encountered. Most of the ore was recovered in this fashion but in a few, and economically important sections, irregular "stoping" or "caving" was done where a high tin content in the pockets, or a local concentration of tin-bearing pockets warranted it. Some colourful and descriptive names such as the Whiskey Stope, Cango Caves and Jewel Box were given to these.

Apart from the distribution of cassiterite *within the confines of the pockets*, it is in some areas also present *around or engulfing the pockets* (Fig. 20). This type of cassiterite mineralisation was first recognised by the author (Labuschagne 1970 a & b) who ascribed it to a later phase of tin mineralisation. It also became apparent that this later phase of mineralisation (cassiterite-2) is generally of a very high grade which had obvious economic implications. Closer attention was thus paid to pockets which had been engulfed with cassiterite, examples of which are shown in Fig 21. In Fig 21A, cassiterite-2 and pyrite are distributed outside the area occupied by tourmaline and completely engulf earlier-formed pockets in Fig 21 B and C.

In the 19N Section of the mine, the presence of cassiterite-2 had been carefully annotated on mine plans. It was found that the earlier-formed pockets were stratiform i.e. essentially parallel to the tin zone with a dip towards the north-east, whereas the confines *embracing all the pockets containing cassiterite-2*, plunges at right angles to the dip of the tin-zone (Fig. 22). This can be considered as a pay shoot with a thickness of about 10 metres and stretching approximately 300 meters along the plunge. Because cassiterite-2 comprised high tin grades, "stoping" or "caving" was done in the

Digitised by the Department of Library Services in support of open access to information, University of Pretoria, 2021

19N and other sections of the mine, such as the Jewel Box and U30.

The concept of a "second tin-phase" was supported until the early 1980s (Dinsdale, 1982; Phillips, 1982). After that time, however, it apparently lost its impact, possibly because this type of ore became depleted in those sections of the mine where it used to be well developed such as the 19N, U30 and Jewel Box. It appears to be absent in the Q22 and Magazine Sections, mined subsequently.

The ore-bodies at the other producing mines were scrutinized for evidence of polyphase mineralisation. At the C Mine, only ankerite, as described by McDonald (1913), exhibits more than one phase of mineralisation, and at B Mine, microscopic evidence indicated that cassiterite was formed during two events (Labuschagne 1970a). It is in the A Mine, however, where polyphase mineralisation is best developed.

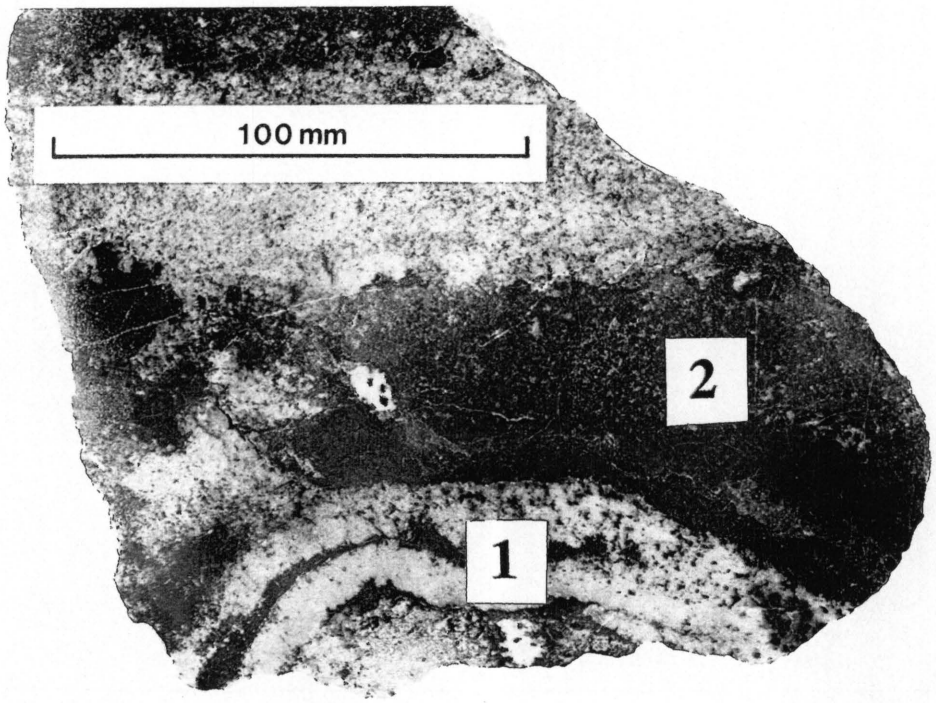

Fig. 20 - Polished slab of a portion of an A Mine pocket (labelled 1), partially engulfed by finely disseminated second generation cassiterite immediately to left, to the right and below label 2. Pyrite, brownish-yellow, is associated with the cassiterite.

A Mine - Jewel Box Section - 680′ level.

Digitised by the Department of Library Services in support of open access to information, University of Pretoria, 2021

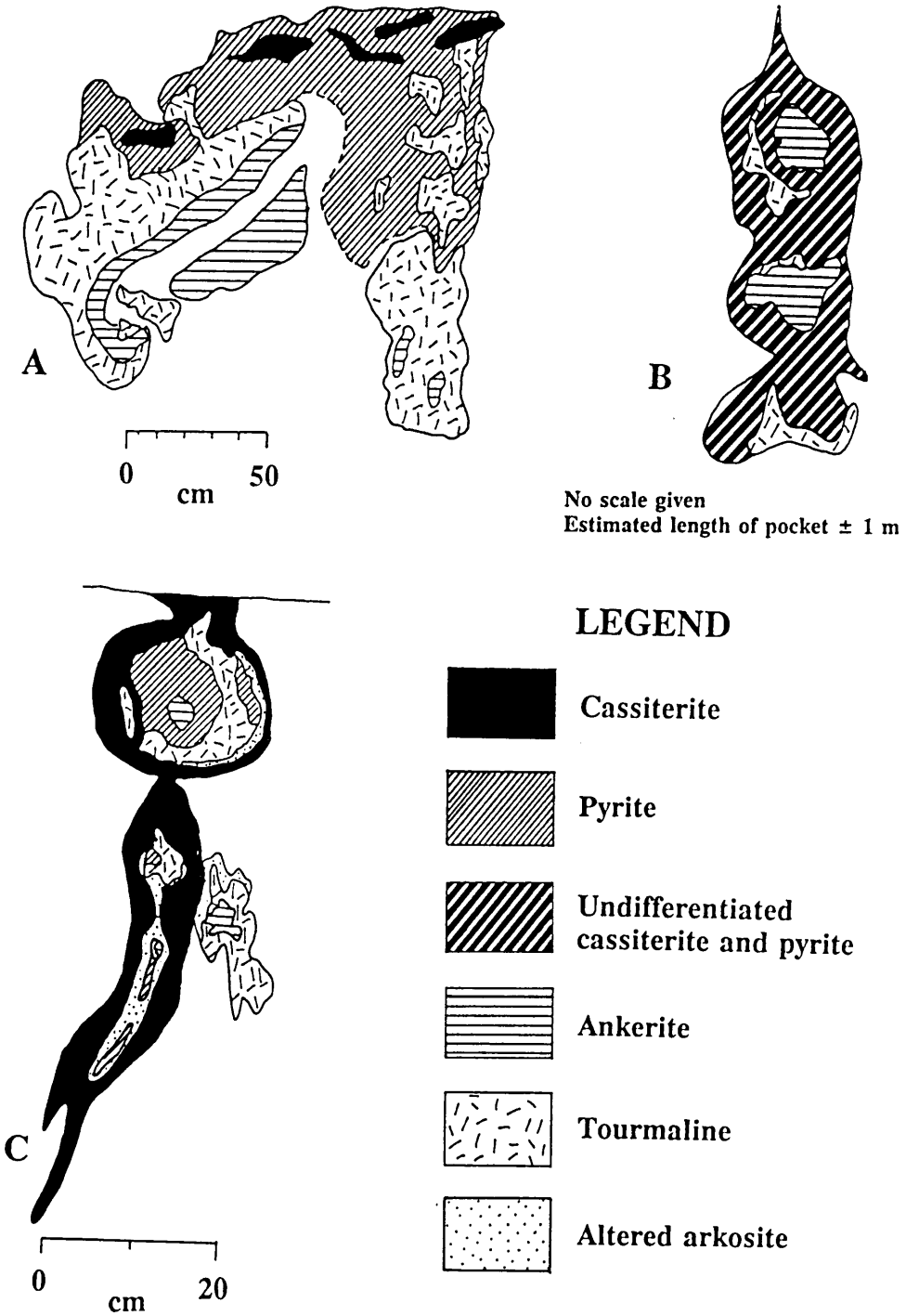

Fig 21 - A Mine pockets showing cassiterite-2 and pyrite engulfing earlier formed tourmaline and ankerite.

A - after Dinsdale (1982)
B - after Stear (1976)
C - after Labuschagne (1970a)

Digitised by the Department of Library Services in support of open access to information, University of Pretoria, 2021

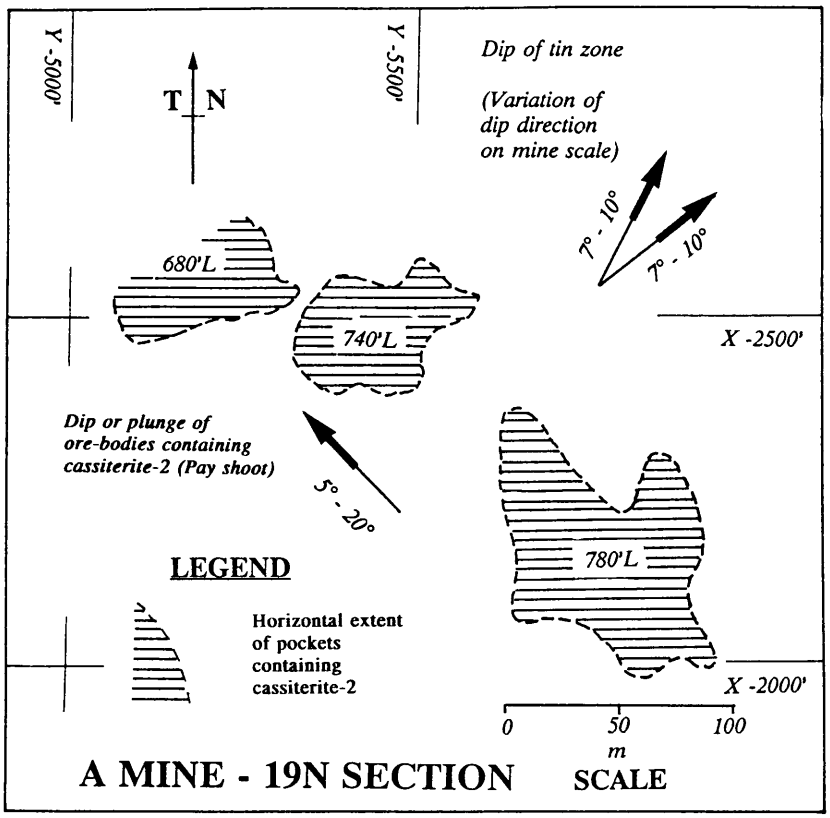

Fig 22 - Portion of the 19N Section, A Mine, showing the horizontal extent of pockets containing cassiterite-2. The plunge of this phase of mineralisation is towards the north-west.

780'L = 780 feet level. The elevations are in English feet and relate to a datum of 1000 feet below the survey benchmark on surface. Thus the 680' level is 100 feet below the 780' level.

Mapped principally by the author with additions by Dr J. Petsnigg.

Rooiberg Tin Limited - Mine plan Ref. A-27

Digitised by the Department of Library Services in support of open access to information, University of Pretoria, 2021

10. TOURMALINE, ANKERITE AND CASSITERITE

The mineralogy of the ore-bodies has been described by Leube and Stumpfl (1963), Labuschagne (1970a), Phillips (1982) and Naude (1993) and the following minerals have been recognised (Table 6):

Table 6 - Minerals present in the Rooiberg ore-bodies

Silicates	*Oxides*	*Carbonates*	*Sulphides*
Tourmaline	Cassiterite	Ankerite	Pyrite
Orthoclase	Magnetite	Siderite	Chalcopyrite
Chlorite	Hematite		Pyrrhotite(*)
Quartz	Rutile(*)		Arsenopyrite(*)
			Bismuthinite(*)
			Galena(*)
			Gersdorffite(*)
			Linnaeite(*)
			Molybdenite(*)
			Sphalerite(*)
			Stannite(?*)

Others	*Secondary minerals*
Fluorite	Sericite
Apatite(*)	Limonite
Scheelite(*)	Bornite(*)
	Covellite(*)
	Neo-digenite(*)

(*) Rare or present in microscopic amounts only

The presence of a rare grey-blue mineral was brought to the attention of the author during this study by J. Misiewicz, and XRD analysis indicated it to be a mixture of 60% luzonite [Cu_3AsS_4] and 40% arsenosulvanite [$Cu_3(As,V)S_4$].

Tourmaline and ankerite are the most common lode- and pocket-forming minerals, and, together with cassiterite, were selected for further analysis. The order in which these minerals are described below does not necessarily reflect their paragenetic sequence.

10.1 Tourmaline

10.1.1 Introduction

Tourmaline is commonly associated with tin deposits and on account of this, some authors suggested that boron, a major constituent of tourmaline, may have

Digitised by the Department of Library Services in support of open access to information, University of Pretoria, 2021

played an important role during the transport and concentration of tin. In the tin-deposits related to the Bushveld Complex, tourmaline is also common; in the Rooiberg tin-field it is one of the most common minerals. However, volumetrically it varies considerably from one deposit to the other.

In the A Mine tourmaline is the predominant mineral in the pockets and on account of its abundance the pockets were often referred to as "tourmaline pockets" by mine personnel. In the NAD Mine it is less common; it may be an important mineral in some of the lodes while in others it occurs in trace amounts only. In the lodes at C Mine, tourmaline is even less common and varies volumetrically within and between the lodes. In those lodes or parts of the lodes where tourmaline is best developed, it is volumetrically less than ankerite, pyrite, feldspar and quartz. In some lodes it may be completely absent. It is, however, common as a wall rock alteration product at the C Mine (Phillips, 1982).

Tourmaline in the A Mine is of special interest: its distribution in some pockets could have been the result of different mineralising events. Moreover, its crystal structure allows extensive substitutions (particulary the Y-site), and possible chemical variations in the compostion of tourmaline could reflect chemical and/or physical variations of the ore-forming fluids.

Underground observations and sampling have been carried out in all the accessible parts of the A Mine and several hundred pockets were studied in detail and sketched or photographed. More than a hundred samples containing tourmaline were collected from which 74 polished thin sections were prepared and examined. In addition, 188 and 73 microprobe analyses were done by Anglo American Research Laboratories (AARL) and the Council for Geoscience (CG) respectively, the results of which are given in Tables VI a and b of the Appendix.

10.1.2 Distribution of tourmaline in the A Mine pockets

The distribution can be summarised as follows:
(1) Tourmaline is always present in the pockets.
(2) Volumetrically, it may occur in trace amounts only e.g. incipient pocket development or it may constitute the bulk of the pocket.

Digitised by the Department of Library Services in support of open access to information, University of Pretoria, 2021

(3) In some pockets it is the only mineral macroscopically visible.
(4) In well developed pockets, tourmaline generally forms the mantle of the pocket thus exhibiting a characteristic "tourmaline ring" when viewed on a plane perpendicular to the long axis of the pocket. Exceptions occur where a later influx of cassiterite-2 formed around the pockets.
(5) In many pockets tourmaline is also present within the core of the pocket which is then commonly separated from the tourmaline in the mantle by altered arkosite, and in some cases by other minerals like ankerite, pyrite and cassiterite.

For descriptive purposes, tourmaline located in the core of the pocket is designated tourmaline L1 and that along the mantle as tourmaline L2 (Fig. 23). However, no temporal relationship is implied and conclusions regarding the genesis and age relationships of tourmaline L1 and L2 are only drawn after all the data have been considered.

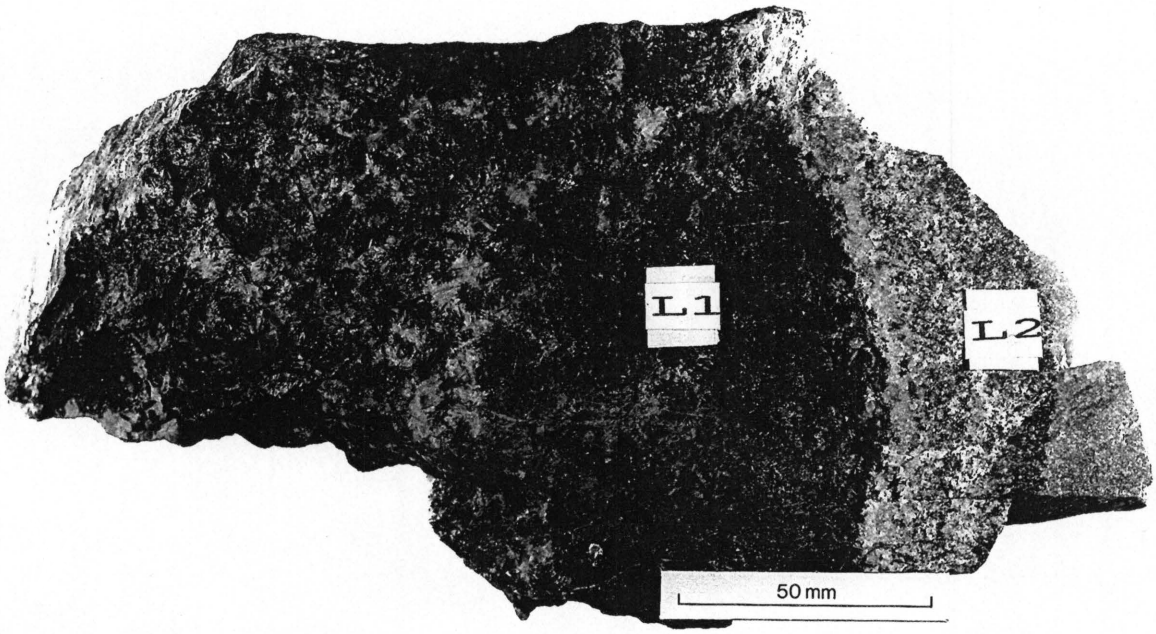

Fig. 23. - Specimen of an A Mine pocket containing coarse-grained and major quantities of tourmaline in the core (L1) and minor quantities of fine-grained tourmaline along the mantle (L2).

Digitised by the Department of Library Services in support of open access to information, University of Pretoria, 2021

10.1.3 Physical and optical properties

Macroscopic. Both tourmaline L1 and L2 are black with diameters of cross-sections of the columnar crystals varying from small to large (Table 7). It appears as if the grain size of tourmaline L1 may be coarser than that of tourmaline L2. In contrast with tourmaline L2, the crystals of tourmaline L1 are commonly arranged in radiating aggregates.

Microscopic. The properties of the tourmalines are summarised in Table 7.

Table 7 - Properties of tourmaline L1 and L2

	Tourmaline L1	Tourmaline L2
Diameter ⊥ c-axis	~ 600 μm	175 - 400 μm
Pleochroism: colours dependent on zoning	O brown-green, khaki-green, dark green, light green E light brown, light bluish green, yellowish brown	
Three types of zoning	(1) Poorly defined, colours patchy; rare (2) *Slightly zoned core*, O dark green; with $\{10\bar{1}0\}$ habit, modified by $\{21\bar{3}0\}$, giving a roughly triangular shape in sections perpendicular to the c-axis (Fig. 24) *Slightly zoned overgrowth*, O light green; with $\{11\bar{2}0\}$ habit giving a hexagonal shape perpendicular to the c-axis. The overgrowth is optically discontinuous (about 20°) with respect to the core (Fig. 25) as it is biaxial with a small 2V (Ford, 1932). (3) *Strongly zoned well developed core*, O light green to almost black; $\{21\bar{3}0\}$ habit giving a convex triangular shape in sections perpendicular to the c-axis (Fig. 26). *Thin, slightly zoned overgrowth*, O light green to khaki green; $\{11\bar{2}0\}$ habit.	

Table 7 is based on the petrographic description of all the thin sections examined. Of these, where zoning could be made out, 45% show the distinct overgrowth (Fig. 24) and in 55% the zoning is either very weak or more commonly developed as (3) in Table 7 (Fig. 27). In 10% of the slides, tourmaline grains with and without the overgrowth are present.

Digitised by the Department of Library Services in support of open access to information, University of Pretoria, 2021

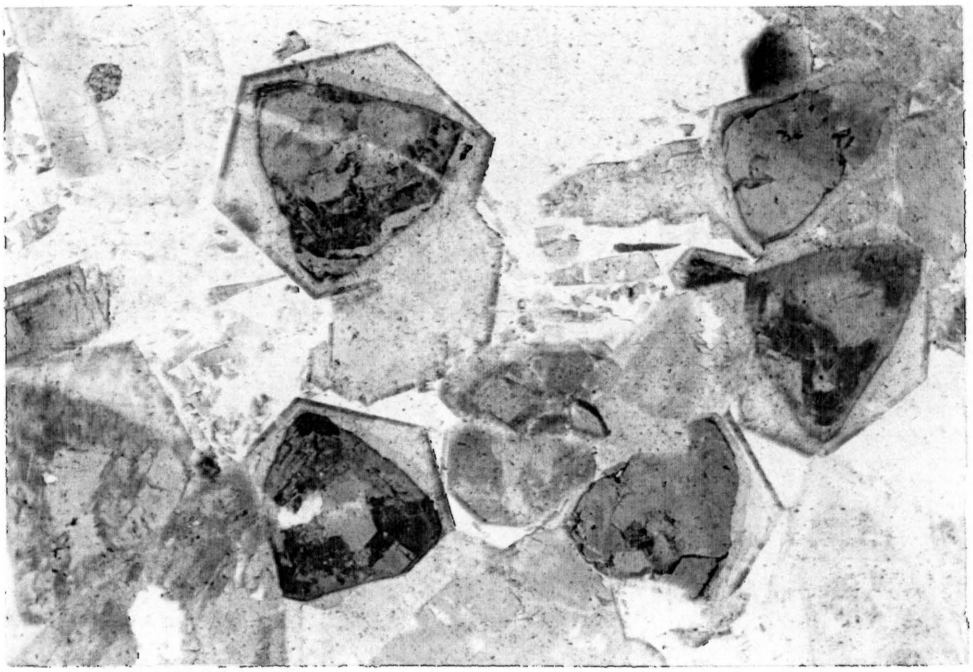

Fig. 24 - Zoning in tourmaline. Core dominated by the trigonal prism $\{10\bar{1}0\}$; overgrowth dominated by the hexagonal prism of the second order $\{11\bar{2}0\}$.

X80 Plane polarised light Sample 265L2

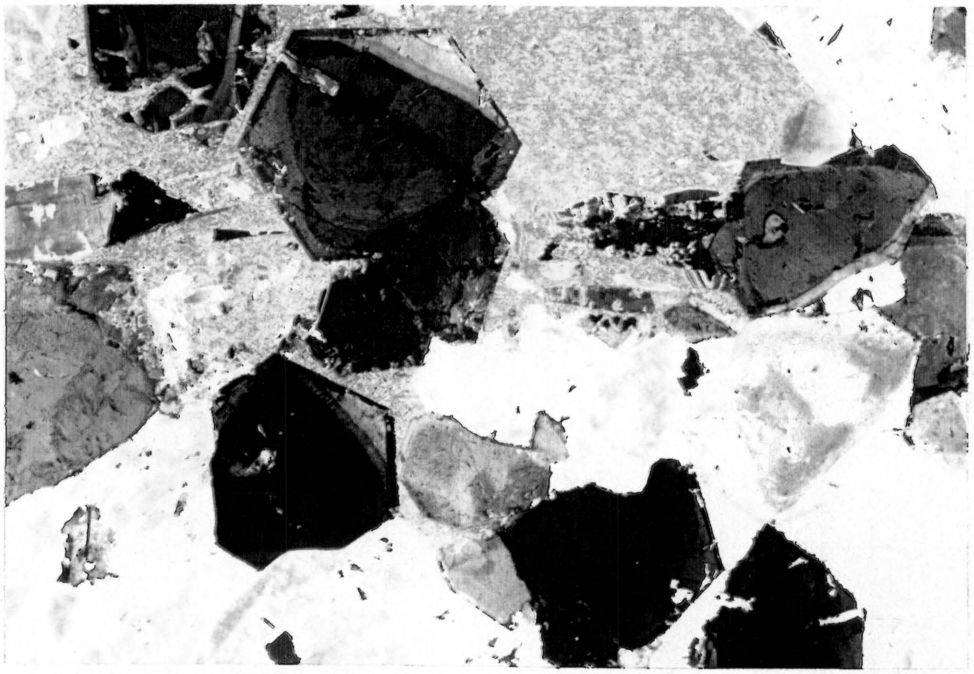

Fig. 25 - Same field as Fig. 24 but with +N to show optical discontinuity between core and overgrowth of tourmaline. Ankerite is present in the upper part of the figure.

X80 +N Sample 265L2

A Mine - U30 Section - 780′ Level

Digitised by the Department of Library Services in support of open access to information, University of Pretoria, 2021

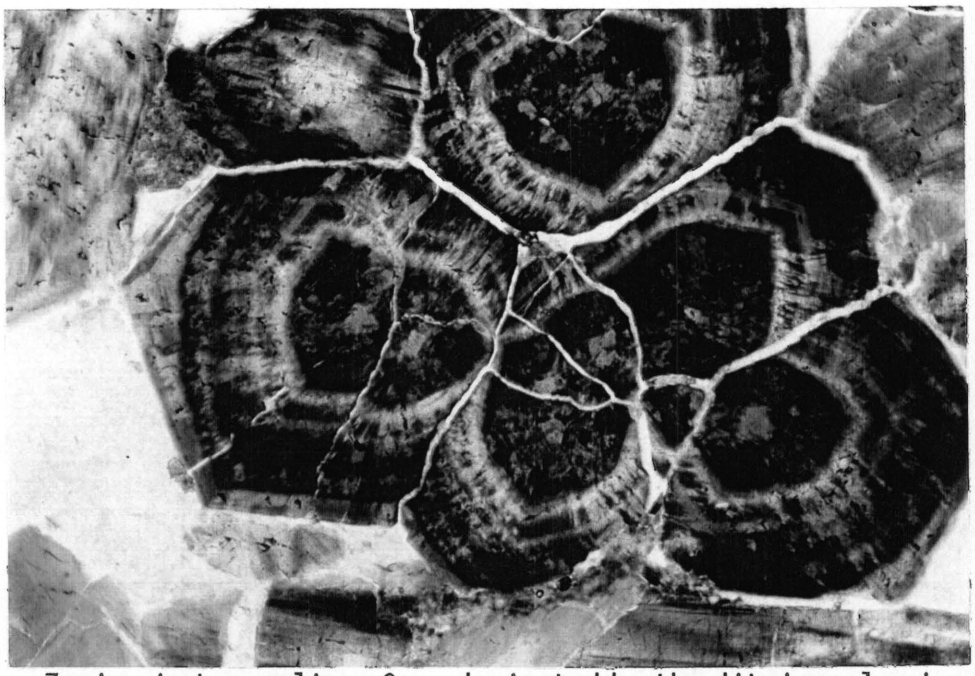

Fig. 26 - Zoning in tourmaline. Core dominated by the ditrigonal prism $\{21\bar{3}0\}$, modified by the trigonal prism $\{10\bar{1}0\}$; overgrowth dominated by the hexagonal prism of the second order $\{11\bar{2}0\}$.

X80 Plane polarised light Sample 124L1

A Mine - Q22 Section - 500′ Level

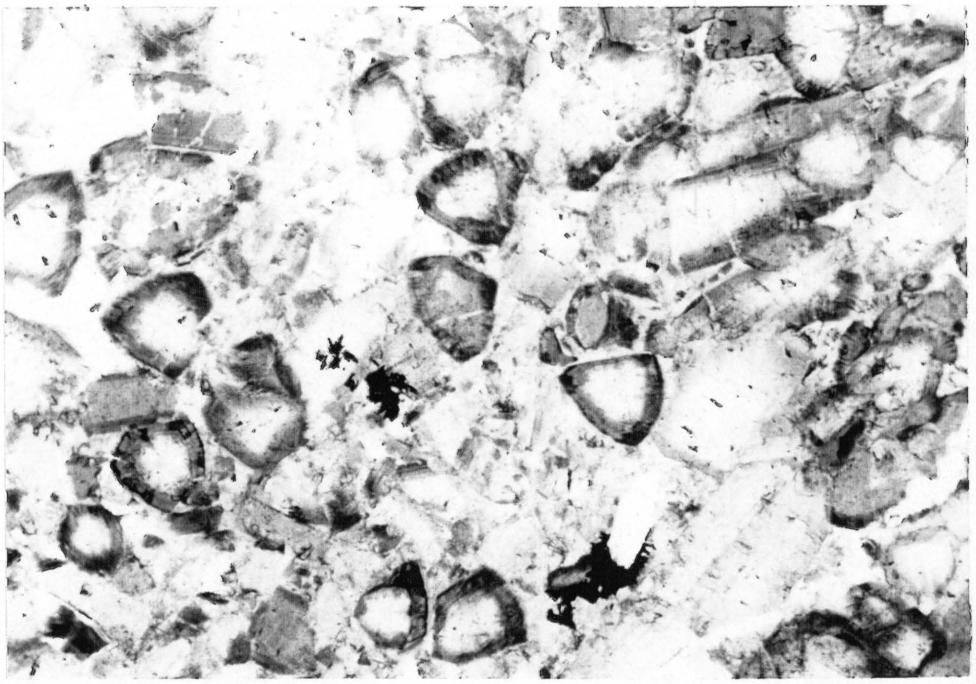

Fig. 27 - Zoning in tourmaline. Note the absence of overgrowth present in the tourmaline in Fig. 24.

X80 Plane polarised light Sample 219L2

A Mine - 19 N Section - 780′ Level

Digitised by the Department of Library Services in support of open access to information, University of Pretoria, 2021

No definite differences in the crystallographic and optical properties of tourmaline L1 and L2 could be found. However, the distinct change in the habits of the cores, and between the cores and the overgrowths of the zoned tourmaline crystals, which are present in both tourmaline L1 and L2, can only be explained by independent episodes of tourmaline formation, or by a sudden change in the characteristics of the ore-forming fluids (e.g. pH, Eh, temperature, composition, concentration etc.).

10.1.4 Mineral chemistry

Tourmaline is a complex boro-silicate with a general formula $XY_3Z_6(BO_3)_3Si_6O_{18}(OH)_4$. The crystal structure of tourmaline was solved by Ito and Sadanaga in 1951 and subsequently several structural refinements by various workers have been done (Grice and Ercit, 1993). This work is still in progress (MacDonald and Hawthorne, 1995) but it is unlikely that future results will show drastic differences from the following site allocations:

X: Usually contains Na but may also accommodate other large cations like Ca and K.

Y: This site has the most varied cation occupancy which accounts for substitutions critical to the formula. Excess Al (after Si and Z positions have been filled), and also Fe^{2+}, Fe^{3+}, Mg and the lesser cations Li, Mn, Zn, V and Ti are accommodated in the Y site.

Z: Typically occupied by Al and relatively few substitutions are possible. Deficiencies in Al are made up largely by Mg and perhaps small amounts of transition metals.

B: This site is assigned to boron. Studies by MacDonald and Hawthorne (1995) indicate that the B in the tourmalines equals the stoichiometric amount of 3 atoms per formula unit.

Si: A deficiency in Si is complemented by Al rather than Mg.

Hydroxyl site: F^- or O^{2-} may substitute for OH^-.

The data in Table VIa have been recalculated to atomic proportions based on the following assumptions:

1. Iron is present as Fe^{2+}. This was necessitated by the fact that the microprobe analyses represent total Fe only.

Digitised by the Department of Library Services in support of open access to information, University of Pretoria, 2021

2. Three boron atoms are present in the structural formula. Boron was not analysed for and B_2O_3 was calculated from the partial analyses. Structural refinements indicated that only boron occupies the B-site and no substitutions have been reported (MacDonald and Hawthorne, 1995).
3. Twenty nine oxygen atoms per unit formula. There are 31 (O, OH) anions in the unit formula and the maximum possible substitution of $4(OH)^-$ by $2O^{2-}$ will reduce the number of oxygen atoms to 27. Since $(OH)^-$ cannot be determined by the microprobe, it was assumed that no $(OH)^-$ is present and hence 29 oxygen anions (Σ negative = 58) were used as the basis for the calculations.

The atomic proportions and site allocations are given in Table VIb in the Appendix.

Comparison between the major element chemistry of tourmaline L1 and L2.

The positions of the microprobe analyses (Tables VI a and b - Appendix) are based on Fig. 28 which was constructed from sketches made and photographs taken during the microscopic examination. Positions 0 - 2 represent the core dominated by the trigonal prism $\{10\bar{1}0\}$ or the *core*; positions 3 - 7 by the zones in the $\{21\bar{3}0\}$ dominated core or the *mantle* and positions 8 - 10 by the overgrowth with the $\{11\bar{2}0\}$ habit or the *overgrowth*. The averaged values of these analyses are given in Table 8. The B_2O_3 values were calculated.

There are distinct differences between the core, mantle and overgrowth within each group as far as major elements are concerned. However, except for TiO_2 and CaO, there are no noteworthy differences between tourmaline L1 and L2. The Cr_2O_3 and K_2O values are discounted on account of the proximity of these values to the detection limit.

Variations in the chemical composition within tourmaline grains

On account of the fact that no noteworthy chemical differences were found between tourmaline L1 and L2, the chemical data of these two groups may be pooled and are forthwith collectively referred to as simply *tourmaline*. All the analyses done on the same position (Fig. 28) can therefore be averaged out.

Digitised by the Department of Library Services in support of open access to information, University of Pretoria, 2021

Table 8 - Averaged microprobe and calculated B_2O_3 values for tourmalines

Mass % as analysed; B_2O_3 calculated

Tourmaline L1		B_2O_3	SiO_2	TiO_2	Al_2O_3	Cr_2O_3	FeO	MgO	CaO	Na_2O	K_2O	Total
Positions 0 - 2	n=22	10.67	37.06	0.39	30.72	0.05	8.53	7.62	0.59	2.26	0.03	97.92
Positions 3 - 7	n=20	10.54	36.64	0.80	28.74	0.03	11.10	7.15	0.79	2.41	0.04	98.23
Positions 8 - 10	n=9	10.60	36.63	0.71	29.04	0.00	11.92	6.95	0.65	2.72	0.05	99.26
Tourmaline L2												
Positions 0 - 2	n=16	10.72	37.22	0.42	30.67	0.22	8.52	7.71	0.60	2.34	0.03	98.45
Positions 3 - 7	n=10	10.41	36.43	1.12	27.30	0.15	11.43	7.26	0.99	2.33	0.04	97.48
Positions 8 - 10	n=15	10.55	36.66	0.69	29.03	0.01	11.13	7.06	0.54	2.66	0.04	98.39
Ratios Tourmaline L2/Tourmaline L1												
Positions 0 - 2			1.00	1.06	1.00		1.00	1.01	1.02	1.03	0.83	1.01
Positions 3 - 7			0.99	1.40	0.95		1.03	1.02	1.25	0.97	1.15	0.99
Positions 8 - 10			1.00	0.98	1.00		0.93	1.02	0.83	0.98	0.80	0.99

Positions 0 - 2: Core dominated by the trigonal prism $\{10\bar{1}0\}$: Core
Positions 3 - 7: Zones in the $\{21\bar{3}0\}$-dominated core : Mantle
Positions 8 - 10: Overgrowth with $\{11\bar{2}0\}$ habit : Overgrowth

Digitised by the Department of Library Services in support of open access to information, University of Pretoria, 2021

The variation in the mass % of the six of the major elements which occupy the X,Y and Z sites relative to the positions of the composite diagram (Fig. 28) is shown in Fig. 29. The value for each position represents the average value of all the analyses (Table VIa- Appendix) for that particular position.

Most noteworthy is that, with the exception of MgO, there is a distinct break between the mantle and the overgrowth i.e. between positions 7 and 8 in Fig. 29. Chemical differences between the core and the overgrowth are also illustrated by Figs. 30 and 31. The analyses of the positions on the mantle were left out for clarity. Fields, with some overlap, exist for the core and overgrowth. A higher FeO, an erratic but overall higher TiO_2, and a lower Al_2O_3 content are recognised for the overgrowth.

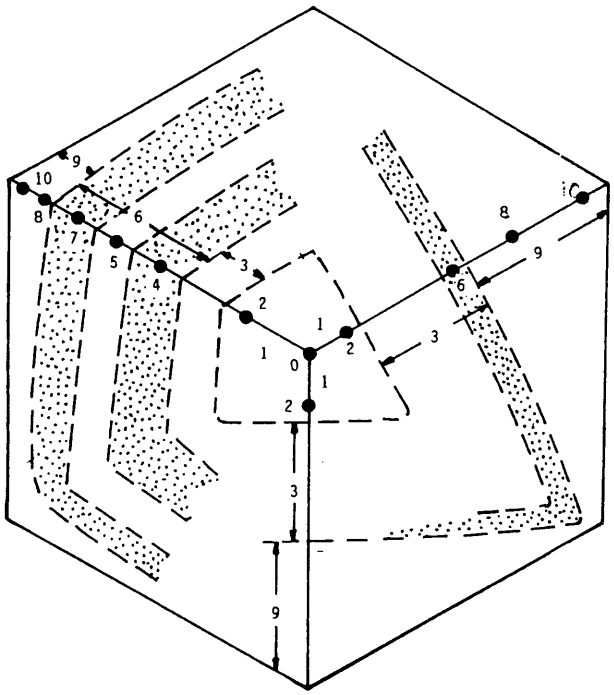

Fig. 28 - Composite diagram of tourmaline grains, perpendicular to the c-axis, showing the positions of microprobe analyses.

Digitised by the Department of Library Services in support of open access to information, University of Pretoria, 2021

The distinct change in the chemistry between the core-mantle and the overgrowth of the tourmaline can, like the optical properties, only be explained by independent episodes of tourmaline formation or by a sudden change in the characteristics of the ore-forming fluids (e.g. pH, Eh, temperature, composition, concentration etc.). This is discussed in Chapter 11 where the atomic proportions and site allocations are also considered.

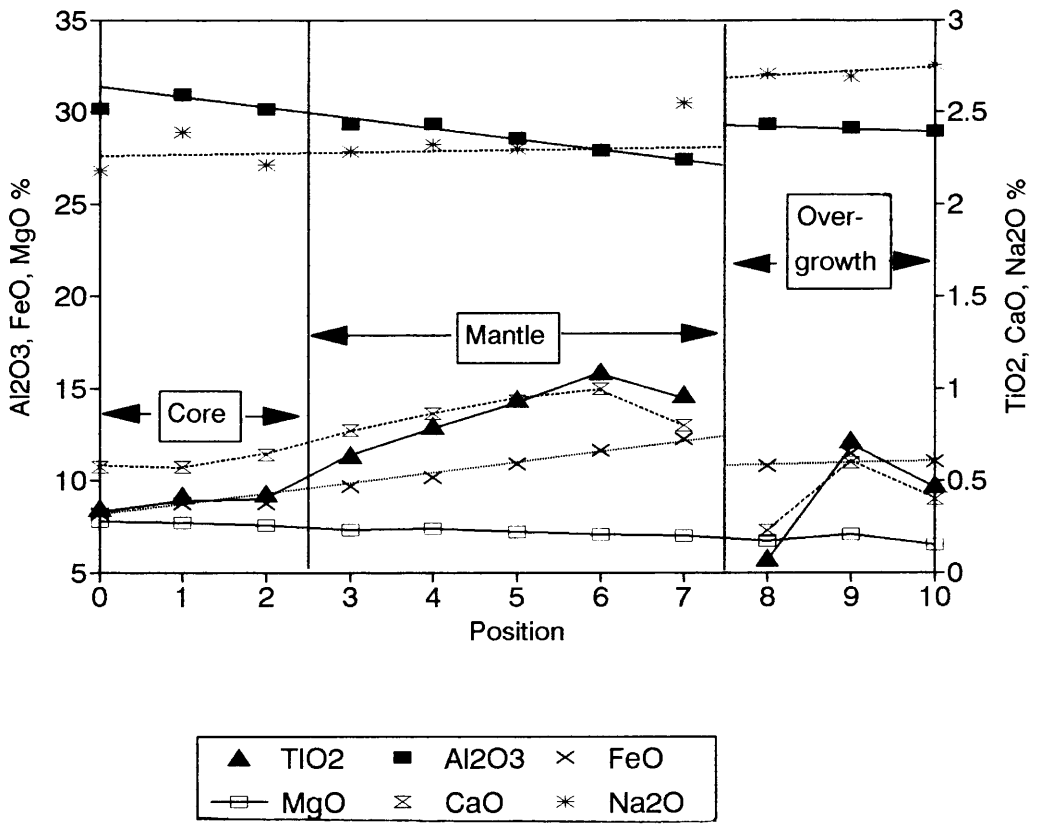

Fig. 29 - Variations in the mass per cent of Al_2O_3, FeO, MgO, TiO_2, CaO and Na_2O relative to the composite tourmaline grain. Note the sharp break between positions 7 and 8 (except for MgO).

Digitised by the Department of Library Services in support of open access to information, University of Pretoria, 2021

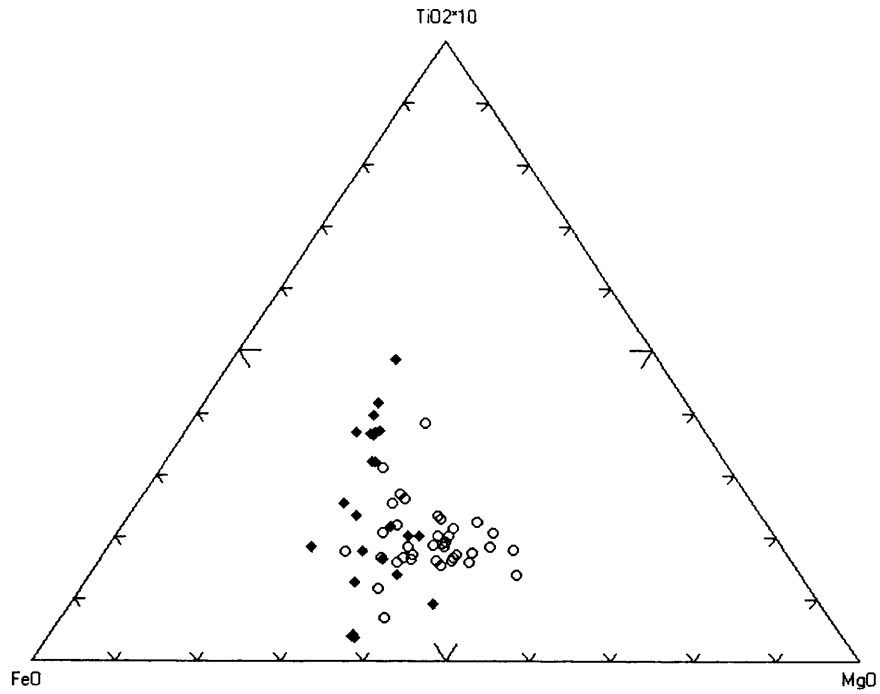

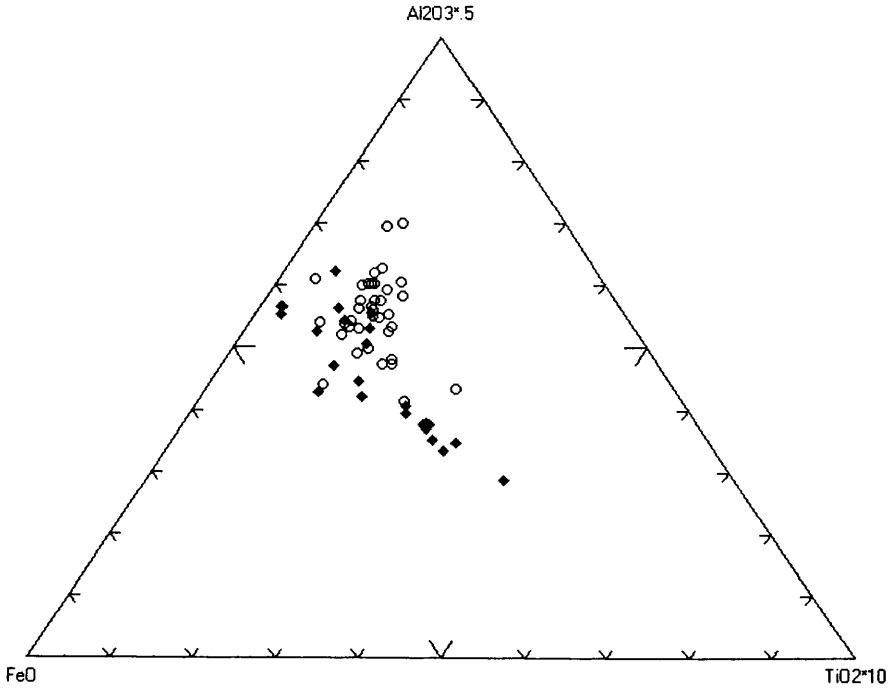

Figs 30 (above) and 31 (below) - Ternary diagrams: TiO_2 - FeO - MgO and Al_2O_3 - FeO - TiO_2 of tourmaline. Fields for the core (circle) and overgrowth (diamond) are recognised. The overgrowth crystallised from a separate pulse of fluids.

Digitised by the Department of Library Services in support of open access to information, University of Pretoria, 2021

10.2 Ankerite

10.2.1 Introduction

Ankerite has the general formula $Ca(Mg,Fe,Mn)(CO_3)_2$. Depending on the Fe/Mg ratio, *ankerite* is used for the more Fe-rich phase and *ferroan dolomite* for the less Fe-rich one, although there is no strict division. Some authors use the terms interchangeably. In this study, *ankerite* is preferred for historical reasons; the term has been used at Rooiberg since it was first reported by McDonald in 1912. The initial identification by McDonald has been reaffirmed during this study by means of chemical and XRD analyses.

Ankerite is widespread and plentiful throughout the Rooiberg tin-field and ranks, next to tourmaline, as the most common mineral in the ore-bodies. This makes it unique in the tin deposits associated with the Bushveld Complex in particular and tin deposits on a world-wide scale in general.

Apart from its abundance, it is of interest for another reason: Ankerite-filled fractures, cutting through apparently earlier-formed ore-bodies, strongly suggest more than one episode of ankerite formation. This was important in the development of the concept of polyphase mineralisation (Labuschagne 1970a). However, prior to this study, petrographic and chemical comparisons between ankerite of these apparently different phases were lacking.

In this study, attention was given to the distribution, petrography and chemistry of ankerite in ore-bodies of A, NAD and C Mines and the ankerite-filled fractures. In addition Pb-Pb isotope determinations were done of which the results are discussed Chapter 11.

10.2.2 Distribution

A Mine pockets. Ankerite occurs mainly within the confines of the pocket, or more specifically, within the confines of the tourmaline mantle (Fig. 32). It may penetrate slightly into the tourmaline mantle, but this is exceptional. Ankerite is also disseminated in the arkosite in the vicinity of pockets in some areas. In these cases, its presence is less obvious and often it can only

Digitised by the Department of Library Services in support of open access to information, University of Pretoria, 2021

be detected microscopically.

Ankerite in the pockets is always associated with one or more of the pocket-forming minerals: tourmaline, sulphides, quartz, cassiterite, etc. and never occurs on its own. Volumetrically, the amount of ankerite ranges from trace to major, and in many pockets, it is the most important mineral.

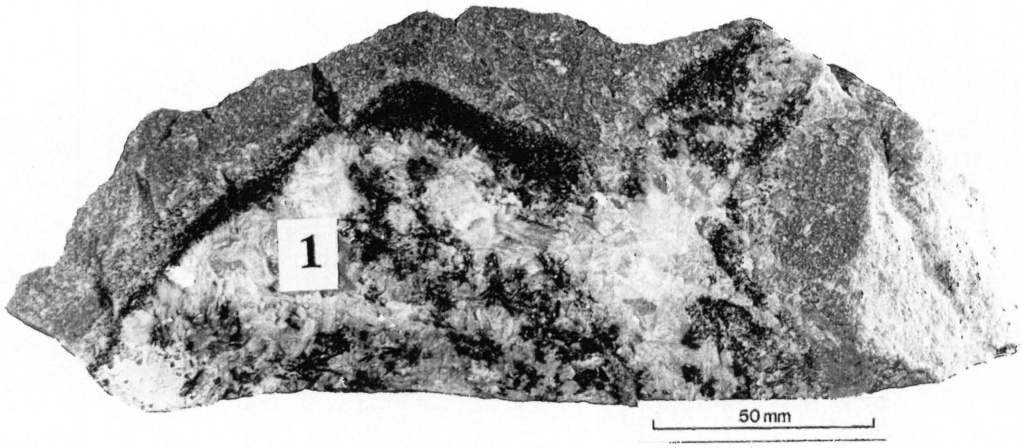

Fig. 32 - Part of a pocket showing a tourmaline mantle (black) and ankerite (labelled 1) within the confines of the pocket. Sulphides and minor tourmaline are present in the core section. The "glassy" mineral is quartz. The arkosite country rock is "bleached" immediately around the pocket as a result of silicification.

A Mine - Q22 Section - 580′ Level Sample 192L0

NAD Mine lodes. Ankerite is present from a trace to a major constituent in all the lodes. In areas where ankerite is well developed, it often contains inclusions of earlier formed minerals, notably tourmaline and cassiterite but also of arkosite up to ± 1 cm in diameter. These lodes can be described as true breccias although some replacement of the inclusions by ankerite is evident from diffused contacts. Excellent examples of this brecciated ore are present in the Bonus and Union lodes, and the volumetric ratio between ankerite cement and inclusions is estimated to be as high as 5:1.

Digitised by the Department of Library Services in support of open access to information, University of Pretoria, 2021

Ankerite occurs together with siderite in the C lode (not C *Mine*) and the Bonus lode. In the C lode in particular, siderite is the main carbonate and in many places it constitutes volumetrically more than 90 per cent of the lode. Where the two carbonates occur together, ankerite appears to have formed before siderite since it is located between cassiterite and siderite. However, microscopically the age relationship could not be established with certainty.

C Mine lodes. Ankerite is volumetrically the most important single lode-forming mineral, although it may not be present everywhere in the lodes. Its thickness is variable and may depend on the width of the lode. Typically, a well developed lode is on average from 10 to 15 cm wide and may it contain 5 cm ankerite (Fig. 33). The most spectacular occurrences are those in the cymoid loops, described by Phillips (1982) and Misiewicz (1992), where thicknesses of up to 1 metre are developed. Phillips (1982) reported thicknesses of more than 2 metres in the Spruit lode, although such thicknesses are exceptional.

Ankerite was the last of the major lode-forming minerals to crystallise, usually filling the central part of the lode, and engulfs the earlier formed minerals. According to Phillips, a depositional overlap exists between ankerite and chalcopyrite and specular haematite. He also reports that it replaces orthoclase, quartz II and possibly pyrite. Only one mineralising phase of ankerite is present in the lodes.

Ankerite-filled fractures. These fractures have been noted during the present study in the A and NAD Mines only, although their presence at B Mine has been reported earlier by Labuschagne (1970a) and at C Mine by McDonald (1913) and later by Leube and Stumpfl (1963). Excellent exposures were found in the Magazine and 19N Sections of the A Mine (Fig. 34).

The term ankerite-filled fracture is used to describe essentially a monomineralic vein filling of ankerite emplaced in a stockwork in which individual fractures are extremely variable in thickness, dip and strike. These fractures cut through the pockets in random orientation, eventually resulting in brecciation (Fig. 35).

Digitised by the Department of Library Services in support of open access to information, University of Pretoria, 2021

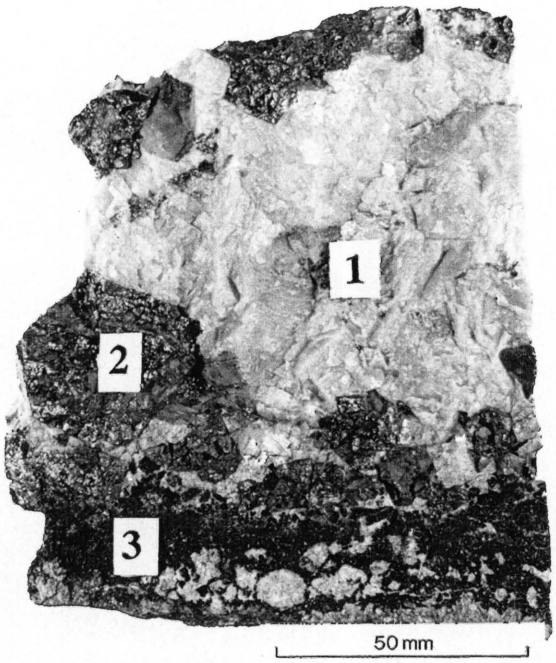

Fig. 33 - A typical well developed C Mine lode. Ankerite (1) occupies the central part. Cassiterite (3) is developed along the bottom part. Pyrite (2) was mainly deposited between cassiterite and ankerite.

C Mine - Hosking Fissure Sample 424LO

Fig. 34 - Ankerite-filled fracture (thin white vein across figure) cutting through earlier-formed pockets. Width of figure = 2 metres.

A Mine - Magazine Section.

Digitised by the Department of Library Services in support of open access to information, University of Pretoria, 2021

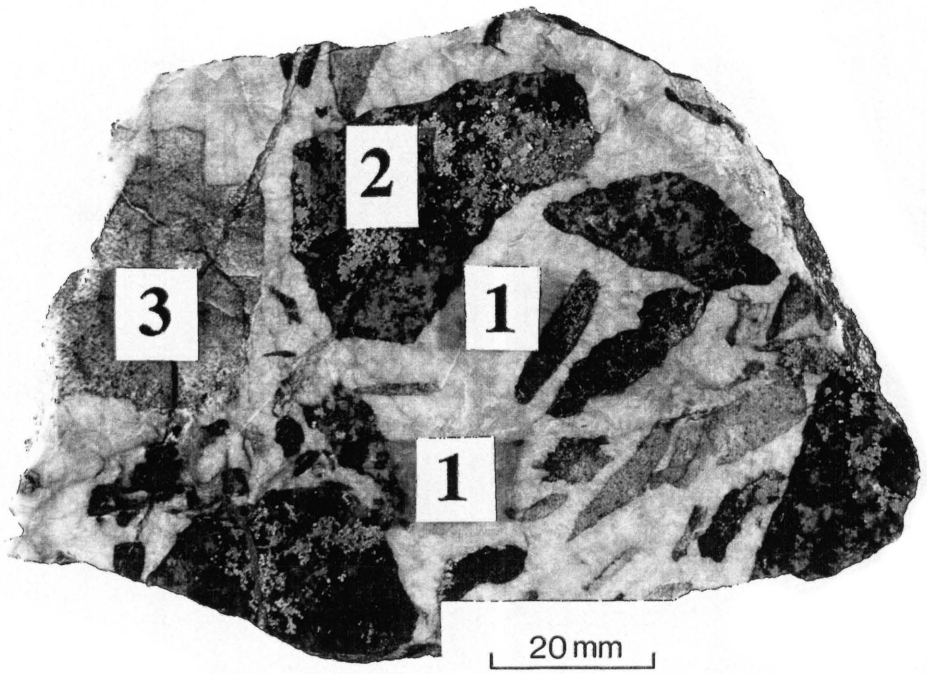

Fig. 35 - Breccia formed by well developed ankerite-filled fractures (labelled 1) cementing fragments of early formed mineralised pockets (labelled 2) and altered arkosite(labelled 3).

A Mine - 19N Section.

Macroscopically, it can be ascertained without any doubt that these fractures constitute a later phase of ankerite mineralisation which is referred to as *ankerite-2* as opposed to earlier-formed *ankerite-1* in the C and NAD Mine lodes and the A Mine pockets. The term *ankerite* is used to discuss the mineral as such without any paragenetic connotation.

10.2.3 Microscopic investigations

Twenty-five thin sections of predominantly ankerite-1 and associated minerals from the A mine pockets, and another 25 of ankerite-2 from the ankerite-filled fractures, were used in a comparative study. These sections are from samples as representative as possible from the A Mine. Microscopic examination of the ankerite from the NAD Mine was limited to establishing the age relationship with siderite, and no microscopic work was done on material from C Mine.

Digitised by the Department of Library Services in support of open access to information, University of Pretoria, 2021

Ankerite-2 was found to be monomineralic and not associated with any other ore-minerals. Ankerite-1 on the other hand, is almost always associated with tourmaline, pyrite, etc. This difference is an excellent microscopic diagnostic feature. The photomicrograph shown as Fig. 36 was taken from a carefully prepared thin section containing both ankerite-1 and -2. Ankerite-1 is associated with earlier-formed tourmaline (on account of total replacement of the arkosite the impression may be gained erroneously that the tourmaline grains are mechanical inclusions) whereas ankerite-2 is not associated with any minerals and cuts through earlier-formed ankerite-1.

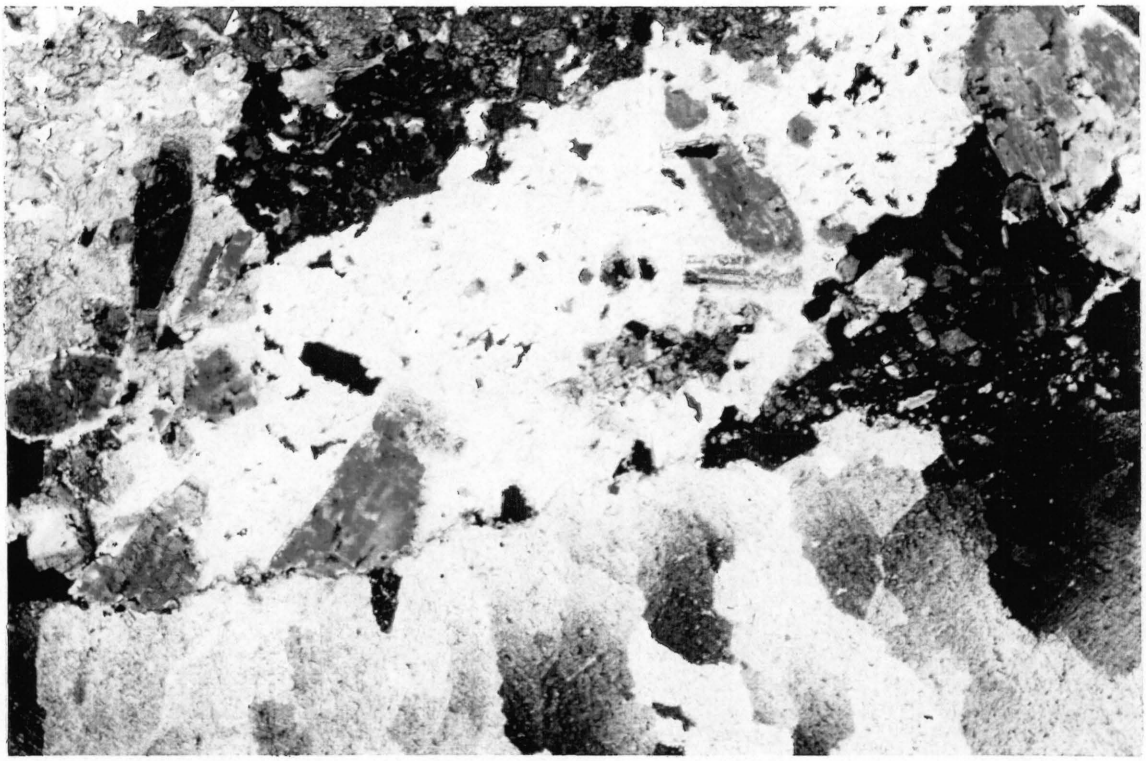

Fig. 36 - Ankerite-2, bottom part of figure, in sharp contact with ankerite-1, associated with tourmaline, centre of figure. Ankerite-2 is younger than ankerite-1.

X80 +N Sample 118L4

A Mine - Magazine Section - 565′ Level

Digitised by the Department of Library Services in support of open access to information, University of Pretoria, 2021

10.2.4 Mineral chemistry

Of the rhombohedral carbonates, ankerite is the only one containing two or more divalent cations in addition to Ca. The three major cations - Ca, Mg and Fe - are distributed over the A and B cation sites. Minor substitution of other cations may occur of which Mn may reach a few per cent. Reeder and Dollase (1989) concluded from the study of three ankerites, which have approximately the same composition as those of Rooiberg, that Ca occupies 94 - 99% of the A site and 1 - 5% of the B site. The difference in the A site is made up by Fe+Mn.

Iron is the most common element substituting for Mg in natural dolomite, with the Fe^{+2} content reaching a *maximum* of 70 mole % $CaFe(CO_3)_2$ (Reeder and Dollase, 1989). The incomplete substitution of Fe for Mg results in the apparent non-existence of the Fe analogue of dolomite, $CaFe(CO_3)_2$, in nature. Moreover, several experimental studies have failed to synthesize this hypothetical mineral. The cause of the instability of $CaFe(CO_3)_2$ and the limited substitution of Fe^{+2} for Mg^{+2} in the dolomite structure, which stands in marked contrast to $MgCO_3$-$FeCO_3$ (magnesite-siderite), is still unknown (Rosenberg, 1991), despite the fact that this incomplete substitution has been known for a few decades and has received considerable attention.

Published data on the trace element chemistry of hydrothermal ankerite are virtually non-existent, a fact corroborated by Reeder (written communication). In a comprehensive discussion on the incorporation of trace elements into carbonates in general, and without any specific reference to ankerite in particular, Veizer (1983) refers to earlier work of other authors (McIntire, 1963; Zemann, 1969). According to them, the trace elements can be incorporated into carbonate minerals by way of:

(1) Substitution for Ca^{2+} in the $CaCO_3$ structure
(2) Interstitial substitution between planes
(3) Substitution at lattice positions which are vacant due to defects in the structure
(4) Adsorption due to remnant ionic charges.

Since the dolomite structure can in simple terms best be described as essentially the same as that of calcite but with substitution of Mg for Ca in every other cation layer (Reeder, 1983), the above ways of incorporation of

Digitised by the Department of Library Services in support of open access to information, University of Pretoria, 2021

trace elements could also apply to dolomite and by implication also to ankerite, as in the latter case, both Fe and Mg substitute for Ca in every other cation layer.

Major elements

Microprobe analyses, and IRS for CO_2 in some cases, were done on 42 samples and the results are given in Tables IV a - d in the Appendix. The mole percentages, calculated from the partial microprobe analyses, are given in Table IVe in the Appendix.

The sample groups and number of analyses are as follows:

Groups	*Description and locality*	*Number of samples*
C	Ankerite from C Mine lodes	12
N	Ankerite from NAD Mine lodes	9
P	Ankerite-1 from A Mine pockets	12
F	Ankerite-2 from A Mine ankerite-filled fractures	9

Two grains were analysed from each sample and two positions, centre and edge, were analysed for each grain. About 10 % of the grains showed a marked variation in the Fe/Mg ratios in the centres and edges which is related to *chemical zoning*. The analyses of the zoned grains in the Rooiberg ankerites are included in the comparisons and variation diagrams since the average of the Fe/Mg ratios in the centres and edges in the zoned grains is about the same as that in the unzoned grains in the same sample.

Little is known about chemical zoning in ankerite (Reeder, written communication) and it was only referred to in two publications to date. Beran (1975) gave a comprehensive account of the zoning in ankerite and siderite in the Styrian Erzberg, Austria, while Reeder and Dollase (1989) only mention that some of the 25 ankerites studied by them show a variation in the Fe/Mg ratio related to "growth zoning".

On account of clear macroscopic and microscopic evidence for separate mineralising episodes for sample groups P and F, most of the discussion below relates to these two.

Digitised by the Department of Library Services in support of open access to information, University of Pretoria, 2021

Calcium. The mole % $CaCO_3$ in sample groups P and F ranges between 48.91 and 51.87, but about three quarters of the samples have a deficiency (less than 50%) $CaCO_3$. It is interesting to compare the Ca deficiency of the Rooiberg ankerites to that of other naturally occurring and experimentally produced ankerite. The compositions of 20 naturally occurring ankerites world-wide (Goldsmith *et al.*, 1962) show that only three of these have a deficiency of Ca which varies between 0.1 and 1.8 mole % $CaCO_3$. The excess of Ca in the remaining 17 is up to 6.8 mole % $CaCO_3$. An excess of Ca was generally also found in synthetically produced ankerite in studies by Goldsmith (op cit.) and Rosenberg (1967). An excess of Ca rather than a deficiency is more common in other ankerites.

Variation diagrams between mole % $CaCO_3$ and $FeCO_3$, $MgCO_3$ and $MnCO_3$ indicate that:

(1) No trend exists between $CaCO_3$ and either $FeCO_3$ or $MgCO_3$ (not shown).

(2) A medium-strong trend exists between $CaCO_3$ and $FeCO_3$ + $MgCO_3$ (Fig. 37). This indicates that both Fe and Mg substitute for Ca and there is no preference for either of the two.

(3) No positive or negative trend exists between $CaCO_3$ and $MnCO_3$ but the ankerite in fractures generally contain more Mn than that of the pockets (Fig. 38).

Iron and magnesium. Two distinct, but slightly overlapping fields for the ankerite in the pockets and in the fractures are recognised (Fig. 39). In general, the ankerite in the pockets contain more Mg than that in the fractures for any given amount of Fe. The medium-strong negative trends indicate mutual substitution between Fe and Mg.

Manganese. No correlation exists between $MnCO_3$ and $FeCO_3$ or $MgCO_3$. However, a medium-strong trend is recognised between $MnCO_3$ v $FeCO_3$ + $MgCO_3$, indicating that both Fe and Mg substitute for Mn with no preference for either of the two (Fig. 40). Except for two or three points, distinctly separated fields are recognised for the pockets and the fractures with more Mn in the ankerite of the fractures as is also indicated in Fig. 41.

Digitised by the Department of Library Services in support of open access to information, University of Pretoria, 2021

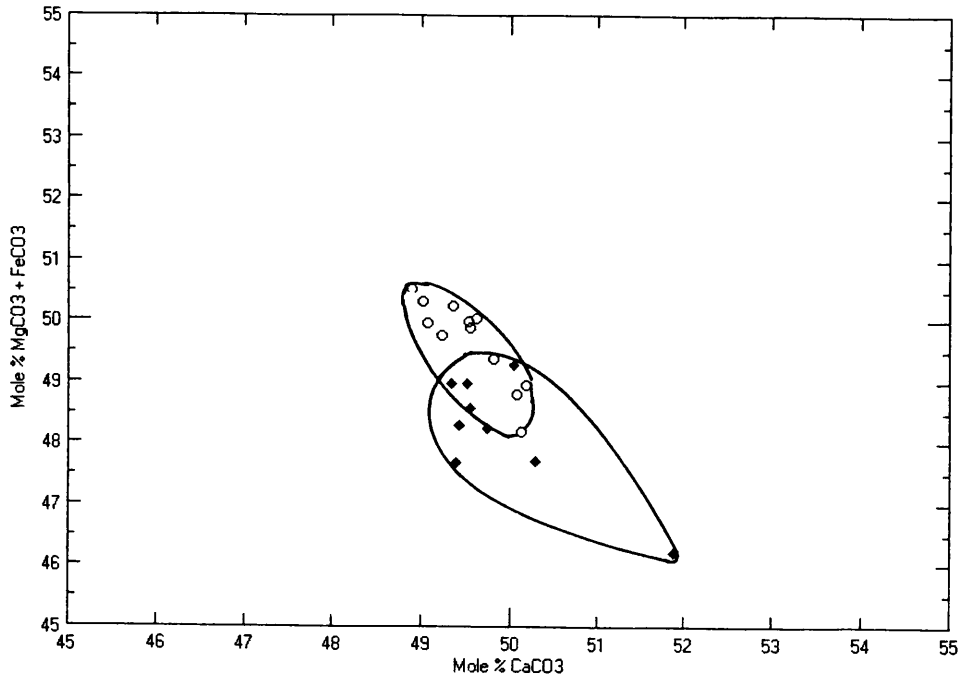

Fig. 37 - Variation diagram of $CaCO_3$ v $MgCO_3$ + $FeCO_3$. A negative trend indicates that both Fe and Mg substitute for Ca. Pockets = circle, ankerite-filled fractures = diamond.

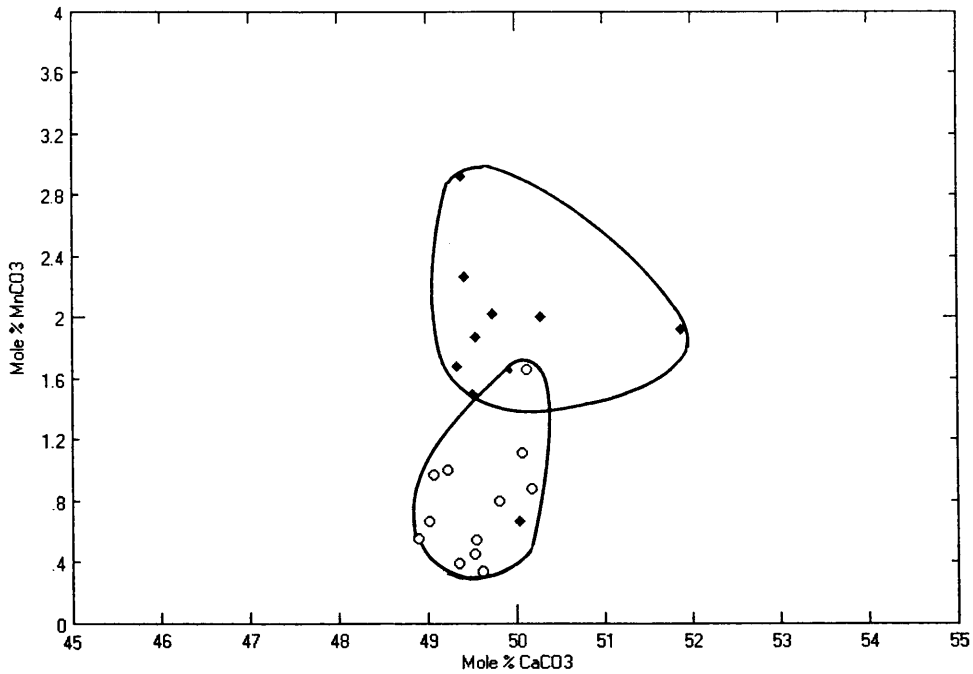

Fig. 38 - Variation diagram of $CaCO_3$ v $MnCO_3$. No trend is apparent but the ankerite in fractures contain more Mn than that in the pockets. Pockets = circle, ankerite-filled fractures = diamond.

Digitised by the Department of Library Services in support of open access to information, University of Pretoria, 2021

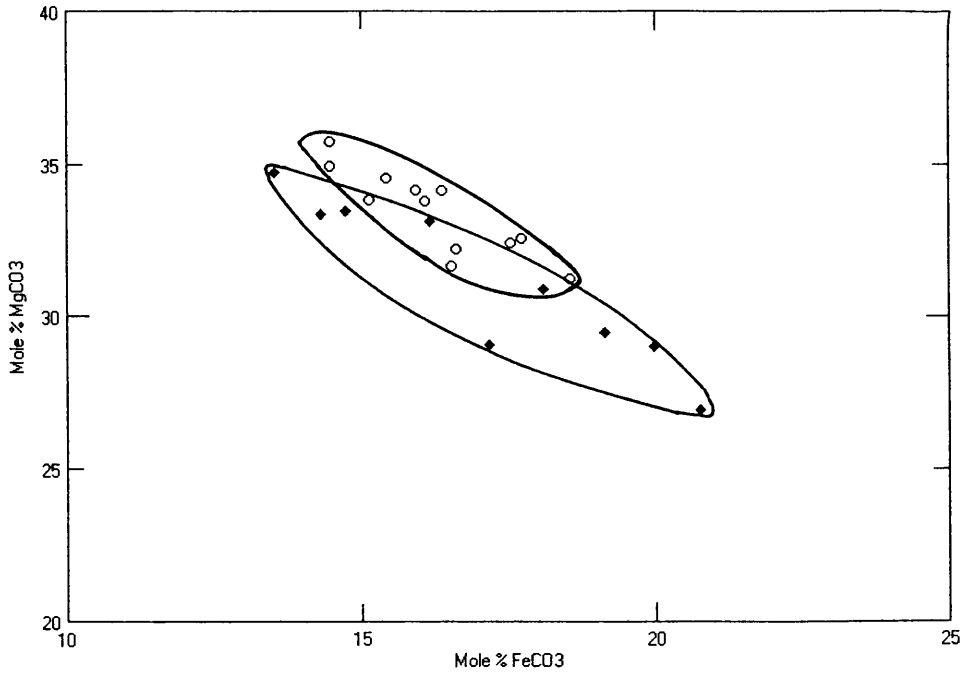

Fig. 39 - Variation diagram of $FeCO_3$ v $MgCO_3$. Overlapping fields for the ankerite in fractures and that of the pockets are apparent. In general the ankerite in the fractures contain more FeCO3 than that in the pockets. Pockets = circle, ankerite-filled fractures = diamond.

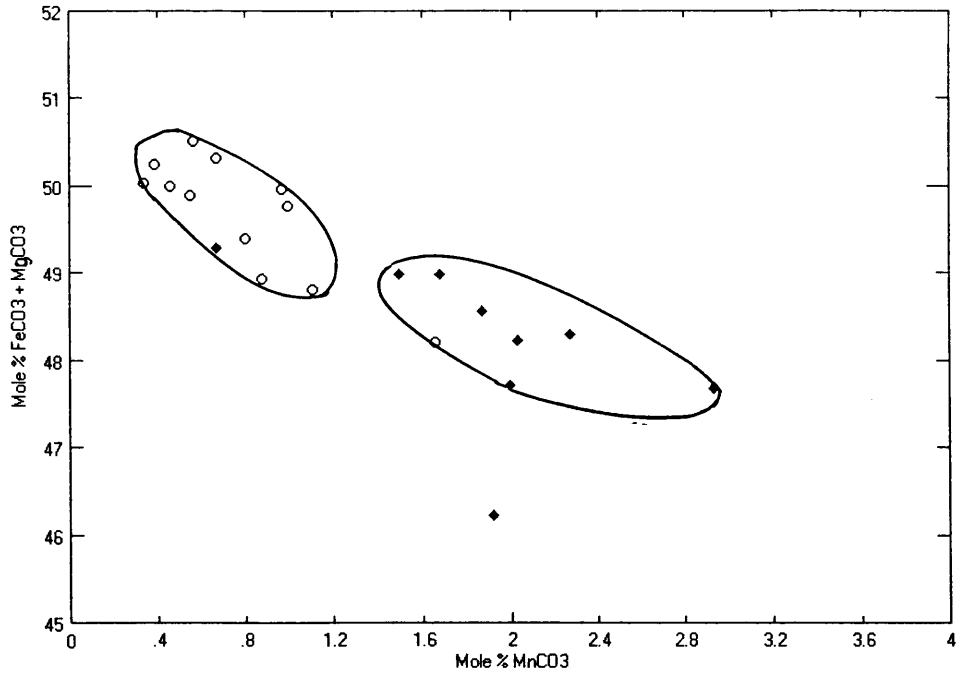

Fig. 40 - Variation diagram of $MnCO_3$ v $FeCO_3$ + $MgCO_3$. Separate fields for the ankerite in fractures and in pockets are apparent. In general, the ankerite in fractures contain more $MnCO_3$ than that in pockets. Pockets = circle, ankerite-filled fractures = diamond.

Digitised by the Department of Library Services in support of open access to information, University of Pretoria, 2021

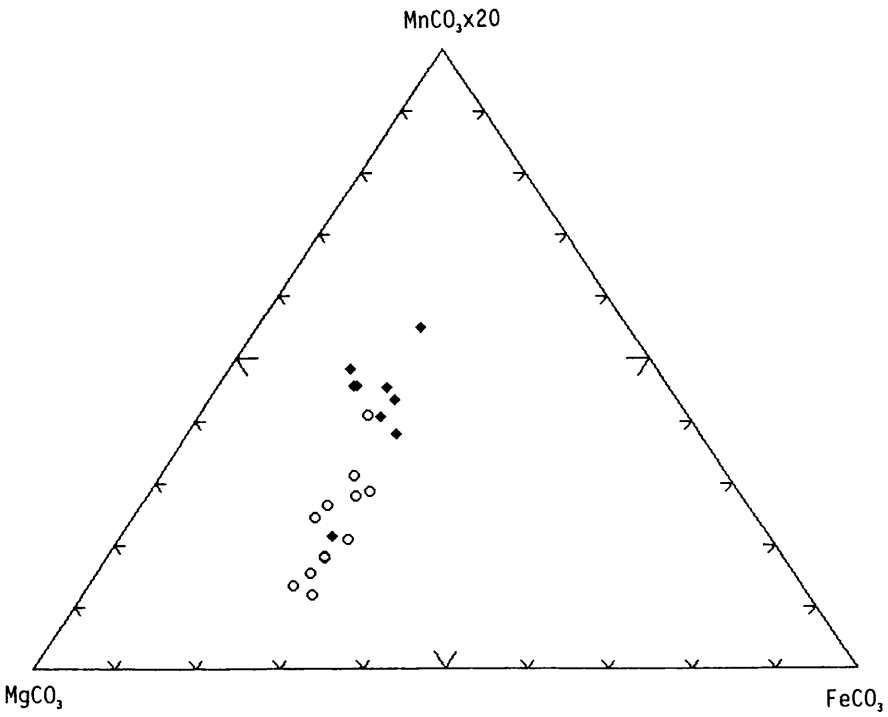

Fig. 41 - Ternary diagram $MnCO_3$ - $MgCO_3$ - $FeCO_3$. The $MnCO_3$ content is the most conspicuous diagnostic difference in ankerite from the pockets and that from the fractures.
Pockets = circle, fractures = diamond.

To summarise:

(1) Ca and Mn do not substitute mutually but Fe and Mg do.

(2) Fe + Mg substitute for Ca and Mn and there appears to be no preference for either Fe or Mg.

(3) The ankerite from fractures contains significantly more Mn, slightly less Ca and more Fe than that from the pockets.

(4) The major element composition of ankerite from fractures differs from that in pockets and Mn is the most diagnostic element.

Brief mention must be made of the possible application of the iron content of ankerite in geothermometry. To date, only two experimental studies on the ternary system $CaCO_3$-$MgCO_3$-$FeCO_3$ have been conducted; one by Goldsmith *et al.* (1961) and the other by Rosenberg (1967). $MnCO_3$ was excluded and the results may therefore not apply to Rooiberg ankerites. However, there are clear inconsistencies in the experimental results. Moreover, some of the more Fe-rich varieties of naturally occurring ankerites would have formed at 700° C -

Digitised by the Department of Library Services in support of open access to information, University of Pretoria, 2021

a temperature clearly too high. Goldsmith *et al.* (op cit) concluded from their studies that the use of the Fe-content for a geologic thermometer is suspect and Goldsmith (1983) reiterated this. Beran (1975), in his microprobe work of the Styrian ankerites, also questioned the validity of the conclusions of Rosenberg (1967).

The Mn and Fe contents of ankerite are probably controlled by the Eh in fluids of similar bulk chemical composition. High oxidation potentials will lead to lower $FeCO_3$ and $MnCO_3$ contents of ankerite relative to $MgCO_3$, independent of the temperature.

The difference in particulary the Mn-content of the ankerite in the pockets, on the one hand and of that in the fractures on the other, may be the result of a difference in the chemical composition of the ore-forming fluids or different physical-chemical conditions. In any case, separate mineralising episodes are indicated.

Trace elements

The following 19 trace elements in ankerite were determined by means of XRF, and those which show a variation in their concentration are indicated in bold: Ba, ***Cu***, Cr, Ga, Hf, Mo, Nb, Ni, ***Rb***, ***Sc***, ***Sr***, Ta, Th, U, ***V***, W, ***Y***, ***Zn***, Zr.

Since no published information on the site occupancies of trace elements in ankerite is available, some of the factors governing the incorporation of trace elements in dolomite may be used as a guide. This should, however, be done with caution because temperature of formation may have a major effect. Kretz (1982) argued that in dolomite, trace elements with ionic radii larger than Ca^{2+} will substitute proportionally more in the Ca sites, whereas those smaller than Ca^{2+} in the Mg, or Mg + Fe sites in the case of ankerite.

The variation diagrams indicate that *no* correlation exists between the major elements and the trace elements selected according to these criteria. In fact, numerous variation diagrams have been constructed using different variables but the only variation diagrams in which trends are present are those where Sc is one of the variables. This is attributed to the fact that Sc values in the C Mine ankerites are relatively high.

Digitised by the Department of Library Services in support of open access to information, University of Pretoria, 2021

Some separation of the fields occupied by the C, N, P and F sample groups is obtained by using *discriminant analysis* of the trace elements indicated in bold above, Sc also being the main contributor. However, overlapping fields are obtained for sample groups P and F only and it appears that trace elements have a limited application in discriminating between ankerite in the pockets and in the ankerite-filled fractures.

10.3 Cassiterite

A microscopic examination and trace element determinations were carried out and comparisons have been made between A Mine cassiterite-1 and -2 as well as with cassiterite from the NAD and C Mines. In addition, the Rooiberg cassiterite was also compared with cassiterite from Zaaiplaats, Mutue Fides, Mmbabane (Swaziland) and Erongo (Namibia).

10.3.1 A microscopic comparison of A Mine cassiterite-1 and -2

No obvious differences exist between cassiterite-1 and -2 from the A Mine. Apart from grain size and intensity of zoning, there are also no significant differences between cassiterite-2 and cassiterite from the NAD and C Mines and from localities outside the Rooiberg tin-field. At the B Mine, however, Labuschagne (1970a) reported a fine-grained and lighter coloured cassiterite, which was apparently formed at a later stage than a coarse-grained and darker coloured variety.

The textural relationship between cassiterite-1 and -2 and ankerite, however, provides valuable evidence regarding the relative ages of the two cassiterite phases. In the interior of the pockets, ankerite-1 replaced cassiterite-1. Cassiterite-2 formed around the earlier pockets in the 19N, U30 and Jewel Box Sections of the Mine (Chapter 9.3) and in the latter it is intimately associated with disseminated ankerite. The thin sections of four samples from the Jewel Box Section clearly show that cassiterite-2 replaced earlier formed ankerite (Figs 42 and 43), thus providing evidence of two mineralising events.

Digitised by the Department of Library Services in support of open access to information, University of Pretoria, 2021

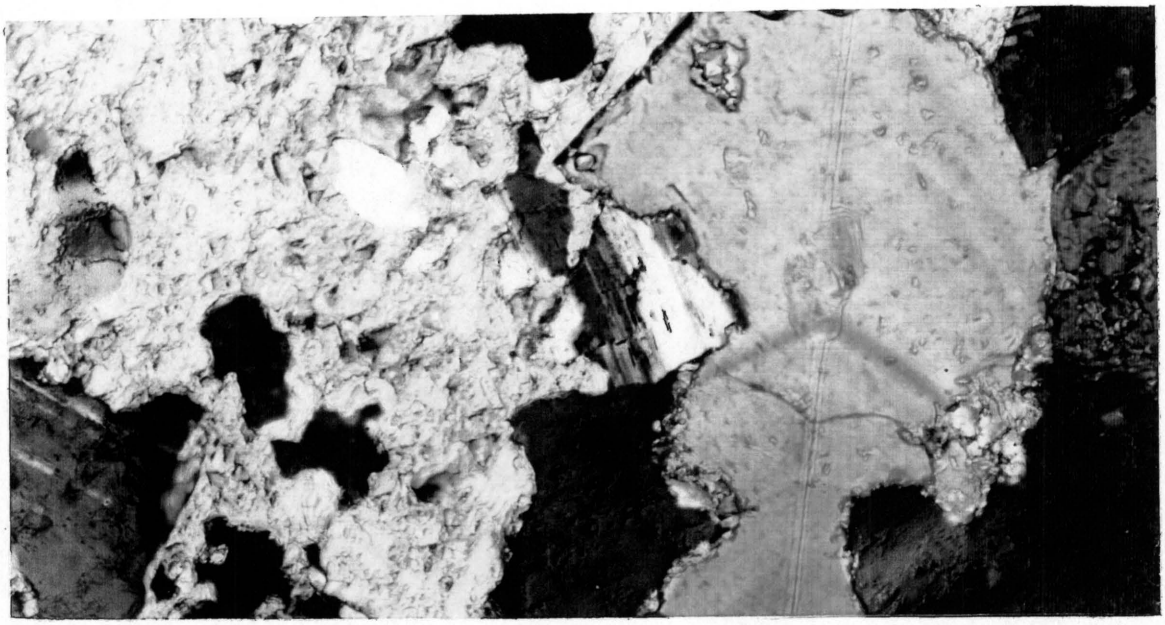

Fig 42 - Cassiterite-2, large subhedral gold-coloured grain at the right, replaced earlier-formed light buff-coloured ankerite. The light- to dark-grey minerals are feldspar and quartz of the arkosite, partly replaced by ankerite.
+N X200 Sample 259L0
A Mine - Jewel Box Section - 680′ Level

Fig 43 - Cassiterite-2, large, subhedral grain with predominantly magenta interference colour, replacing earlier-formed light buff-coloured ankerite. The grey to dark-grey minerals are feldspar and quartz of the arkosite.
+N X200 Sample 250L7
A Mine - Jewel Box Section - 680′ Level

Digitised by the Department of Library Services in support of open access to information, University of Pretoria, 2021

10.3.2 Trace element content

In a purely ionic model cassiterite would consist of close packed O^{2-} ions with Sn^{4+} ions occupying half the octahedral interstices. However, since the length of the Sn-O bonds in cassiterite is 20,5 nm and the sum of the ionic radii is 21,1 nm, it is evident that electron sharing between Sn and O occurs. This gives cassiterite the property of a n-type semiconductor and permits a wide range of impurity elements to enter the structure diadochically (Farmer *et al.*, 1991).

The documented studies are dominated by the trace elements Fe, Ti, Nb, Ta, Mn, W, Zr and Hf and in only two studies were REE and elements like Sc, Ga, Rb and In also considered.
This is ascribed to the fact that

(1) The former mentioned trace elements are the most common ones present in cassiterite
(2) Concentrations are high and may reach 1 per cent or more
(3) Their ionic radii are very similar to that of Sn^{4+}. Substitution is readily affected and can be homovalent e.g. Ti^{4+} or heterovalent, involving pairs, e.g $(Ta, Nb)^{5+}$ - Fe^{3+}, to balance the valency.

The studies can be broadly divided into three categories:

(1) Correlation between trace element content and zoning and/or cathodoluminescence.
(2) Mechanism of substitution into the crystal structure of cassiterite.
(3) Physico-chemical control.

A summary of the studies in each of these categories is given in Table 9.

10.3.3 Comparison of the trace element content in cassiterite-1 and -2

Six samples form the A Mine containing suspected cassiterite-1 and nine containing suspected cassiterite-2 were analysed by means of instrumental neutron activation analysis (INAA). The sample selection of the two types of cassiterite was done underground and was based on their macroscopic distribution. On account of technical difficulties, it was not possible to

Digitised by the Department of Library Services in support of open access to information, University of Pretoria, 2021

Table 9 - Summary of trace elements studied in cassiterite and main conclusions as documented in the literature

Locality (Number of samples) (If available)	Trace elements	Main conclusions	References
Correlation between trace elements and zoning and/or cathodoluminescence			
Various (40)	Ta, Nb, Fe, Ti	Cathodoluminescence related to Ta and Nb	Hall & Ribbe (1971)
Maritime	Fe, Ti	(1) Zoning related to Fe, Ti (2) Relative abundance related to temperature Fe = Low temp; Ti = High temp	Kanischcheva & Romanenko (1977)
Galicia, Spain (9)	Fe, Ta, Ti, Nb	(1) Dark zones enriched with Ti, Fe, Nb, Ta (2) Fe^{3+} depends on ratios of Fe^{3+} and $(Nb,Ta)^{5+}$	Izoret et al. (1985)
Morocco	Ti, Ta, Fe, Nb, Mn	Darker zones = Fe, Ti, Nb	Giullani (1987)
Mechanism of substitutions in crystal structure of cassiterite			
Various (15)	Fe, Mn, Ti, Ta, Nb	Unit cell volume of SnO_2 related to concentration of trace elements	Clark et al. (1976)
Cornwall (16)	Fe, Si, Nb, W, In, Ti, Ta, Ir	Magnetic cassiterite contains inclusions of wolframite	Moore & Howie (1979)
Various - Five continents (190)	Ta, Nb, W, Fe, Mn	Coupled substitutions: $2(Ta, Nb)^{5+} + (Fe, Mn)^{2+} = 3Sn^{4+}$ $W^{6+} + 2Fe^{3+} = 3Sn^{4+}$	Möller et al. (1988)
Experimental	Fe, Ti, Na, Nb	Substitution $2Sn^{4+} \rightarrow Fe^{3+} + Nb^{5+}$	Ruck et al. (1989)
Physico-chemical control			
Bolivia (50)	W, Nb, Ta, Zr, Ti, Ga, Zn, Pb, Sr, As, V, F, Cl	W, Nb, Ta, Zr, Ti, Ga correlated with geotectonic setting	Schneider et al. (1978)
Various	W, Ga, Sc, Ti, Zr, Hf, Ta, Nb	(1) Decrease in time in province: Ta, Nb, decrease. W, Ga, Sc also decrease (2) W controlled by chemistry of the fluids	Möller et al. (1981)
Southeastern Desert, Egypt (10)	Nb, Ta, W, Zr, Ti, Mn, Pb, Cu	Nb used as indicator of temperature of formation	Soliman (1982)
Various continents (117)	Zr, Hf	Zr/Hf: Pegmatite = ± 5; Hydrothermal = ± 30	Möller & Dulski (1983)
Cornwall	Ti, Fe, W	(1) Fe related to conc. in fluids (2) Ti reflects changes in solution chemistry (3) Cathodoluminescence indicates sector zoning	Farmer et al. (1991)
Mole Granite, Australia	REE In,Cs,Rb,Sr,Zr,Sc,Be,As,Sb,Bi	(1) REE reflects chemistry of Granite (2) Rb, Cs, Sc in granite-hosted cassiterite	Plimer et al. (1991)

Digitised by the Department of Library Services in support of open access to information, University of Pretoria, 2021

analyse for Ti, Nb and W - three of the most commonly found trace elements. For comparative purposes this is, however, not too serious since Ti and Nb are related to zoning, and unless microprobe analyses are also done, these elements are of limited use in bulk chemical analyses. Moreover, Ti and W may, in addition to isomorphous substitutions, also be present as rutile (Leube and Stumpfl, 1963) and wolframite inclusions (Moore and Howie, 1979), which may yield misleading bulk analytical results.

A cursory comparison of the trace element content (Table VII - Appendix) indicates significant differences in Na, Gd, Th and Zr between cassiterite-1 and -2. Accepting a value equal to the lower analytical detection limit for those analyses below the detection limit, the arithmetic averages are as follows:

	Na	**Gd**	**Th**	**Zr**
Cassiterite-1	267 ± 136	2 ± 2	4 ± 3	99 ± 82
Cassiterite-2	1066 ± 815	14 ± 22	1 ± 1	8 ± 0

Additional statistical treatment involved a stepwise regression to ascertain which elements should be used in discriminant analysis and the results are as follows:

Elements	**R-squared** (95 % confidence level)
Fe, Ca, Na, La, Sm, Gd, Sc, Th, U, Zr	0,96335
Na, La, Sc, Zr	0,92494
Na, La, Zr	0,86963
La, Zr	0,71426
Zr	0,62498

The difference in the R-squared value between all ten elements and the four selected by the stepwise regression, Na, La, Sc and Zr, is insignificant and is in fact very high for these four elements at 0,92494. These four elements were used in the discriminant analysis from which the plot of the discriminant function values for cassiterite-1 and -2 (Fig. 44) was constructed. Two well separated fields representing cassiterite-1 and -2 are recognised indicating that cassiterite-1 can be clearly distinguished from -2, based on Na, La, Sc and Zr.

If more elements are forced out, R-squared decreases rapidly but is still reasonably high at 0,62498 for Zr only. This implies that only one element, Zr, can be used to distinguish between cassiterite-1 and -2.

Digitised by the Department of Library Services in support of open access to information, University of Pretoria, 2021

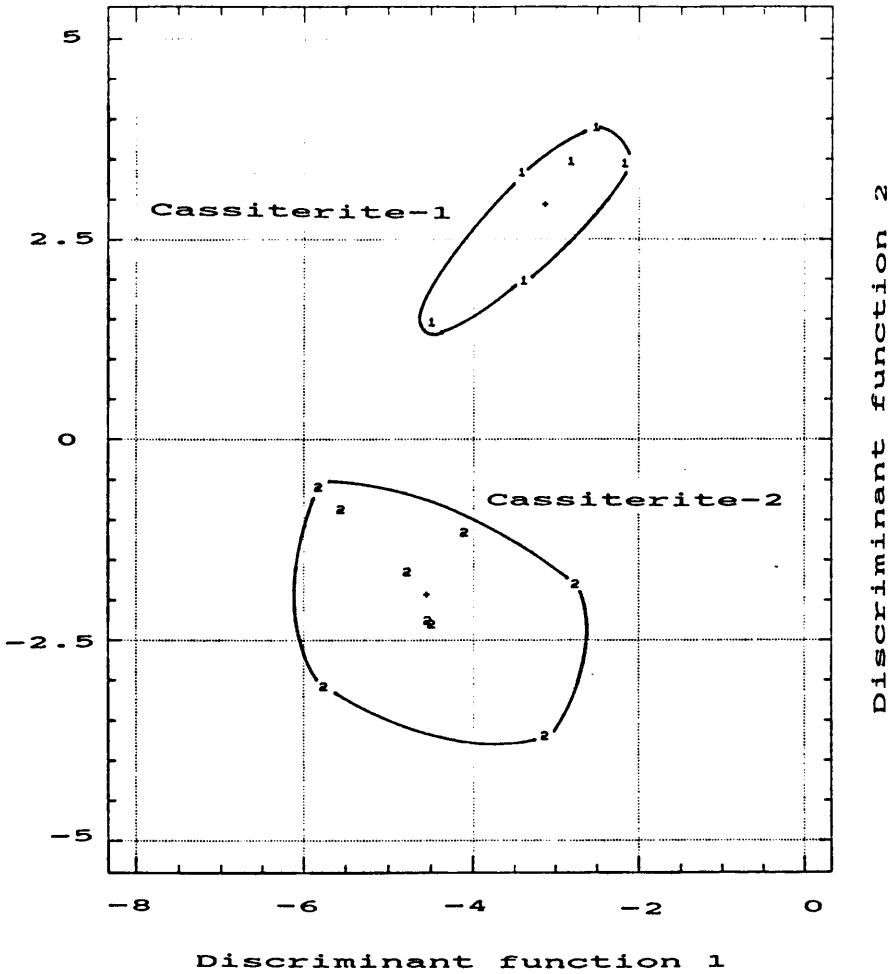

Fig. 44 - Plot of discriminant function values by using the trace element contents of Na, La, Sc and Th in cassiterite from the A Mine. A clear separation between the fields of cassiterite-1 and -2 is indicated.

10.3.4 Comparison of the trace element content in cassiterites from the A and C Mines

The same statistical analysis as before was applied and the results of the stepwise regression are as follows:

Elements	R-squared (95 % confidence level)
Fe, Ca, Na, La, Co, Gd, Lu, Sb, Sc, Th, U, Zr	0,96894
*	
Ca, La, Gd, Sb, Sc, Th, Zr	0,94557
*	
La, Sc, Th, Zr	0,84842
*	
Sc, Th	0,79172
Sc	0,68687

* Intermediate steps not shown

Digitised by the Department of Library Services in support of open access to information, University of Pretoria, 2021

From this it is concluded that while excellent discrimination between A Mine cassiterite-1 and -2 and C Mine cassiterite will be obtained by using Ca, La, Gd, Sb, Sc, Th and Zr (R-squared = 0,94557) in the discriminant analysis, Sc alone (R-squared = 0,68687) is adequate to discriminate between A and C Mine cassiterite. The Sc content in the C Mine cassiterite is consistently high at 152 ± 31 as against 9 ± 6 for A Mine (Table VII - Appendix).

Fig. 45 represents the plot of the discriminant function values using these seven elements and distinct separate fields for A Mine cassiterite-1 and -2 and C Mine cassiterite are recognised. In Fig 46, only Sc and Th were used and while the A Mine cassiterite fields overlap, they are clearly separated from C Mine.

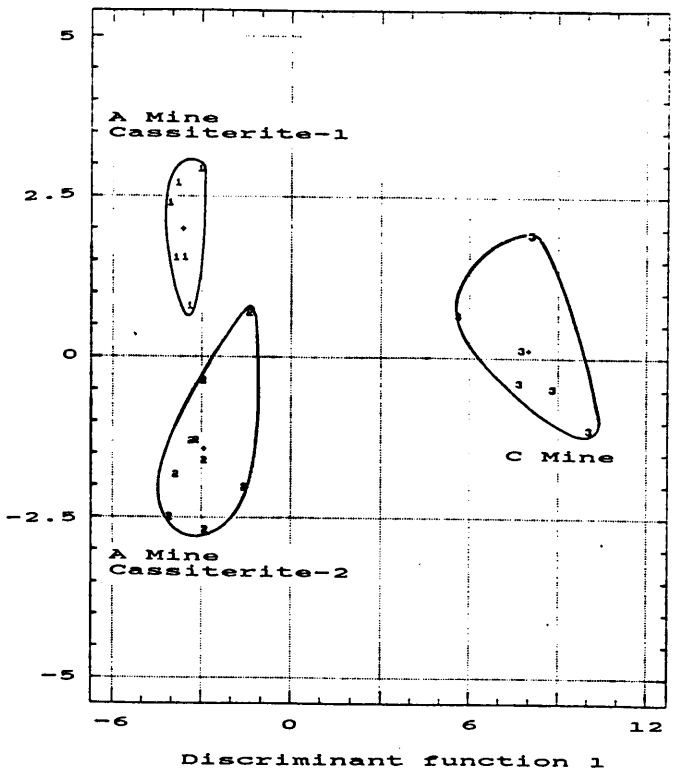

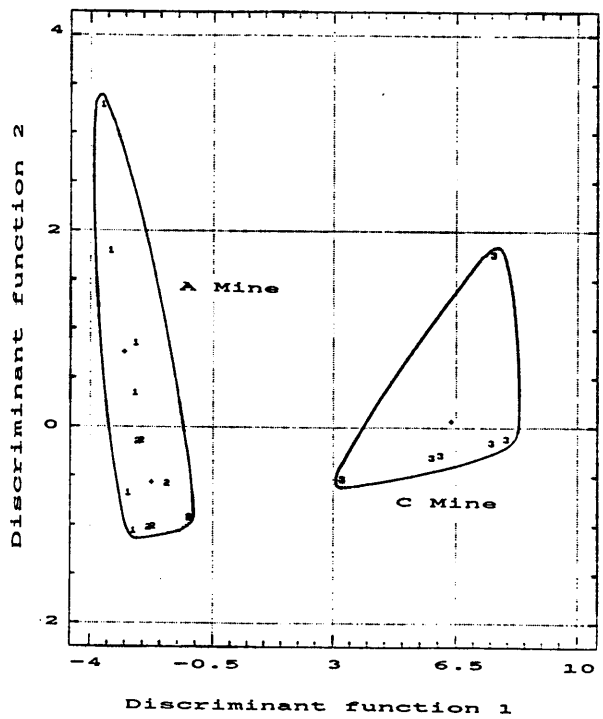

Figs. 45 (left) and 46 (right) - Plot of discriminant function values of A and C Mine cassiterites showing a clear separation between the fields of the A and C Mines. In Fig. 45, Ca, La, Gd, Sb, Sc, Th and Zr were used as against Sc and Th only in Fig. 46.

Digitised by the Department of Library Services in support of open access to information, University of Pretoria, 2021

11. EVOLUTION OF THE ORE-FORMING FLUIDS

This chapter deals with the *source* of the ore-forming fluids, their *migration history*, the changes in the composition of the fluids during *mineral deposition* and, finally, *polyphase mineralisation.*

11.1 Evolution of the ore-forming fluids in the granite

11.1.1 The alternative models

Tin deposits are almost invariably associated with granitic plutons and more than 99 per cent of the historic world production of tin is from deposits directly or indirectly related to granitic rocks (Lehmann, 1990). This close relationship is so ubiquitous that it was in fact recognised two centuries ago (Lehmann, 1990 quoting Werner, 1791 and Zimmermann, 1808). Historically, the tin deposits of the Bushveld Complex have also been related to the granitic rocks and particulary those in the Rooiberg area (Recknagel, 1908). Despite this, some authors (Hunter, 1976; Rozendaal *et. al*, 1986) proposed that serious consideration should be given to an alternative model apparently implying a possible volcanic origin for the tin.

In the light of these apparently conflicting views, three possible hypothetical alternatives for the origin of the Rooiberg tin deposits will be considered, viz. (1) a genetic relationship to magmatism older or younger than the Bushveld Complex, (2) the volcanic model as mooted by Hunter (1976) and Rozendaal *et. al* (1986) and (3) a synsedimentary origin of the tin which was later redistributed and concentrated by fluids related to the Bushveld granite(s)

(1) Mineralisation caused by magmatism other than the Bushveld. In view of the possibility that the sedimentary host rocks of the tin mineralisation at Rooiberg may be uplifted floor rocks of the Bushveld Complex, now forming a detached roof pendant, a possible genetic relationship of the mineralisation to much older source rocks can be considered. In this case several possibilities exist: The quartz porphyry of the Makwassie Formation, dated at 2709 ± 4 Ma by Armstrong *et al.* (1990) could be a candidate, but the closest known occurrence of this is 200 km south-west of the Rooiberg Fragment. Basalt of the Klipriviersberg Group is dated at 2714 ± 8 Ma (Armstrong *et al.*, 1990)

Digitised by the Department of Library Services in support of open access to information, University of Pretoria, 2021

but nowhere is tin known to be associated with basalt in significant quantities. Still older magmatism such as the granitic rocks in the Makoppa Dome, north-west of Rooiberg can also be discounted, since tin has not been reported to be associated with this granite. The only worthwhile example of igneous rocks younger than the Bushveld Complex are those of Karoo age but they can also be discounted as likely candidates for the mineralising fluids since tin is nowhere reported to be present in, or associated with them.

Mineralisation related to magmatism other than the Bushveld episode is therefore discounted.

(2) Mineralisation derived from Rooiberg volcanics. The alternative hypothetical source for the ore-forming fluids, namely volcanics, was initially proposed by Hunter (1976). Tin deposits associated with rhyolite are common; in the Bushveld it occurs in the dormant Union Tin Mine and is closely associated with the Union Tin shale (Menge, 1963) which according to R.H. Rastall (pers. comm.) may be a tuff. Tin-bearing rhyolite of the Black Range, New Mexico is another example (Rye *et al.*, 1990; Reece *et al.*, 1990) and the mineralisation is ascribed to a process of eruptive fountaining (Duffield, 1990). At Rooiberg it is difficult to reconcile the ore bodies with the rhyolite of the Rooiberg Group. Dykes which may represent feeders for the rhyolite were neither found on surface nor underground. A genetic relationship would therefore imply that the ore-forming fluids, whether dispersed by fountaining or another process, had to move *downwards* to mineralise the arkosite a few hundred metres *below the base* of the rhyolite. Clearly, this cannot be the case and proponents of a volcanic origin for the Rooiberg tin deposits must be more specific regarding the migration paths of the ore-forming fluids.

(3) Synsedimentary origin for the tin. This hypothesis presupposes that the tin had been in place prior to granite magmatism. Söhnge (1963) suggested that the pipes in the Zaaiplaats area could have formed by granitisation of sediments which contained tin deposits. He did not elaborate on the primary origin of these deposits but implied that it was in fact earlier than the granite.

Digitised by the Department of Library Services in support of open access to information, University of Pretoria, 2021

The arkosite at Rooiberg contains a considerable amount of disseminated tin, calculated to be more than the tin contained in the known ore-bodies. The presence of this disseminated tin was indicated by both the regional geochemical programme of the Council for Geoscience (Chapter 8) and also by analyses of the cores of exploration boreholes.

A histogram (Fig. 47) shows the distribution of tin in the upper part of the arkosite in the vicinity of the A Mine. The tin values were determined from the cores of surface boreholes and only the values below 50 ppm were used in the compilation. Values up to 2000 ppm were encountered in the cores but these obviously indicate mineralised portions in the arkosite.

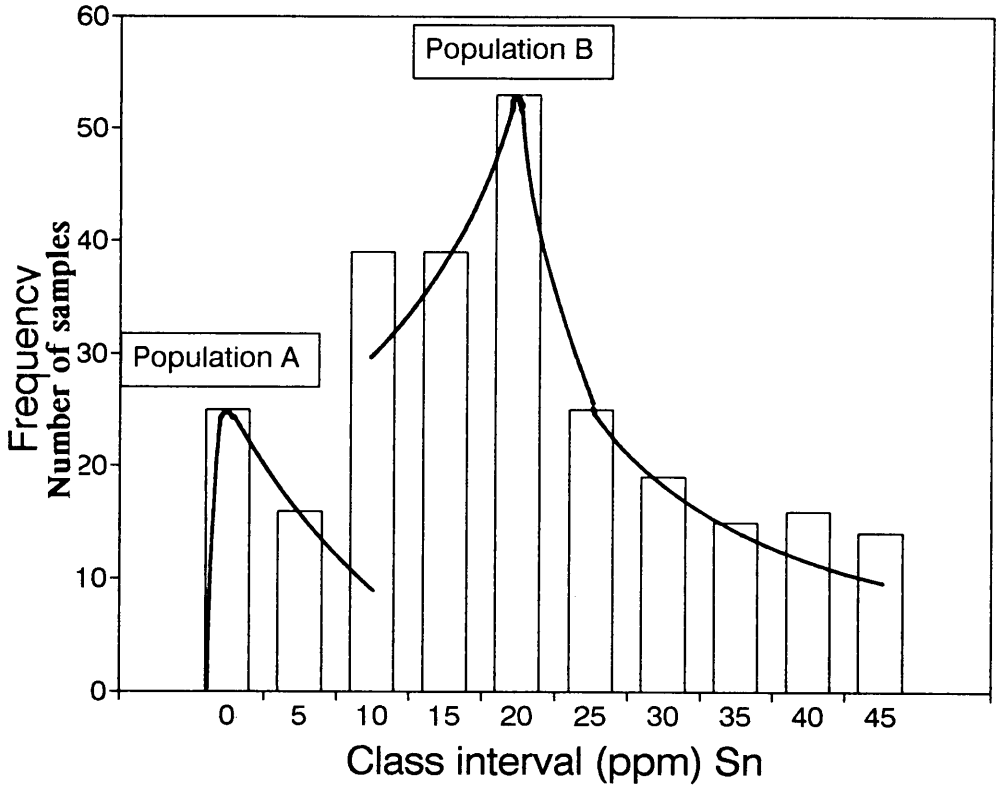

Fig. 47 - Distribution of Populations A (synsedimentary tin) and B (hydrothermally introduced tin) in arkosite.

The overall distribution is bimodal and two curves, or populations A and B, can be recognised. Both are positively skewed, typical of the distribution of trace elements in rocks as first formulated by Ahrens (1957) and later substantiated by many workers particulary Rose *et al.* (1979) and Sinclair (1991).

Digitised by the Department of Library Services in support of open access to information, University of Pretoria, 2021

Population A represents the background distribution of tin in the unmineralised arkosite, and with the upper threshold of 50 ppm, comprises 18% of the total. This tin was derived from the same provenance as the sediments, which Rozendaal *et al.* (1986) have shown to be tonalitic-granodioritic. Population B represents the hydrothermal overprint of the tin added to the arkosite and with the 50 ppm threshold, comprises 82% of the total.

If population B and the values above 50 ppm represent reconstituted tin, this tin could only have been derived from population A and A would have disappeared. If it did not, and A represents the residual tin after tin had been reconstituted to form B and the other deposits, then it becomes impossible to explain the positively skewed log normal distribution of A since it would require that the digestion of tin followed a positively skewed log normal pattern.

A synsedimentary origin for the tin which later was reconstituted by mineralising fluids to form ore deposits is therefore discounted.

It is concluded that the Bushveld granites were the only primary source for the ore-forming fluids.

11.1.2 Physical evolution of the ore-forming fluids

The physical evolution of the ore-forming fluids is considered on the premise that the Bobbejaankop Granite, geochemically the most evolved of the four granites, was the source for these fluids. It is also accepted that both the magma from which the fluids evolved and the fluids themselves were encapsulated by the granophyric granite.

West of the Rooiberg Fragment, the variation in the TEDI of the samples from the Bobbejaankop Granite is too small to ascertain the direction of crystallisation. However, it is assumed to have proceeded from the rim towards the core of the Bobbejaankop Granite scallop.

Digitised by the Department of Library Services in support of open access to information, University of Pretoria, 2021

The average fluorine content of the Bobbejaankop Granite is 0,25% as against 0,23% for the granophyric granite, 0,21% for the Klipkloof Granite and 0,10% for the Nebo Granite. The (slightly) higher fluorine content of the Bobbejaankop Granite depressed the solidus temperatures more than in the other granites and also prevented quenching. Cooling therefore proceeded to temperatures below that where without F, the melt would have solidified.

After the initial crystallisation of anhydrous minerals, the hydrous fluids exsolved and concentrated along the rim. The water content in the melt increased with increasing crystallisation. At some point, the lithostatic pressure could no longer sustain water in the melt and boiling (the so-called second boiling point of a magma) resulted. Depending on the temperature and pressure, CO_2, SO_2 and Cl_2 also boiled off. The residual elements e.g. Mg and Ca which remained in the hydrous fluids after all the Bobbejaankop Granite had solidified, together with the vapour (from boiling), accumulated between the solidified Bobbejaankop Granite and the enclosing granophyric granite.

The physical separation of the ore-forming fluids from the solidifying silicates in the Bobbejaankop Granite as outlined above, is very similar to the elegant model developed by Jackson *et al.* (1982) for Sn-W deposits in general, and adopted by Eugster (1985). In essence this model is an extension of that proposed by Burnham (1979) and really has its roots in the work of Niggli and Morey during the 1910s-1930s. Jackson *et al.* (1982) proposed that crystallisation of anhydrous phases, largely feldspars, leads to the formation of an H_2O-saturated carapace and, through vesiculation and boiling, separation of an aqueous phase. When the pressure of the fluid exceeds the strength of the wall rock, hydrofracturing occurs and an extensive fracture system develops, permitting escape of the fluids and marking the onset of hydrothermal circulation. Eugster (1985) pointed out that the circulating fluids cannot penetrate the still-liquid centre of the granite body which is impervious to the addition of water, but hydrothermal fluids may react with solidified granite. In the Bobbejaankop Granite, however, it was essential for the formation of tin deposits that these fluids penetrated and migrated pervasively through the semi-solidified crystal mush.

Digitised by the Department of Library Services in support of open access to information, University of Pretoria, 2021

11.1.3 Geochemical evolution of ore-forming fluids in the granite

It is theoretically possible to determine the composition of the exsolved fluids if the following are known:

(1) The combined composition of the deposit(s) and the wall rock alteration.

(2) The composition as well as the amount of fluids which did not form products but escaped from the hydrothermal system during or after mineralisation.

(3) The nature of the fluids which took part in the mineralising process but were derived from elsewhere e.g. meteoric water.

For a number of reasons it is impossible to determine these exactly and the most important limitations are:

(1) In replacement type ore-bodies both fluid and pre-existing rock compositions played a role.

(2) Wall rock alteration is invariably present but the extent is not always known or difficult to calculate. Truly large quantities of fluid may be required during various types of wall rock alteration such as silicification, felspathisation, sericitisation etc.

(3) Some elements e.g. chlorine, were undoubtedly present as indicated by fluid inclusion studies and may have played an important role during the mineralisation. However, they never formed any permanent *in situ* products and escaped during or after mineralisation.

The best that can be achieved is an approximation of the composition of the exsolved fluids. This was done for the fluids responsible for the A Mine mineralisation, and this mine was chosen for the following reasons:

(1) The ore-bodies (pockets) are relatively simple in composition as far as main minerals are concerned. They are well zoned and relatively large compared to the thin bedded lodes, and lend themselves to the macroscopic determination of the minerals.

(2) Such determinations have already been done by Haikney (1986) and in total, she determined the main mineral composition of 996 pockets. Her raw data were used in this study.

Digitised by the Department of Library Services in support of open access to information, University of Pretoria, 2021

(3) The A Mine pockets were the first deposits formed and constitute the bulk of the mineralisation at the A and NAD Mines.

The data of Haikney (op cit.) were averaged out and the following bulk mineralogical composition of the pockets of the A Mine was calculated:

Mineral	**Volumetric %**	**Mass %**
Tourmaline	46 ± 6	45
Ankerite	21 ± 7	20
Sericite/chlorite	15 ± 9	14
K-feldspar	5 ± 5	4
Quartz	4 ± 3	3
Pyrite	4 ± 3	6
Chalcopyrite	3 ± 3	4
Cassiterite	2 ± 2	4
Total	100	100

The difference in the value of 4% by mass for cassiterite and an average mine "blast value" of 0.4 % Sn (0,5% SnO_2) is the result of dilution of the pocket-ore by unmineralised arkosite.

From the mineralogical composition of the pockets as well as the determined averaged compositions of tourmaline and ankerite (Tables VI and IV a - d - Appendix) and the idealised chemical composition of the other minerals, the chemical composition of the pockets could be calculated (Table 10). This is compared with the averaged composition of the Bobbejaankop Granite (calculated from Table III - Appendix) and the averaged composition of the arkosite in the tin-zone (Rozendaal *et al.* 1995b) (Table 11).

Table 10 - Composition of the A Mine pockets calculated from the relative mass %.

	SiO2	TiO2	Al2O3	FeO	MnO	MgO	CaO	Na2O	K2O	CO2	S	B2O3	SnO2	Cu
Tourmaline	17.63	0.31	14.04	4.82	0.00	3.48	0.32	1.15	0.02	0.00	0.00	5.03	0.00	0.00
Ankerite	0.00	0.00	0.00	2.76	0.21	2.61	5.91	0.00	0.00	9.18	0.00	0.00	0.00	0.00
Sericite	5.76	0.00	6.67	0.00	0.00	0.00	0.00	0.00	2.05	0.00	0.00	0.00	0.00	0.00
K-feldspar	2.38	0.00	0.92	0.00	0.00	0.00	0.00	0.00	0.84	0.00	0.00	0.00	0.00	0.00
Quartz	3.00	0.00	0.00	0.00	0.00	0.00	0.00	0.00	0.00	0.00	0.00	0.00	0.00	0.00
Pyrite	0.00	0.00	0.00	2.15	0.00	0.00	0.00	0.00	0.00	0.00	1.66	0.00	0.00	0.00
Chalcopyrite	0.00	0.00	0.00	0.98	0.00	0.00	0.00	0.00	0.00	0.00	0.72	0.00	0.00	1.43
Cassiterite	0.00	0.00	0.00	0.00	0.00	0.00	0.00	0.00	0.00	0.00	0.00	0.00	4.00	0.00
Total	28.77	0.31	21.62	10.70	0.21	6.09	6.23	1.15	2.92	9.18	2.38	5.03	4.00	1.41

Digitised by the Department of Library Services in support of open access to information, University of Pretoria, 2021

Table 11 - Averaged chemical composition of Bobbejaankop Granite, tin-zone arkosite and A Mine pockets

	B.kop Granite	Arkosite Tin zone	A Mine pockets	Ratio Pockets/Granite
SiO_2	75,80	72,55	28,77	0,4
TiO_2	0,09	0,47	0,31	3,4
Al_2O_3	12,34	13,25	21,62	1,8
FeO	2,60[1]	1,83[1]	10,70	3,9
MnO	0,02	0,04	0,21	10,5
MgO	0,14	0,94	6,09	43,5
CaO	0,54	0,95	6,23	45,1
Na_2O	3,34	4,30	1,15	0,3
K_2O	4,69	2,43	2,92	0,6
Subtotal	99,56	96,76	78,00	0,8
CO_2	0,08	1,28	9,18	115
S	0,01	0,08	2,38	238
B_2O_3	0,10	nd	5,03	50
Subtotal	0,19	1,36	16,59	87
Sn	0,0006	0,05	4,00	*
F	0,25	nd	nd	
Cu	0,005	0,02	1,41	282
Total	100,00	98,19	100,00	

[1] = Fe_2O_3 recalculated to FeO

* See remarks in Section 11.1.4 below.

Mineralogical studies showed the arkosites to be extensively altered, to such a degree that the original composition could not be established with certainty (Rozendaal *et al.* 1995b). It was suggested in Chapter 8 that the alteration of the arkosite represents the footprint of the ore-forming fluids. Rozendaal *et al.* (1995b), however, considered it to be early pervasive hydrothermal alteration which apparently preceded pocket mineralisation. In either event, it is concluded from Table 11 that the pockets, in relation to the Bobbejaankop Granite, contain less SiO_2, Na_2O and K_2O, more TiO2, Al_2O_3, FeO, and MnO, substantially more MgO and CaO, and a hundred times more of the volatiles CO_2, S, B_2O_3. The metals Sn and Cu became highly enriched during pocket formation.

The composition of the pockets should agree with that of dissolved solids in the exsolved fluids if initial reactions with the wall rock took place and no fluid escaped from the system. This was obviously not the case. The ratio

Digitised by the Department of Library Services in support of open access to information, University of Pretoria, 2021

between the composition of the pockets and the Bobbejaankop Granite therefore provides *merely an indication* of which elements became enriched in the exsolved fluids in relation to solidified magma.

11.1.4 Evolution of tin in the ore-forming fluids

This can be considered in three stages: (1) The initial level of concentration of tin in the magma, (2) concentration by means of magmatic differentiation after the magma separated from its source and (3) concentration of tin in the exsolved fluids.

(1) Initial concentration

Irrespective of the fact that the Bobbejaankop Granite is the most differentiated of the four types of granite and should therefore contain more tin (as also inferred from the chemical data), two other factors which apparently could have governed the initial tin concentration are considered.

(a) Geochemical heritage. Lehmann (1990) showed that the magmatic trends of a number of tin-granites indicate an initial tin content higher than the Clarke value of the upper crust and bulk crust (1- 3 ppm) and may be as high as 10 ppm (average upper limit of shale). Elevated initial tin values above the crustal levels are regarded to be the result of geochemical heritage.

Extrapolation of the magmatic trends of the pooled chemical data of the granites at Rooiberg (diagrams not shown) indicates an initial concentration of tin of about 1 - 2 ppm, which corresponds with the lower Clarke values of the upper crust. Geochemical heritage from a premagmatic source is therefore of no consequence to the granites at Rooiberg.

(b) Redox conditions. Within certain limitations (i.e. limited water/rock interaction, similar temperature range of crystallisation and melt composition), the log[Fe^{3+}/Fe^{2+}] ratios in granite rocks can be used as a simplistic approximation of the magmatic oxygen fugacity. Lehmann (1990) showed that for six tin provinces, these ratios fall, with the exception of very few data points, below the magnetite/ilmenite division of granites on the diagram adopted from Ishihara *et al*. (1979) (Fig 48). These granites have a sufficiently high tin content to be classed as tin-bearing granites in the

Digitised by the Department of Library Services in support of open access to information, University of Pretoria, 2021

classical sense. Some, notably those of the particulary rich tin districts (Phuket, Thailand and Tin Islands, Indonesia) fall well below the division and have ratios of 0.01 or less. A low fO_2 represented by the granites of the ilmenite series was apparently conducive for the formation of tin ore systems, but the causes are still not fully understood.

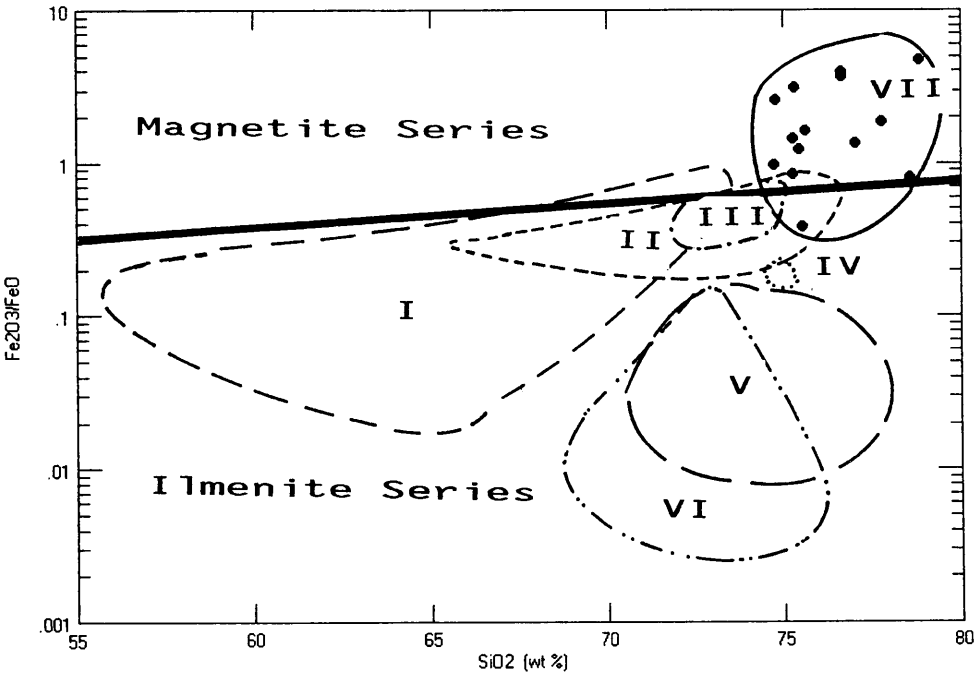

Fig. 48 - Variation diagram of SiO_2 v Fe_2O_3/FeO for various granitic rocks associated with tin deposits.

I - Portugal, II - Malaysian West Coast, III - Jos Plateau (Nigeria), IV - Erzgebirge (Germany), V - Banka & Beilitung (Indonesia), VI - Phuket (Thailand), VII - Rooiberg.
I - VI : After Lehmann (1990)
VII : Bobbejaankop Granite - this study.

The individual plots of the four granite types at Rooiberg indicate that there is no difference in the Fe^{3+}/Fe^{2+} ratios and only the Bobbejaankop Granite is plotted in Fig. 48. The ratios are close to the magnetite/ilmenite division but the majority fall within the magnetite series which indicates that the Bobbejaankop Granite (and the other granites) formed under relatively

Digitised by the Department of Library Services in support of open access to information, University of Pretoria, 2021

oxidising conditions compared to the other tin granites. It is in fact the only granite with a preponderance of data points in the magnetite field. Significantly, the granites at Rooiberg have very low tin values (± 5 ppm) and should strictly be classed as tin-barren granites in the classical sense. The Bobbejaankop Granite at Rooiberg contains even less tin than the unmineralised Bobbejaankop Granite in the Groblersdal area.

Taylor and Wall (1992) concluded from experimental data that the distribution of tin in a granite, after separation from its source, was controlled by melt composition and redox conditions. Within limitations, reducing conditions will favour the stability of Sn^{+2} and consequently the retention of tin in the *melt*. Oxidising conditions, on the other hand, stabilize sufficient Sn^{+4} to partition a proportion of tin into *minerals* such as biotite and other mafic minerals and magnetite. The melt containing *retained* tin can be equilibrated with either water or acidic fluids. The sodic species, under Sn^{+4} dominated systems and equilibrated with H_2O, is given as an example:

$$Na_4SnO_{4(melt)\ (retained\ portion)} + H_2O_{(fluid)} = SnO_{2(solid)} + O^{-2}_{(melt)} + 4Na^{+}_{(melt)} + 2OH^{-}_{(fluid)}$$

The work of Wall and Taylor merely showed that the redox conditions governed the relative partitioning of the tin into minerals such biotite as against SnO_2 as cassiterite, and *not the initial* tin content. As far as Rooiberg is concerned, their work would suggest that not all the initial tin in the Bobbejaankop Granite crystallised as cassiterite but a certain proportion was partitioned into other minerals, probably biotite and muscovite.

(2) Concentration by magmatic differentiation

Issues related to magmatic differentiation are the following:

(a) Lehmann (1982, 1987) considers the bulk solid-liquid distribution coefficient (K_D) in the fractionation process described by Rayleigh (1896) as important. Those elements where .."K_D <1 becomes enriched, whereas other elements with K_D > 1 are impoverished in residual melts" (Lehmann, 1987, p.178). Lehmann (1987, p.184) concluded that "a tin granite is formed by a prolonged fractionation history combined with a small Sn bulk distribution coefficient. Geochemical heritage plays only a minor or no role. The actual formation of a tin deposit is, in addition, dependent on the release of a fluid phase... for hydrothermal mineralization".

Digitised by the Department of Library Services in support of open access to information, University of Pretoria, 2021

(b) Coetzee and Twist (1989, p.1831) and Twist (pers. comm.) questioned whether fractional crystallisation of the granite at Zaaiplaats in particular, and granites in general, can *directly* produce significant concentrations of magmatic tin. They calculated (p.1831) "that significant tin enrichments can only be attained when F [in the equation of Rayleigh, 1896] falls well below 0.01 (i.e.> 99% crystallisation). However, because initial water contents in the Nebo magma were probably about 2.2 wt percent (Kleemann and Twist, 1989)... fluid-dominated processes must have controlled crystallization trends long before F could fall to 0.01. At most, therefore, little more than a twofold enrichment of tin could have occurred during fractional crystallisation of the Nebo magma". They emphasised (p. 1832) that..."the significance of fractional crystallization in producing endogranitic tin mineralization is not that it significantly concentrates tin, but that it enhances the water and volatile contents and thereby promotes conditions that facilitate the exsolution of an appropriate, tin-scavenging fluid phase from the melt".

(c) Newberry *et al.* (1990) proposed that liquid-liquid (ultra) fractionation might have played a role. They concluded that in order to concentrate Rb, B, F and Sn to amounts found in the plutons in the Fairbanks Circle, Alaska (their study area) the most evolved rocks required 97 to 99 per cent Rayleigh fractionation and at these levels, concentration of Rb, B, F and Sn was effected by liquid-liquid (ultra) fractionation.

Binary plots of the differentiation index versus Rb, W, F and Sn of the granites at Rooiberg show no sharp increase in the concentration of these elements towards the higher differentiation indices as found by Newberry *et al.*. Liquid-liquid (ultra) fractionation can be ruled out as a mechanism for concentrating tin at Rooiberg.

(3) Concentration of tin in the exsolved fluids

The fundamental agreement in the proposals of Lehmann (1982, 1987), Coetzee and Twist (1989) and Newberry *et al.* (1990) is that a separate fluid phase developed during the final stages of fractionation of a granitic magma. This could have exsolved as a hydrothermal fluid enriched in tin (Lehmann) or exsolved as a discrete fluid phase initially poor in tin that became enriched in tin by scavenging it (Coetzee and Twist), or underwent liquid-liquid (ultra) fractionation, concentrating tin in the same process (Newberry *et*

Digitised by the Department of Library Services in support of open access to information, University of Pretoria, 2021

al.). In a batholith comprising several phases of granite which have crystallised *directly from the same parent magma*, these fluids will emanate from the most evolved granite phase.

Two features are of considerable importance with regard to the granites at Rooiberg, more specifically the Bobbejaankop Granite.

(1) The Bobbejaankop Granite, though generally low in tin compared to other tin-granites, became enriched with tin during magmatic differentiation.

(2) After this initial enrichment, depletion of tin took place as indicated by the plot of TEDI v Sn (Fig. 49). It is proposed that this depletion was caused by interaction between the exsolved fluid and crystal mush.

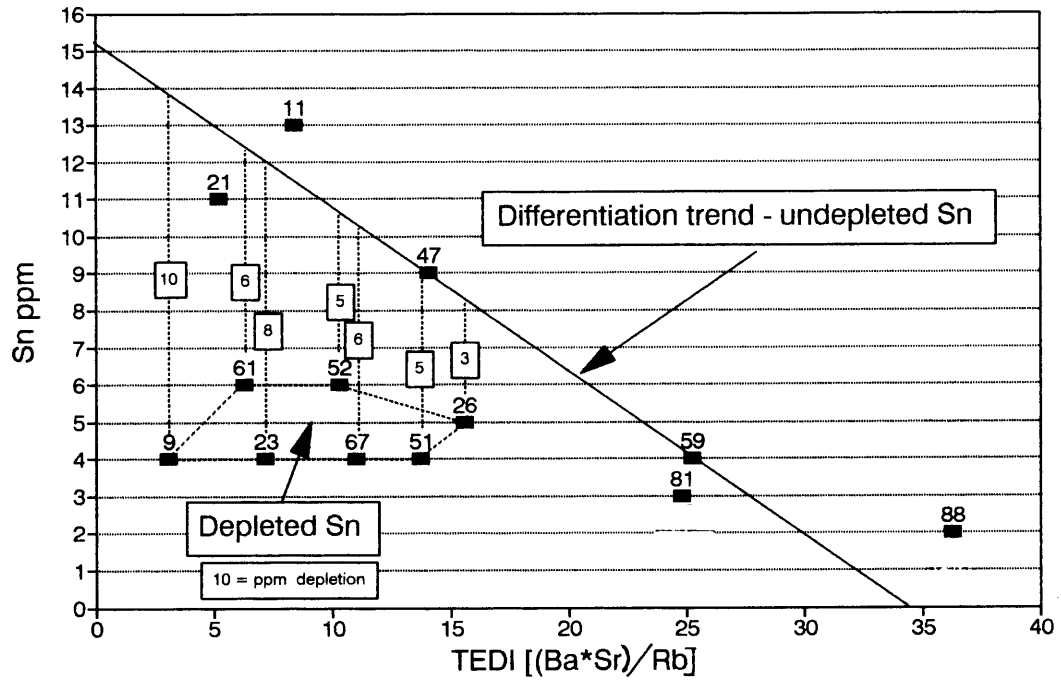

Fig. 49 - Variation diagram of TEDI v Sn showing the differentiation trend of undepleted tin and the field of depleted tin. Numbers above the data points are laboratory sample numbers; those in squares indicate the depletion with respect to the differentiation trend.

Since the amount of depletion can be estimated as well as the total tons tin deposited, a *hypothetical metal balance* can be calculated. This is based on the suggestion that each focus of mineralisation is related to scallops in the Bobbejaankop Granite of about 5 km in diameter (Chapter 7).

Digitised by the Department of Library Services in support of open access to information, University of Pretoria, 2021

Metal balance:

Volume of granite body 5 km X 5 km X 1 km	= 25 X 10^9 m^3
Tons @ RD of 2,6	= 65 X 10^9
Reduce to ± 75 % for scallop shape	= 50 X 10^9 tons
Depleted @ 6 ppm (Averaged from Fig. 49)	= 300 000 tons (1)
Rooiberg A Mine:	
Historic production	= 50 000 tons
Reserve	= 50 000 tons
Tin discarded as waste	= 10 000 tons
Tin eroded	= 10 000 tons
Tin-zone:	
Volume - 3000 m X 1500 m X 80 m	= 360 X 10^6 m^3
Tons @ RD of 2,6	= 936 X 10^6
At 500 ppm Sn (After Rozendaal *et al.* 1995b)	= 468 000 tons
Total A Mine	= 588 000 tons
Say	600 000 tons (2)
Shortfall (2) minus (1)	= 300 000 tons

The shortfall indicates that for the A Mine, the depletion should have been 12 ppm on average rather than 6 ppm. A depletion of 6 ppm may have been sufficient for the smaller deposits such as the B or Vellefontein Mines but not for the larger A or C Mines, particulary if the relatively large quantities of tin in the tin-zone are brought into the calculations. However, a tin content of no more than 18 - 20 ppm, that is 12 - 14 ppm depletion plus 6 ppm residual tin, was required for the Bobbejaankop Granite prior to fluid interaction.

The water content in the original granitic magma was, by analogy of the Groblersdal area (Kleemann and Twist, 1989), approximately 2,2 % by mass. A certain proportion of water was used for the formation of biotite and muscovite after which it is *assumed* that approximately 2 % remained and was eventually exsolved. A depletion of 12 ppm tin in the granite equates to an enrichment of 600 ppm tin (100 - 1000 ppm range) in the exsolved water.

Ollila (1981, 1984) concluded from fluid inclusion studies that the ore-forming fluids at Rooiberg (and Zaaiplaats) were moderately saline, indicating that chlorine was present in the ore-forming fluids. Chlorine is a very effective solvent and carrier of tin but the solubility is highly dependent on temperature, pH and oxygen fugacity (Eugster, 1986). Exsolution of water

Digitised by the Department of Library Services in support of open access to information, University of Pretoria, 2021

in the Bobbejaankop Granite took place between 500 - 700 °C (Ollila, 1981). At a temperature of say 600 °C and 100 - 1000 ppm Sn in solution, the oxygen fugacity was moderate.

11.2 Migration history

The events during the migration of the ore-forming fluids are important since these may have changed the chemical composition of the fluids and also effected different mineralising episodes. Three aspects are considered: (1) the migration path, (2) the compositional changes and (3) the time lapsed between the release of the fluids from the source and ore deposition (residence time).

11.2.1 The migration path

Pb - Pb isotope systematics of ankerite were initially done in an attempt to discriminate between the ankerites of the various types of deposits, but it proved to be of more value in reconstructing the migration path of the ore-forming fluids.

A total of 59 ankerites were selected and these are distributed over the four sample groups as follows:

Sample group		**Number of samples**
C Mine lodes -	C:	16
NAD Mine lodes -	N:	13
A Mine pockets -	P:	15
Ankerite-filled fractures -	F:	15

Sample selection was based on the availability of clean ankerite and the largest possible distribution on a mine scale. The samples, localities and isotope data are given in Tables V a - d in the Appendix. The results of the regressions of all the data as well as the individual sample groups are summarised in Table 12.

Digitised by the Department of Library Services in support of open access to information, University of Pretoria, 2021

Table 12 - Summary of Pb-Pb isotopic dates for ankerite

Sample Group	Number of samples	MSWD*	Pb-Pb Age/Date Ma (95% conf.)
All	59	49,3	2588+47-49
C Mine lodes	16	21,2	2712+150-167
NAD Mine lodes	13	16,3	2712+45-46
A Mine pockets	15	37,0	2181+170-192
Ankerite-filled fractures	15	69,2	2469+247-298

* Mean square of weighted deviates

All Sample Groups - C N P F

A large scatter of the data (in terms of $^{207}Pb/^{204}Pb$:$^{206}Pb/^{204}Pb$ ratios) is present as indicated in Fig. 50 and by the relatively high mean square of weighted deviates (MSWD) of 49,3. The Pb-Pb isotope "ages" are calculated to be 2588+47-49 Ma. Since the mineralisation is related to the Bobbejaankop Granite, it must therefore be younger than 2054.4 ± 1.8 Ma - the age of the Nebo Granite (Walraven and Hattingh, 1993). The apparent anomalous "older ages" are considered to be the result of the scavenging of lead by the ore-forming fluids during their migration through the sediments, and the present day $^{207}Pb/^{204}Pb$ and $^{206}Pb/^{204}Pb$ ratios are the result of two components as shown in Fig. 51. Component A-B represents the extraneous Pb of the contaminant and the position of B is determined by the amount of contamination. Component B-C is the result of radiogenic decay after the ankerite was deposited, and the slope of B-C would be parallel to the isochron of the Nebo Granite if ankerite mineralisation was temporally exactly coincidental with the closure of the isotope system in the Nebo Granite. Since the exact position of any point B for the corresponding point C is unknown, the slope of B-C, and hence the age of mineralisation, cannot be determined. Also, the large scatter of the data can be explained by the contamination of the ore-forming fluids with the sediments.

The "ages" of the ankerite are meaningless from a geochronological point of view and the term *age* is misleading; *date* is more appropriate, and is used forthwith. The initial isotope ratios can likewise, as a result of mixing, not be determined. However, some additional important conclusions regarding the migration and evolution of the ore-forming fluids can be drawn.

Digitised by the Department of Library Services in support of open access to information, University of Pretoria, 2021

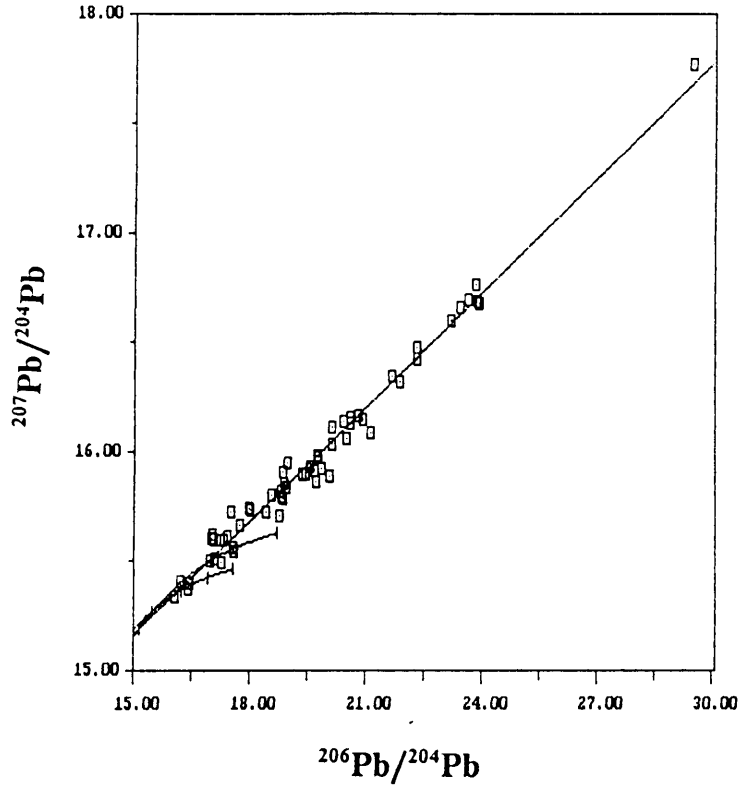

Fig. 50 - Regression of Pb-Pb isotope data for all sample groups. Short curves = single stage growth (top) and two stage growth (bottom) of Stacey and Kramers (1975).

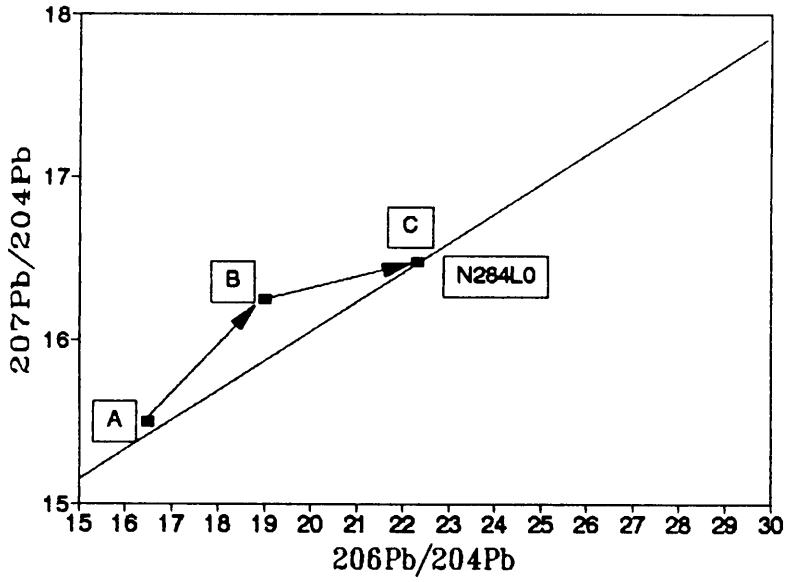

Fig. 51 - Diagram showing relative contributions of contaminant, A-B, and radiogenic decay, B-C, after crystallisation of ankerite. Position C was plotted from actual data of sample N284L0. The exact positions of points A and B are unknown and hence the slopes A-B and B-C are only illustrative.

Digitised by the Department of Library Services in support of open access to information, University of Pretoria, 2021

Sample Group C - C Mine Lodes

The fact that the date of 2712 Ma is (along with the NAD Mine lodes) the "oldest", cannot be interpreted as a higher degree of contamination; it only indicates that extraneous Pb was indeed scavenged by the ore-forming fluids. In fact, this sample group has the least scatter of $^{207}Pb/^{204}Pb$: $^{206}Pb/^{204}Pb$ ratios compared to any of the other groups (Fig. 52) from which it *may* be concluded that the ore-bodies at the C Mine were the closest to the source of the fluids i.e. the granite, or that pervasive migration took place during a shorter interval of time. Hence, the C Mine lodes may have formed at a higher temperature than the A Mine pockets or the NAD Mine lodes.

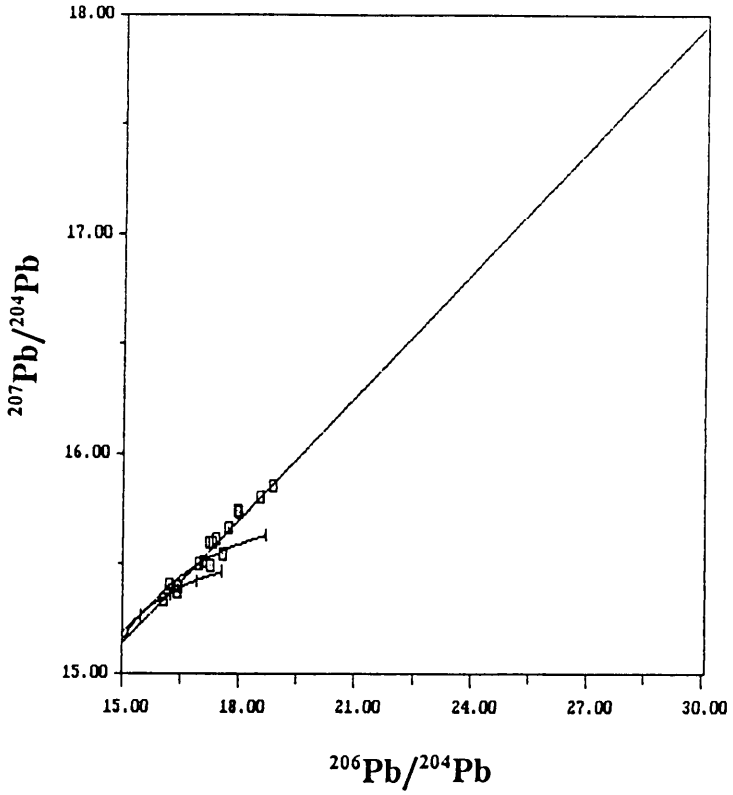

Fig. 52 - Regression of Pb-Pb isotope data for Sample Group C. Data points have the least scatter of all the sample groups. Short curves = single stage growth (top) and two stage growth (bottom) of Stacey and Kramers (1975).

Digitised by the Department of Library Services in support of open access to information, University of Pretoria, 2021

Sample Group N - NAD Mine Lodes

This sample group has the highest overall scatter of the $^{207}Pb/^{204}Pb$: $^{206}Pb/^{204}Pb$ ratios, which *may* indicate a substantial amount of contamination with the arkosite during the migration of the ore-forming fluids (Fig. 53). This may be interpreted in two ways: (1) The ore-bodies were situated the farthest away from the source, resulting in a long path of migration of the fluids, or (2) the migration of the fluids extended over a longer period of time than in the case of the other sample groups.

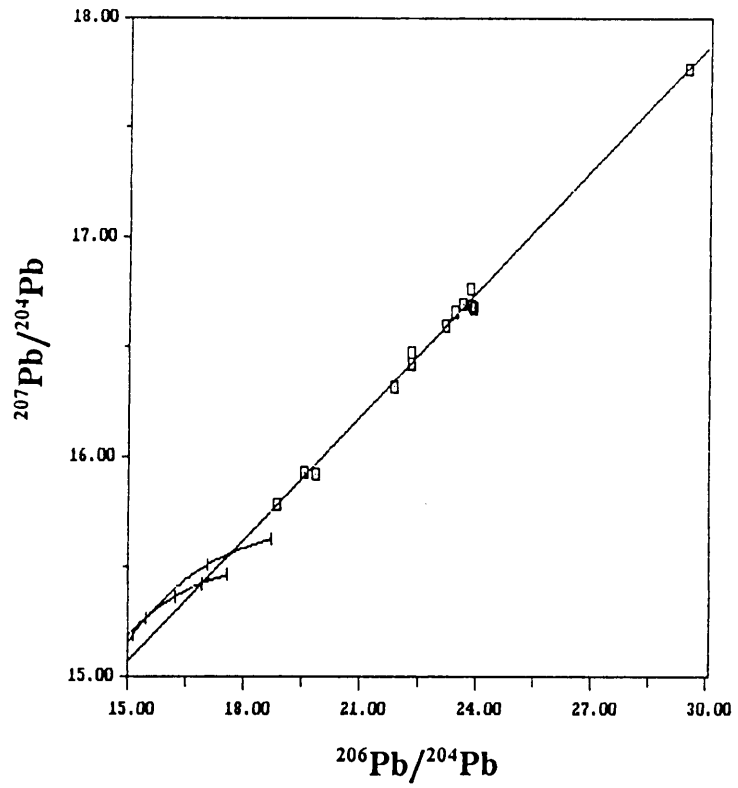

Fig. 53 - Regression of Pb-Pb isotope data for Sample Group N. Data points have the highest amount of scatter of all the sample groups.
Short curves = single stage growth (top) and two stage growth (bottom) of Stacey and Kramers (1975).

Digitised by the Department of Library Services in support of open access to information, University of Pretoria, 2021

Sample Group P - A Mine pockets

A comparison between the isotopic data of this sample group (Fig. 54) with that of the NAD Mine, and in conjunction with their age relationships, may provide further clues regarding the migration history of the fluids. The NAD Mine lodes and the A Mine pockets are spatially closely related and hence the distance from the respective ore-bodies to their source was approximately the same. The isotopic data, however, *may* indicate that more contamination took place between the fluids and arkosite which mineralised the NAD Mine lodes than those which mineralised the A Mine pockets. The NAD Mine lodes are younger than the A Mine pockets (Chapter 9), but this does imply a separate pulse of the fluids. The *residence time* of the fluids which mineralised the NAD Mine lodes was simply longer and the fluids were released into the fracture-structures to form NAD Mine lodes *after* the A Mine pockets had formed completely.

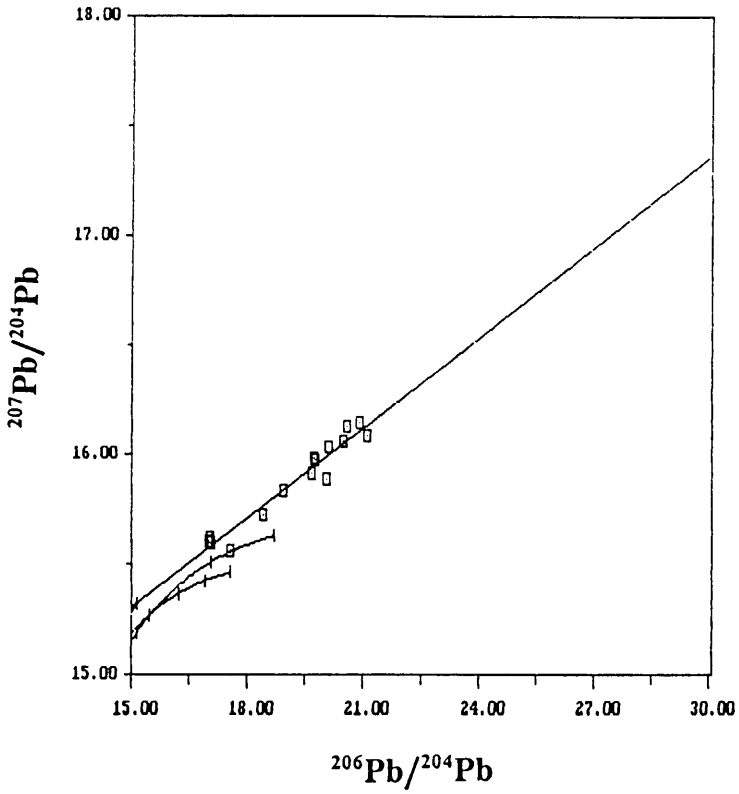

Fig. 54 - Regression of Pb-Pb isotope data for Sample Group P.
Amount of scatter of the data indicate less contamination with the arkosite than in the case of the NAD Mine lodes.
Short curves = single stage growth (top) and two stage growth (bottom) of Stacey and Kramers (1975).

Digitised by the Department of Library Services in support of open access to information, University of Pretoria, 2021

The role of primary feeder channels. Pervasive migration of the fluids through interconnected pores in the permeable arkosite negates the role of primary feeder-channels for the ore-forming fluids. Fracture-structures which exercised structural control on mineralisation, only attained importance *after the ore-forming fluids had migrated from the arkosite into them, and only then was a* ***local*** *plumbing system established on a mine scale.*

Moreover, wall rock alteration is thus not the result of migration of the fluids from the fracture(s) into the arkosite, but are the footprints left behind by the migrating fluids.

The pervasive migration of the ore-forming fluids also offers a plausible explanation for the apparently large scale geochemical alteration of the sediments (Stear 1977 a & b; Phillips, 1982; Rozendaal *et al.*, 1986, 1995 a & b).

11.2.2 Compositional changes

The geochemical alteration of the upper 500 - 600 metres of the arkosite was studied comprehensively by Rozendaal *et al.* (1995b) and the most significant averaged chemical changes are as follows:

		Relation to tin-zone		
		Footwall	**Tin-zone**	**Hanging wall**
Al_2O_3	(mass %)	12,11	13,25	14,42
Na_2O	(mass %)	5,37	4,30	3,67
K_2O	(mass %)	0,78	2,43	4,23

Unfortunately, the original composition of the arkosite could not be determined but it is clear that substantial amounts of aluminum, sodium and potassium have been introduced to the arkosite, which led to a depletion of these elements in the ore-forming fluids *prior* to ore-deposition. This may account for the relatively low pockets/Bobbejaankop Granite ratios of these elements (Table 11). More orthoclase feldspar would probably have formed if more potassium and aluminum had been available.

Digitised by the Department of Library Services in support of open access to information, University of Pretoria, 2021

11.2.3 Residence time

In the *Rooiberg tin-field*, the age relationship between the NAD Mine lodes and the pockets indicates a prolonged period of mineralisation which is also supported by the Pb-Pb isotopic data. The pockets formed first, at a stage when only the numerous and relatively thin, steeply dipping fractures of limited extent, were developed. Subsequent structural deformation resulted in the formation of fracture-structures which cut through the already-formed pockets, and the ore-forming fluids migrated from the arkosite into these structures to form mineralised lodes.

Since both pockets and lodes are present at the C Mine (Phillips, 1982) and since the same age relationship was established, a prolonged period of mineralisation is also indicated for the C Mine, although the isotopic data suggest that the migration time was probably less than at the A Mine complex.

Long-lived hydrothermal systems for the granites of the *Bushveld Complex outside the Rooiberg tin-field* have been demonstrated by other workers as well. Walraven *et al.* (1985) concluded from Rb/Sr isotopic disturbance that hydrothermal reticulation within the Lebowa Granite Suite may have been as long as 400 Ma. Robb *et al.* (1994) regarded both endo-granitic and exo-granitic poly-metallic mineralisation related to the Bushveld granites as a result of hydrothermal systems which persisted for "several hundred million years" after the granites solidified. At Zaaiplaats, McNaughton *et al.* (1993) proposed a long-lived hydrothermal system of 1000 Ma (1 Ga) based on Pb-Pb isotopic evidence.

Walraven *et al.* (1985) and McNaughton *et al.* (1993) suggested that high levels of heat were produced by radioactive processes which caused the prolonged period of hydrothermal fluid circulation. The possibility that the emplacement of the Bushveld Complex was related to a mantle plume (Hatton and Schweitzer, 1995) which could have generated anomalous heat, should also be considered.

The heat producing characteristics of various granites calculated according to McNaughton *et al.* (1993), using uranium, thorium and potassium radioactive decay, are given in Table 13.

Digitised by the Department of Library Services in support of open access to information, University of Pretoria, 2021

Table 13 - Heat producing characteristics of granites from various localities

Granite	U ppm	Th ppm	K_2O %	$\mu W/m^3$
Rooiberg				
Bobbejaankop	12	42	4,75	6,4
Granophyric	11	46	4,81	6,5
Klipkloof	12	41	4,40	6,3
Nebo	7	34	4,79	4,5
Zaaiplaats[1]				
Bobbejaankop	15	55	5,13	8,2
Lease	24	66	5,59	11,5
SW England[1]				<6
Western Australia[1]				9
Average granite	3,9	18,5	2,82	2,5

$\mu W/m^3$ = Microwatt per cubic metre

[1] McNaughton *et al.* (1993)

McNaughton *et al.* (1993) argued that the long-lived hydrothermal actively at Zaaiplaats was due to relatively high $\mu W/m^3$ values of the granites compared to the granites at SW England and Western Australia, which are also regarded as high heat producing granites.

The granites at Rooiberg have lower $\mu W/m^3$ values compared to those at Zaaiplaats but they have higher values than those of the average granite. In comparison with those in SW England, the granites at Rooiberg may also be considered as high heat producing. This, and probably also because of the fact that the migration of the ore-forming fluids was pervasive throughout the arkosite, as against *direct* channelling via open fracture-structures (trunk feeders) from the granite to the site of ore deposition, contributed towards the prolonged period of migration.

It has not been possible to calculate the absolute residence time of the ore-forming fluids at Rooiberg from the data gathered during this study. Long-lived hydrothermal systems in the range of 400 Ma to 1000 Ma for other areas

Digitised by the Department of Library Services in support of open access to information, University of Pretoria, 2021

of the Bushveld Complex may appear to be excessive, since this constitutes up of half of the absolute age of 2054 Ma of the Bushveld granites. While it may not have been several hundred millions years in the Rooiberg area, there is no reason to question times shorter than of a few tens of millions of years.

11.3 Deposition of tourmaline, ankerite and cassiterite

The chemical variation in some of the trace and major elements of these minerals has been demonstrated in Chapter 10. The causes of these changes and how they may be related to the evolution of the ore-forming fluids are now considered.

11.3.1 Tourmaline

The chemical variations in tourmaline (10.1.4) appear to be broadly consistent with those found in naturally occurring tourmaline elsewhere (Table 14). The consensus amongst authors who documented these changes is that the MgO content can be related to magmatic differentiation of the granite which supplied the fluids for tourmaline formation. A decrease in the magnesium content is supplemented by iron. In the case of Rooiberg, a negative correlation with a reasonably good correlation coefficient of -0,7 exists between MgO and FeO. Two possibilities are considered:

(1) A decrease in magnesium attributed to magmatic differentiation. This implies that the ore-forming fluids were exsolved and released from the Bobbejaankop Granite while magmatic differentiation *was still in progress*. The variation diagram of TEDI versus MgO (Fig. 14, p. 40) indicates a positive but *weak* trend, suggesting that, to a certain extent, magnesium in the melt decreased with increasing magmatic differentiation.

Synchronous magmatic differentiation and fluid exsolution is essential for the development of these fluids. In addition, this process could only have taken place during the final stages of magmatic differentiation, since the fluids were not exsolved while the lithostatic pressure was greater than the

Digitised by the Department of Library Services in support of open access to information, University of Pretoria, 2021

Table 14 - Variation of the major element content of tourmaline and intrepretation as proposed by various authors.

Setting and locality	Variation	Interpretation	Remarks	Reference
1. Experimental	*0.92Mg0.08:600°C *0.04Mg0.96:450°C	Alkali-free member at lower temperature	No Fe used-only Mg	Rosenberg & Foit (1979)
2. Maleba pluton, Tanzania	Core -> Rim: Ti, Fe, F increase Mg, Ca decrease; Na constant	Trends due to: Mg: Magmatic differentiation Ti: Uncertain		Ikingura (1989)
3. Aplite Pegmatite, Hub Kapong, Thailand	Core -> Rim: Mg decreases, Ti increases Rims: More alkali-free	Lower temperature: alkali-free	Mg not according to experimental data as per 1. above	Manning (1982)
4. Granite, SW England	Early pegmatite: Mg-rich Late pegmatite: Fe-rich	Magmatic differentiation		Lister (1979)
5. Muscovite-biotite granite, Portugal	Granite -> aplite -> pegamite Mg, Ti decrease; Fe increases	Fractionation of late stage magmatic fluids		Neiva (1974)
General summary	Tourmaline in or close to granitoids: Core -> Rim: Mg decreases, Fe increases Ti: Variable	Magmatic differentiation or temperature decrease		
	Experimental: Lower T :>*, high Mg Higher T:<*, low Mg	Temperature control	Mg trend opposite to magmatic differentiation	
Hydrothermal tourmaline, Rooiberg	Core -> Mantle: As per mass %: MgO, Al2O3: decrease FeO, CaO, TiO2: increase Core -> Rim: As per atomic proportion: Na and Na+Ca+K, i.e. *: increase Mg: decreases	Temperature rather than magmatic differentiation exercised control		This study

* Denotes alkali-free component

Digitised by the Department of Library Services in support of open access to information, University of Pretoria, 2021

hydrostatic pressure and water was retained in the melt. It is also imperative that, despite the long residence time of the fluids, no homogenisation of the exsolved fluids should take place -- those fluids which were exsolved and released first, also had to "arrive" first at the site of tourmaline formation.

(2) The temperature of formation. The atomic proportions (Table VIb - Appendix) indicate a deficiency of sodium and potassium in the X (alkali) site and since potassium is negligible, the deficiency is reflected by the atomic proportion of sodium only.

Rosenberg and Foit (1979) synthesized alkali-free tourmaline at two different temperatures and found the following:

Temperature	**Partial formula**	**Mole %**	
		MgO	Al_2O_3
600°C:	$\square_{0.92}Mg_{0.08}\ (Mg_{1.98}\ Al_{1.02})Al_6$	18,0	32,8
450°C:	$\square_{0.04}Mg_{0.96}\ (Mg_{1.52}\ Al_{1.48})Al_6$	20,9	34,9

$\square$ denotes alkali deficiency

They concluded that the alkali site occupancy by Mg is higher at lower temperatures and consequently more Mg is present at lower temperatures.

The amount of magnesium used to compensate the deficiency of sodium in the Rooiberg tourmalines was calculated and this was deducted from the total atomic proportion of magnesium.

The total atomic proportion of sodium and the remaining atomic proportion of magnesium, after its allocation to the X site, are shown in Fig. 55. The sodium increases from the core to the mantle (positions 0 - 7) but is always less than 1. The magnesium which remained in the Y and Z sites after allocation to the X site (to compensate for the sodium deficiency) is almost constant at an atomic proportion of about 1,5. This horizontal trend suggests that the magnesium content of tourmaline was *not controlled by its concentration in the ore-forming fluids but rather by temperature.*

The alternative, that magmatic differentiation exercised control, would be untenable, as it would be impossible to explain why the fluids did not homogenise during their prolonged migration, and it would also require that

Digitised by the Department of Library Services in support of open access to information, University of Pretoria, 2021

the ore-forming fluids would be exsolved from the melt and released into the overlying arkosite instantaneously. Otherwise, homogenisation would have occurred while the fluids were still within the granite carapace.

Temperature control, however, requires that the temperature increased during the formation of tourmaline. The experimental data indicate a variation of almost 1 alkali cation deficiency over a temperature difference of 150 °C. In the Rooiberg tourmaline, this variation in deficiency is only ± 0,2 alkali cation and although the exact corresponding temperature cannot be extrapolated, a much lower temperature variation than 150 °C is suggested and it may well be as low as 20 - 30 °C. Such a small variation is perfectly acceptable within a hydrothermal system operating at much higher temperatures — three or four times the 150°C used in the experiments.

Compositional control due to magmatic differentiation, as advocated by some authors, must therefore be seriously questioned.

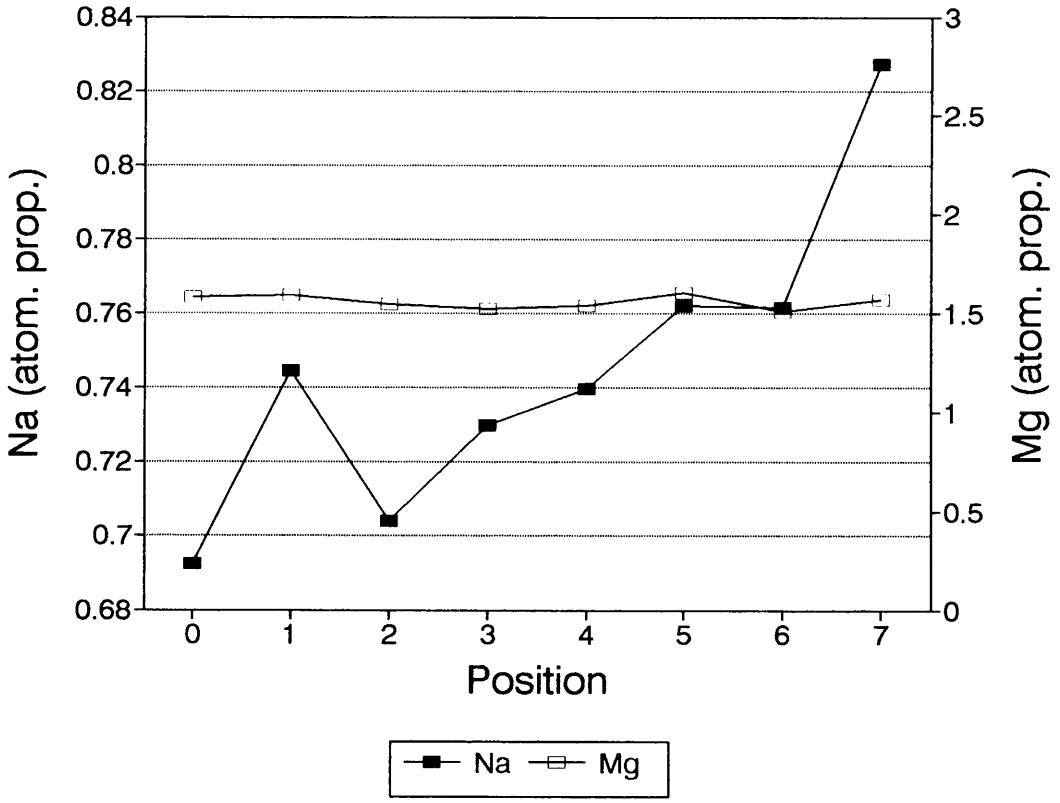

Fig. 55 - Variation in the atomic proportions of sodium and magnesium $_{(remaining)}$ after allocation was made for the alkali deficiency. Sodium increases but magnesium $_{(remaining)}$ is constant from positions 0 - 7. Positions 8 - 10 (overgrowth) not shown but are discussed in the text.

Digitised by the Department of Library Services in support of open access to information, University of Pretoria, 2021

Chemical variation in the overgrowth. Since the trends in the variation in the composition of the overgrowth are about the same as that in the core-mantle, the same conditions which governed them in the core-mantle were most probably also responsible for the compositional changes in the overgrowth.

11.3.2 Cassiterite and ankerite

Since cassiterite-1 crystallised *before* ankerite-1 and cassiterite-2 *after* ankerite-1 (Fig. 42), these minerals are discussed in the chronological order of their deposition. No evidence could be found of two mineralising events of cassiterite at the NAD and C Mines and on account of the fact that cassiterite is distinctly older than ankerite at these mines, it is discussed together with cassiterite-1 of the A Mine. The average tin content of the tin-zone is only 0,05 % and it was impossible to extract material for analyses - in fact, no cassiterite which could possibly be "background" was observed in any of the thin sections. The discussion below is thus limited to cassiterite in the ore-bodies only.

Cassiterite in the NAD and C Mine lodes and cassiterite-1 in the A Mine pockets

A solution buffered with Ni-Ni Oxide and at a temperature of 600 °C can transport 1000 ppm tinchloride in solution, but this can drop to a mere 1 ppm at 450 °C (Eugster, 1986). An increase in the oxygen fugacity also reduces the cassiterite solubility sharply. It is probable that all three - temperature, pH and increased oxygen fugacity - played a role in the precipitation of cassiterite. After injection of the ore-forming fluids from the arkosite into the numerous small fractures at A Mine or open fracture-structures at the NAD and C Mines, a pressure release resulted in a drop of temperature which could have been one of the factors which triggered precipitation of cassiterite and is considered to be:

$$SnCl^{+} + H_2O + \tfrac{1}{2}O_2 \rightarrow SnO_2 + 2H^{+} + Cl^{-} \quad \ldots\ldots 1$$

This reaction must be accompanied by a H^{+} consuming process which can be achieved by feldspar destruction:

Digitised by the Department of Library Services in support of open access to information, University of Pretoria, 2021

$3NaAlSi_3O_8 + 2H^+ \rightarrow NaAl_2[Si_3AlO_{10}(OH)_2]$ (mica group - sericite) $+ 6SiO_2 + 2Na^+$ ... 2

The products are cassiterite, sericite, quartz and sodium chloride.

At A Mine, sericite is a common mineral in the pockets. The white halo of few centimetres wide and comprising silicified arkosite, found around many of the pockets throughout the mine (Fig. 32, p. 69), and pink-white silicified arkosite, resulted from silica liberated by the above reaction. Dinsdale (1982) showed that the modal quartz increases from 20 - 40 per cent in the arkosite to 50 -70 per cent in the silicified areas. Sodium chloride was either released into the ore-forming fluids or became entrapped in cassiterite as fluid inclusions as described by Ollila (1981), or both.

The trace element contents. The high scandium values of C Mine as against the A Mine warrants attention. Leube and Stumpfl (1963) also found higher Nb in the C Mine cassiterites and their reported values are as follows:

Table 15 - Sc and Nb values in the C Mine lodes and A Mine pockets

	A Mine		**C Mine**	
	1	*2*	*1*	*2*
Sc	37 ± 11	10 ± 3	130 ± 52	152 ± 31
Nb	18 ± 15	nd	44 ± 29	nd

1 = Leube and Stumpfl (1963)
2 = This study - Table VII - Appendix

The Sc values of this study generally agree with those reported by Leube and Stumpfl (op cit). (The higher values in the A Mine by Leube and Stumpfl compared to those obtained during this study might have been the result of a higher lower limit of detection in the method used by the former authors). Leube and Stumpfl (op cit) considered the higher values of these elements in the cassiterite of the C Mine lodes to be indicative of a higher temperature of formation than that of the A Mine pockets.

Although it appears that the C Mine lodes formed at a higher temperature, it does not necessarily imply that the lodes formed during an earlier stage as proposed by Leube and Stumpfl. On the contrary, Phillips (1982) mentioned that

Digitised by the Department of Library Services in support of open access to information, University of Pretoria, 2021

the lodes at C Mine cut through the few pockets present there which implies a later period of formation for the lodes. Also, the NAD Mine lodes are distinctly younger than the A Mine pockets. The Pb-Pb isotope results suggest the C Mine lodes were either closer to the granite or that the residence time of the ore-forming fluids were shorter than the A Mine pockets or both. In either case, a higher temperature of formation for cassiterite would have resulted.

Ankerite of the NAD Mine and ankerite-1 in the A Mine pockets

The ore-forming fluids which mineralised the C Mine lodes were derived from a different Bobbejaankop Granite scallop and hence the chemical composition may also have been different. Hence, it is unjustified to draw conclusions based on chemical differences of ankerites in the A Mine complex (NAD and A Mine proper) and the C Mine. The ankerite of the NAD Mine, however, crystallised from the same fluids as ankerite-1 of the A Mine and these two may be compared.

The major element content.The negative trend between iron and magnesium as expressed as mole % $FeCO_3$ and $MgCO_3$ (Fig. 56) indicates that a decrease of one is complemented by an increase of the other and vice versa. Fig. 56 also indicates that, in general, the NAD Mine lodes contains more iron and less magnesium than the A Mine pockets. Three possibilities, which may account for this, are considered.

(1) Magmatic differentiation. This was evaluated to account for the decrease in magnesium during tourmaline growth. The same arguments which militate against it, applies *mutatis mutandis* for ankerite.

(2) Temperature. To date, only two experimental studies were done on the ternary system $CaCO_3$ - $MgCO_3$ - $FeCO_3$; one by Goldsmith *et al.* (1961) and another by Rosenberg (1967). While the results of Rosenberg (1967) apparently suggest the use of iron as a geologic thermometer, Goldsmith (*op cit*) concluded from his work that it is suspect and reiterated this conclusion in a later publication (Goldsmith, 1983). Beran (1975), in his microprobe work of naturally occurring ankerite, also questioned the validity of the suggestion of Rosenberg (1967). For these reasons, temperature is ruled out.

(3) Depletion of magnesium as a result of ore deposition.
The distribution of the mole % $FeCO_3$ and $MgCO_3$ of ankerite in the A Mine

Digitised by the Department of Library Services in support of open access to information, University of Pretoria, 2021

pockets and the ankerite-filled fractures (Fig. 39) shows two statistical populations, indicating a *separate* influx of fluids for each. In contrast, the distribution of the data points in Fig. 56 is along the same linear trend, indicating chemical evolution of the *same* fluid to form chemically different A Mine pockets and NAD Mine lodes.

Since large quantities of ankerite were deposited during pocket formation and since the ore-forming fluids were not replenished by a renewed influx from the source, it is suggested that the fluids which remained after ankerite was deposited in the pockets, were depleted with respect of magnesium. Less magnesium was therefore available during the formation of the NAD Mine lodes.

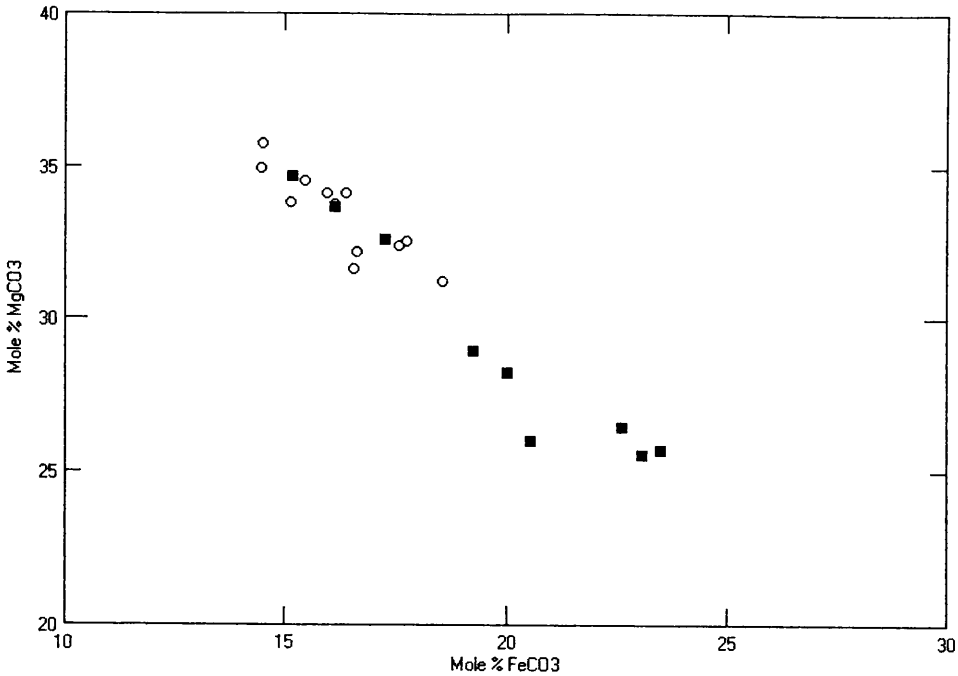

Fig. 56 - Variation diagram of mole % $FeCO_3$ v $MgCO_3$ in ankerite from the A Mine pockets (circle) and NAD Mine lodes (square). Each point represents the average of four analyses of two grains of each sample. The A Mine pockets contain, in general, more $MgCO_3$ than the NAD Mine lodes, but only one statistical population for both mines is indicated.

Fluid interaction. At the NAD Mine, no interaction took place between cassiterite and the fluids from which ankerite crystallised. In the A Mine pockets, however, clear evidence exists of fluid interaction. This interaction was fairly common and has been noted in samples from the Jewel Box, 19N,

Digitised by the Department of Library Services in support of open access to information, University of Pretoria, 2021

Magazine and Q22 Sections of the A Mine. It was arrested at different stages, and three examples, illustrating different stages of fluid interaction, are given below:

Stage 1. A small amount of fluid interaction is indicated by incipient replacement of cassiterite-1 (Fig. 57). Replacement was apparently not by way of corrosion of anhedral crystal faces of these minerals but the fluids actually penetrated the crystals, probably via micro-fractures.
Stage 2. Fluid interaction reached an advanced stage resulting in doughnut-shaped cassiterite-1 remnants in Fig. 58.
Stage 3. Fluid interaction almost completely dissolved (replaced) cassiterite-1 and only cassiterite-1 near the crystal faces remains (Fig. 59).

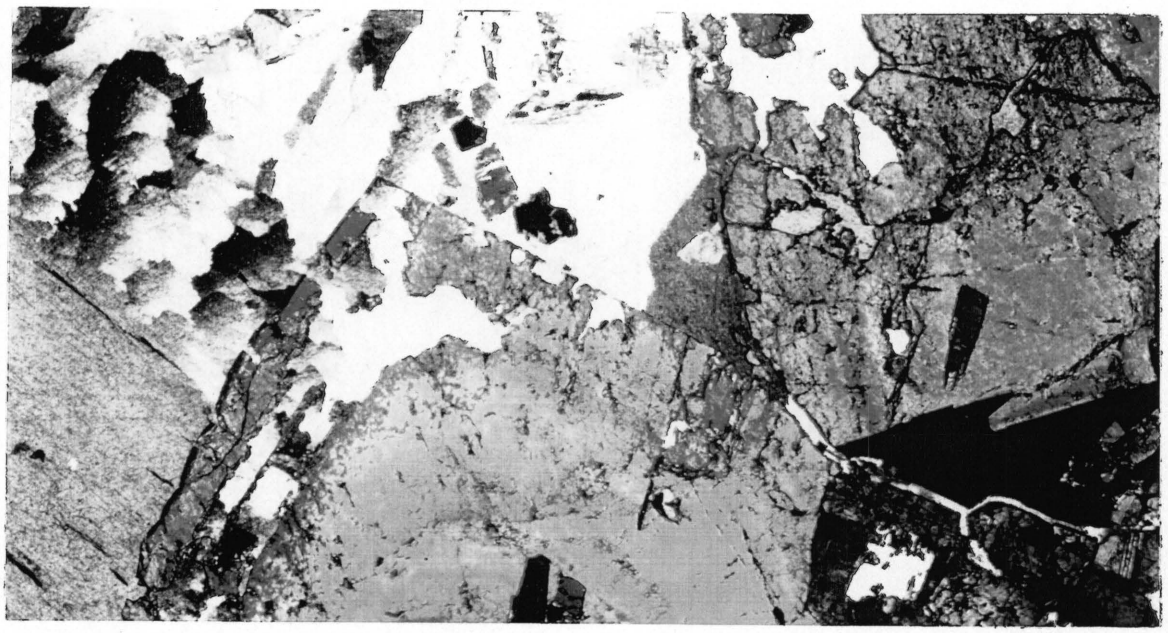

Fig. 57 - Incipient replacement of cassiterite, yellow-green, by ankerite-1, white and beige.
X30 +N Sample 453L5

A Mine - Jewel Box Section - 680′ Level

Digitised by the Department of Library Services in support of open access to information, University of Pretoria, 2021

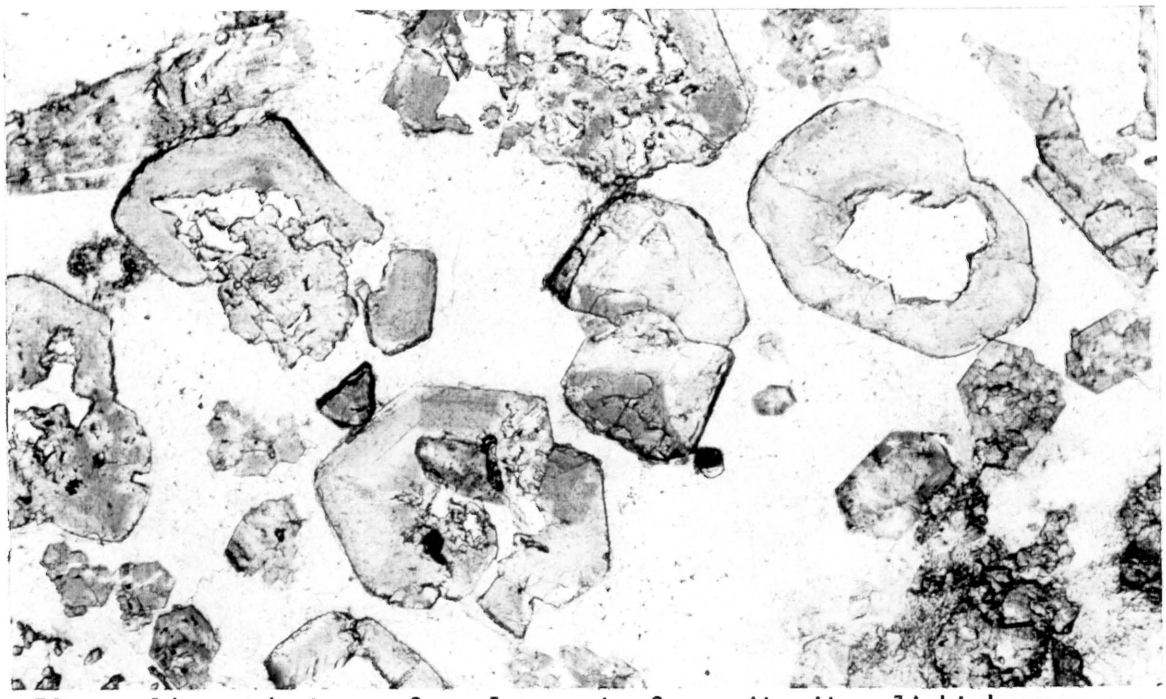

Fig. 58 - Advanced stage of replacement of cassiterite, light brown and doughnut-shaped, by ankerite-1, very light beige. Tourmaline, light green is mainly unreplaced.

X80 Plane polarised light Sample 117L5

A Mine - Q22-Magazine Sections

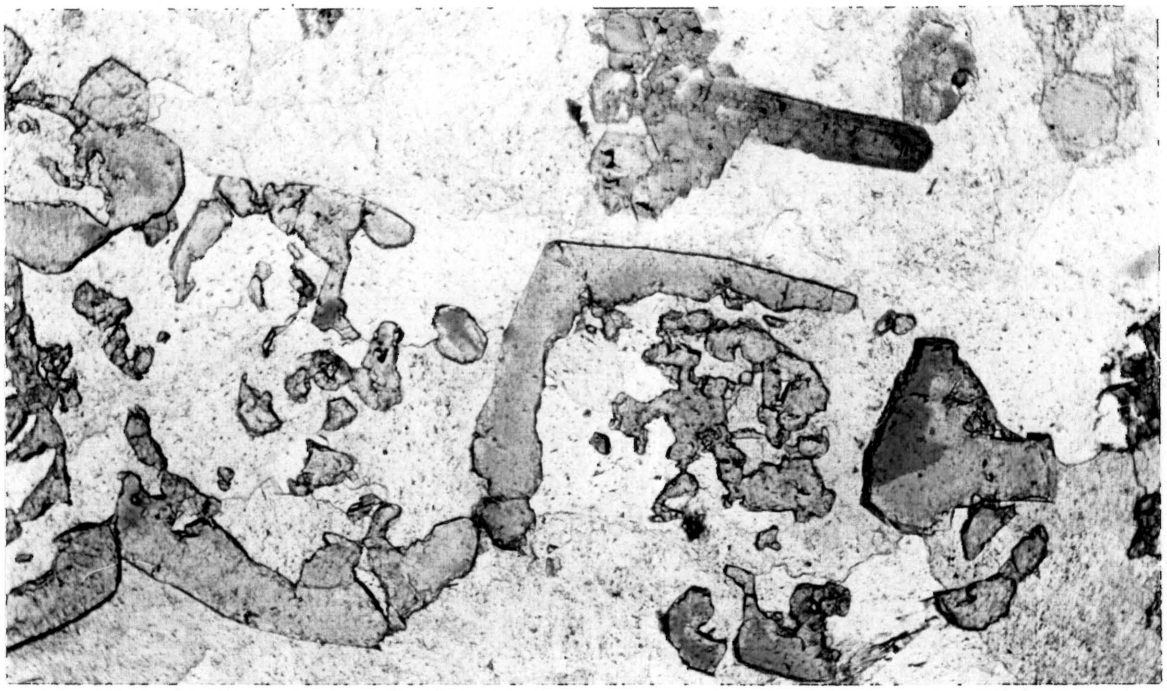

Fig. 59 - Almost total replacement of cassiterite, light brown, by ankerite-1, light beige. Tourmaline, green, is unreplaced.
X80 Plane polarised light Sample 117L5

A Mine - Q22-Magazine Sections

Digitised by the Department of Library Services in support of open access to information, University of Pretoria, 2021

Replacement of cassiterite-1 took place under reducing conditions according to:

$$Ca^{2+} + (Mg,Fe)^{2+} + 2CO_2 + SnO_2 + 2e^- \rightarrow Ca(Mg,Fe)(CO_3)_2 + Sn^{2+} \quad \ldots\ldots\ldots \quad 3$$

Two important conclusions can be drawn. Firstly, pockets which were originally mineralised with cassiterite may become economically uninteresting with advanced stages of ankerite replacement. Secondly, and more importantly, is that the ore-forming fluids from which ankerite-1 were deposited, changed geochemically as replacement of cassiterite proceeded.

The fluids became enriched in tin (Sn^{2+}) and could have either (1) escaped to the surface without depositing their metal content, or (2) circulated and caused further mineralisation. From a purely stratigraphic point of view, the first possibility appears unlikely since it would have required upward migration of the fluids through several hundred metres of country rock, including impervious argillites as well as rhyolite, now eroded away. The second possibility is more likely.

Cassiterite-2 in the A Mine

The Sn^{2+} liberated by the above reaction could have reacted with the ore-forming fluids to form $SnCl^+$, which is soluble under reducing conditions, and migrated together with the remaining fluids. Deposition of cassiterite from these fluids took place when the redox conditions changed according to reaction 1. This would have resulted in a *separate and later phase of cassiterite mineralisation* thus causing polyphase mineralisation. It may be argued that the ore-forming fluids, charged with $SnCl^+$, did not migrate for extended distances but cassiterite-2 deposition took place around nearby existing pockets such as in the 19N Section.

Since the ore-forming fluids discharged most, if not all, of the originally contained Ca, Fe, Mg etc. and volatiles such as B_2O_3 and CO_2 prior to the liberation of $SnCl^+$, this $SnCl^+$ was probably, apart from water and chlorine (which did not form discrete minerals), the only major constituent left. Hence cassiterite-2 is not associated with the major minerals - tourmaline and ankerite.

Digitised by the Department of Library Services in support of open access to information, University of Pretoria, 2021

Trace element content

Zirconium. On account of both similar charge and ionic radius, Zr^{4+} (0.79 Å) can replace Sn^{4+} (0.71 Å) but saturation is reached at about 2 750 ppm Zr (Möller *et al.*, 1981). Möller and Dulski (1983) studied 117 cassiterite samples from a large number of localities distributed over five continents. They concluded that Zr is present in all of them and the Zr content is higher in pegmatitic than in hydrothermal tin deposits, which they ascribed to magmatic differentiation.

Of all the trace elements, zirconium shows the largest variation between cassiterite-1, containing about 100 ppm Zr, as against less than 8 ppm in cassiterite-2 (Table VII - Appendix). It is suggested that the much lower Zr in cassiterite-2 resulted from the fluid action which dissolved cassiterite-1 and only the Sn cations, and not the Zr, were subsequently redeposited as cassiterite-2. This process in effect purified cassiterite-2 of Zr.

Because no Zr was found in cassiterite-2, a renewed influx of fluids *from the source* can be ruled out, since this would have resulted in some level of concentration of Zr in cassiterite-2.

Sodium shows the second largest variation in the trace element content (Table VII - Appendix).

The chemical reaction (2) (p. 116) indicates that the ore-forming fluids became enriched in Na^+ as a result of the breakdown of feldspar during the precipitation of cassiterite-1. Some of this Na^+ reacted with Cl^-, which was liberated during cassiterite deposition, and formed NaCl, but a portion could have remained in the fluids and was later incorporated in cassiterite-2.

The actual incorporation of Na into the crystal structure of cassiterite, however, presents a problem on account of its large ionic radius (0.98 Å), even after allowing for a ± 12 per cent tolerance as proposed by Goldschmidt (1937). This problem is also relevant for all other samples of cassiterite but to a smaller extent.

Digitised by the Department of Library Services in support of open access to information, University of Pretoria, 2021

Two possibilities may account for the Sn - Na association:

(i) *Fluid inclusions* contain NaCl but they are very small and it is unlikely that the Na content would have been affected by them. Fluid inclusions, comprising 0,05 % by volume, account for 10 - 15 ppm Na.

(ii) *Surface adsorption*. Na^+ may be held in a diffuse layer at the surface of cassiterite crystals where bonding is not completely satisfied. This may explain the Sn - Na association but not the increase in Na in cassiterite-2 since the amount of Na^+ adsorbed is controlled by the bonding configuration rather than by the availability of sodium in the ore-forming fluids.

Ankerite-2

The closing event of mineralisation in the Rooiberg tin-field is represented by the ankerite-filled fractures. As mentioned above, a separate influx of ore-forming fluids is indicated. Moreover, the ankerite-filled fractures contain no other minerals and were formed after the pockets and the lodes.

Structural deformation of the Rooiberg Fragment resulted in faulting, development of fracture-structures either along the bedding planes of the sediments or steeply dipping and numerous small fractures aligned along set directions. The ankerite-filled fractures are, on the other hand, localised, highly irregular in both dip and strike and more often than not resemble brecciation. A forceful injection of fluids, causing fracturing, and in places brecciation, with concurrent emplacement of ankerite-2 only, is suggested.

11.4 Polyphase mineralisation

Polyphase mineralisation in the Rooiberg tin-field is manifested by:

(1) The temporal relationship between pockets and lodes. The lodes at both the A Mine complex and the C Mine were emplaced after all the minerals in the pockets had been deposited and are clearly of a later phase.

In a way, this type may be compared with the polyphase mineralisation of the Cornish tin deposits. Major tin veins at Cornwall are usually multiphase and have formed as a result of continued reopening and deposition of successive phases of mineralisation (Garnett, 1965; 1966 a & b; Edmonds et al., 1975; Taylor, 1978)

Digitised by the Department of Library Services in support of open access to information, University of Pretoria, 2021

(2) An abrupt change in the chemistry of the ore-forming fluids. The overgrowth of tourmaline and the ankerite-filled fractures are ascribed to separate pulses of the ore-forming fluids.

(3) Solution and redeposition as in the case of cassiterite-1 and -2. This type is comparable with the tin pipes in Herberton, Queensland, Australia, where two types of cassiterite are frequently closely associated with each other. Georgees (1974) suggested that the younger and lighter coloured variety of cassiterite has resulted from dissolution of the older and darker coloured variety. Taylor (1978) pointed out that in " many ores" elsewhere, which contain more than one phase of cassiterite, it is quite common for the later generations to be lighter coloured and he suggested that this type of mineralisation may "indeed be more widespread than suspected".

The second phase cassiterite at the B Mine recognised by Labuschagne (1970a) is lighter-coloured than the first phase and may also have resulted from fluid interaction and subsequent redeposition of younger cassiterite.

Polyphase mineralisation may result from either the poly-ascent or mono-ascent of the ore-forming fluids with respect to their source. In the case of poly-ascent, polyphase mineralisation may result.

In the Rooiberg tin-field, the tourmaline overgrowth and the ankerite-filled fractures are considered to be the result of poly-ascent of ore-forming fluids. However, only a relatively small volume of fluids was involved. The separate pulses also occurred during at very early stage (tourmaline) and at the final stage of mineralisation (ankerite-filled fractures).

In the case of mono-ascent, the fluids were released during a single event, but during the migration, several factors could have led to the arrival of fluids as poly-ascendent pulses at the site of ore deposition.

Release of the ore-forming fluids in the Rooiberg tin-field is considered to be predominantly mono-ascendent and the greater part of the ore-forming fluids was released this way. The fluids remained in the arkosite for a considerable period which may have been in the order of tens of million years. The pockets were formed at a relatively early stage and the lodes were emplaced at a later

Digitised by the Department of Library Services in support of open access to information, University of Pretoria, 2021

stage, but both types were formed from the same fluids.

Fluid interaction dissolved cassiterite-1 and redeposited it as cassiterite-2 and the two phases of cassiterite cannot be related to separate pulses of the fluids.

SUMMARY AND CONCLUSIONS

1. Four granite types, Nebo, Klipkloof, granophyric and Bobbejaankop Granites, are present in the west and in the east of the Rooiberg tin-field and these four granites evolved from the same parent magma.

2. The Bobbejaankop Granite is geochemically the most evolved of the four and supplied the ore-forming fluids.

3. The Bobbejaankop Granite was emplaced in the form of a series of scallops which may or may not be interconnected. The apices of these scallops are about 5 km apart and coincide with the loci of mineralisation on a regional scale: eight major and six minor loci are indicated by regional stream sediment geochemistry.

4. The ore-forming fluids exsolved from the Bobbejaankop Granite towards the final stages of magmatic differentiation and contained Si, Ti, Al, Mg, Fe, Mn, and Ca as major constituents together with the volatiles CO_2, SO_2, B_2O_3 and Cl and water. Metals such Sn and Cu were present in the ppm range; 100 -1000 in the case of Sn.

5. The exsolved fluids scavenged tin from the Bobbejaankop Granite mush, and as result depleted the granite of tin. Tin was transported as tinchloride.

6. The ore-forming fluids were not channelled via "primary feeders" from their source, but were discharged into the arkosite and pervasive migration through the pores of the arkosite took place. It was only at the site of ore-deposition that the fluids migrated from the arkosite into a local plumbing system of channelways on a mine scale.

Digitised by the Department of Library Services in support of open access to information, University of Pretoria, 2021

7. As a result of this pervasive migration, the residence time of the ore-forming fluids was prolonged. In addition, the granites at Rooiberg can be considered to be high heat producing and such granites can generate long-lived systems of hydrothermal activity. At Rooiberg, it was probably a few tens of million years.

8. Pervasive sodic, potassic and sericitic (increased Al_2O_3) alteration of the arkosite represents the footprints of the migrating ore-forming fluids and did not result from fluids migrating from fracture-structures into the wall rock.

9. The main pulse of the ore-forming fluids from the Bobbejaankop Granite was monoascendant. Only at the very beginning and towards the end of the mineralising events did separate and far less intense polyascendant pulses occur.

10. Polyphase mineralisation is manifested by:

(1) Temporal relationship between pockets and lodes. The pockets were formed first and the same fluids, which resided in the arkosite for a prolonged period, also mineralised fracture-structures. These developed later and cut through the earlier-formed pockets.

(2) Overgrowth of tourmaline and ankerite-filled fractures which formed from separate pulses.

(3) Dissolution of cassiterite-1 which was redeposited to form the later phase of cassiterite-2. Cassiterite of this phase was of high grade and supplied a substantial amount of the tin from the A Mine.

Digitised by the Department of Library Services in support of open access to information, University of Pretoria, 2021

REFERENCES

Ahrens, L. H, 1957. A survey of the quality of some principal abundance data of geochemistry. *Phys. Chem. Earth*, **2**, 30-45

Alderton, D.H.M., Pearce, J.A. and Potts, P.J., 1980. Rare earth element mobility during granite alteration: evidence from Southwest England. *Earth Planet. Sci. Lett.*, **49**, 149-165.

Armstrong, R.A., Retief, E., Compston, W. and Williams, I.S., 1990. Geochronological constraints on the evolution of the Witwatersrand Basin, as deduced from single zircon U/Pb microprobe studies. *Ext. Abs. Geocongress 90*. Geol. Soc. S. Afr., 24-27.

Barsukov, V.L., 1957. The geochemistry of tin. *Geochemistry 1. (Translated)* 41-52.

Beran, A., 1975. Mikrosondenuntersuchen von Ankeriten und Sideriten des Steirischen Erzberges. *Tschermaks Mineral. Petrogr. Mitt.*, **22**, 250-265.

_____ and Zemann, J., 1977. Refinement and comparison of the crystal structures in a dolomite and an Fe-rich ankerite. *Tschermaks Mineral. Petrogr. Mitt.*, **24**, 279-286.

Bernard, F., Moutou, P. and Pichavant, M., 1985. Phase relations of tourmaline leucogranites and the significance of tourmaline in silicic magmas. *Journ. Geol.*, **93**, 271-291.

Boardman, L.G., 1946. The geology of a portion of the Rooiberg tinfields. *Trans. geol. Soc. S. Afr.*, **49**, 103-132.

Brown, C. E. and Ayuso, R.A., 1985. Significance of tourmaline-rich rocks in the Grenville Complex of St. Lawrence County, New York. *U.S. Geological Survey Bulletin 1626*, ***Chapter C.***, C1-C32.

Burnham, C.W., 1979. Magmas and hydrothermal fluids. In: Barnes (Ed.) *Geochemistry of hydrothermal ore deposits.* **2nd Ed.** John Wiley. New York. 34-76.

Clark, E.E.F, Donaldson, J.D. and Silver, J., 1976. The ^{119}Sn Mössbauer spectra, cell dimensions, and minor element contents of some cassiterites. *Min. Mag. (Short Communications)*, **40**, 895 -898.

Clark, A.H., Farrar, E., Caelles,J.C., Haynes, S.J., Lortie, R.B., McBride, S.L., Quirt, G.S., Robertson, R.C.R. and Zentilli, M., 1976. Longitudinal variations in the metallogenic evolution of the Central Andes: A progress report. *Geological Association of Canada*. Special Paper **Number 14**. 58p.

_____ and Robertson, R.C.R., 1978. The evolution and origin of the northern plutonic sub-provinces of the Bolivian tin field. In: *Abstracts of Papers - International Symposium, Geology of Tin Deposits*. Geological Society of Malaysia, Annex to Warti-Geologi. **Vol. 4**, No 2. 42-43.

Digitised by the Department of Library Services in support of open access to information, University of Pretoria, 2021

Coetzee, J., 1984. A geochemical and petrological investigation of the low-grade tin deposits in the Bobbejaankop Granite at the Zaaiplaats tin mine. *M.Sc. thesis (Unpubl.)* Univ. Pretoria. 126p.

_____ 1986. The Lease granite - a granophyric miarolitic mineralised granite at the apical region of a tin-tungsten system. *Trans. geol. Soc. S. Afr.*, **89**, 335-345.

_____ and Twist, D., 1989. Disseminated tin mineralisation in the roof of the Bushveld Granite pluton at the Zaaiplaats Mine, with implications for the genesis of magmatic hydrothermal tin systems. *Econ. Geol.*, **84**, 1817-1834.

Crocker, I.T., 1976. Fluorite mineralisation in the Bushveld Granites south east of Rooiberg. *M.Sc. thesis (unpubl.)* Univ. Stellenbosch. 118p.

_____ 1986. The Zaaiplaats tinfield, Potgietersrus district. In: Anhaeusser, C.R., and Maske, S. (Eds.). *Mineral Deposits of Southern Africa.* **Vol. II**, Geol. Soc. S. Afr., Johannesburg. 1307-1327.

Dinsdale, J.L., 1982. The development and control of pocket - mineralisation in the Rooiberg Quartzites. *M.Sc. thesis (Unpubl.)* Univ. Pretoria. 150p.

Du Plessis, C.P. and Walraven, F., 1990. The tectonic setting of the Bushveld Complex in Southern Africa.I. Structural deformation and distribution. *Tectonophysics*, **176**, 305-319.

Duffield, W.A., 1990. Eruptive fountains of silicic magma and their possible effects on the tin content of fountain-fed lavas, Taylor Creek Rhyolite, New Mexico. In: *H.J. Stein and J.L Hannah (Eds). Ore-bearing Granite Systems; Petrogenesis and Mineralizing Processes.* Geol. Soc. Am. Special Paper 246. 251-262.

Edmonds, E.A., McKeown, M.C. and Williams, M., 1975. *British Regional Geology: South-West England.* **Fourth Ed.** British Geological Survey. London. 138p.

Eglington, B.M. and Harmer, R.E., 1989. GEODATE: a program for the processing and regression of isotope data using IBM-compatible microcomputers. *CSIR Manual EMA-H 8901*, 57p.

Erasmus, C.S., Fesq, H.W., Cable, E.G.D., Rasmussen, S.E. and Sellschop, J.P.F., 1977. The NIMROC samples as reference material for neutron activation. *Journ. Radioanalytical Chem.*, **39**, 323 - 329.

Eriksson, P.G., Meyer, R. and Botha, W.J. 1988. A hypothesis on the Pretoria Group basin. *S. Afr. J. Geol.*, **94**, 490-497.

_____, Schreiber, U.M. and Van der Neut, M. 1991. A review of the sedimentology of the early Proterozoic Pretoria Group, Transvaal Sequence, South Africa: implications for tectonic setting. *J. Afr. Earth Sci.*, **13**, 107-119.

Eugster, H.P., 1985. Granites and hydrothermal ore deposits: a geochemical framework. *Min. Mag.*, **49**, 7-23.

Digitised by the Department of Library Services in support of open access to information, University of Pretoria, 2021

_____, 1986. Minerals in hot water. *Am. Mineral.* **71**, 665-673.

Farmer, C.B., Searl, A. and Halls, C., 1991. Cathodoluminescence and growth of cassiterite in the composite lodes at South Crofty Mine, Cornwall, England. *Min. Mag.*, **55**, 447 - 458.

Ford, W.E., 1932. *Dana's textbook of mineralogy.* **Fourth Edition**, John Wiley & Sons, New York, 851p.

Feather, C. E. and Willis, J.P., 1976. A simple method for background and matrix correction of spectral peaks in trace element determinations by X-ray spectrometry. *X-ray spectrometry*, **5**, 41-48

Flinter, B.H., 1971. Tin in acid granitoids: The search for a geochemical scheme of mineral exploration. In: *Boyle, R.W. (Ed.) : Geochemical Exploration.* **CIMM Spec. Vol. II**, 323-330.

Foit, F.F., Jr. and Rosenberg, P.E., 1977. Coupled substitutions in the tourmaline group. *Contrib. Mineral. Petrol.*, **62**, 109-127.

Fourie, P.J., 1968. Die geochemie van granitiese gesteentes van die Bosveldstollingskompleks. *DSc thesis (unpubl.)* Univ. Pretoria. 290p.

Garnett, R.H.T., 1965. Polyascendent zoning in the No.3 Branch Lode of Geevor Tin Mine, Cornwall. *Symp. Post-magm. Ore Dep.*, Prague. 97-103.

_____, 1966a. Relationship between tin content and structure of lodes at Geevor Mine, Cornwall., *Bull. Inst. Min. Met.*, **75**. B1-B22.

_____, 1966b. Distribution of cassiterite in vein tin deposits., *Bull. Inst. Min. Met.*, **75**. B245-B273.

Georgees, C., 1974. Geology and mineralisation at Herberton Hill, Herberton, North Queensland, Australia. *Unpubl. Honours thesis.* James Cook University of North Queensland, Australia.

Giuliani, G., 1987. La cassitérite zonée du gisement de Sokhret Allal (Granite des Zaër; Maroc Central): Composition chimique et phases fluides associées. *Mineral. Deposita*, **22**, 253 - 261.

Goldschmidt, V. M., 1937. The principles of distribution of chemical elements in minerals and rocks. *J. Chem. Soc.*, 655 -673.

Goldsmith, J.R., 1983. Phase relations of rhombohedral carbonates. In: Reeder Richard J (Ed.), *Carbonates: Mineralogy and Chemistry. Reviews in Mineralogy*, **11**, 49-76.

_____, Graf, D.L. and Heard, H.C., 1961. Lattice constants of the calcium-magnesium carbonates. *Am. Mineral.*, **46**, 453-457.

_____, Graf, D.L., Witters, J. and Northrop, D.A., 1962. Studies in the system $CaCO_3$-$MgCO_3$-$FeCO_3$: 1. Phase relations; 2. A method for major-element spectrochemical analysis; 3. Composition of some ferroan dolomites. *J. Geol.*, **70**, 659-688.

Digitised by the Department of Library Services in support of open access to information, University of Pretoria, 2021

Grice, J.D. and Robinson, G.W., 1989. Feruvite, a new member of the tourmaline group, and its crystal structure. *Canadian Min.*, **27**, 199-203.

_____ and Ercit, T.S., 1993. Ordering of Fe and Mg in the tourmaline crystal structure: The correct formula. *Neues Jahrbuch Miner. Abh.*, **165**, 245-266.

Haikney, S.A., 1986. Report on the compilation of geochemical data of the Rooiberg Fragment. *Unpubl. rep. Gold Fields of South Africa.* Johannesburg. 32p.

Hall, M.R. and Ribbe, P.H., 1971. An electron microprobe study of luminescence centers in cassiterite. *Am. Min.*, **56**, 31 - 45.

Hannah, J.L. and Stein, H.J., 1990. Magmatic and hydrothermal processes in ore-bearing systems. In: *H.J. Stein and J.L Hannah (Eds). Ore-bearing Granite Systems; Petrogenesis and Mineralizing Processes.* Geol. Soc. Am. Special Paper 246, 1-10.

Harmer, R.E. and Farrow, D., 1995. An isotopic study of the Rooiberg Group: age implications and a potential exploration tool. *Mineral. Deposita*, **30**, 188-195

Hatton, C.J. and Schweitzer, J.K., 1995. Evidence for synchronous extrusive and intrusive Bushveld magmatism. *Journ. Afr. Earth Sciences*, **4**, 579-594.

Henry, S.J. and Guidotti, C.V., 1985. Tourmaline as a petrogenetic indicator mineral: an example from the staurolite-grade metapelites of NW Maine. *Am. Miner.*, **70**, 1-15.

Hunter, D.R., 1973. The localisation of tin mineralisation with reference to Southern Africa. *Miner. Sci. Eng.*, **5**, 53-77.

_____, 1976. Some enigmas of the Bushveld Complex. *Econ. Geol.*, **71**, 229 - 248.

Iannello, P., 1970. The geology of the country between the Boshofsberg and the Crocodile River. *M.Sc. thesis*, Univ. Pretoria. 74p.

_____, 1971. The Bushveld Granites around Rooiberg, Transvaal, South Africa. *Geol. Rundschau*, **60**, 630-655.

Ikingura, J.R., 1989. Geology, geochemistry and genesis of stanniferous granites in the southern part of the Karagwe-Ankolean Belt, NW Tanzania. *Ph.D thesis (Unpubl)*, Carleton Univ. Ottawa. 326p.

Ishihara, S., Sawata, H., Arpornsuwan, S., Busaracome, P. and Bungbrakearti, N., 1979. The magnetite-series and ilmenite-series granitoids and their bearing on tin mineralization, particulary of the Malay Peninsula region. *Geol. Soc. Malaysia Bull.*, **11**, 103-110.

_____, 1981. The granitoid series and mineralization. *Econ. Geol.* **75th Anniv. Vol.** 458-484.

Digitised by the Department of Library Services in support of open access to information, University of Pretoria, 2021

Ito, T and Sadanaga, R., 1951. A Fourier analysis of the structure of tourmaline. *Acta Cryst.*, **4**. 385-390.

Izoret, L., Marnier, G. and Dusuavoy, Y., 1985. Caractérisation cristallochimique de la cassitérite des gisements d'étain et de tungstène de Galice, Espange. *Canadian Mineralogist*, **23**, 221 -231.

Jackson, N.J., Halliday, A.N., Sheppard, S.M.F. and Mitchell, J.G., 1982. Hydrothermal activity in the St. Just Mining District, Cornwall, England. In: *Metallization Associated with Acid Magmatism . Evans, A.M. (Ed)*. John Wiley. New York. 137-179.

Kanishcheva, L.I. and Romanenko, I.M., 1977. Zoning of cassiterite in tourmaline-type tin-ore deposits of the Maritime Region. *Doklady Akad. Nauk SSSR*, **236**, 176 -178.

Kleeman, G.J., and Twist, D., 1989. The compositionally-zoned sheet-like granite pluton of the Bushveld Complex: evidence bearing on the nature of A-type magmatism. *Journ. Petrology*, **6**, 1383-1414.

Kretz, R., 1982. A model for the distribution of trace elements between calcite and dolomite. *Geochim. Cosmochim. Acta*, **46**, 1979-1981.

Labuschagne, L.S., 1970a. The structure and mineralisation of the ore-bodies at Blaauwbank and Nieuwpoort, Rooiberg tin-field, Transvaal. *M.Sc. thesis (unpubl.)*, Univ. Pretoria. 77p.

_____, 1970b. The mineralisation of the Rooiberg A Mine. *Unpubl. mine report*, Rooiberg Tin Ltd. 8p.

_____, Holdsworth, R. and Stone, T.P., 1993. Regional stream sediment geochemical survey of South Africa. *Journ. Geochem. Expl.*, **47**, 282-296.

Lebedev, L. M., 1967. Metacolloids in endogenetic deposits. *Inst. of Geol. of Ore Dep., Petr., Min. and Geochem. Acad. of Sciences, USSR, Moscow.* Translated by: Southard., John B., Plenum Press. New York. 298p.

Leube, A., 1960. Structural control in the Rooiberg tinfields, South Africa. *Trans. geol. Soc. S. Afr.*, **63**, 265-282.

_____ and Stumpfl, E.F., 1963. The Rooiberg and Leeuwpoort Tin Mines, Transvaal, S. Africa. *Econ. Geol.*, **58**, 391-418.

Lehmann, B., 1990. Metallogeny of Tin. *Lecture Notes in Earth Sciences*, **32**, Springer-Verlag. 211p.

_____, 1982. Metallogeny of tin: magmatic differentiation versus geochemical heritage. *Econ. Geol.*, **77**, 50-59.

_____, 1987. Tin granites, geochemical heritage, magmatic differentiation. *Geol. Rundschau*, **76/1**, 177-185.

Lenthall, D.H., 1972. Progress report on the Bushveld Project. *Annual Rep. 1971. Econ. Geol. Res. Unit.*, Univ. Wits.

Digitised by the Department of Library Services in support of open access to information, University of Pretoria, 2021

Lister, C.J., 1979. Quartz-cored tourmalines from Cape Cornwall and other localities. *Proc. Ussher Soc.*,**4, Part 3**, Bristol, United Kingdom, 402-418

London, D., 1987. Internal differentiation of rare-element pegmatites. Effects of boron, phosphorous and fluorine. *Geochim. Cosmochim. Acta*, **51**, 403-420.

MacDonald, D.J. and Hawthorne, F.C., 1995. The crystal chemistry of Si-Al substitution in tourmaline. *Canadian Min.*, **33**, 849-858.

Manning, D.A.C., 1982. Chemical and morphological variation in tourmalines from the Hub Kapong batholith of peninsular Thailand. *Min. Mag.*, **45**, 139-147.

_____, and Pichavant, M., 1983. The role of fluorine and boron in the generation of granitic melts. *In: Alderton, M.P., and Gribble, C.D., (Eds). Migmatites melting and metamorphism*: Nantwich, Shiva Publications, 94-109.

McCarthy, T.S., and Hasty, R.A., 1976. Trace element distribution patterns and their relationship to the crystallization of granitic melts. *Geochim. Cosmochim. Acta*, **40**, 1351-1358.

McDonald, D.P., 1912. The occurrence of sideroplesite and ankerite in the cassiterite lodes at Rooiberg. *Trans. geol. Soc. S. Afr.*, **15**, 107-112.

_____, 1913. The cassiterite deposits of Leeuwpoort (938); the paragenesis of the lode-forming minerals. *Trans. geol. Soc. S. Afr.*, **16**, 107-141.

McIntire, W.L., 1963. Trace element partitioning coefficients - a review of theory and application to geology. *Geochim. Cosmochim. Acta*, **27**, 1209-1264

Menge, G.F.W., 1963. The cassiterite deposits on Doornhoek 342KR and vicinity, west of Naboomspruit, Transvaal. *M.Sc.thesis (unpubl.)*, Univ. Pretoria. 54p.

McNaughton, N.J., Pollard, P.J., Groves, D.I. and Taylor, R.G., 1993. A long-lived hydrothermal system in the Bushveld granites at the Zaaiplaats Tin Mine: Lead isotope evidence. *Econ. Geol.*, **88**, 27-43.

Misiewicz, J.E., 1992. The application of resource management at Rooiberg Tin Limited. *MASSMIN 92*. Johannesburg, SAIMM.

Möller, P., Dulski, P., Schley, F., Luck, J. and Szacki, W., 1981. A new way of interpreting trace element concentrations with respect to modes of mineral formation. *Journ. Geochem. Expl.*, **15**, 271 - 284.

_____ and Dulski, P., 1983. Fractionation of Zr and Hf in cassiterite. *Chemical Geology*, **12**, 1 - 12.

_____, Dulski, P., Szacki, W., Malow, G, and Riedel,E., 1988. Substitution of tin in cassiterite by tantalum, niobium, tungsten, iron and manganese. *Geochim. Cosmochim. Acta*, **52**, 1497 -1503.

Digitised by the Department of Library Services in support of open access to information, University of Pretoria, 2021

Moore, F. and Howie, R.A., 1979. Geochemistry of some Cornubian cassiterites. *Mineral. Deposita*, **14**, 103 -107.

Naude, K., 1993. A mineralogical and geochemical study of the tin deposit at the NAD-Mine in the Rooiberg tin field regarding cassiterite, tourmaline, carbonate, sulphide and quartz, wall rock alteration and fluid composition. *M.Sc. thesis (Unpubl.)* Univ. Stellenbosch. 89p.

Neiva, A. M. R., 1974. Geochemistry of tourmaline (schorlite) from granites, aplites and pegmatites from Northern Portugal. *Geochim. Cosmochim. Acta*, **38**, 1307-1317.

Newberry, R.J., Burns, L.E., Swanson, S.E. and Smith, T.E., 1990. Comparative petrologic evolution of the Sn and W granites of the Fairbanks-Circle area, interior Alaska. In: *H.J. Stein and J.L Hannah (Eds). Ore-bearing Granite Systems; Petrogenesis and Mineralizing Processes*. Geol. Soc. Am. Special Paper 246. 121-142.

Niggli, P. and Morey, G.W. ca 1910-1930. See Bowen, N.L. *Evolution of Igneous Rocks* for a summary of the work of Niggli and Morey.

Norrish, K. and Hutton, J.T., 1969. An accurate X-ray spectrographic method for the analysis of a wide range of geological samples. *Geochim. Cosmochim. Acta*, **33**, 431-453.

Olade, M.A., 1980. Geochemical characteristics of tin-bearing and tin-barren granites, Northern Nigeria. *Econ. Geol.*, **75**, 71-82.

Ollila, J.T., 1981. A fluid inclusion and mineralogical study of tin deposits and rocks associated with the Bushveld Complex at the Zaaiplaats, Rooiberg and Union Tin Mines in the Central Transvaal, South Africa. *PhD thesis*. Rand Afr. Univ. 257p.

_____, 1984. Fluid inclusions and tin deposition at Zaaiplaats, the central Transvaal, South Africa. *Bull. Geol. Soc. Finland*, **56** (1-2) 59-73.

Phillips, A. H., 1982. The geology of the Leeuwpoort tin deposit and selected aspects of its environs. *M.Sc. thesis (unpubl.)*, Wits. Univ., 297p.

Pitcher, W.S., 1979. The nature, ascent and emplacement of granitic magmas. *J. geol. Soc. London.*, **136**, 627-662.

Plimer, I.R., 1980. Exhalative Sn and W deposits associated with mafic volcanism as precursors to Sn and W deposits associated with granites. *Mineral. Deposita*, **15**, 275-289.

_____, Lu, J. and Kleeman, J.D., 1991. Trace and rare earth elements in cassiterite - sources of components for tin deposits of the Mole Granite, Australia. *Mineral. Deposita*, **26**, 267 - 274.

Pollard, P.J., Taylor, R.G. and Tate, N.M., 1989. Textural evidence for quartz and feldspar dissolutions as a mechanism of formation for Maggs Pipe, Zaaiplaats tin mine, South Africa. *Mineral. Deposita*, **24**, 210-218.

Digitised by the Department of Library Services in support of open access to information, University of Pretoria, 2021

_____, Andrew, A.S. and Taylor, R.G., 1991a. Fluid inclusions and stable isotope evidence for interpretation between granites and magmatic hydrothermal fluids during formation of disseminated and pipe-style mineralisation at Zaaiplaats Tin Mine. *Econ. Geol.*, **86**, 121-141.

_____, Taylor, R.G, Taylor, R.P. and Groves, D.I., 1991b. Petrographic and geochemical evolution of pervasively altered Bushveld granites at the Zaaiplaats Tin Mine. *Econ. Geol.*, **86**, 1401-1433.

_____ , R.P. and Blenkinsop, J., 1991c. Rb/Sr isotope systematics of Sn-W-REE mineralisation in miarolitic cavities at the Zaaiplaats Tin Mine, Bushveld Complex. *[Abs.] : Geol. Soc. Canada-Mineralog. Assoc. Canada*. Program with Abstracts. **16**, p A100.

Rayleigh, J.W.S., 1896. Theoretical considerations respecting the separation of gases by diffusion and similar processes. *Philos. Mag.*, **42**, 77-107.

Recknagel, R., 1908. On some mineral deposits in the Rooiberg District. *Trans. geol. Soc. S. Afr.*, **11**, 83-106.

Reece, C., Ruiz, J., Duffield, W.A. and Patchett, J.P., 1990. Origin of Taylor Creek rhyolite magma, Black Range, New Mexico, based on Nd-Sr isotope studies. In: *H.J. Stein and J.L Hannah (Eds). Ore-bearing Granite Systems; Petrogenesis and Mineralizing Processes*. Geol. Soc. Am. Special Paper 246, 263-274.

Reeder, R.J., 1983. Crystal chemistry of the rhombohedral carbonates. In: Reeder Richard J., (Ed.), *Carbonates: Mineralogy and Chemistry. Reviews in Mineralogy*, **11**, 1-47.

_____ and Dollase, W.A., 1989. Structural variation in the dolomite-ankerite solid-solution series: An X-ray, Mössbauer, and TEM study. *Am. Mineral.*, **74**, 1159-1167.

Reinecke, L., 1929. Report on the mines of the Rooiberg Minerals Development Co. Ltd. *Unpubl. Mine Report*.

Richards, R.J., and Eriksson, P.G. 1988. The sedimentology of the Pretoria Group in selected areas in the northern portion of the Rooiberg Fragment. *S. Afr. J. Geol.*, **91**, 498-508

Robb, L.J., Robb, V.M. and Walraven, F., 1994. The Albert silver mine revisited: towards a model for polymetallic mineralisation in granites of the Bushveld Complex, South Africa. *Expl. Mining Geol.*, **4**, 219-230

Robinson, B.W. and Kusakabe, M., 1975. Quantitative preparation of SO_2 for $^{34}S/^{32}S$ analyses from sulphides by combustion with cuprous oxide. *Analytical Chemistry*, **47**, 1179-1181.

Rose, A.W., Hawkes, H.E. and Webb, J.S., 1979. *Geochemistry in Mineral Exploration*. Academic Press, New York.

Rosenberg, P.E., 1967. Subsolidus relations in the system CaCO3-MgCO3-FeCO3 between 350 and 550°C. *Am. Mineral.*, **52**, 787-796

Digitised by the Department of Library Services in support of open access to information, University of Pretoria, 2021

_____, 1991. Structural variation in the dolomite-ankerite solid solution series: An X-ray, Mössbauer, and TEM study - a discussion. *Am. Mineral.*, **76**, 659-660.

_____ and Foit, Jr., F.F., 1979. Synthesis and characterization of alkali-free tourmaline. *Am. Mineral.*, **64**, 180-186.

Rozendaal, A., Toros, M.S. and Anderson, J.R., 1986. The Rooiberg tin deposits, west-central Transvaal. In: Anhaeusser, C.R. and Maske, S. (Eds.). *Mineral Deposits of Southern Africa*. **Vol. II**,. Geol. Soc. S. Afr., Johannesburg., 1307-1327

_____, Misiewicz, J.E and Scheepers, R., 1995a. The tin-zone: sediment-hosted hydrothermal tin mineralisation at Rooiberg, South Africa. *Mineral. Deposita*, **30**, 178-187.

_____, Misiewicz, J.E and Scheepers, R., 1995b. Hydrothermal alteration associated with sediment-hosted Rooiberg tin deposits, South Africa. *Trans. Inst. Min. Metall.* ***(Sect. B: Appl. earth sci.)***, **104**, B121-B135.

Ruck, R., Dusausoy, Y., Nguyen Trung, C., Gaite, J-M. and Murciego, A., 1989. Powder EPR study of natural cassiterites and synthetic SnO_2 doped with Fe, Ti, Na and Nb. *Eur. J. Mineral.*, **1**, 343 -352.

Rye, R.O., Lufkin, J.L. and Wasserman, M. D., 1990. Genesis of the rhyolite-hosted tin occurrences in the Black Range, New Mexico, as indicated by stable isotope studies. In: *H.J. Stein and J.L Hannah (Eds). Ore-bearing Granite Systems; Petrogenesis and Mineralizing Processes*. Geol. Soc. Am. Special Paper 246, 233-250.

Schneider, H-J., Dulski, P., Möller, P., Luck, J. and Villalpando, A., 1978. Correlation of trace element distribution in cassiterites and geotectonic position of their deposits in Bolivia. *Mineral. Deposita*, **13**, 119 -122.

Schweitzer, J.K, Hatton, C.J. and de Waal, S.A., 1995. Economic potential of the Rooiberg Group: Volcanic rocks in the floor and roof of the Bushveld Complex. *Mineral. Deposita*, **30**, 168-177

Simpson, P.R., and Hurdley, J., 1985. Relationship between metalliferous mineralization and Sn-U-F-rich mildly alkaline high heat production granites in the Bushveld Complex, South Africa. In: *High Heat Production Granites. Hydrothermal circulation and ore genesis.* Inst. Min. Met., London., 365-382

Sinclair, A.J., 1991. A fundamental approach to threshold estimation in exploration geochemistry: probability plots revisited. *Journ. Geochem.*, **41**, 1-72

Söhnge, A.P.G., 1963. Genetic problems of pipe deposits in South Africa. *Trans. geol. Soc. S. Afr.*, **66**, xx-lxxii.

Solliman, M.M., 1982. Chemical and physical properties of beryl and cassiterite ores, Southeastern Desert, Egypt. *Trans. Instn. Min. Metall. (Sect. B: Appl. earth sci.)*, **91**, B17 - B20.

Digitised by the Department of Library Services in support of open access to information, University of Pretoria, 2021

South African Committee for Stratigraphy (SACS). 1980. Stratigraphy of South Africa, Part I (Comp. L.E. Kent). Lithostratigraphy of the Republic of South Africa, South West Africa/Namibia, and the Republics of Bophuthatswana, Transkei and Venda. *Handbk. geol. Surv. S. Afr.*, **8**, 690p.

Stear, W.M., 1976. The geology and ore controls of the northern Rooiberg tin-field, Transvaal. *M.Sc. thesis*, Univ. Stellenbosch. 89p.

_____, 1997a. The stratigraphy and sedimentation of the Pretoria Group at Rooiberg, Transvaal. *Trans. geol. Soc. S. Afr.*, **80**, 53-65.

_____, 1977b. The stratabound tin-deposits and structure of the Rooiberg Fragment. *Trans. geol. Soc. S. Afr.*, **80**, 67-78.

Stacey, J.S. and Kramers, J.D., 1975. Approximation of terrestrial lead isotope evolution by a two stage model. *Earth Planet. Sci. Lett.*, **26**, 207-221.

Sun, S.-s., and McDonough, W.F., 1989. Chemical and isotopic systematics of oceanic basalts: implications for mantle composition and processes. In: *Magmatism in the Ocean Basalts. Saunders, A.D., and Norry, M.J., (Eds).* Geological Society Special Publication, 42, 313-345.

Taylor, Roger G., 1978. Geology of tin deposits. *Developments in Economic Geology*, **11**, Elsevier Scientific Publishing Company, 543p.

Taylor, B.E. and Slack, J.F., 1984. Tourmalines from Appalachian-Caledonian massive sulfide deposits: Textural, chemical and isotope relationships. *Econ. Geol.*, **79**, 1703-1726.

Taylor, J.R., and Wall, V.J., 1992. The behaviour of tin in granitoid magmas. *Econ. Geol.*, **87**, 403-420.

van Biljon, S., 1949. The transformation of the Pretoria Series in the Bushveld Complex. *Trans. geol. Soc. S. Afr.*, **52**, 1-175.

Veizer, J., 1983. Trace elements and isotopes in sedimentary carbonates. In: Reeder Richard J., (Ed.), *Carbonates: Mineralogy and Chemistry. Reviews in Mineralogy*, **11**, 265-300.

Visser, D.J.L., 1970. Johannes Willemse. *Symposium on the Bushveld Igneous Complex and other layered intrusions.* Von Gruenewaldt, G. and Visser, D.J.L., (Eds.). Geol. Soc. S. Afr. Spec. Publ. No. 1, 1-4

Von Gruenewaldt, G., and Strydom, J.H., 1985. Geochemical distribution patterns surrounding tin-bearing pipes and the origin of the mineralising fluids at the Zaaiplaats Tin Mine, Potgietersrus District. *Econ. Geol.*, **80**, 1201-1211.

Walraven, F., 1986. Stratigraphy and structure of the Nebo Granite, Bushveld Complex, South Africa. *Geocongress 86 Abstr.*, Geol. Soc. S. Afr. Johannesburg.

Digitised by the Department of Library Services in support of open access to information, University of Pretoria, 2021

_____, 1987. Textural, geochemical and genetic aspects of the granophyric rocks of the Bushveld Complex. *Mem. geol. Surv. S. Afr.*, **72**, 145p.

_____, 1997. Geochronology of the Rooiberg Group, Transvaal Supergroup, South Africa. *Inf. Circ., Econ. Geol. Res. Unit*, **316**, 21p.

_____, Kleemann, G.J., Allsopp, H.L., 1985. Disturbance of trace element or isotope systems and its bearing on mineralisation in acid rocks of the Bushveld Complex, South Africa. In: *High Heat Production Granites. Hydrothermal circulation and ore genesis.* Inst. Min. Met., London. 393-408

_____, Armstrong, R.A. and Kruger, F.J., 1990. A chronostratigraphic framework for the north-central Kaapvaal craton, the Bushveld Complex and the Vredefort structure. *Tectophysics*, **171**, 23-48.

_____, and Hattingh, E., 1993. Geochronology of the Nebo Granite, Bushveld Complex. *S. Afr. J. Geol.*, **96**, 31-41.

Webster, J.D., and Holloway, J.R., 1990. Partitioning of F and Cl between magmatic hydrothermal fluids and highly evolved granitic magmas. In: *H.J. Stein and J.L Hannah (Eds). Ore-bearing Granite Systems; Petrogenesis and Mineralizing Processes.* Geol. Soc. Am. Special Paper 246. 21-34.

Zemann, J., 1969. Crystal chemistry. In: Wedepohl, K.H., (Ed.), *Handbook of Geochemistry*, **1**, Springer: Berlin, 12-36

Digitised by the Department of Library Services in support of open access to information, University of Pretoria, 2021

APPENDIX

Table I - Sample number, rock type and co-ordinates of granitoids

Table II - Rooiberg A, NAD and C Mines - Underground samples : Sample number, locality and main minerals

Table III - Major, trace and REE analyses of Rooiberg granitoids

Table IV - Major and trace element analyses of Rooiberg ankerite, including mole percentages

Table V - Pb-Pb isotopic data of Rooiberg ankerite

Table VI - Partial analyses of Rooiberg tourmalines, including atomic proportions and site allocations

Table VII- Trace element content of cassiterite

Digitised by the Department of Library Services in support of open access to information, University of Pretoria, 2021

Table I - Sample number, rock type and co-ordinates of granitoids

Digitised by the Department of Library Services in support of open access to information, University of Pretoria, 2021

Table I - Sample number, rock type and co-ordinates of granitoids

Station	Field No	Lab No	Rock type	Co-ordinates South	Co-ordinates East	Locality
1	501L0	SL1	Rashoop Granophyre	24 47 17	27 34 53	West
2	502L0	SL2	Rashoop Granophyre	24 46 39	27 34 58	West
3	503L0	SL3	Rashoop Granophyre	24 47 42	27 25 05	West
4	504L0	SL4	Rashoop Granophyre	24 48 17	27 35 28	West
5	505L0	SL5	Rashoop Granophyre	24 49 07	27 35 59	West
6	506L0	SL6	Rashoop Granophyre	24 48 54	27 35 31	West
7	507L0	SL7A	Rashoop Granophyre	24 49 37	27 36 14	West
8	508L0	SL8	Rashoop Granophyre	24 49 49	27 35 37	West
9	509L0	SL9	Bobbejaankop Granite	24 50 01	27 35 24	West
10	510L0	SL10	Lease Granite	24 49 30	27 35 32	West
11	511L0	SL11	Bobbejaankop Granite	24 50 01	27 35 00	West
12	512L0	SL12	Lease Granite	24 50 18	27 34 41	West
13	513L0	SL13	Lease Granite	24 50 46	27 34 32	West
14	514L0	SL14	Lease Granite	24 50 22	27 34 13	West
15	515L0	SL15	Lease Granite	24 50 06	27 33 59	West
16	516L0	SL16	Lease Granite	24 50 10	27 33 27	West
17	517L0	SL17	Lease Granite	24 49 13	27 33 36	West
18	518L0	SL18	Not classified	24 49 42	27 33 31	West
19	519L0	SL19	Nebo Granite	24 48 54	27 33 49	West
20	520L0	SL20	Lease Granite	24 48 15	27 35 10	West
21	521L0	SL21	Bobbejaankop Granite	24 48 27	27 34 49	West
22	522L0	SL22A&B	Bobbejaankop Granite	24 48 46	27 34 35	West
23	523L0	SL23	Bobbejaankop Granite	24 49 01	27 34 05	West
24	524L0	SL24	Klipkloof Granite	24 49 57	27 32 27	West
25	525L0	SL25&A	Klipkloof Granite	24 49 35	27 32 46	West
26	526L0	SL26	Bobbejaankop Granite	24 49 27	27 33 18	West
27	527L0	SL27	Klipkloof Granite	24 48 43	27 33 33	West
28	528L0	SL28&A	Klipkloof Granite	24 48 19	27 33 30	West
29	529L0	SL29	Klipkloof Granite	24 48 59	27 33 32	West
30	530L0	SL30	Lease Granite	24 50 09	27 32 21	West
31	531L0	SL31	Lease Granite	24 49 30	27 32 11	West
32	532L0	SL32	Klipkloof Granite	24 49 02	27 32 04	West
33	533L0	SL33	Lease Granite	24 48 35	27 32 27	West
34	534L0	SL34	Nebo Granite	24 52 24	27 34 14	West
35	535L0	SL35	Nebo Granite	24 52 00	27 34 54	West
36	536L0	SL36	Nebo Granite	24 51 46	27 35 16	West
37	537L0	SL37	Nebo Granite	24 51 35	27 35 57	West
38	538L0	SL38	Nebo Granite	24 51 30	27 36 27	West
39	539L0	SL39	Nebo Granite	24 51 17	27 36 13	West
40	540L0	SL40	Not classified	24 51 06	27 36 12	West
41	541L0	SL41	Not classified	24 48 21	27 32 39	West
42	542L0	SL42	Nebo Granite	24 51 28	27 34 45	West
43	543L0	SL43	Nebo Granite	24 48 05	27 33 11	West
44	544L0	SL44	Nebo Granite	24 48 02	27 33 37	West
45	545L0	SL45	Lease Granite	24 47 56	27 34 03	West
46	546L0	SL46	Lease Granite	24 47 55	27 33 04	West
47	547L0	SL47	Bobbejaankop Granite	24 47 38	27 33 18	West
48	548L0	SL48	Not classified	24 52 19	27 33 34	West
49	549L0	SL49	Nebo Granite	24 51 31	27 34 02	West
50	550L0	SL50	Lease Granite	24 50 52	27 34 56	West

Digitised by the Department of Library Services in support of open access to information, University of Pretoria, 2021

Table I (contd) - Sample number, rock type and co-ordinates of granitoids

Station	Field No	Lab No	Rock type	Co-ordinates South	Co-ordinates East	Locality
51	551L0	SL51	Bobbejaankop Granite	24 50 45	27 35 31	West
52	552L0	SL52	Bobbejaankop Granite	24 50 28	27 36 08	West
53	553L0	SL53	Nebo Granite	24 51 04	27 35 42	West
54	554L0	SL54	Lease Granite	24 46 24	27 33 09	West
55	555L0	SL55	Lease Granite	24 46 32	27 32 51	West
56	556L0	SL56	Not classified	24 46 46	27 32 32	West
57	557L0	SL57	Klipkloof Granite	24 47 09	27 32 48	West
58	558L0	SL58	Lease Granite	24 46 27	27 32 19	West
59	559L0	SL59	Bobbejaankop Granite	24 46 02	27 32 18	West
60	560L0	SL60	Lease Granite	24 46 43	27 33 26	West
61	561L0	SL61	Bobbejaankop Granite	24 46 49	27 33 19	West
62	562L0	SL62	Lease Granite	24 46 49	27 33 19	West
63	563L0	SL63	Lease Granite	24 47 56	27 34 01	West
64	564L0	SL64	Lease Granite	24 48 08	27 32 53	West
65	565L0	SL65	Lease Granite	24 50 11	27 34 44	West
66	566L0	SL66	Klipkloof Granite	24 50 24	27 34 32	West
67	567L0	SL67	Bobbejaankop Granite	24 48 50	27 34 23	West
68	568L0	SL68	Not classified	24 53 20	27 32 32	West
69	569L0	SL69	Lease Granite	24 49 08	27 51 19	East
70	570L0	SL70	Lease Granite	24 49 48	27 51 21	East
71	571L0	SL71	Klipkloof Granite	24 50 13	27 51 19	East
72	572L0	SL72	Bobbejaankop Granite	24 51 11	27 51 06	East
73	573L0	SL73	Klipkloof Granite	24 52 20	27 52 07	East
74	574L0	SL74	Klipkloof Granite	24 52 07	27 52 44	East
75	575L0	SL75	Klipkloof Granite	24 57 54	27 53 19	East
76	576L0	SL76	Klipkloof Granite	24 51 37	27 54 04	East
77	577L0	SL77	Klipkloof Granite	24 50 33	27 54 30	East
78	578L0	SL78	Lease Granite	24 49 50	27 53 13	East
79	579L0	SL79	Klipkloof Granite	24 50 14	27 54 23	East
80	580L0	SL80	Nebo Granite	24 49 55	27 53 46	East
81	581L0	SL81	Bobbejaankop Granite	24 51 09	27 52 17	East
82	582L0	SL82	Lease Granite	24 51 37	27 51 58	East
83	583L0	SL83	Nebo Granite	24 50 30	27 53 21	East
84	584L0	SL84	Lease Granite	24 51 27	27 54 40	East
85	585L0	SL85	Nebo Granite	24 49 04	27 57 25	East
86	586L0	SL86	Nebo Granite	24 48 48	27 55 51	East
87	587L0	SL87	Lease Granite	24 48 36	27 54 19	East
88	588L0	SL88	Bobbejaankop Granite	24 48 43	27 52 01	East
89	589L0	SL89	Lease Granite	24 48 43	27 52 01	East
90	590L0	SL90	Not classified	24 49 51	27 57 30	East
91	591L0	SL91	Nebo Granite	24 49 02	27 54 29	East
92	592L0	SL92	Nebo Granite	24 48 49	27 56 24	East
93	593L0	SL93	Nebo Granite	24 48 58	27 56 12	East
94	594L0	SL94	Not classified	24 50 58	27 55 50	East
95	595L0	SL95	Not classified	24 51 37	27 54 38	East
96	596L0	SL96	Nebo Granite	24 48 21	27 53 32	East
97	597L0	SL79	Klipkloof Granite	24 47 57	27 54 23	East
98	598L0	SL98	Not classified	24 46 49	27 54 36	East
99	599L0	SL99	Nebo Granite	24 41 49	27 54 33	East
100	600L0	SL100	Nebo Granite	24 47 31	27 54 30	East

Digitised by the Department of Library Services in support of open access to information, University of Pretoria, 2021

Table I (contd) - Sample number, rock type and co-ordinates of granitoids

Station	Field No	Lab No	Rock type	Co-ordinates South	Co-ordinates East	Locality
101	601L0	SL101	Nebo Granite	24 46 49	27 54 10	East
102	602L0	SL102	Not classified	24 46 23	27 53 11	East
103	603L0	SL103	Nebo Granite	24 47 29	27 56 51	East
104	604L0	SL104	Not classified	24 49 34	27 58 49	East
105	605L0	SL105	Lease Granite	24 52 48	27 52 39	East
106	606L0	SL106	Lease Granite	24 53 32	27 53 10	East
107	607L0	SL107	Nebo Granite	24 54 12	27 53 43	East
108	608L0	SL108	Nebo Granite	24 45 36	27 56 49	East
109	609L0	SL109	Lease Granite	24 45 18	27 57 23	East
110	610L0	SL110	Nebo Granite	24 44 46	27 58 34	East
111	611L0	SL111	Not classified	24 45 27	27 58 10	East
112	612L0	SL112	Nebo Granite	24 47 29	27 58 43	East
113	613L0	SL113	Nebo Granite	24 54 09	27 53 20	East
114	614L0	SL114	Nebo Granite	24 54 08	27 53 13	East
115	615L0	SL115	Lease Granite	24 53 41	27 50 45	East
116	616L0	SL116	Lease Granite	24 54 06	27 50 54	East
117	617L0	SL117	Not classified	24 54 15	27 50 49	East
118	618L0	SL118	Lease Granite	24 54 26	27 50 49	East
119	619L0	SL119	Lease Granite	24 54 23	27 50 29	East
120	620L0	SL120	Nebo Granite	24 55 32	27 53 50	East
121	621L0	SL121	Klipkloof Granite	24 55 48	27 53 17	East
122	622L0	SL122	Klipkloof Granite	24 55 33	27 52 06	East
123	623L0	SL123	Lease Granite	24 55 17	27 50 50	East
124	624L0	SL124	Nebo Granite	24 53 53	27 33 54	East
125	625L0	SL125	Nebo Granite	24 54 30	27 53 15	East

Digitised by the Department of Library Services in support of open access to information, University of Pretoria, 2021

Table II - Rooiberg A, NAD and C Mines

Underground samples: Sample number, locality and main minerals

Digitised by the Department of Library Services in support of open access to information, University of Pretoria, 2021

TABLE II - Rooiberg A NAD And C Mines. Underground samples: Sample number, locality and main minerals

Sample	Mine	Section/ Lode	Level	Wall rock	Tourm. L2	Tourm L1	Cass.1	Cass.2	Pyrite	Sulph.	Ank.1	Ank.2	Quartz	Ser./Cl	Fluors
100L0	A	Q-22	500	X											
101L0	A	Q-22	500								X				
102L0	A	Q-22	500	X											
103L0	A	Q-22	500		X	X									
104L0	A	Q-22	580	X										X	
105L0	A	Q-22	580												
106L0	A	Q-22	500	X											
107L0	A	Q-22	500	X											
108L0	A	Q-22	500		X	X				X	X				
109L0	A	Q-22	500		X	X					X				
110L0	A	Q-22	500		X				X						
111L0	A	Q-22	500								X				
112L0	A	Q-22	580		X							X	X		
113L0	A	Q-22	580	X								X			
114L0	A	Q-22	580		X	X						X	X		
115L0	A	Q-22	565			X									
116L0	A	Q-22	565		X					X	X				
117L0	A	Q-22	565			X	X				X				
118L0	A	Q-22	565	X					X						
119L0	A	Q-22	565												
120L0	A	Q-22	565			X									
121L0	A	Q-22	500	X	X	X									
122L0	A	Q-22	500			X									
123L0	A	Q-22	500	X	X	X									
124L0	A	Q-22	500			X					X				
125L0	A	Q-22	500											X	
126L0	A	Q-22	500											X	
127L0	A	Q-22	500			X									
128L0	A	Q-22	500							X					
129L0	A	Q-22	500	X									X		

Digitised by the Department of Library Services in support of open access to information, University of Pretoria, 2021

TABLE II (contd) - Rooiberg A NAD And C Mines. Underground samples: Sample number, locality and main minerals

Sample	Mine	Section/ Lode	Level	Wall rock	Tourm L2	Tourm L1	Cass.1	Cass.2	Pyrite	Sulph.	Ank.1	Ank.2	Quartz	Ser./Cl	Fluors
130L0	A	Q-22	500									X			
131L0	A	Q-22	500												
132L0	A	Q-22	500												
133L0	A	Q-22	500												
134L0	A	Q-22	500			X				X			X		
135L0	A	Q-22	500												
143L0	A	Q-22	500	X											
144L0	A	Q-22	500	X											
145L0	A	Q-22	500	X											
146L0	A	Q-22	500	X											
147L0	A	Q-22	500									X			
148L0	A	Q-22	500	X	X						X				
149L0	A	Q-22	500		X						X				
150L0	A	Q-22	525	X									X		
151L0	A	Q-22	525		X	X			X						
152L0	A	Q-22	565		X		X				X				
153L0	A	Q-22	565		X	X				X		X			
154L0	A	Q-22	565			X									
155L0	A	Q-22	565	X	X										
156L0	A	Q-22	565		X						X				
157L0	A	Q-22	565		X					X	X				
158L0	A	Q-22	565	X	X	X				X					
159L0	A	Q-22	565		X					X	X				
160L0	A	Q-22	565		X					X	X				
161L0	A	Q-22	565		X	X									
162L0	A	Q-22	565	X								X			
163L0	A	Q-22	580						X		X				
164L0	A	Q-22	580						X						
165L0	A	Q-22	580												
166L0	A	Q-22	580												
167L0	A	Q-22	580				X								

Digitised by the Department of Library Services in support of open access to information, University of Pretoria, 2021

TABLE II (contd) - Rooiberg A NAD And C Mines. Underground samples: Sample number, locality and main minerals

Sample	Mine	Section/ Lode	Level	Wall rock	Tourm L2	Tourm L1	Cass.1	Cass.2	Pyrite	Sulph.	Ank.1	Ank.2	Quartz	Ser./Cl	Fluors
168L0	A	Q-22	580												
169L0	A	Q-22	580												
170L0	A	Q-22	580												
171L0	A	Q-22	580												
172L0	A	Q-22	580												
173L0	A	Q-22	580												
174L0	A	Q-22	580												
175L0	A	Q-22	580												
176L0	A	Q-22	580				X					X			
177L0	A	Q-22	580												
178L0	A	Q-22	580												
179L0	A	Q-22	580												
180L0	A	Q-22	580												
188L0	A	Q-22	580									X			
189L0	A	Q-22	580		X				X		X				
190L0	A	Q-22	580	X	X				X					X	
191L0	A	Q-22	580									X			
192L0	A	Q-22	580	X	X	X			X		X		X		
193L0	A	Q-22	580		X		X		X		X			X	
194L0	A	Q-22	580	X			X		X		X				
195L0	A	Q-22	580		X	X	X		X		X				
196L0	A	Q-22	580		X	X					X				
197L0	A	Q-22	580												
198L0	A	19N	760									X			
199L0	A	19N	760		X				X						
200L0	A	19N	760	X								X			
201L0	A	19N	760		X				X						
202L0	A	19N	760		X				X	X					
203L0	A	19N	640		X				X	X					
205L0	A	19N	640			X			X		X				

Digitised by the Department of Library Services in support of open access to information, University of Pretoria, 2021

TABLE II (contd) - Rooiberg A NAD and C Mines. Underground samples: Sample number, locality and main minerals

Sample	Mine	Section/ Lode	Level	Wall rock	Tourm L2	Tourm L1	Cass.1	Cass.2	Pyrite	Sulph.	Ank.1	Ank.2	Quartz	Ser./Cl	Fluors
206L0	A	19N	640		X		X	X	X						
207L0	A	19N	640		X	X	X	X	X						
208L0	A	19N	640	X			X	X	X		X				
209L0	A	19N	640		X		X	X	X		X				
210L0	A	19N	640		X				X		X	X			
211L0	A	19N	640	X											
212L0	A	19N	640		X		X	X	X						
213L0	A	19N	640		X				X		X				
214L0	A	19N	640			X	X	X	X						
215L0	A	19N	640		X		X		X						
216L0	A	M-18	780			X	X				X				
217L0	A	M-18	780	X		X									
218L0	A	M-18	780	X	X						X				
219L0	A	M-18	780	X	X				X						
220L0	A	M-18	780			X			X						
221L0	A	M-18	780		X		X		X						
222L0	A	Jewel Box	680			X	X		X						
223L0	A	Jewel Box	680		X	X		X	X						
224L0	A	Jewel Box	680		X						X	X			
225L0	A	Jewel Box	680	X											
226L0	A	Jewel Box	680		X		X	X	X						
227L0	A	Jewel Box	680			X				X		X			
228L0	A	M-18	780			X									
229L0	A	M-18	780	X		X				X					
230L0	A	M-18	780				X		X						
231L0	A	M-18	780	X					X						
232L0	A	M-18	780				X			X					
233L0	A	M-18	780			X									
234L0	A	M-18	780												
235L0	A	M-18	780		X		X		X	X				X	
236L0	A	M-18	780		X		X			X					

Digitised by the Department of Library Services in support of open access to information, University of Pretoria, 2021

TABLE II (contd) - Rooiberg A NAD and C Mines. Underground samples: Sample number, locality and main minerals

Sample	Mine	Section/ Lode	Level	Wall rock	Tourm L2	Tourm L1	Cass.1	Cass.2	Pyrite	Sulph.	Ank.1	Ank.2	Quartz	Ser./Cl	Fluors
237L0	A	M-18	780	X		X	X		X	X					
238L0	A	M-18	780	X	X				X						
239L0	A	M-18	780		X		X		X					X	
240L0	A	M-18	780	X	X		X		X	X					
241L0	A	M-18	780	X	X				X						
242L0	A	M-18	780		X										
243L0	A	M-18	780	X	X					X					
244L0	A	M-18	780			X									
245L0	A	Jewel Box	680		X				X						
246L0	A	Jewel Box	680		X				X						
247L0	A	Jewel Box	680		X		X	X							
248L0	A	Jewel Box	680	X			X								
249L0	A	Jewel Box	680	X			X								
250L0	A	Jewel Box	680	X			X								
251L0	A	Jewel Box	680	X			X								
252L0	A	Jewel Box	680		X		X								
253L0	A	Jewel Box	680	X			X								
254L0	A	Jewel Box	680	X	X		X								
255L0	A	Jewel Box	680	X	X		X								
256L0	A	Jewel Box	680				X	X							
257L0	A	Jewel Box	680				X								
258L0	A	Jewel Box	680				X								
259L0	A	Jewel Box	680	X	X		X								
260L0	A	Jewel Box	680	X	X		X								
261L0	A	Jewel Box	680	X	X		X								
262L0	A	U30	780	X	X		X								
263L0	A	U30	780		X		X		X						
264L0	A	U30	780		X						X		X	X	
265L0	A	U30	780	X	X		X				X				
266L0	A	U30	780		X				X						

Digitised by the Department of Library Services in support of open access to information, University of Pretoria, 2021

TABLE II (contd) - Rooiberg A NAD and C Mines. Underground samples: Sample number, locality and main minerals

Sample	Mine	Section/ Lode	Level	Wall rock	Tourm L2	Tourm L1	Cass.1	Cass.2	Pyrite	Sulph.	Ank.1	Ank.2	Quartz	Ser./Cl	Fluors
267L0	A	U30	780	X	X				X						
268L0	A	U30	780		X		X		X						
269L0	A	U30	780												
270L0	A	U30	780	X			X								
271L0	A	U30	780	X	X		X								
272L0	A	U30	780		X		X	X							
273L0	A	U30	780		X				X			X		X	
274L0	A	U30	780		X		X		X						
275L0	A	U30	780									X			
276L0	A	U30	780	X	X		X								
277L0	A	U30	780		X		X								
425L0	A	Jewel Box	680						X		X	X			
428L0	A	Q-22	500											X	
429L0	A	Q-22	500			X									
430L0	A	Q-22	500			X									
432L0	A	Q-22	565		X		X			X					
433L0	A	Q-22	565		X										
434L0	A	Q-22	565			X								X	
435L0	A	Q-22	580		X		X		X						
436L0	A	Magazine	580		X		X		X						
437L0	A	Magazine	580		X				X						
438L0	A	Magazine	580		X				X						
439L0	A	19N	760		X				X						
440L0	A	19N	640		X		X	X	X						
441L0	A	19N	640		X		X	X	X						
442L0	A	19N	640		X		X	X	X						
443L0	A	19N	640		X		X	X	X						
444L0	A	19N	640		X		X	X	X						
445L0	A	19N	640		X		X	X	X						
446L0	A	19N	640		X		X	X	X						
447L0	A	19N	640		X		X	X	X		X				
448L0	A	19N	640		X		X	X	X		X				
449L0	A	19N	640				X	X			X				
450L0	A	19N	640				X	X			X				
451L0	A	19N	640				X	X	X		X				
453L0	A	Jewel Box	680			X			X		X				
455L0	A	Q-22	500							X					

Digitised by the Department of Library Services in support of open access to information, University of Pretoria, 2021

TABLE II (contd) - Rooiberg A NAD and C Mines. Underground samples: Sample number, locality and main minerals

Sample	Mine	Section/ Lode	Level	Wall rock	Tourm	Cassit.	Pyrite	Sulph.	Ank.	Siderite	Qrtz	Ser./Cl	Fluors
136L0	NAD	C Lode	1480	X		X			X				
137L0	NAD	C Lode	1480	X		X			X				
138L0	NAD	C Lode	1480										
139L0	NAD	C Lode	1480	X		X			X				
140L0	NAD		1480										
141L0	NAD		1480										
142L0	NAD	AMS Lode	1480	X									
278L0	NAD	C	1480					X		X			
279L0	NAD	C	1480							X			
280L0	NAD	C	1480			X				X			
281L0	NAD	C	1480	X		X		X	X		X		
282L0	NAD	C	1480										
283L0	NAD	C	1480										
283/4L0	NAD	C	1480										
284L0	NAD	C	1480	X		X	X		X				
285L0	NAD	C	1480						X	X			
286L0	NAD	C	1480						X	X			
287L0	NAD	Cotton	1580		X					X	X		
288L0	NAD	Cotton	1580		X	X	X		X				
289L0	NAD	Cotton	1580		X						X	X	
290L0	NAD	Cotton	1580		X				X		X	X	
291L0	NAD	Cotton	1580	X	X				X		X	X	
292L0	NAD	C	1480							X			
293L0	NAD	C	1480	X	X	X				X		X	
294L0	NAD	C	1480	X		X		X	X				
295L0	NAD	C	1480			X		X	X				
296L0	NAD	C	1480		X	X		X	X				
297L0	NAD	C	1480			X							
298L0	NAD	C	1480		X	X	X		X				
299L0	NAD	C	1480		X	X	X		X				
300L0	NAD	Union	1480	X	X	X	X		X		X	X	

Digitised by the Department of Library Services in support of open access to information, University of Pretoria, 2021

TABLE II (contd) - Rooiberg A NAD and C Mines. Underground samples: Sample number, locality and main minerals

Sample	Mine	Section/ Lode	Level	Wall rock	Tourm	Cassit.	Pyrite	Sulph.	Ank.	Siderite	Qrtz	Ser./Cl	Fluors
301L0	NAD	Union	1480										
302L0	NAD	Union	1480		X		X		X				
303L0	NAD	Union	1480		X				X		X	X	
304L0	NAD	Union	1480		X	X			X		X	X	
305L0	NAD	Union	1480		X		X		X				
306L0	NAD	Union	1480	X	X		X		X				
307L0	NAD	Union	1480	X	X		X		X			X	
308L0	NAD	Union	1480		X				X				
309L0	NAD	Bonus	1380	X		X			X				
310L0	NAD	Bonus	1380	X		X	X						
311L0	NAD	U	1380	X	X	X							
312L0	NAD	U	1380	X	X	X			X				
313L0	NAD	U	1380		X		X				X		
314L0	NAD	Ross-Watt	1380				X		X		X	X	
315L0	NAD	Ross-Watt	1380								X	X	
316L0	NAD	Ross-Watt	1380									X	
317L0	NAD	Ross-Watt	1380									X	
318L0	NAD	Ross-Watt	1380									X	
319L0	NAD	U	1380	X	X								
320L0	NAD	Bonus	1380		X	X			X		X		
321L0	NAD	Bonus	1380		X				X				
322L0	NAD	Bonus	1380	X			X		X				
323L0	NAD	Bonus	1380						X		X		
324L0	NAD	Bonus	1380		X								
325L0	NAD	Bonus	1380			X							
326L0	NAD	Bonus	1380			X							
327L0	NAD	Bonus	1380		X	X	X						
328L0	NAD	Bonus	1380			X		X					
329L0	NAD	Bonus	1380		X	X	X		X				
330L0	NAD	Bonus	1380		X	X							

Digitised by the Department of Library Services in support of open access to information, University of Pretoria, 2021

TABLE II (contd) - Rooiberg A NAD and C Mines. Underground samples: Sample number, locality and main minerals

Sample	Mine	Section/ Lode	Level	Wall rock	Tourm	Cassit.	Pyrite	Sulph.	Ank.	Siderite	Qrtz	Ser./Cl	Fluors
331L0	NAD	U	1380	X	X	X			X				
332L0	NAD	U	1380	X	X				X				
333L0	NAD	U	1380	X	X				X				
334L0	NAD	U	1380	X	X	X			X				
335L0	NAD	U	1380	X	X	X			X				
336L0	NAD	U	1380	X	X	X			X				
337L0	NAD	U	1380	X	X	X			X				
338L0	NAD	U	1380		X	X			X				
339L0	NAD	U	1380	X	X	X			X				
340L0	NAD	U	1380	X	X	X			X				
341L0	NAD	U	1380		X	X							
342L0	NAD	U	1380		X	X							
431L0	NAD	C Lode	1480	X		X			X				
455L0	NAD	C	1480		X	X	X		X				

Digitised by the Department of Library Services in support of open access to information, University of Pretoria, 2021

TABLE II (contd) - Rooiberg A NAD and C Mines. Underground samples: Sample number, locality and main minerals

Sample	Mine	Section/ Lode	Level	Wall rock	Chlorit	Tourm	Cassit.	Pyrite	Sulph.	Ank.	Feldspar	Qrtz	Ser./Cl	Fluors
343L0	C	CA	1740		X		X				X			X
344L0	C	CA	1740		X		X				X			
345L0	C	CA	1740		X		X				X			
346L0	C	CA	1740	X			X				X		X	
347L0	C	CA	1740				X			X	X			
348L0	C	CA	1740		X		X		X	X	X		X	
349L0	C	CA	1740		X		X				X	X	X	
350L0	C	CA	1740		X		X					X	X	
351L0	C	CA	1740	X										
352L0	C	CA	1740	X										
353L0	C	CA	1740	X										
354L0	C	CA	1740		X				X			XX		
355L0	C	CA	1740		X							XXX		
356L0	C	CA	1740		X							X		
357L0	C	New	1740		X			X				X		
358L0	C	New	1740					X		X	X			
359L0	C	New	1740					X			X	XX		
360L0	C	FLFract	1740										X	
361L0	C	Gap	1740	X			X	X						
362L0	C	Gap	1740	X									X	
363L0	C	Gap	1740	X			X	X						
364L0	C	Gap	1740		X			X						
365L0	C	Gap	1740	X										X
366L0	C	Gap	1740	X			X	X						
367L0	C	Gap	1740				X	X				X		
368L0	C	Gap	1740	X			X							
369L0	C	Gap	1740				X	X						
370L0	C	Gap	1740	X			X							
371L0	C	Gap	1740				X	X						
372L0	C	Gap	1740					X				X		X
373L0	C	Gap	1740				X	X						

Digitised by the Department of Library Services in support of open access to information, University of Pretoria, 2021

TABLE II (contd) - Rooiberg A NAD and C Mines. Underground samples: Sample number, locality and main minerals

Sample	Mine	Section/ Lode	Level	Wall rock	Chlorit	Tourm	Cassit.	Pyrite	Sulph.	Ank.	Feldspar	Qrtz	Ser./Cl	Fluors
374L0	C	Gap	1740									X		
375L0	C	Gap	1740				X	X						
376L0	C	Gap	1740				X					X		
377L0	C	Gap	1740				X	X	X					
378L0	C	Gap	1740											X
379L0	C	Gap	1740									X		X
380L0	C	Gap	1740				X	X						
381L0	C	Gap	1740											X
382L0	C	Gap	1740				X							
383L0	C	Gap	1740											
384L0	C	Gap Lower	1870					X						
385L0	C	Gap Lower	1870				X	X						
386L0	C	Gap Lower	1870											X
387L0	C	Gap Lower	1870				X			X				X
388L0	C	Gap Lower	1870				X	X						
389L0	C	Gap Lower	1870				X	X						X
390L0	C	Gap Lower	1870				X	X		X				
391L0	C	Gap Lower	1870				X	X						
392L0	C	Gap Lower	1870				X	X		X				
393L0	C	Gap Lower	1870				X	X		X		X		
394L0	C	Gap Lower	1870									X		X
395L0	C	Gap Lower	1870				X	X		X				X
396L0	C	Gap Lower	1870		X		X						X	
397L0	C	Gap Lower	1870				X	X					X	
398L0	C	Gap Lower	1870				X	X		X		X	X	
399L0	C	Gap Lower	1870				X	X		X				
400L0	C	Gap Lower	1870				X	X						
401L0	C	Gap Lower	1870				X	X						X
402L0	C	Gap Lower	1870				X	XX						
403L0	C	Gap Lower	1870				X	X		X				
404L0	C	Gap Lower	1870											

Digitised by the Department of Library Services in support of open access to information, University of Pretoria, 2021

TABLE II (contd) - Rooiberg A NAD and C Mines. Underground samples: Sample number, locality and main minerals

Sample	Mine	Section/ Level Lode	Wall rock	ChloritTourm	Cassit.	Pyrite	Sulph.	Ank.	Feldspar	Qrtz	Ser./Cl	Fluors
405L0	C	Gap Lower 1870										
406L0	C	GLLoopO/D 1740			X	X		X				
407L0	C	GLLoopO/D 1740			X	X		X				
408L0	C	GLLoopO/D 1740			X	X		X				
409L0	C	GLLoopO/D 1740			X	X						
410L0	C	GLLoopO/D 1740			X	X		X				
411L0	C	GLLoopO/D 1740			X	X		X				
412L0	C	GLLoopO/D 1740				X						
413L0	C	GLLoopO/D 1740			X	X						
414L0	C	GLLoopO/D 1740	X		X	X						
415L0	C	GLLoopO/D 1740			X	X		X				
416L0	C	GLLoopO/D 1740				X						
417L0	C	GLLoopO/D 1740				X		X			X	
418L0	C	GLLoopO/D 1740										X
419L0	C	A Upper 1870	X		X							
420L0	C	A Upper 1870			X	X		X				
421L0	C	A Upper 1870			X	X		X				
422L0	C	A Upper 1870			X	X		X				
423L0	C	Hosking 1870	X		X	X						
424L0	C	Hosking 1870			X	X		X				
425L0	C	Hosking 1870			X							
426L0	C	Hosking 1870	X		X	X						
427L0	C	Hosking 1870	X		X	X		X				

Digitised by the Department of Library Services in support of open access to information, University of Pretoria, 2021

Table III - Major, trace and rare earth element analyses of Rooiberg granitoids

Digitised by the Department of Library Services in support of open access to information, University of Pretoria, 2021

Table III - Major, trace and REE analyses of Rooiberg granitoids

SL No	1	2	3	4	5	6	7	8	9	10	11	12	13	14	15	16
SiO2	75.55	75.36	74.40	73.99	74.32	74.86	75.97	72.52	78.80	77.41	77.02	75.03	77.10	76.64	76.62	74.34
TiO2	0.27	0.25	0.27	0.23	0.23	0.25	0.26	0.09	0.04	0.08	0.13	0.12	0.15	0.18	0.11	0.17
Al2O3	11.50	11.54	11.39	12.10	12.24	11.46	11.56	12.90	12.15	12.10	11.75	11.88	11.70	12.57	12.41	12.17
FeO	1.22	1.53	2.68	2.58	2.75	1.98	2.02	2.65	0.17	0.17	1.06	1.70	1.90	1.56	0.90	2.08
Fe2O3	3.08	2.70	1.54	1.06	1.57	1.94	1.25	1.89	0.81	2.69	1.42	1.77	0.84	1.12	1.30	1.03
MnO	0.04	0.02	0.05	0.06	0.04	0.03	0.04	0.05	0.02	0.02	0.02	0.01	0.04	0.03	0.02	0.04
MgO	0.03	0.00	0.09	0.16	0.16	0.03	0.01	0.16	0.00	0.08	0.03	0.05	0.02	0.00	0.00	0.08
CaO	0.66	0.79	0.88	0.64	0.78	0.73	0.99	0.58	0.72	0.16	0.49	1.07	0.35	0.78	0.67	0.33
Na2O	3.36	4.03	3.06	2.96	3.12	3.05	3.25	3.19	4.39	2.96	3.51	2.97	3.55	4.17	3.84	3.59
K2O	5.16	3.89	5.41	5.06	4.39	4.79	5.38	4.91	4.20	5.13	5.31	5.20	4.52	4.46	5.07	5.26
P2O5	0.02	0.02	0.02	0.02	0.02	0.02	0.02	0.01	0.01	0.00	0.01	0.01	0.01	0.01	0.00	0.01
H2O-	0.04	0.09	0.09	0.07	0.09	0.17	0.07	0.09	0.04	0.06	0.02	0.08	0.07	0.05	0.07	0.03
H2O+	0.41	0.24	0.52	0.62	0.44	0.68	0.40	0.73	0.23	0.55	0.60	0.78	0.63	0.39	0.40	0.71
CO2	0.05	0.07	0.16	0.40	0.04	0.32	0.04	0.38	0.05	0.04	0.05	0.07	0.13	0.06	0.06	0.26
S	0.01	0.01	0.01	0.01	0.01	0.00	0.01	0.01	0.00	0.01	0.00	0.01	0.00	0.00	0.01	0.00
Total	101.4	100.6	100.6	100.0	100.2	100.3	101.3	100.2	101.6	101.5	101.4	100.7	101.0	102.0	101.5	100.1
Ba	1105	1085	1140	1138	1177	1015	1132	542	159	255	287	603	341	542	319	684
B	343	299	354	344	626	232	264	663	88	135	187	185	195	217	207	239
Cr	119	172	183	168	143	176	131	162	138	131	193	176	128	195	224	130
Cu	13	12	13	10	11	9	9	10	11	14	9	10	10	9	10	12
F	0.13	0.14	0.1	0.1	0.1	0.06	0.11	0.1	0.35	0.09	0.21	0.455	0.1	0.19	0.295	0.04
Ga	21	21	19	20	20	19	21	27	30	34	27	28	22	26	28	25
Li	2	2	8	6	18	8	7		1	2	4	4	11	13	7	9
Mo	3	4	6	4	6	5	3	2	2	3	10	4	2	3	4	2
Nb	23	23	22	20	22	20	22	45	51	72	34	57	19	34	38	32
Ni	6	10	9	7	7	7	6	14	6	7	10	15	8	14	10	10
Pb	18	15	18	17	14	10	11	33	7	5	18	39	21	24	31	23
Rb	212	135	194	168	166	171	201	271	257	348	307	284	212	250	293	251
Sc	6	10	10	8	12	7	10	5	6	4	9	9	8	7	5	11
Sn	9	5	9	3	4	10	5	6	4	9	13	8	4	6	5	5
Sr	33	51	33	63	60	46	37	13	5	7	9	5	18	20	8	13
Th	24	22	23	25	23	21	25	64	50	54	40	63	39	76	43	78
U	6	5	7	6	4	5	5	13	9	5	15	17	9	19	13	11
V	8	7	9	9	7	9	10	5	6	7	6	5	4	5	6	4
W	9	17	13	11	11	11	10	21	14	12	16	24	15	24	20	19
Y	71	171	73	71	74	78	90	226	86	74	131	302	121	267	156	179
Zn	59	50	58	45	35	49	83	43	10	15	55	69	57	52	50	47
Zr	405	462	406	411	436	392	396	209	214	260	273	295	136	215	230	164
La		199	89			94.8	97.8	202	25.6	15.3	76.5	188	80.4	175		198
Ce		282	164			174	180	405	41.2	70.8	149	359	172	312		393
Pr		39.3	18.5			18.9	20	39.6	4.2	6.3	14.8	36	23.1	38		46.6
Nd		163	65.2			67	71.5	160	14.6	29.6	56.7	144	88.4	179		174
Sm		32.7	12.2			12.8	13.9	35.2	4.2	5.2	13.2	35.9	19.9	46.3		33.3
Eu		5.1	1.7			1.5	1.5	0	0.1	0.2	0.3	0.1	0.8	1		1.3
Gd		32.6	11.6			12.1	13.6	35.8	4.5	5.2	14.4	40.5	20.8	52.2		30.7
Tb		4.7	1.8			1.9	2.1	5.8	0.9	1.4	2.4	6.4	3.1	7.8		4.5
Dy		27.7	11			11.2	12.8	34.1	6.8	10.8	15.5	39.6	17.4	43.1		25.4
Ho		131	52.5			64.5	70.5	161	59.2	66.6	99.7	227	79.2	217		101
Er		15.7	7			7	8	18.8	5.7	9.1	10.6	24.8	8.8	23		14.5
Tm		2.1	1			1	1.2	2.6	1	1.6	1.6	3.6	1.2	3		2
Yb		13.5	7.3			7.1	8.2	16.6	7.4	11.6	10.8	22.8	7.4	19		13.3

Digitised by the Department of Library Services in support of open access to information, University of Pretoria, 2021

Table III (contd) - Major, trace and REE analyses of Rooiberg granitoids

SL No	17	18	19	20	21	22A	22B	23	24	25	25A	26	27	28	28A	29
SiO2	75.67	76.16	76.26	73.48	74.75	74.03	75.41	74.74	76.72	74.63	76.71	77.74	75.40	76.69	74.98	75.70
TiO2	0.19	0.18	0.09	0.23	0.06	0.27	0.09	0.11	0.11	0.08	0.11	0.12	0.13	0.10	0.12	0.12
Al2O3	12.11	11.93	12.55	12.00	12.57	12.30	12.85	12.58	11.63	13.15	12.07	11.90	12.21	11.87	12.60	12.63
FeO	1.59	1.42	0.71	3.03	0.57	1.13	1.01	1.32	1.25	1.13	1.21	0.71	1.45	1.35	1.14	0.83
Fe2O3	1.27	1.20	1.55	1.31	1.48	3.60	1.23	1.29	0.86	1.18	0.84	1.34	1.19	0.83	1.38	1.91
MnO	0.04	0.04	0.05	0.04	0.02	0.04	0.02	0.04	0.04	0.04	0.04	0.03	0.04	0.04	0.04	0.03
MgO	0.08	0.03	0.11	0.13	0.13	0.12	0.13	0.17	0.12	0.15	0.10	0.00	0.17	0.07	0.12	0.11
CaO	0.64	0.49	0.39	0.68	1.27	0.56	0.66	0.70	0.62	0.64	0.41	0.39	0.65	0.62	0.63	0.30
Na2O	3.41	3.30	3.71	2.86	3.27	3.39	3.69	3.36	3.10	3.41	3.51	3.32	3.37	3.64	3.48	3.41
K2O	5.24	5.03	3.87	4.67	4.88	4.00	4.19	4.96	4.31	4.84	4.41	5.45	5.04	5.19	4.76	4.09
P2O5	0.02	0.01	0.01	0.02	0.01	0.03	0.01	0.01	0.01	0.01	0.01	0.00	0.01	0.01	0.01	0.01
H2O-	0.06	0.06	0.11	0.13	0.10	0.06	0.04	0.04	0.09	0.09	0.08	0.06	0.09	0.08	0.08	0.16
H2O+	0.35	0.57	0.34	1.01	0.48	0.35	0.40	0.51	0.51	0.47	0.44	0.42	0.56	0.42	0.46	0.54
CO2	0.05	0.11	0.05	0.36	0.08	0.08	0.08	0.25	0.34	0.05	0.11	0.05	0.31	0.14	0.08	0.05
S	0.00	0.00	0.01	0.01	0.01	0.01	0.01	0.01	0.01	0.01	0.01	0.01	0.01	0.01	0.01	0.01
Total	100.7	100.5	99.8	100.0	99.7	100.0	99.8	100.1	99.7	99.9	100.1	101.5	100.6	101.1	99.9	99.9
Ba	678	443	361	791	351	1092	397	365	494	542	316	411	429	488	435	287
B	209	232	594	645	274	641	566	605	553	586	558	208	602	599	583	609
Cr	189	183	181	168	159	170	188	186	151	173	183	182	162	223	135	180
Cu	9	9	11	12	29	9	10	15	10	8	11	9	10	9	10	10
F	0.09	0.25	0.2	0.16	0.71	0.12	0.31	0.19	0.16	0.16	0.24	0.17	0.16	0.24	0.24	0.15
Ga	22	25	27	19	31	20	30	26	22	22	30	25	24	27	26	25
Li	6	4	11	10	7	15	13	11	21	16	17	5	13	15	10	16
Mo	3	2	3	5	3	4	3	3	3	2	3	3	2	4	2	3
Nb	19	31	34	22	71	22	55	36	27	22	40	37	28	34	36	23
Ni	8	11	10	9	11	7	12	11	10	9	12	8	11	12	11	12
Pb	16	15	44	15	7	18	12	14	23	38	27	29	25	40	31	23
Rb	255	261	325	261	403	155	344	357	221	241	263	316	288	309	306	305
Sc	6	3	8	11	8	9	4	5	7	6	5	7	5	8	8	8
Sn	5	5	10	11	11	7	6	4	7	6	3	5	3	6	4	5
Sr	40	12	7	19	6	74	6	7	18	27	14	12	10	10	11	11
Th	27	49	41	23	59	24	53	46	40	32	40	35	45	46	43	37
U	5	10	11	7	23	6	21	12	8	6	12	12	14	10	8	16
V	9	6	7	7	7	11	7	7	7	8	7	7	5	6	6	5
W	15	20	18	12	18	12	20	21	17	14	19	14	19	23	17	18
Y	98	196	122	62	184	66	157	145	111	116	179	92	167	170	178	168
Zn	50	49	85	62	22	41	41	48	59	89	88	89	76	92	90	66
Zr	279	134	225	429	250	364	276	265	211	154	150	258	322	296	226	309
La	110		118		95.6				107		70.3			201		
Ce	210		214		160				206		145			300		
Pr	22		20.6		13.7				23.4		16.5			31.1		
Nd	90.4		73.6		50.6				81.6		74			102		
Sm	19.2		16.4		11.8				17.1		16.2			18.2		
Eu	1.2		1.1		0.1				1.8		1			0.1		
Gd	19		16.1		13.4				16.3		16.9			19		
Tb	2.9		3		2.3				2.5		2.5			3		
Dy	16.6		17.7		16.5				14.7		15.6			18.7		
Ho	80.8		92		150				69.7		83.5			143		
Er	9.6		11.4		14				8.9		9.7			13		
Tm	1.4		2		2.5				1.3		1.4			2.1		
Yb	8.9		11.6		18.8				8.2		9			13.1		

Digitised by the Department of Library Services in support of open access to information, University of Pretoria, 2021

Table III (contd) - Major, trace and REE analyses of Rooiberg granitoids

SL No	30	31	32	33	34	35	36	37	38	39	40	41	42	43	44	45
SiO2	74.37	76.60	76.60	75.08	76.56	77.48	76.43	74.71	77.21	76.74	74.14	77.73	75.55	75.85	75.06	74.78
TiO2	0.10	0.12	0.11	0.09	0.12	0.10	0.12	0.14	0.10	0.11	0.14	0.04	0.12	0.13	0.13	0.11
Al2O3	12.67	12.26	12.35	12.87	12.54	12.96	12.34	12.80	11.82	11.90	11.98	12.83	12.53	12.29	12.82	12.85
FeO	1.37	0.98	0.79	0.65	0.43	0.26	0.71	1.01	0.73	0.43	1.66	0.83	0.75	1.60	0.98	1.43
Fe2O3	0.99	0.41	1.61	1.55	1.23	0.59	1.39	1.59	1.27	1.40	1.01	0.66	1.84	0.94	1.90	1.13
MnO	0.05	0.03	0.03	0.03	0.02	0.01	0.04	0.03	0.02	0.04	0.04	0.02	0.03	0.04	0.03	0.05
MgO	0.12	0.02	0.09	0.11	0.20	0.09	0.09	0.17	0.16	0.17	0.43	0.05	0.09	0.11	0.12	0.13
CaO	0.62	0.52	0.33	0.38	0.14	0.09	0.64	0.23	0.10	0.86	1.08	0.30	0.53	0.57	0.44	0.69
Na2O	3.31	3.35	3.02	3.63	4.08	4.68	3.80	3.52	3.10	3.46	3.08	4.60	3.39	3.18	3.49	3.57
K2O	5.31	5.71	4.61	4.59	4.54	4.65	4.67	4.67	4.68	4.38	5.29	3.74	4.67	4.19	4.20	4.37
P2O5	0.01	0.00	0.01	0.01	0.01	0.01	0.01	0.03	0.01	0.01	0.03	0.02	0.02	0.02	0.02	0.01
H2O-	0.17	0.07	0.06	0.14	0.13	0.06	0.07	0.13	0.22	0.13	0.07	0.04	0.33	0.17	0.13	0.16
H2O+	0.57	0.38	0.43	0.46	0.25	0.20	0.22	0.50	0.51	0.31	0.56	0.18	0.40	0.58	0.40	0.48
CO2	0.11	0.06	0.03	0.25	0.07	0.05	0.05	0.07	0.06	0.76	0.56	0.04	0.09	0.04	0.06	0.08
S	0.01	0.01	0.01	0.01	0.01	0.01	0.01	0.01	0.01	0.01	0.02	0.01	0.01	0.01	0.01	0.01
Total	99.8	100.5	100.1	99.9	100.3	101.2	100.6	99.6	100.0	100.7	100.1	101.1	100.4	99.7	99.8	99.9
Ba	373	368	357	273	498	446	644	531	643	462	462	108	391	468	432	396
B	601	234	634	526	568	350	410	576	126	449	263	567	670	630	207	163
Cr	183	149	124	127	149	171	178	147	190	138	134	156	160	159	167	157
Cu	10	10	11	11	7	9	8	24	10	11	14	11	10	9	10	8
F	0.32	0.22	0.16	0.09	0.06	0.05	0.24	0.09	0.06	0.08	0.31	0.24	0.22	0.08	0.17	0.3
Ga	25	28	24	30	24	25	25	25	24	25	23	33	26	21	26	28
Li	18	6	12	16	6	5	18	13	3	13	15	204	5	20	10	7
Mo	2	2	3	2	2	3	2	3	3	2	2	3	2	3	3	3
Nb	33	37	22	48	17	25	31	30	27	27	26	46	16	19	26	47
Ni	14	11	11	12	10	9	10	12	12	9	10	13	9	8	12	12
Pb	24	27	20	29	22	7	25	22	22	8	13	32	24	20	21	35
Rb	253	283	307	415	205	161	245	309	242	225	210	469	261	288	340	350
Sc	5	10	8	7	7	6	9	11	7	8	11	9	7	8	4	7
Sn	6	6	4	5	4	3	4	4	5	5	2	12	2	5	5	4
Sr	11	17	11	13	30	16	20	20	13	16	20	8	11	28	10	7
Th	50	24	42	55	35	16	49	37	38	39	33	82	44	24	45	52
U	26	9	14	17	8	5	10	10	11	9	10	17	10	4	13	19
V	5	7	5	6	6	6	6	9	6	10	10	7	5	7	6	6
W	25	20	17	13	19	16	18	17	21	19	17	20	15	17	20	18
Y	269	143	159	98	130	131	142	114	190	128	127	177	113	86	172	171
Zn	53	183	61	39	35	15	33	55	42	17	29	18	31	47	66	74
Zr	149	.89	415	229	253	304	240	274	215	212	236	341	234	157	282	311
La	96.7			80		113		109						69.4		146
Ce	201			173		161		216						133		265
Pr	29			24.3		27.6		24.5						15.2		25.9
Nd	122			62		93.7		87						63.1		92
Sm	33			14.6		20.8		18.6						14.7		21.3
Eu	0.6			1.5		1.1		1						1.2		0.1
Gd	41.6			12.6		20		17.3						15.2		21
Tb	6.5			2.1		2.8		2.9						2.4		4.4
Dy	36.4			14.5		15.3		17.8						15		26.7
Ho	218			77		76.8		89.8						76.1		155
Er	19.3			10.3		7.5		10.9						8.7		15.4
Tm	2.8			1.7		1.1		1.7						1.2		2.3
Yb	17.9			11.4		6.9		11						8.3		15.5

Digitised by the Department of Library Services in support of open access to information, University of Pretoria, 2021

Table III (contd) - Major, trace and REE analyses of Rooiberg granitoids

SL No	46	47	48	49	50	51	52	53	54	55	56	57	58	59	60	61
SiO2	74.99	75.32	74.42	76.38	73.43	76.60	75.24	76.95	76.13	76.34	77.80	76.44	73.93	75.24	74.83	75.60
TiO2	0.14	0.10	0.20	0.13	0.13	0.08	0.07	0.22	0.08	0.11	0.04	0.11	0.10	0.13	0.07	0.09
Al2O3	12.76	12.76	12.63	12.38	13.00	12.65	12.88	11.62	12.72	12.46	13.11	12.28	13.21	12.78	12.93	12.43
FeO	0.94	0.59	2.19	1.39	2.17	0.39	1.00	1.15	0.68	1.06	0.39	1.50	1.55	1.35	0.48	0.88
Fe2O3	1.77	1.86	0.83	0.86	1.00	1.43	1.44	2.03	1.06	1.37	1.00	0.95	1.02	1.13	2.04	1.42
MnO	0.02	0.02	0.06	0.04	0.03	0.01	0.02	0.04	0.01	0.03	0.02	0.03	0.04	0.04	0.01	0.03
MgO	0.10	0.13	0.22	0.10	0.21	0.14	0.18	0.02	0.12	0.11	0.11	0.17	0.21	0.22	0.13	0.15
CaO	0.67	0.63	0.80	0.61	0.71	0.30	0.73	0.63	0.55	0.44	0.10	0.38	0.57	0.27	0.49	0.26
Na2O	3.71	3.57	3.24	3.34	3.52	3.52	3.67	3.50	4.08	3.17	4.21	3.21	3.39	3.15	4.55	3.33
K2O	3.96	4.68	4.73	4.02	3.94	4.16	3.57	4.80	4.59	4.69	3.62	4.85	4.41	4.61	3.00	4.86
P2O5	0.01	0.01	0.02	0.02	0.01	0.01	0.01	0.02	0.01	0.01	0.01	0.01	0.01	0.02	0.01	0.02
H2O-	0.11	0.09	0.08	0.20	0.16	0.21	0.28	0.01	0.14	0.06	0.02	0.07	0.15	0.18	0.29	0.09
H2O+	0.52	0.52	0.56	0.29	0.65	0.34	0.58	0.31	0.44	0.48	0.23	0.53	0.48	0.62	0.32	0.44
CO2	0.07	0.10	0.45	0.05	0.23	0.08	0.04	0.04	0.05	0.10	0.04	0.08	0.06	0.06	0.05	0.07
S	0.01	0.01	0.01	0.01	0.01	0.01	0.01	0.00	0.01	0.01	0.01	0.01	0.01	0.01	0.01	0.01
Total	99.8	100.4	100.4	99.8	99.2	99.9	99.7	101.3	100.7	100.5	100.7	100.6	99.1	99.8	99.2	99.7
Ba	510	575	680	579	414	319	307	600	283	383	203	563	526	500	238	280
B	660	640	658	206	201	257	186	293	158	194	152	268	173	247	258	193
Cr	114	105	120	175	186	153	168	174	139	182	146	165	177	184	162	204
Cu	10	15	12	8	8	12	8	10	10	8	7	9	10	11	12	9
F	0.25	0.31	0.07	0.09	0.24	0.12	0.33	0.1	0.21	0.26	0.16	0.14	0.23	0.12	0.23	0.19
Ga	27	28	23	23	26	27	29	22	29	26	35	25	25	22	32	25
Li	16	9	24	18	4	1	5	6	1	3	108	2	5	4	3	8
Mo	6	2	3	2	2	3	3	3	2	3	2	2	2	3	3	3
Nb	29	47	25	23	33	31	44	23	43	43	50	20	42	27	64	33
Ni	13	12	10	6	11	10	9	8	9	11	10	10	10	8	9	10
Pb	23	13	18	20	25	12	8	23	6	24	29	45	22	17	8	28
Rb	308	326	234	218	224	278	239	219	319	329	641	299	293	297	272	356
Sc	8	9	7	7	4	5	7	9	7	8	5	7	7	7	3	6
Sn	5	9	3	5	4	4	6	5	7	7	8	5	5	4	4	6
Sr	15	8	43	36	15	12	8	38	6	11	4	12	20	15	6	8
Th	55	43	28	29	59	49	36	32	43	45	58	41	53	30	47	41
U	16	12	6	8	12	8	8	6	15	15	15	10	14	9	9	10
V	6	7	11	8	7	6	7	6	8	4	5	5	5	8	7	6
W	19	14	13	16	21	17	17	13	14	17	14	16	16	14	15	15
Y	236	136	88	81	189	115	124	69	135	141	92	149	140	107	88	94
Zn	49	47	57	43	52	24	33	41	27	52	24	63	58	60	20	46
Zr	278	286	334	161	132	259	180	297	335	272	229	272	148	335	296	252
La				107		199				132				91.2		57.7
Ce				199		219				244				154		118
Pr				24.1		36.6				29.8				22.5		8.2
Nd				80.4		109				98.8				78.5		34
Sm				15.3		19.7				20.8				15.9		9
Eu				1.2		0.1				0.1				0.1		0.01
Gd				14		15.8				20				15		9
Tb				2.4		3				4				2.6		1.9
Dy				14.3		17.7				23.5				15.3		12.5
Ho				61.7		103				121				71.6		71.2
Er				8		10.2				13				8.5		8.6
Tm				1.2		1.6				1.9				1.2		1.4
Yb				8		10.6				12.5				7.8		9.3

Digitised by the Department of Library Services in support of open access to information, University of Pretoria, 2021

Table III (contd) - Major, trace and REE analyses of Rooiberg granitoids

SL No	62	63	64	65	66	67	68	69	70	71	72	73	74	75	76	77
SiO2	74.13	75.73	73.38	75.10	75.37	75.53	75.17	74.82	74.84	74.21	74.56	75.31	75.48	74.86	75.92	72.09
TiO2	0.10	0.10	0.08	0.11	0.11	0.09	0.17	0.16	0.14	0.21	0.20	0.10	0.10	0.11	0.10	0.15
Al2O3	13.62	12.55	13.71	12.71	12.37	12.67	12.55	12.51	12.28	12.89	12.44	12.24	12.53	12.54	12.82	13.92
FeO	1.10	1.16	1.18	1.30	0.99	1.53	1.67	1.88	2.36	2.04	1.10	1.69	1.50	1.57	1.58	2.18
Fe2O3	1.42	1.04	0.88	0.88	1.39	0.58	1.06	1.37	1.38	1.40	2.28	0.99	0.78	0.83	0.00	0.54
MnO	0.03	0.02	0.04	0.02	0.04	0.04	0.04	0.02	0.03	0.03	0.03	0.03	0.02	0.02	0.01	0.04
MgO	0.23	0.11	0.27	0.13	0.10	0.15	0.19	0.18	0.21	0.26	0.20	0.24	0.14	0.15	0.15	0.32
CaO	0.49	0.48	0.71	0.48	0.71	1.24	0.49	0.31	0.83	0.40	0.16	0.91	0.72	0.57	0.52	0.91
Na2O	3.52	3.48	3.50	3.56	3.70	3.44	3.89	3.47	3.11	3.29	3.16	3.22	3.57	3.41	3.70	3.38
K2O	3.63	4.67	4.11	5.98	4.65	4.65	4.63	4.39	3.48	3.75	4.51	5.43	3.22	4.26	4.28	3.95
P2O5	0.01	0.01	0.02	0.02	0.01	0.01	0.03	0.02	0.02	0.02	0.02	0.02	0.01	0.01	0.01	0.03
H2O-	0.11	0.17	0.08	0.09	0.26	0.12	0.09	0.06	0.06	0.02	0.08	0.16	0.06	0.26	0.23	0.08
H2O+	0.49	0.48	0.37	0.47	0.30	0.40	0.26	0.51	0.67	0.49	0.55	0.52	0.37	0.54	0.47	0.61
CO2	0.07	0.06	0.16	0.07	0.03	0.08	0.09	0.06	0.11	0.13	0.06	0.13	0.08	0.07	0.05	0.58
S	0.01	0.01	0.01	0.01	0.01	0.01	0.01	0.01	0.02	0.01	0.01	0.01	0.01	0.02	0.01	0.01
Total	99.0	100.1	98.5	100.9	100.0	100.5	100.3	99.8	99.5	99.2	99.4	101.0	98.6	99.2	99.9	98.8
Ba	582	408	496	349	323	522	665	674	809	783	1429	1430	583	647	328	740
B	416	465	332	317	417	340	586	593	683	602	674	533	319	322	309	196
Cr	150	164	223	168	178	180	148	181	221	189	148	188	187	198	183	129
Cu	12	12	8	10	11	9	9	9	12	8	11	181	33	68	12	7
F	0.22	0.22	0.26	0.33	0.29	0.58	0.08	0.13	0.35	0.1	0.07	0.45	0.42	0.3	0.3	0.08
Ga	26	26	27	27	26	27	21	26	22	23	22	28	26	29	27	25
Li	4	4	6	7	15	6	10	5	5	5	5	5	4	4	5	7
Mo	2	2	5	3	4	2	2	4	6	4	8	15	21	9	4	3
Nb	46	25	44	43	27	53	18	26	29	25	27	51	42	41	43	26
Ni	14	11	10	11	11	15	9	8	10	7	8	15	14	10	9	7
Pb	26	13	27	24	16	20	16	20	15	14	12	12	16	16	20	7
Rb	361	333	310	316	292	331	171	250	256	239	216	234	201	205	210	214
Sc	7	7	9	4	7	8	12	7	8	7	6	10	9	10	6	8
Sn	9	6	6	4	4	4	5	4	5	6	5	5	4	5	3	3
Sr	7	8	12	8	9	7	43	32	27	35	33	11	14	16	14	20
Th	56	36	56	46	40	48	17	37	44	29	29	64	49	81	42	43
U	14	9	18	13	10	10	4	6	12	5	17	24	16	15	12	19
V	5	6	5	7	5	5	6	6	7	8	7	5	6	5	6	8
W	19	18	21	18	18	24	14	16	21	14	13	25	18	18	19	9
Y	221	141	155	142	147	279	89	95	145	89	98	300	200	152	134	69
Zn	46	40	45	47	31	44	42	32	32	29	54	16	18	19	17	13
Zr	257	236	268	241	258	259	291	289	282	376	356	279	266	302	265	275
La						187			179			642		232		139
Ce						308			319			942		351		243
Pr						35.5			35.5			95		41		28
Nd						110			117			268		123		103
Sm						23.6			22.6			44		22.7		18
Eu						0.01			1.2			0.1		0.1		1.4
Gd						24.5			19.9			38		19.2		13
Tb						5.5			3.3			7.2		3.8		1.8
Dy						31.8			18.4			48.3		22.2		9.6
Ho						234			85.6			236		108		43.9
Er						18.8			9.3			24.5		12.6		5.3
Tm						3			1.4			3.3		1.9		0.8
Yb						19.6			9.2			22		12.5		5.4

Digitised by the Department of Library Services in support of open access to information, University of Pretoria, 2021

Table III (contd) - Major, trace and REE analyses of Rooiberg granitoids

SL No	78	79	80	81	82	83	84	85	86	87	88	89	90	91	92	93
SiO2	75.70	71.61	72.39	78.57	75.58	74.95	74.65	77.31	72.47	77.89	76.62	73.35	87.08	69.69	72.25	73.38
TiO2	0.05	0.22	0.13	0.03	0.11	0.22	0.23	0.23	0.23	0.05	0.08	0.05	0.38	0.20	0.26	0.22
Al2O3	13.04	14.59	13.61	10.97	11.96	12.57	13.08	12.44	13.78	12.98	12.55	12.81	5.85	15.35	12.56	13.28
FeO	0.86	0.20	1.67	0.43	0.31	0.30	2.46	0.57	0.30	0.21	0.32	0.40	1.93	1.94	3.23	2.67
Fe2O3	0.63	3.60	1.28	0.35	2.77	3.03	1.12	1.85	4.14	0.40	1.26	0.98	0.00	1.81	1.14	0.55
MnO	0.01	0.01	0.02	0.01	0.01	0.02	0.02	0.02	0.06	0.01	0.01	0.01	0.05	0.04	0.07	0.05
MgO	0.13	0.25	0.23	0.33	0.05	0.13	0.33	0.09	0.26	0.00	0.16	0.16	0.12	0.45	0.19	0.19
CaO	0.77	0.22	1.09	0.05	0.17	0.81	0.15	0.36	1.48	0.09	0.29	0.45	0.40	0.82	1.13	1.28
Na2O	3.80	4.04	3.07	1.89	2.93	3.12	3.71	3.15	4.06	3.99	3.07	3.55	1.48	3.92	3.88	4.21
K2O	4.34	4.79	5.90	4.94	6.32	5.49	4.94	5.17	4.66	5.73	5.71	5.82	2.50	4.70	4.76	4.69
P2O5	0.01	0.04	0.02	0.01	0.06	0.03	0.03	0.02	0.04	0.00	0.02	0.01	0.03	0.04	0.05	0.05
H2O-	0.07	0.48	0.33	0.02	0.10	0.54	0.07	0.01	0.16	0.02	0.10	0.20	0.74	0.10	0.17	0.02
H2O+	0.33	0.53	0.38	0.21	0.32	0.70	0.86	0.59	0.31	0.17	0.30	0.40	0.53	0.52	0.39	0.33
CO2	0.06	0.06	0.06	0.05	0.06	0.06	0.05	0.08	0.08	0.05	0.09	0.07	0.11	0.08	0.18	0.27
S	0.01	0.01	0.01	0.03	0.01	0.01	0.01	0.01	0.01	0.01	0.01	0.01	0.01	0.01	0.01	0.01
Total	99.8	100.7	100.2	97.9	100.8	102.0	101.7	101.9	102.1	101.6	100.6	98.3	101.2	99.7	100.3	101.2
Ba	262	905	535	562	433	765	856	947	783	248	388	381	401	862	954	852
B	166	130	97	110	106	112	137	127	108	112	132	147	182	111	105	104
Cr	163	164	167	232	208	164	165	218	177	176	203	210	313	207	203	205
Cu	21	8	25	59	18	17	9	7	7	7	12	7	7	7	7	6
F	0.58	0.07	0.51	0.05	0.08	0.33	0.05	0.03	0.14	0.03	0.1	0.24	0.12	0.16	0.15	0.15
Ga	27	27	26	15	30	26	26	21	25	27	27	29	11	25	25	24
Li	5	1	1	1	3	2	3	8	8	1	3	2	21	2	14	10
Mo	7	3	30	5	3	7	3	4	3	2	3	4	7	4	28	4
Nb	29	26	31	34	78	30	33	17	27	36	37	46	30	26	30	25
Ni	10	10	9	10	8	12	8	9	9	6	7	9	10	10	9	9
Pb	7	11	21	14	11	8	7	14	14	9	13	15	8	10	13	14
Rb	208	183	238	204	278	210	149	146	148	190	246	246	93	183	144	140
Sc	5	7	7	6	9	8	7	4	11	3	10	3	6	8	11	9
Sn	2	2	2	3	2	5	2	4	4	2	2	2	3	4	2	1
Sr	16	42	39	9	33	42	26	76	60	23	23	15	28	65	65	67
Th	50	29	56	34	53	32	36	17	39	42	51	44	10	37	22	38
U	6	4	16	8	6	8	6		10	9	5	28	3	10	2	10
V	7	10	8	7	8	9	9	8	10	7	6	7	15	10	11	10
W	15	15	17	23	16	15	14	15	16	13	14	17	16	15	13	16
Y	95	123	93	113	54	126	109	56	110	44	75	107	69	114	116	98
Zn	10	10	17	6	11	17	17	50	30	10	13	11	16	22	38	26
Zr	129	347	229	166	183	300	336	299	372	132	195	188	802	361	410	341
La	32.9						136	191		15.4				140	154	
Ce	74						258	129		22.7				218	269	
Pr	9.7						27.9	38.8		8.3				27.6	34.7	
Nd	30.5						98.7	137		19.6				99.4	113	
Sm	7.8						18.8	20.7		3.8				18.6	20.1	
Eu	0.6						1.4	3.3		0.4				1.7	1.7	
Gd	8.6						16.6	15		4.7				17.6	18.3	
Tb	1.7						2.5	2		1				2.9	3	
Dy	11.4						13.7	10.5		7.1				16.7	19	
Ho	58						54.8	45.6		40.8				95.8	99	
Er	7.7						7.1	5.3		6.3				9.8	10.8	
Tm	1.2						1.1	0.8		1.1				1.5	1.6	
Yb	8.7						7.1	5.3		7.2				10.1	11	

Digitised by the Department of Library Services in support of open access to information, University of Pretoria, 2021

Table III (contd) - Major, trace and REE analyses of Rooiberg granitoids

SL No	94	95	96	97	98	99	100	101	102	103	104	105	106	107	108	109
SiO2	40.74	75.29	74.63	73.70	76.88	74.16	74.60	75.41	76.10	76.65	83.40	76.00	75.81	76.87	78.23	75.89
TiO2	0.38	0.20	0.20	0.20	0.15	0.15	0.24	0.24	0.14	0.20	0.21	0.12	0.10	0.18	0.16	0.23
Al2O3	12.16	12.48	12.52	13.40	12.18	13.28	12.28	12.47	12.35	12.52	4.99	12.03	12.29	11.74	11.66	13.00
FeO	0.10	2.91	2.15	2.55	1.10	1.30	2.21	1.66	1.61	1.43	0.47	1.86	1.54	1.37	1.30	1.40
Fe2O3	33.08	0.89	1.06	0.44	1.49	1.50	1.38	2.03	0.65	0.48	6.34	0.70	0.34	1.29	0.37	0.64
MnO	0.14	0.07	0.03	0.04	0.03	0.03	0.04	0.06	0.02	0.03	0.03	0.02	0.03	0.03	0.03	0.04
MgO	0.18	0.69	0.12	0.30	0.06	0.16	0.11	0.08	0.09	0.11	0.12	0.10	0.07	0.08	0.07	0.19
CaO	0.03	0.39	0.65	0.94	0.37	0.37	0.77	0.52	0.41	0.66	0.03	1.33	0.76	0.46	0.46	0.56
Na2O	0.14	4.25	3.74	4.37	3.39	3.61	3.50	3.46	3.91	5.02	0.11	3.13	3.68	3.51	3.61	4.08
K2O	9.97	3.39	5.13	4.11	4.99	5.13	4.96	5.12	4.99	3.56	1.76	5.27	5.37	5.00	4.98	4.16
P2O5	0.05	0.02	0.03	0.04	0.02	0.03	0.03	0.03	0.02	0.02	0.02	0.01	0.01	0.02	0.02	0.03
H2O-	0.41	0.02	0.10	0.06	0.30	0.40	0.19	0.13	0.02	0.24	0.98	0.03	0.16	0.35	0.06	0.09
H2O+	3.61	0.97	0.34	0.68	0.52	0.50	0.42	0.50	0.37	0.25	1.92	0.48	0.34	0.34	0.16	0.19
CO2	0.07	0.30	0.08	0.36	0.13	0.08	0.11	0.09	0.23	0.14	0.06	0.06	0.11	0.07	0.04	0.09
S	0.01	0.01	0.01	0.01	0.01	0.01	0.01	0.01	0.01	0.01	0.01	0.01	0.01	0.01	0.01	0.01
Total	101.1	101.9	100.8	101.2	101.6	100.7	100.9	101.8	100.9	101.3	100.5	101.2	100.6	101.3	101.2	100.6
Ba	1733	881	761	566	785	508	767	987	595	740	423	500	314	738	774	1001
B	54	112	106	103	90	105	118	104	119	122	289	106	106	126	102	147
Cr	54	223	214	188	239	199	218	237	227	230	302	228	252	244	211	180
Cu	18	8	8	7	7	7	8	8	8	6	11	17	10	7	6	8
F	0.04	0.04	0.13	0.15	0.04	0.04	0.04	0.04	0.06	0.03	0.04	1.06	0.29	0.04	0.04	0.04
Ga	12	27	25	24	22	23	23	23	25	23	13	27	28	22	21	21
Li	6	8	6	5	4	4	3	2	2	1	19	2	1	6	3	3
Mo	2	3	3	3	4	3	3	4	3	4	6	7	4	3	2	3
Nb	62	31	26	25	20	21	31	33	22	22	15	43	39	24	16	22
Ni	14	10	9	8	8	8	11	11	8	8	9	13	12	10	7	9
Pb	7	5	12	11	11	13	7	13	14	13	12	17	23	15	14	9
Rb	305	113	217	144	183	190	167	226	231	87	69	239	286	207	127	96
Sc	17	8	9	8	8	7	10	9	8	8	9	5	5	5	10	9
Sn	8	4	4	3	3	3	2	5	4	3	1	5	5	4	3	4
Sr	5	24	37	67	43	42	42	44	31	57	13	15	13	44	55	52
Th	27	36	35	17	19	29	15	48	36	34	8	48	49	30	33	30
U	13	2	11	7	5	6	4	7	10	2	3	11	6	6	3	2
V	29	7	9	14	9	9	9	6	8	8	16	5	7	6	8	6
W	5	18	17	16	19	18	19	20	18	19	16	20	24	21	15	19
Y	192	140	119	83	69	89	177	115	82	93	34	222	164	137	44	108
Zn	12	16	20	35	25	19	26	24	17	19	22	29	23	31	17	10
Zr	302	344	272	268	197	294	326	369	239	316	304	335	262	265	211	342
La				79.6				136		170				321		285
Ce				137				321		152				187		307
Pr				11.6				37.7		42.7				78.9		58.6
Nd				52.7				118		140				234		205
Sm				11.5				21.2		23.6				45		31.9
Eu				0.9				0.1		2.7				2.7		3.1
Gd				11.6				18.3		18.4				36.5		25.8
Tb				2				3.2		3				5		3.8
Dy				11.9				21.5		17.7				28		21.7
Ho				62.6				98.7		61.2				131		87.8
Er				7.8				10.8		8.9				12.8		11.1
Tm				1.2				1.5		1.4				2.2		1.8
Yb				8.1				11.1		9.1				12.8		10.8

Digitised by the Department of Library Services in support of open access to information, University of Pretoria, 2021

Table III (contd) - Major, trace and REE analyses of Rooiberg granitoids

SL No	110	111	112	113	114	115	116	117	118	119	120	121	122	123	124	125
SiO2	74.40	71.17	73.74	72.91	77.32	76.55	76.31	74.03	75.92	76.72	77.93	75.74	72.58	75.93	71.16	75.32
TiO2	0.27	0.43	0.39	0.20	0.16	0.13	0.12	0.10	0.14	0.15	0.11	0.15	0.09	0.13	0.19	0.24
Al2O3	12.56	14.32	12.14	12.99	11.70	12.56	11.69	13.24	11.80	11.68	12.19	12.67	13.41	12.70	14.30	12.71
FeO	1.36	0.10	3.33	2.00	1.75	0.97	1.18	1.73	1.96	1.88	1.00	1.93	2.24	0.94	1.96	2.34
Fe2O3	2.17	2.61	1.19	0.91	1.19	1.90	1.23	0.61	0.89	1.16	0.43	0.64	0.68	1.47	1.05	0.36
MnO	0.06	0.02	0.09	0.04	0.02	0.02	0.01	0.03	0.03	0.04	0.03	0.03	0.05	0.02	0.05	0.04
MgO	0.14	0.20	0.20	0.25	0.13	0.12	0.03	0.23	0.07	0.08	0.09	0.18	0.37	0.14	0.19	0.12
CaO	0.40	0.12	1.62	0.56	0.24	0.39	0.50	0.66	0.80	0.34	0.46	0.29	0.75	0.40	0.97	1.16
Na2O	3.29	0.20	3.49	3.45	3.45	3.03	3.36	3.69	3.39	2.74	3.20	3.38	4.71	3.53	3.69	3.91
K2O	5.11	10.39	4.79	5.16	4.97	5.19	5.12	5.21	5.08	5.34	5.38	5.00	2.83	4.85	5.57	5.10
P2O5	0.03	0.06	0.06	0.03	0.02	0.02	0.00	0.01	0.01	0.02	0.01	0.02	0.07	0.02	0.02	0.03
H2O-	0.02	0.16	0.02	0.12	0.22	0.08	0.21	0.02	0.03	0.10	0.07	0.07	0.07	0.14	0.12	0.02
H2O+	0.80	1.01	0.26	0.30	0.62	0.50	0.40	0.38	0.45	0.55	0.24	0.54	0.63	0.47	0.41	0.21
CO2	0.12	0.22	0.06	0.09	0.13	0.11	0.08	0.21	0.32	0.07	0.06	0.15	0.45	0.10	0.06	0.11
S	0.01	0.06	0.01	0.02	0.01	0.01	0.01	0.01	0.07	0.01	0.01	0.01	0.01	0.01	0.01	0.01
Total	100.7	101.1	101.4	99.0	102.0	101.6	100.3	100.2	101.0	100.9	101.2	100.8	98.9	100.9	99.8	101.7
Ba	1220	2120	1103	822	591	546	437	408	494	573	795	431	399	521	707	802
B	251	221	235	266	249	230	224	242	269	290	177	206	210	214	214	209
Cr	174	65	166	208	207	205	208	216	229	207	169	229	227	237	181	167
Cu	6	8	10	10	10	9	7	8	34	10		9	43	11	12	7
F	0.04	0.03	0.06	0.05	0.04	0.14	0.22	0.3	0.15	0.15	0.05	0.06	0.08	0.16	0.28	0.15
Ga	22	16	21	23	23	24	26	27	24	23	23	24	28	25	27	25
Li	3	20	16	4	3	4	4	6	5	3	5	5	6	5	10	8
Mo	3	7	5	4	3	5	4	7	4	5	2	3	6	4	3	3
Nb	26	27	21	29	22	31	37	37	29	28	18	22	28	27	29	30
Ni	12	9	7	8	8	8	11	10	9	9	9	10	10	10	9	9
Pb	16	50	21	12	7	9	15	14	17	7	20	12	9	11	24	20
Rb	188	421	123	198	186	299	256	261	242	267	185	194	129	221	255	200
Sc	7	8	12	8	8	4	7	11	6	9	8	8	3	9	5	7
Sn	3	2	2	5	4	6	8	5	6	8	3	4	9	4	3	3
Sr	67	67	92	34	24	14	12	15	17	12	38	20	16	13	41	50
Th	29	19	15	34	34	36	41	39	36	33	32	37	31	38	45	43
U	4	11	4	5	4	6	10	10	11	4	6	9	8	11	7	8
V	11	13	13	8	7	6	5	5	6	8	6	7	10	5	6	8
W	15	10	13	15	16	18	20	18	21	21	18	22	19	20	19	14
Y	87	38	57	92	54	120	130	129	120	109	115	127	123	120	121	119
Zn	36	16	81	27	26	34	40	37	33	30	28	24	28	20	54	27
Zr	409	576	488	339	248	295	270	296	252	305	155	256	279	346	299	342
La	127		61.1			145			114		155		79.8	102	148	141
Ce	226		101			256			195		238		149	178	270	254
Pr	29.2		11.6			33.1			28		43.8		13.9	14.2	41.7	33.4
Nd	98.4		53.1			108			79.8		115		54.9	59.6	106	104
Sm	16.8		10.3			19.5			15.4		22.3		13.6	13.8	21.7	19
Eu	2		2.4			0.1			1.3		3.2		0.1	0.7	3.5	1.4
Gd	14.2		9.7			17.4			13.6		16.5		11.2	12.8	17.4	16.8
Tb	2.5		1.6			2.9			2.4		3.1		1.9	2.5	3.7	3.1
Dy	17		10.6			18.4			14		15.8		12	16.2	20	19.1
Ho	78.1		44.9			65.2			60.6		65.9		55.3	68.5	82.8	75.6
Er	8.5		5.6			8.5			7.9		8.4		6.7	9.2	11.4	10.4
Tm	1.2		0.8			1.3			1.3		1.5		1.1	1.5	2	1.6
Yb	8.5		5.7			8			7.7		8.5		7	9.2	11.3	10.2

Digitised by the Department of Library Services in support of open access to information, University of Pretoria, 2021

Tables IV a - d: Major and trace element analyses of Rooiberg ankerite

Table IVe - Mole percentages

Digitised by the Department of Library Services in support of open access to information, University of Pretoria, 2021

Table IVa - Major and trace element analyses of Rooiberg ankerite
Group C - C Mine lodes

Sample	C387L0	C387L0	C387L0	C387L0	C422L0	C422L0	C422L0	C422L0	C347L0	C347L0	C347L0	C347L0	C403L0	C403L0	C403L0	C403L0
FeO	13.08	14.19	10.28	15.32	12.01	12.85	17.41	17.93	14.09	14.42	14.12	13.78	16.31	15.17	12.38	15.90
MnO	0.72	0.75	1.83	0.56	1.54	1.45	1.21	0.94	0.56	0.40	0.52	0.90	1.32	1.23	2.07	1.30
MgO	12.93	12.32	12.25	12.20	13.51	12.73	9.69	9.81	12.10	12.09	12.27	12.33	10.40	11.18	12.38	10.52
CaO	28.49	28.67	28.30	27.99	28.91	29.36	28.92	28.62	29.09	29.39	28.84	29.54	28.86	28.84	28.69	28.39

Sample	C358L0	C358L0	C358L0	C358L0	C399L0	C399L0	C399L0	C399L0	C406L0	C406L0	C406L0	C406L0	C410L0	C410L0	C410L0	C410L0
FeO	16.73	12.25	12.21	13.33	13.09	12.14	10.05	12.26	16.66	14.65	11.64	13.62	14.98	15.90	16.95	15.62
MnO	1.75	1.28	2.59	1.93	0.79	1.74	1.44	1.10	1.03	0.95	0.86	0.93	1.30	0.95	1.03	1.03
MgO	10.03	12.98	12.44	12.11	13.22	12.89	14.30	13.39	10.83	11.94	13.74	12.06	11.63	10.88	10.67	11.19
CaO	29.08	29.00	28.53	28.60	28.95	28.84	29.34	29.15	28.39	28.26	28.72	29.06	28.12	27.80	28.45	28.56

Sample	C411L0	C411L0	C411L0	C411L0	C417L0	C417L0	C417L0	C417L0	C424L0	C424L0	C424L0	C424L0	C427L0	C427L0	C427L0	C427L0
FeO	13.65	12.35	13.84	12.79	16.85	16.43	14.62	16.60	11.40	14.91	13.01	13.55	17.99	18.14	17.22	18.01
MnO	1.10	1.00	1.40	1.24	0.84	1.02	1.73	0.88	0.85	0.96	2.34	2.45	1.23	1.01	1.17	1.18
MgO	12.57	13.31	12.23	12.78	10.73	10.70	11.85	10.87	13.03	10.78	10.92	10.52	9.28	8.90	10.01	9.46
CaO	27.70	28.36	28.02	28.55	28.27	28.21	28.23	28.00	28.69	28.12	28.51	28.29	28.30	28.61	28.37	28.47

Sample	C387L0*	C422L0*	C347L0*	C403L0*	C358L0*	C399L0*	C406L0*	C410L0*	C411L0*	C417L0*	C424L0*	C427L0*	Ave(48)
FeO	13.21	15.05	14.10	14.94	13.63	11.88	14.14	15.86	13.16	16.12	13.22	17.84	14.43
MnO	0.97	1.29	0.60	1.48	1.89	1.27	0.94	1.08	1.19	1.12	1.65	1.15	1.22
MgO	12.43	11.44	12.20	11.12	11.89	13.45	12.14	11.09	12.72	11.04	11.31	9.41	11.69
CaO	28.36	28.95	29.22	28.70	28.80	29.07	28.61	28.23	28.16	28.18	28.40	28.44	28.59
H2O-	.....	.....	.....	.....	.....	.....	0.10	0.04	0.04	0.03	0.05	0.11	0.06
H2O+	.....	.....	.....	.....	.....	.....	0.12	0.06	0.06	0.07	0.08	0.16	0.09
CO2	.....	.....	.....	.....	.....	.....	45.10	42.90	45.83	44.74	44.75	43.27	44.43
S	.....	.....	.....	.....	.....	.....	0.02	0.01	0.01	0.01	0.00	0.01	0.01
Total	.....	.....	.....	.....	.....	.....	101.17	99.27	101.16	101.30	99.46	100.38	
													Ave(5)
Cu	.....	.....	.....	.....	.....	.....	12	10	16	11	10		12
Ni	.....	.....	.....	.....	.....	.....	10	11	12	12	11		11
Rb	.....	.....	.....	.....	.....	.....	3	3	3	3	3		3
Sc	.....	.....	.....	.....	.....	.....	85	87	81	93	87		87
Sr	.....	.....	.....	.....	.....	.....	34	88	49	61	88		64
V	.....	.....	.....	.....	.....	.....	19	30	21	33	30		27
Y	.....	.....	.....	.....	.....	.....	16	60	17	56	60		42
Zn	.....	.....	.....	.....	.....	.....	82	43	61	52	43		56

* = Averages

Digitised by the Department of Library Services in support of open access to information, University of Pretoria, 2021

Table IVb - Major and trace element analyses of Rooiberg ankerite
Group N - NAD Mine lodes

Sample	N281L0	N281L0	N304L0	N304L0	N304L0	N304L0	N303L0	N303L0	N303L0	N303L0	N308L0	N308L0	N308L0	N308L0
FeO	16.32	16.67	15.26	14.79	14.88	13.96	16.94	16.66	17.62	17.11	14.13	13.38	14.50	14.96
MnO	1.36	1.57	0.70	0.96	0.81	0.88	1.06	1.09	0.98	0.99	1.74	1.69	0.80	0.89
MgO	10.62	10.34	11.15	11.44	11.85	11.88	11.04	10.58	10.14	10.27	11.94	11.82	12.17	12.16
CaO	29.14	28.87	28.89	28.87	28.56	28.86	28.01	28.10	28.17	27.85	29.26	28.84	29.15	28.40

Sample	N284L0	N284L0	N284L0	N284L0	N286L0	N286L0	N286L0	N286L0	N309L0	N309L0	N309L0	N309L0	N335L0	N335L0
FeO	16.18	16.90	17.06	16.55	15.45	17.96	17.50	15.51	13.93	15.35	15.19	15.24	11.35	11.62
MnO	1.55	1.09	1.18	0.91	1.25	0.62	1.00	0.93	1.79	2.03	1.76	1.96	0.49	0.49
MgO	10.27	10.20	9.89	11.05	10.79	11.70	9.83	11.27	9.99	10.93	10.85	10.68	14.25	14.04
CaO	27.88	27.99	27.84	28.39	27.92	30.38	27.65	27.72	30.02	28.43	28.11	28.59	28.37	28.22

Sample	N335L0	N335L0	N336L0	N336L0	N336L0	N336L0	N339L0	N339L0	N339L0	N339L0
FeO	10.92	10.60	11.91	13.30	13.29	12.07	11.97	10.14	13.91	12.00
MnO	0.32	0.41	0.47	0.34	0.48	0.45	0.44	0.31	0.66	0.54
MgO	14.36	14.41	13.74	12.88	13.14	13.91	14.10	15.35	12.71	14.14
CaO	28.22	28.55	28.40	28.37	28.66	28.14	28.90	29.49	28.22	28.57

Sample	N281L0*	N304L0*	N303L0*	N308L0*	N284L0*	N309L0*	N335L0*	N336L0*	N339L0*	Ave(40)
FeO	16.49	14.42	17.36	14.73	16.67	14.93	11.12	12.64	12.01	13.83
MnO	1.46	0.84	0.99	0.85	1.18	1.88	0.43	0.43	0.48	0.92
MgO	10.48	11.86	10.20	12.16	10.35	10.62	14.27	13.42	14.07	11.30
CaO	29.00	28.71	28.01	28.78	28.02	28.79	28.34	28.39	28.79	27.10
H2O-	.....	.....	.....	.....	0.02	0.08	0.05	0.02	0.03	0.04
H2O+	.....	.....	.....	.....	0.11	0.03	0.11	0.10	0.11	0.09
CO2	.....	.....	.....	.....	44.74	44.42	45.10	45.46	45.10	44.96
S	.....	.....	.....	.....	0.01	0.00	0.00	0.00	0.00	0.00
Total	.....	.....	.....	.....	101.11	100.74	99.42	100.47	100.60	

	N286L0				Ave(4)
Cu	10	12	11	8	10
Ni	20	10	22	21	18
Rb	5	8	11	6	8
Sc	28	36	37	34	34
Sr	196	46	102	100	111
V	9	27	23	20	20
Y	61	94	66	41	66
Zn	30	36	54	64	46

* = Averages

Digitised by the Department of Library Services in support of open access to information, University of Pretoria, 2021

Table IVc - Major and trace element analyses of Rooiberg ankerite
Group P - Rooiberg A Mine POCKETS

Sample	132L5	132L5	132L5	132L5	101L5	101L5	101L5	101L5	152L5	152L5	152L5	152L5	157L5	157L5
FeO	13.02	13.62	14.57	13.84	10.63	10.42	13.59	13.49	14.67	12.36	13.63	12.46	12.50	14.08
MnO	0.65	0.78	0.84	0.66	0.49	0.59	1.11	0.99	0.54	0.29	0.74	0.44	0.53	0.59
MgO	13.71	12.92	12.35	13.00	14.50	13.97	12.11	11.73	12.75	13.95	13.66	14.39	14.04	14.04
CaO	28.65	28.38	28.60	28.38	28.18	28.29	28.16	28.56	28.25	28.32	29.25	28.80	28.56	28.25

Sample	213L5	213L5	213L5	213L5	153L5	153L5	153L5	153L5	148L5	148L5	148L5	148L5	163L5	163L5
FeO	11.05	12.68	11.77	10.97	11.22	10.44	13.30	13.01	9.95	10.32	13.62	13.84	13.47	13.81
MnO	0.23	0.46	0.28	0.41	0.18	0.19	0.37	0.25	0.18	0.28	0.69	0.45	1.07	0.60
MgO	15.15	13.68	14.75	14.72	14.98	15.32	13.62	13.70	15.66	15.03	12.77	12.75	12.90	12.87
CaO	29.25	28.61	29.03	29.42	29.46	29.04	29.15	28.99	28.95	28.90	28.38	28.48	28.07	28.68

Sample	192L5	192L5	192L5	192L5	193L5	193L5	193L5	193L5	206L5	206L5	206L5	206L5	216L5	216L5
FeO	13.35	10.98	9.15	9.40	10.02	12.27	10.75	9.75	13.13	12.01	12.34	11.09	11.52	11.87
MnO	0.36	0.31	0.30	0.15	0.82	0.80	0.45	0.27	1.70	0.98	0.99	1.15	0.60	0.87
MgO	13.08	14.63	15.61	16.03	14.49	13.62	14.65	15.21	12.02	13.36	12.90	13.89	13.66	13.07
CaO	28.05	28.86	28.73	28.34	28.73	29.14	28.47	28.74	28.67	28.94	28.82	28.51	28.73	28.63

Sample	132L5*	101L5*	152L5*	157L5*	213L5*	153L5*	148L5*	163L5*	192L5*	193L5*	216L5*	Ave(48)
FeO	13.76	12.03	13.28	12.24	11.61	11.99	11.93	13.04	10.72	10.70	11.08	12.04
MnO	0.73	0.79	0.50	0.42	0.34	0.25	0.40	0.71	0.28	0.58	0.63	0.57
MgO	12.99	13.07	13.69	13.98	14.58	14.40	14.05	13.51	14.84	14.49	13.89	13.88
CaO	28.51	28.30	28.65	28.55	29.08	29.16	28.68	28.46	28.50	28.77	28.70	28.67
H2O-		.....					0.09	0.07	0.03	0.04	0.05	0.06
H2O+		.....					0.14	0.14	0.06	0.05	0.07	0.09
CO2		.....					42.16	44.00	44.70	45.12	45.46	44.29
S		.....					0.01	0.03	0.00	0.01	0.00	0.01
Total		.....					97.46	99.95	99.12	99.76	99.89	

					N134L5	Ave(4)
Cu	5	.....	20	42	5	18
Ni	18	.....	30	16	16	20
Rb	4	.....	4	4	3	4
Sc	29	.....	27	23	20	25
Sr	798	.....	209	72	1052	533
V	23	.....	43	21	18	26
Y	16	.....	15	48	26	26
Zn	73	.....	65	26	74	60

* = Averages

Digitised by the Department of Library Services in support of open access to information, University of Pretoria, 2021

Table IVd - Major and trace element analyses of Rooiberg ankerite
Group F - Ankerite-filled FRACTURES

Sample	113L4	113L4	113L4	113L4	114L4	114L4	114L4	114L4	130L4	130L4	130L4	188L4	188L4	188L4	188L4
FeO	10.72	10.79	10.29	10.80	11.40	10.82	10.69	10.63	10.85	10.58	10.60	12.08	12.26	12.45	11.62
MnO	1.45	1.37	1.62	1.44	1.50	1.52	1.47	1.44	1.98	1.99	1.72	1.23	1.17	1.47	1.45
MgO	14.13	13.64	14.01	13.90	13.38	13.86	13.96	14.00	13.49	13.69	13.57	11.72	11.15	11.12	11.92
CaO	29.17	29.26	29.56	28.72	28.37	28.59	29.01	28.74	28.82	28.99	29.20	28.43	28.54	28.29	28.83

Sample	147L4	147L4	147L4	147L4	162L4	162L4	162L4	162L4	176L4	176L4	176L4	176L4	191L4	191L4	191L4	191L4
FeO	12.50	12.09	15.76	15.94	11.72	11.02	13.14	11.45	15.16	13.76	14.64	14.83	9.35	10.67	10.40	10.20
MnO	1.28	1.26	1.42	1.47	0.46	0.38	0.49	0.61	0.80	1.63	1.00	0.90	1.56	1.92	1.81	1.44
MgO	13.03	13.40	11.15	11.05	13.92	14.08	12.36	14.08	11.81	12.18	11.84	11.80	15.13	14.23	14.56	14.57
CaO	28.51	28.48	28.58	28.30	28.47	28.83	28.43	28.67	28.44	28.19	28.04	28.40	28.80	29.04	29.12	28.78

Sample	198L4	198L4	198L4	198L4	200L4	200L4	200L4	200L4
FeO	13.38	13.29	13.42	12.69	14.78	14.95	14.93	15.55
MnO	1.34	1.13	1.15	1.21	1.71	2.09	2.02	2.56
MgO	12.58	12.44	12.58	12.97	11.41	11.05	11.13	10.24
CaO	28.08	27.98	28.02	28.30	28.04	27.96	27.69	28.20

Sample	113L4*	114L4*	130L4*	188L4*	147L4*	162L4*	176L4*	191L4*	198L4*	200L4*	Ave(39)
FeO	10.65	10.89	10.68	12.10	14.07	11.83	14.60	10.15	13.19	15.05	12.36
MnO	1.47	1.48	1.90	1.33	1.36	0.48	1.08	1.68	1.21	2.09	1.40
MgO	13.92	13.80	13.58	11.48	12.16	13.61	11.90	14.62	12.64	10.96	12.85
CaO	29.18	28.68	29.00	28.53	28.47	28.60	28.27	28.94	28.09	27.97	28.56
H_2O^-					0.02	0.03	0.04	0.01	0.04	0.02	0.03
H_2O^+					0.06	0.07	0.06	0.20	0.07	0.07	0.09
CO_2					42.53	44.36	45.10	45.47	45.46	44.21	44.52
S					0.01	0.00	0.00	0.00	0.01	0.01	0.01
Total					98.67	98.98	101.05	101.07	100.72	100.39	

					Ave (4)
Cu	5	5	74	122	52
Ni	20	16	9	9	14
Rb	7	5	3	3	5
Sc	25	23	18	24	23
Sr	672	712	23	82	372
V	42	27	4	9	21
Y	11	10	97	28	37
Zn	72	76	35	37	55

* = Averages

Digitised by the Department of Library Services in support of open access to information, University of Pretoria, 2021

Table IVe - Mole % calculated from the partial microprobe analyses

Ankerite-filled fractures

Sample	FeCO3	MnCO3	MgCO3	CaCO3	Total
147L4	19.12	1.87	29.45	49.56	100.00
162L4	16.16	0.67	33.13	50.04	100.00
176L4	19.96	1.50	29.02	49.52	100.00
191L4	13.54	2.27	34.75	49.43	100.00
198L4	18.09	1.68	30.89	49.34	100.00
200L4	20.75	2.93	26.93	49.40	100.00
113L4	14.33	2.00	33.38	50.29	100.00
114L4	14.74	2.03	33.49	49.74	100.00
188L4	17.18	1.92	29.04	51.87	100.00

A Mine pockets

Sample	FeCO3	MnCO3	MgCO3	CaCO3	Total
148L5	16.10	0.55	33.79	49.56	100.00
163L5	17.55	0.97	32.41	49.07	100.00
192L5	14.49	0.39	35.76	49.36	100.00
193L5	14.47	0.80	34.92	49.81	100.00
206L5	16.53	1.66	31.67	50.14	100.00
216L5	15.13	0.88	33.81	50.19	100.00
132L5	18.55	1.00	31.22	49.23	100.00
101L5	16.62	1.11	32.19	50.08	100.00
152L5	17.73	0.67	32.58	49.02	100.00
157L5	16.37	0.56	34.15	48.91	100.00
213L5	15.44	0.46	34.55	49.54	100.00
153L5	15.93	0.34	34.11	49.63	100.00

C Mine lodes

Sample	FeCO3	MnCO3	MgCO3	CaCO3	Total
C406L0	19.27	1.30	29.49	49.94	100.00
C410L0	21.76	1.50	27.13	49.62	100.00
C411L0	18.00	1.64	31.02	49.34	100.00
C417L0	22.08	1.55	26.94	49.43	100.00
C424L0	18.50	2.34	28.22	50.93	100.00
C427L0	24.70	1.61	23.23	50.45	100.00
C387L0	18.18	1.34	30.49	49.99	100.00
C422L0	20.38	1.77	27.61	50.24	100.00
C347L0	19.09	0.82	29.43	50.66	100.00
C403L0	20.46	2.06	27.14	50.34	100.00
C358L0	18.51	2.60	28.78	50.11	100.00
C399L0	15.98	1.73	32.23	50.06	100.00

NAD Mine lodes

Sample	FeCO3	MnCO3	MgCO3	CaCO3	Total
N284L0	23.08	1.66	25.55	49.71	100.00
N286L0	22.62	1.31	26.46	49.60	100.00
N309L0	20.55	2.63	26.05	50.77	100.00
N335L0	15.18	0.59	34.70	49.53	100.00
N336L0	17.23	0.60	32.60	49.57	100.00
N339L0	16.12	0.66	33.68	49.53	100.00
N304L0	20.03	1.16	28.27	50.54	100.00
N303L0	23.48	1.43	25.74	49.35	100.00
N308L0	19.24	1.75	28.96	50.05	100.00

Digitised by the Department of Library Services in support of open access to information, University of Pretoria, 2021

Pb - Pb isotopic data of Rooiberg ankerite

Table V - All sample groups

Table V a - d - Individual sample groups - $^{206}Pb/^{204}Pb$ $^{207}Pb/^{204}Pb$ ratios only

Tables V e - h - Individual sample groups - All relevant information

Digitised by the Department of Library Services in support of open access to information, University of Pretoria, 2021

Table V - All sample groups

Sample no.	206Pb/204Pb	X Wt	207Pb/204Pb	Y Wt	R	X Error	Y Error	Include
101L5	21.091769	0.010000	16.086978	0.010000	0.960	0.151682	0.160728	Y
112L4	19.423398	0.010000	15.898798	0.010000	0.960	0.038094	0.040365	Y
113L4	18.758804	0.010000	15.710969	0.010000	0.960	0.120165	0.127332	Y
113L4	18.782182	0.010000	15.819798	0.010000	0.960	0.001968	0.002085	Y
113L4	18.802921	0.010000	15.794037	0.010000	0.960	0.035078	0.037170	Y
114L4	20.393407	0.010000	16.137354	0.010000	0.960	-0.041547	-0.044025	Y
117L0	20.897725	0.010000	16.150920	0.010000	0.960	0.041652	0.044136	Y
117L5	20.054155	0.010000	15.892660	0.010000	0.960	0.168216	0.178248	Y
130L4	20.564473	0.010000	16.129316	0.010000	0.960	0.000932	0.000988	Y
147L4	20.573642	0.010000	16.157119	0.010000	0.960	-0.028640	-0.030348	Y
148L5	20.103472	0.010000	16.036416	0.010000	0.960	0.015685	0.016621	Y
149L5	19.755654	0.010000	15.979358	0.010000	0.960	0.012114	0.012837	Y
149L5	19.716520	0.010000	15.986337	0.010000	0.960	-0.003402	-0.003605	Y
152L5	18.932441	0.010000	15.840675	0.010000	0.960	0.007766	0.008229	Y
153L4	19.695585	0.010000	15.865048	0.010000	0.960	0.129328	0.137041	Y
156L5	17.006460	0.010000	15.609467	0.010000	0.960	-0.107602	-0.114019	Y
156L5	17.015075	0.010000	15.622512	0.010000	0.960	-0.120634	-0.127829	Y
157L5	20.500723	0.010000	16.064453	0.010000	0.960	0.061649	0.065326	Y
162L4	17.495839	0.010000	15.727115	0.010000	0.960	-0.144729	-0.153360	Y
163L5	20.572432	0.010000	16.131670	0.010000	0.960	-0.000169	-0.000179	Y
176L4	18.851246	0.010000	15.905917	0.010000	0.960	-0.081689	-0.086561	Y
176L4	18.960350	0.010000	15.954717	0.010000	0.960	-0.115428	-0.122312	Y
188L4	19.334865	0.010000	15.895639	0.010000	0.960	0.024365	0.025818	Y
191L4	20.104791	0.010000	16.116280	0.010000	0.960	-0.074147	-0.078569	Y
192L5	18.415137	0.010000	15.725351	0.010000	0.960	0.036817	0.039013	Y
213L5	19.667819	0.010000	15.915900	0.010000	0.960	0.066542	0.070510	Y
216L5	17.567698	0.010000	15.563715	0.010000	0.960	0.053629	0.056827	Y
273L4	21.665571	0.010000	16.352966	0.010000	0.960	-0.036290	-0.038454	Y
275L4	20.776805	0.010000	16.170345	0.010000	0.960	-0.003878	-0.004109	Y
453L5	17.046257	0.010000	15.600389	0.010000	0.960	-0.089588	-0.094931	Y
C343L0	17.082981	0.010000	15.509599	0.010000	0.960	0.020000	0.021193	Y
C347L0	17.589238	0.010000	15.546539	0.010000	0.960	0.077212	0.081816	Y
C348L0	16.978256	0.010000	15.499883	0.010000	0.960	0.010505	0.011132	Y
C387L0	17.272327	0.010000	15.490284	0.010000	0.960	0.078771	0.083469	Y
C392L0	16.395679	0.010000	15.373858	0.010000	0.960	0.038879	0.041198	Y
C399L0	16.443068	0.010000	15.398984	0.010000	0.960	0.019792	0.020972	Y
C402L0	17.743772	0.010000	15.665661	0.010000	0.960	-0.026980	-0.028589	Y
C403L0	16.052265	0.010000	15.338635	0.010000	0.960	0.011537	0.012225	Y
C410L0	17.965946	0.010000	15.739696	0.010000	0.960	-0.067100	-0.071102	Y
C411L0	18.878651	0.010000	15.852673	0.010000	0.960	-0.016275	-0.017245	Y
C420L0	17.332256	0.010000	15.593119	0.010000	0.960	-0.025526	-0.027049	Y
C422L0	17.421389	0.010000	15.612507	0.010000	0.960	-0.029987	-0.031776	Y
C424L0	17.995690	0.010000	15.735964	0.010000	0.960	-0.057081	-0.060485	Y
C427L0	16.200793	0.010000	15.404388	0.010000	0.960	-0.033625	-0.035630	Y
N281L0	22.306450	0.010000	16.425195	0.010000	0.960	0.007408	0.007850	Y
N284L0	22.308538	0.010000	16.477256	0.010000	0.960	-0.050911	-0.053947	Y
N286L0	21.867028	0.010000	16.323125	0.010000	0.960	0.036721	0.038910	Y
N288L0	23.877836	0.010000	16.686681	0.010000	0.960	0.019362	0.020516	Y
N291L0	29.504244	0.010000	17.764281	0.010000	0.960	-0.097276	-0.103078	Y
N303L0	23.917063	0.010000	16.681258	0.010000	0.960	0.033141	0.035117	Y
N304L0	23.198576	0.010000	16.597477	0.010000	0.960	-0.012685	-0.013441	Y
N308L0	23.418291	0.010000	16.658306	0.010000	0.960	-0.038388	-0.040677	Y

Digitised by the Department of Library Services in support of open access to information, University of Pretoria, 2021

N309LO	23.833450	0.010000	16.767226	0.010000	0.960	-0.080166	-0.084947	Y
N326LO	18.841845	0.010000	15.783377	0.010000	0.960	0.054705	0.057968	Y
N329LO	23.632029	0.010000	16.690877	0.010000	0.960	-0.033382	-0.035373	Y
N335LO	19.854848	0.010000	15.928767	0.010000	0.960	0.088558	0.093839	Y
N339LO	19.555122	0.010000	15.931984	0.010000	0.960	0.026386	0.027960	Y
C417LO	17.231500	0.010000	15.592400	0.010000	0.960	-0.044395	-0.047042	Y
C358LO	18.537300	0.010000	15.803200	0.010000	0.960	-0.027139	-0.028758	Y

Sample uncertainties are 1 sigma and based on 60 replicates Students t = 2.00

Regression converged after 7 iterations F (0.025; 60; 57) = 1.55

Centroid 206Pb/204Pb = 19.589214 207Pb/204Pb = 15.961278
Slope = 0.1731481 +/- 0.0024930 1 sigma
Intercept = 12.569444 +/- 0.049221 1 sigma

MSWD = 49.291 on 59 points Errors augmented by Sqrt(MSWD/1.55)

Age = 2588.31 + 47.27 - 48.88 95% conf.

Mu = 11.058 + 0.213 - 0.217 95% conf. - S & K two stage

Decay constants 238U = 1.55125E-0010 235U = 9.84850E-0010

Digitised by the Department of Library Services in support of open access to information, University of Pretoria, 2021

Table V a - Pb/Pb isotope data of ankerite
C Mine lodes - Group C

Sample Number	Lab Number	Pb206/ Pb204	Pb207/ Pb204
C343L0	562	17.083	15.5096
C347L0	573	17.5892	15.5465
C348L0	588	16.9783	15.4999
C387L0	572	17.2723	15.4903
C392L0	559	16.3957	15.3739
C399L0	571	16.4431	15.399
C402L0	560	17.7438	15.6657
C403L0	587	16.0523	15.3386
C410L0	581	17.9659	15.7397
C411L0	574	18.8787	15.8527
C420L0	579	17.3323	15.5931
C422L0	561	17.4214	15.6125
C424L0	582	17.9957	15.736
C427L0	580	16.2008	15.4044

Table V b - Pb/Pb isotope data of ankerite
NAD Mine lodes - Group N

Sample Number	Lab Number	Pb206/ Pb204	Pb207/ Pb204
N281L0	576	22.3064	16.4252
N284L0	569	22.3085	16.4773
N286L0	578	21.867	16.3231
N288L0	583	23.8778	16.6867
N290L0	586	31.1514	17.4035
N291L0	584	29.5042	17.7643
N303L0	567	23.9171	16.6813
N304L0	568	23.1986	16.5975
N308L0	577	23.4183	16.6583
N309L0	566	23.8335	16.7672
N314L0	575	33.8484	17.6941
N320L0	564	25.238	16.717
N326L0	565	18.8418	15.7834
N329L0	563	23.632	16.6909
N335L0	570	19.8548	15.9288
N339L0	585	19.5551	15.932

Table V c - Pb/Pb isotope data of ankerite
A Mine pockets - Group P

Sample Number	Lab Number	Pb206/ Pb204	Pb207/ Pb204
101L5	477	21.0918	16.087
117L5	479	20.0542	15.8927
148L5	499	20.1035	16.0364
149L5	558	19.7165	15.9863
149L5	503	19.7557	15.9794
152L5	501	18.9324	15.8407
156L5	557	17.0151	15.6225
156L5	478	17.0065	15.6095
157L5	505	20.5007	16.0645
163L5	502	20.5724	16.1317
192L5	498	18.4151	15.7254
213L5	500	19.6678	15.9159
216L5	504	17.5677	15.5637
453L5	476	17.0463	15.6004

Table V d - Pb/Pb isotope data of ankerite
Ankerite-filled fractures - Group F

Sample Number	Lab Number	Pb206/ Pb204	Pb207/ Pb204
112L4	457	19.4234	15.8988
113L4	458	18.7588	15.711
113L4	555	18.8029	15.794
113L4	555	18.7822	15.8198
114L4	475	20.3934	16.1374
130L4	461	20.5645	16.1293
147L4	453	20.5736	16.1571
153L4	454	19.6956	15.865
162L4	456	17.4958	15.7271
176L4	452	18.8512	15.9059
176L4	556	18.9604	15.9547
188L4	455	19.3349	15.8956
191L4	474	20.1048	16.1163
273L4	450	21.6656	16.353
275L4	460	20.7768	16.1703

Digitised by the Department of Library Services in support of open access to information, University of Pretoria, 2021

Table V e - C Mine lodes - Group C

Sample no.	206Pb/204Pb	X Wt	207Pb/204Pb	Y Wt	R	X Error	Y Error	Include
C343L0	17.082981	0.010000	15.509599	0.010000	0.960	0.021157	0.022455	Y
C347L0	17.589238	0.010000	15.546539	0.010000	0.960	0.086889	0.092221	Y
C348L0	15.978256	0.010000	15.499883	0.010000	0.960	0.009931	0.010541	Y
C387L0	17.272327	0.010000	15.490284	0.010000	0.960	0.083614	0.088745	Y
C392L0	16.395679	0.010000	15.373858	0.010000	0.960	0.029757	0.031583	Y
C399L0	16.443068	0.010000	15.398984	0.010000	0.960	0.011141	0.011825	Y
C402L0	17.743772	0.010000	15.665661	0.010000	0.960	-0.016325	-0.017327	Y
C403L0	16.052265	0.010000	15.338635	0.010000	0.960	-0.003211	-0.003409	Y
C410L0	17.965946	0.010000	15.739696	0.010000	0.960	-0.053577	-0.056864	Y
C411L0	18.878651	0.010000	15.852673	0.010000	0.960	0.011911	0.012642	Y
C420L0	17.332256	0.010000	15.593119	0.010000	0.960	-0.021157	-0.022456	Y
C422L0	17.421389	0.010000	15.612507	0.010000	0.960	-0.024312	-0.025804	Y
C424L0	17.995690	0.010000	15.735964	0.010000	0.960	-0.042968	-0.045604	Y
C427L0	16.200793	0.010000	15.404388	0.010000	0.960	-0.046700	-0.049566	Y
C417L0	17.231500	0.010000	15.592400	0.010000	0.960	-0.041821	-0.044388	Y
C358L0	18.537300	0.010000	15.803200	0.010000	0.960	-0.004328	-0.004594	Y

Sample uncertainties are 1 sigma and based on 60 replicates Students t = 2.00

Regression converged after 8 iterations F (0.025; 60; 14) = 1.86

Centroid 206Pb/204Pb = 17.320069 207Pb/204Pb = 15.572337
Slope = 0.1865519 +/- 0.0089187 1 sigma
Intercept = 12.341245 +/- 0.154629 1 sigma

MSWD = 21.183 on 16 points Errors augmented by Sqrt(MSWD/1.86)

Age = 2712.00 + 149.58 - 167.08 95% conf.

Mu = 11.346 + 0.467 - 0.500 95% conf. - S & K two stage

Decay constants 238U = 1.55125E-0010 235U = 9.84850E-0010

Digitised by the Department of Library Services in support of open access to information, University of Pretoria, 2021

Table V f - NAD Mine lodes - Group N

Sample no.	206Pb/204Pb	X Wt	207Pb/204Pb	Y Wt	R	X Error	Y Error	Include
N281L0	22.306450	0.010000	16.425195	0.010000	0.960	0.003927	0.004168	Y
N284L0	22.308538	0.010000	16.477256	0.010000	0.960	-0.055136	-0.058519	Y
N286L0	21.867028	0.010000	16.323125	0.010000	0.960	0.026916	0.028567	Y
N288L0	23.877836	0.010000	16.686681	0.010000	0.960	0.040049	0.042506	Y
N291L0	29.504244	0.010000	17.764281	0.010000	0.960	0.007824	0.008304	Y
N303L0	23.917063	0.010000	16.681258	0.010000	0.960	0.054611	0.057962	Y
N304L0	23.198576	0.010000	16.597477	0.010000	0.960	-0.002802	-0.002974	Y
N308L0	23.418291	0.010000	16.658306	0.010000	0.960	-0.025491	-0.027055	Y
N309L0	23.833450	0.010000	16.767226	0.010000	0.960	-0.061482	-0.065254	Y
N326L0	18.841845	0.010000	15.783377	0.010000	0.960	-0.001082	-0.001148	Y
N329L0	23.632029	0.010000	16.690877	0.010000	0.960	-0.017153	-0.018205	Y
N335L0	19.854848	0.010000	15.928767	0.010000	0.960	0.048699	0.051687	Y
N339L0	19.555122	0.010000	15.931984	0.010000	0.960	-0.018879	-0.020038	Y

Sample uncertainties are 1 sigma and based on 60 replicates Students t = 2.00

Regression converged after 8 iterations F (0.025; 60; 11) = 1.95

Centroid 206Pb/204Pb = 22.778102 207Pb/204Pb = 16.516601
Slope = 0.1865148 +/- 0.0025696 1 sigma
Intercept = 12.268148 +/- 0.058901 1 sigma

MSWD = 16.337 on 13 points Errors augmented by Sqrt(MSWD/1.95)

Age = 2711.67 + 44.74 - 46.18 95% conf.

Mu = 10.758 + 0.376 - 0.384 95% conf. - S & K two stage

Decay constants 238U = 1.55125E-0010 235U = 9.84850E-0010

Digitised by the Department of Library Services in support of open access to information, University of Pretoria, 2021

Table V g - A Mine pockets - Group P

Sample no.	206Pb/204Pb	X Wt	207Pb/204Pb	Y Wt	R	X Error	Y Error	Include
101L5	21.091769	0.010000	16.086978	0.010000	0.960	0.052524	0.055422	Y
117L0	20.897725	0.010000	16.150920	0.010000	0.960	-0.045856	-0.048386	Y
117L5	20.054155	0.010000	15.892660	0.010000	0.960	0.110051	0.116124	Y
148L5	20.103472	0.010000	16.036416	0.010000	0.960	-0.039083	-0.041240	Y
149L5	19.755654	0.010000	15.979358	0.010000	0.960	-0.028592	-0.030170	Y
149L5	19.716520	0.010000	15.986337	0.010000	0.960	-0.041994	-0.044312	Y
152L5	18.932441	0.010000	15.840675	0.010000	0.960	0.000197	0.000208	Y
156L5	17.006460	0.010000	15.609467	0.010000	0.960	-0.033935	-0.035808	Y
156L5	17.015075	0.010000	15.622512	0.010000	0.960	-0.046854	-0.049440	Y
157L5	20.500723	0.010000	16.064453	0.010000	0.960	-0.010656	-0.011244	Y
163L5	20.572432	0.010000	16.131670	0.010000	0.960	-0.073170	-0.077207	Y
192L5	18.415137	0.010000	15.725351	0.010000	0.960	0.048953	0.051655	Y
213L5	19.667819	0.010000	15.915900	0.010000	0.960	0.027438	0.028952	Y
216L5	17.567698	0.010000	15.563715	0.010000	0.960	0.099129	0.104599	Y
453L5	17.046257	0.010000	15.600389	0.010000	0.960	-0.018151	-0.019153	Y

Sample uncertainties are 1 sigma and based on 60 replicates Students t = 2.00

Regression converged after 7 iterations F (0.025; 60; 13) = 1.89

Centroid 206Pb/204Pb = 19.222889 207Pb/204Pb = 15.880453
Slope = 0.1363310 +/- 0.0070460 1 sigma
Intercept = 13.259778 +/- 0.135809 1 sigma

MSWD = 37.072 on 15 points Errors augmented by Sqrt(MSWD/1.89)

Age = 2181.10 + 169.65 - 191.96 95% conf.

Mu = 10.839 + 0.355 - 0.378 95% conf. - S & K two stage

Decay constants 238U = 1.55125E-0010 235U = 9.84850E-0010

Digitised by the Department of Library Services in support of open access to information, University of Pretoria, 2021

Table V h - Ankerite-filled fractures - Group F

Sample no.	206Pb/204Pb	X Wt	207Pb/204Pb	Y Wt	R	X Error	Y Error	Include
112L4	19.423398	0.010000	15.898798	0.010000	0.960	0.051786	0.054797	Y
113L4	18.758804	0.010000	15.710969	0.010000	0.960	0.141740	0.149982	Y
113L4	18.782182	0.010000	15.819798	0.010000	0.960	0.024607	0.026038	Y
113L4	18.802921	0.010000	15.794037	0.010000	0.960	0.057056	0.060374	Y
114L4	20.393407	0.010000	16.137354	0.010000	0.960	-0.039827	-0.042143	Y
130L4	20.564473	0.010000	16.129316	0.010000	0.960	-0.000117	-0.000124	Y
147L4	20.573642	0.010000	16.157119	0.010000	0.960	-0.029467	-0.031180	Y
153L4	19.695585	0.010000	15.865048	0.010000	0.960	0.138339	0.146384	Y
162L4	17.495839	0.010000	15.727115	0.010000	0.960	-0.103276	-0.109282	Y
176L4	18.851246	0.010000	15.905917	0.010000	0.960	-0.058994	-0.062425	Y
176L4	18.960350	0.010000	15.954717	0.010000	0.960	-0.093791	-0.099245	Y
188L4	19.334865	0.010000	15.895639	0.010000	0.960	0.039394	0.041685	Y
191L4	20.104791	0.010000	16.116280	0.010000	0.960	-0.068209	-0.072176	Y
273L4	21.665571	0.010000	16.352966	0.010000	0.960	-0.051548	-0.054545	Y
275L4	20.776805	0.010000	16.170345	0.010000	0.960	-0.007694	-0.008142	Y

Sample uncertainties are 1 sigma and based on 60 replicates Students t = 2.00

Regression converged after 4 iterations F (0.025; 60; 13) = 1.89

Centroid 206Pb/204Pb = 19.612259 207Pb/204Pb = 15.975695
Slope = 0.1612208 +/- 0.0128620 1 sigma
Intercept = 12.813791 +/- 0.252600 1 sigma

MSWD = 69.177 on 15 points Errors augmented by Sqrt(MSWD/1.89)

Age = 2468.50 + 246.98 - 298.11 95% conf.

Mu = 11.119 + 0.864 - 0.962 95% conf. - S & K two stage

Decay constants 238U = 1.55125E-0010 235U = 9.84850E-0010

Digitised by the Department of Library Services in support of open access to information, University of Pretoria, 2021

Table VI - Partial analyses of tourmaline

Samples nnnL1 and nnnL2 are from Rooiberg A Mine
Sample L105 is from a stanniferous pegmatite: Erongo, Namibia

Digitised by the Department of Library Services in support of open access to information, University of Pretoria, 2021

Table V1 - Partial analyses of tourmaline

Lab	Sample	Pos	SiO2	TiO2	Al2O3	Cr2O3	FeO	MnO	MgO	CaO	Na2O	K2O	F	Total
Tourmaline L1														
CG	127L1-1	1	37.68	0.51	31.19	0.06	8.56	0.00	8.17	0.70	2.22	0.03		89.13
CG	127L1-1	4	37.47	0.52	32.86	0.02	8.01	0.00	7.55	0.87	2.20	0.04		89.53
CG	127L1-1	7	36.92	0.67	29.35	0.00	11.77	0.01	7.12	0.42	2.89	0.04		89.19
CG	127L1-1	9	36.96	0.48	30.64	0.01	10.16	0.00	7.25	0.43	2.99	0.04		88.97
CG	127L1-2	1	37.78	0.45	32.10	0.08	6.99	0.02	8.50	0.67	2.22	0.04		88.87
CG	127L1-2	6	36.99	0.88	31.43	0.04	9.27	0.01	7.01	1.20	2.02	0.04		88.88
CG	127L1-2	9	37.03	1.14	28.80	0.02	12.34	0.00	7.12	0.97	2.45	0.04		89.90
AARL	127L1-3	0	37.50	0.37	29.96	0.20	7.99	0.01	7.85	0.52	2.06	0.03	0.01	86.50
AARL	127L1-3	0	37.65	0.37	29.96	0.19	7.97	0.00	7.84	0.51	2.07	0.02	0.00	86.57
AARL	127L1-3	0	37.35	0.36	29.96	0.21	8.01	0.01	7.87	0.54	2.06	0.03	0.01	86.42
AARL	127L1-3	2	37.37	0.32	30.65	0.15	7.71	0.00	7.93	0.57	2.11	0.04	0.01	86.84
AARL	127L1-3	2	37.26	0.28	32.31	0.16	6.97	0.00	7.38	0.84	2.07	0.01	0.01	87.31
AARL	127L1-3	3	36.90	0.64	29.40	0.03	9.59	0.00	7.22	0.78	2.38	0.03	0.02	87.00
AARL	127L1-3	3	37.02	0.63	29.37	0.02	9.58	0.00	7.30	0.78	2.41	0.03	0.03	87.18
AARL	127L1-3	3	36.78	0.65	29.43	0.04	9.60	0.01	7.15	0.78	2.34	0.03	0.00	86.81
AARL	127L1-3	6	36.30	0.95	29.70	0.25	8.96	0.00	7.23	1.20	1.93	0.03	0.04	86.57
AARL	127L1-3	6	36.19	1.41	26.25	0.01	12.76	0.01	7.02	1.05	2.25	0.04	0.02	87.01
AARL	127L1-3	6	36.70	0.65	27.81	0.00	11.81	0.00	6.80	0.61	2.57	0.04	0.02	87.01
AARL	127L1-3	6	36.47	0.66	27.81	0.00	11.86	0.01	6.90	0.61	2.55	0.03	0.01	86.90
AARL	127L1-3	6	36.58	0.66	27.81	0.00	11.84	0.00	6.85	0.61	2.56	0.04	0.01	86.96
AARL	127L1-4	0	37.46	0.49	29.70	0.08	8.41	0.01	8.14	0.65	2.27	0.02	0.00	87.23
AARL	127L1-4	1	37.40	0.44	29.90	0.07	7.84	0.00	8.12	0.66	2.16	0.01	0.02	86.62
AARL	127L1-4	1	37.29	0.40	30.44	0.04	7.61	0.00	8.25	0.68	2.24	0.03	0.00	86.98
AARL	127L1-4	1	37.36	0.46	29.83	0.04	8.10	0.00	8.22	0.68	2.20	0.02	0.00	86.92
AARL	127L1-4	1	36.71	0.47	30.48	0.03	7.72	0.00	8.18	0.77	2.30	0.03	0.01	86.69
AARL	127L1-4	3	37.22	0.31	31.74	0.12	6.80	0.02	7.81	0.69	2.11	0.02	0.00	86.83
AARL	127L1-4	3	37.26	0.28	32.51	0.19	6.78	0.00	7.26	0.88	1.99	0.03	0.02	87.20
AARL	127L1-4	4	37.27	0.47	31.07	0.10	8.10	0.00	7.30	0.86	2.22	0.03	0.03	87.45
AARL	127L1-4	4	37.02	0.29	31.88	0.15	7.42	0.01	7.09	0.77	2.14	0.03	0.04	86.84
AARL	127L1-4	4	37.10	0.82	29.99	0.06	9.32	0.00	7.37	0.88	2.35	0.04	0.03	87.97
AARL	127L1-4	7	36.41	1.22	26.41	0.01	13.14	0.00	6.87	0.70	2.50	0.05	0.00	87.32
AARL	127L1-4	7	36.45	0.91	27.58	0.00	12.30	0.00	6.93	0.55	2.63	0.05	0.03	87.44
AARL	127L1-4	7	36.32	0.53	28.65	0.02	11.40	0.00	6.79	0.47	2.65	0.04	0.07	86.94
CG	205L1-1	1	37.58	0.25	30.63	0.00	10.05	0.00	7.26	0.20	2.95	0.04		88.96
CG	205L1-1	1	36.53	0.22	29.02	0.00	10.52	0.00	6.93	0.27	2.77	0.03		86.30
CG	205L1-1	9	35.92	1.40	27.73	0.00	13.23	0.02	5.98	0.75	2.75	0.07		87.84
CG	205L1-1	9	36.99	0.80	29.59	0.00	12.03	0.00	6.44	0.52	2.90	0.06		89.32
CG	205L1-2	1	37.18	0.50	30.43	0.03	10.22	0.01	7.57	0.76	2.57	0.04		89.33
CG	205L1-2	6	35.92	1.22	24.38	0.02	16.53	0.00	6.77	0.80	2.69	0.06		88.40
CG	205L1-2	9	35.87	0.46	28.42	0.00	14.29	0.01	6.19	0.40	2.93	0.04		88.62
CG	124L1-1	1	37.06	0.34	31.86	0.02	8.90	0.00	7.36	0.65	2.24	0.03		88.47
CG	124L1-1	4	37.23	0.43	32.19	0.08	8.49	0.00	7.49	0.75	2.52	0.02		89.21
CG	124L1-1	7	36.56	0.62	29.34	0.01	12.72	0.03	7.05	0.44	2.86	0.04		89.68
CG	124L1-1	9	36.96	0.27	31.65	0.00	9.53	0.01	7.24	0.16	3.06	0.07		88.95
CG	124L1-2	1	37.11	0.34	31.90	0.01	8.93	0.00	7.35	0.52	2.03	0.03		88.23
CG	124L1-2	6	36.08	1.83	26.99	0.01	13.63	0.00	7.06	1.15	2.34	0.04		89.13
CG	124L1-2	9	36.74	0.26	30.62	0.00	11.25	0.02	6.77	0.38	2.82	0.04		88.91

Digitised by the Department of Library Services in support of open access to information, University of Pretoria, 2021

Table V1 (contd) - Partial analyses of tourmaline - Page 2

Lab	Sample	Pos	SiO2	TiO2	Al2O3	Cr2O3	FeO	MnO	MgO	CaO	Na2O	K2O	F	Total
AARL	124L1-3	0	37.52	0.32	30.67	0.24	7.90	0.02	7.74	0.48	2.02	0.02	0.03	86.97
AARL	124L1-3	0	37.63	0.25	32.08	0.17	6.28	0.00	7.80	0.64	1.94	0.03	0.00	86.81
AARL	124L1-3	0	37.52	0.26	32.14	0.17	6.37	0.01	7.88	0.65	1.93	0.04	0.00	86.98
AARL	124L1-3	2	37.50	0.27	32.20	0.18	6.17	0.00	7.92	0.68	1.98	0.03	0.00	86.92
AARL	124L1-3	2	36.93	0.28	32.36	0.17	6.31	0.03	7.85	0.65	1.96	0.02	0.01	86.58
AARL	124L1-3	2	37.00	0.34	32.29	0.09	7.18	0.00	7.27	0.81	1.99	0.03	0.01	87.01
AARL	124L1-3	4	37.23	0.92	29.99	0.68	8.15	0.02	7.59	1.00	2.12	0.03	0.02	87.75
AARL	124L1-3	4	37.14	0.41	31.60	0.10	8.30	0.00	7.19	0.91	2.02	0.03	0.01	87.72
AARL	124L1-3	4	37.45	0.26	32.50	0.18	6.26	0.01	7.83	0.66	1.97	0.03	0.03	87.16
AARL	124L1-3	4	36.98	0.42	31.64	0.13	7.76	0.02	7.24	0.88	1.94	0.02	0.00	87.03
AARL	124L1-3	4	35.84	1.20	26.24	0.04	12.21	0.00	7.12	0.82	2.30	0.04	0.04	85.86
AARL	124L1-3	4	36.16	0.81	27.96	0.04	11.08	0.01	7.32	0.79	2.48	0.05	0.02	86.71
AARL	124L1-3	4	35.77	1.25	27.63	0.14	10.73	0.00	7.41	1.07	2.25	0.02	0.03	86.31
AARL	124L1-3	7	36.85	0.68	30.52	0.12	8.13	0.01	7.53	0.92	2.17	0.04	0.03	87.01
AARL	124L1-3	7	36.47	1.02	28.76	0.11	9.84	0.00	7.61	0.96	2.27	0.04	0.01	87.09
AARL	124L1-3	7	36.46	1.12	26.71	0.01	13.34	0.00	6.85	0.62	2.53	0.04	0.03	87.70
AARL	124L1-3	7	35.66	1.35	24.09	0.03	14.54	0.00	7.12	1.02	2.28	0.05	0.05	86.19
AARL	124L1-3	7	36.56	1.04	29.04	0.04	9.92	0.00	7.24	0.91	2.24	0.04	0.03	87.06
AARL	124L1-4	0	36.49	0.32	29.84	0.07	9.58	0.00	7.25	0.57	2.07	0.04	0.02	86.23
AARL	124L1-4	2	36.88	0.35	29.85	0.07	10.25	0.00	7.07	0.49	2.12	0.03	0.00	87.11
AARL	124L1-4	3	36.22	0.96	26.62	0.01	12.50	0.00	7.21	0.80	2.43	0.03	0.03	86.80
AARL	124L1-4	4	36.60	0.42	28.49	0.00	11.03	0.00	7.24	0.72	2.49	0.04	0.00	87.03
AARL	124L1-4	7	36.18	0.80	26.56	0.00	13.02	0.00	6.20	0.37	2.52	0.03	0.01	85.69
AARL	124L1-4	7	36.30	0.60	26.51	0.00	13.41	0.00	6.32	0.26	2.64	0.06	0.02	86.13
AARL	124L1-4	7	36.79	0.30	28.70	0.01	10.53	0.02	6.75	0.35	2.65	0.04	0.04	86.17
CG	227L1-1	1	37.33	0.36	31.37	0.03	7.93	0.00	7.87	0.37	2.58	0.03		87.87
CG	227L1-1	9	28.48	0.98	22.18	0.03	8.12	0.00	5.76	0.69	1.94	0.13		68.32
CG	227L1-2	1	36.73	0.86	28.73	0.02	10.20	0.01	7.50	0.70	2.49	0.04		87.28
CG	227L1-2	1	36.87	0.37	31.08	0.00	9.50	0.02	7.56	0.36	2.55	0.03		88.33
CG	227L1-2	9	36.60	0.66	28.85	0.00	12.01	0.03	7.40	0.83	2.60	0.05		89.01
CG	227L1-2	9	36.55	1.18	26.84	0.00	12.28	0.00	7.13	1.05	2.48	0.05		87.57
AARL	227L1-3	0	37.07	0.32	29.60	0.01	9.26	0.00	7.42	0.33	2.42	0.03	0.01	86.47
AARL	227L1-3	0	37.09	0.37	29.23	0.02	9.61	0.00	7.37	0.35	2.50	0.03	0.02	86.58
AARL	227L1-3	1	36.96	0.38	29.51	0.00	9.25	0.00	7.43	0.35	2.41	0.03	0.01	86.33
AARL	227L1-3	2	37.34	0.34	29.41	0.00	9.43	0.00	7.54	0.37	2.38	0.03	0.01	86.86
AARL	227L1-3	2	37.31	0.34	29.49	0.00	9.21	0.00	7.50	0.39	2.44	0.03	0.03	86.75
AARL	227L1-3	2	37.25	0.31	29.98	0.01	8.91	0.01	7.54	0.37	2.46	0.03	0.00	86.87
AARL	227L1-3	6	36.54	0.61	27.67	0.02	11.80	0.01	7.08	0.93	2.37	0.05	0.04	87.12
AARL	227L1-3	6	36.47	0.95	26.91	0.00	11.93	0.01	7.30	0.89	2.32	0.05	0.03	86.87
AARL	227L1-3	6	36.61	0.68	27.69	0.01	11.60	0.00	7.09	0.86	2.43	0.04	0.05	87.07
AARL	227L1-3	9	35.44	0.85	26.14	0.01	13.20	0.00	7.12	1.04	2.31	0.06	0.04	86.23
AARL	227L1-4	0	37.32	0.31	31.35	0.02	7.20	0.03	7.70	0.74	2.23	0.04	0.02	86.95
AARL	227L1-4	2	35.88	0.84	27.88	0.01	11.27	0.01	7.26	0.86	2.37	0.05	0.00	86.41
AARL	227L1-4	3	36.41	0.94	26.62	0.02	12.41	0.00	6.94	0.93	2.37	0.05	0.05	86.75
AARL	227L1-4	3	36.86	0.75	27.71	0.01	11.59	0.02	7.20	0.91	2.42	0.04	0.02	87.53
AARL	227L1-4	3	35.95	1.44	25.71	0.02	13.15	0.00	7.34	1.10	2.24	0.06	0.03	87.03
AARL	227L1-4	6	36.28	1.10	26.35	0.01	12.73	0.01	7.18	0.94	2.32	0.05	0.04	87.01
AARL	227L1-4	9	36.61	0.40	28.14	0.01	11.14	0.00	7.16	0.78	2.42	0.06	0.03	86.74
AARL	227L1-4	9	36.67	0.39	27.65	0.01	12.08	0.00	7.03	0.79	2.37	0.04	0.03	87.05

Digitised by the Department of Library Services in support of open access to information, University of Pretoria, 2021

Table V1 (contd) - Partial analyses of tourmaline - Page 3

Lab	Sample	Pos	SiO2	TiO2	Al2O3	Cr2O3	FeO	MnO	MgO	CaO	Na2O	K2O	F	Total
CG	244L1-1	1	37.04	0.18	35.90	0.04	4.90	0.00	7.83	0.86	2.07	0.03		88.84
CG	244L1-1	1	33.35	0.34	33.29	0.02	4.69	0.00	6.44	1.06	1.64	0.03		80.86
CG	244L1-1	9	36.50	1.47	26.79	0.02	12.88	0.00	7.62	1.11	2.47	0.05		88.92
CG	244L1-1	9	36.37	1.25	26.93	0.00	13.72	0.02	7.19	1.19	2.40	0.04		89.11
CG	155L2-1	1	37.41	0.33	32.03	0.88	8.04	0.00	7.57	0.36	2.33	0.01		88.96
CG	155L2-1	1	37.68	0.23	31.85	1.00	7.62	0.00	7.65	0.43	2.30	0.02		88.77
CG	155L2-1	9	36.76	0.67	30.19	0.00	11.89	0.01	6.53	0.19	2.92	0.04		89.19
CG	155L2-1	9	36.50	0.49	27.76	0.00	12.49	0.03	7.23	0.21	2.66	0.10		87.45
Tourmaline L2														
CG	155L2-2	1	36.79	0.39	31.60	0.03	7.71	0.00	7.41	0.34	2.35	0.05		86.66
CG	155L2-2	1	37.32	0.38	32.49	0.15	8.06	0.00	7.59	0.73	2.47	0.05		89.24
CG	155L2-2	9	35.59	1.69	25.77	0.22	13.44	0.00	6.91	0.91	2.37	0.06		86.95
CG	155L2-2	9	37.31	0.50	31.09	0.01	11.00	0.00	6.66	0.24	3.03	0.05		89.89
AARL	155L2-3	0	37.35	0.30	29.91	0.91	7.96	0.00	7.55	0.39	2.17	0.02	0.03	86.59
AARL	155L2-3	1	37.56	0.36	30.36	0.66	8.04	0.01	7.50	0.55	2.26	0.03	0.01	87.34
AARL	155L2-3	2	37.10	0.63	29.17	0.12	9.88	0.03	7.28	0.74	2.38	0.04	0.02	87.39
AARL	155L2-3	3	37.11	0.70	29.35	0.00	10.34	0.03	7.08	0.65	2.45	0.04	0.01	87.74
AARL	155L2-3	6	35.24	1.05	27.35	0.10	10.85	0.04	7.17	1.11	2.29	0.04	0.00	85.23
AARL	155L2-3	6	36.84	1.21	27.17	0.10	11.28	0.01	7.23	0.90	2.35	0.05	0.06	87.20
AARL	155L2-3	8	36.51	0.08	29.17	0.00	10.94	0.01	6.83	0.07	2.69	0.04	0.05	86.38
AARL	155L2-3	10	36.40	0.48	27.29	0.01	13.30	0.01	6.24	0.30	2.66	0.04	0.03	86.78
AARL	155L2-3	10	36.21	0.80	28.02	0.00	11.71	0.01	6.48	0.87	2.66	0.03	0.09	86.86
AARL	155L2-4	2	38.03	0.20	31.97	0.01	6.30	0.00	7.96	0.48	2.02	0.02	0.01	87.01
AARL	155L2-4	2	37.52	0.30	30.80	0.11	8.37	0.02	7.48	0.56	2.25	0.03	0.03	87.46
AARL	155L2-4	2	37.36	0.36	30.72	0.06	7.48	0.00	7.59	0.47	2.13	0.01	0.05	86.23
AARL	155L2-4	4	36.37	1.50	25.41	0.12	12.90	0.02	7.24	1.00	2.30	0.06	0.02	86.94
AARL	155L2-4	5	36.28	1.68	25.90	0.14	12.60	0.01	7.36	1.06	2.34	0.06	0.01	87.42
AARL	155L2-4	7	36.56	1.58	25.98	0.23	12.66	0.01	7.08	1.05	2.34	0.04	0.00	87.51
AARL	155L2-4	7	36.39	1.47	26.72	0.17	11.93	0.02	7.17	1.02	2.27	0.04	0.03	87.24
AARL	155L2-4	8	36.98	0.07	29.57	0.00	10.69	0.02	6.63	0.38	2.72	0.03	0.03	87.11
AARL	155L2-4	9	36.49	0.07	29.68	0.00	10.70	0.02	6.74	0.38	2.70	0.03	0.03	86.83
AARL	155L2-4	10	36.88	0.32	30.23	0.00	9.54	0.00	6.62	0.22	2.85	0.02	0.03	86.71
AARL	155L2-5	1	37.09	0.59	29.01	0.08	10.18	0.02	7.20	0.78	2.42	0.04	0.01	87.42
AARL	155L2-5	3	37.07	0.25	30.94	0.77	7.49	0.00	7.57	0.43	2.13	0.02	0.00	86.67
AARL	155L2-5	3	37.38	0.30	31.12	0.58	7.40	0.01	7.67	0.49	2.16	0.02	0.03	87.17
AARL	155L2-5	3	37.70	0.31	30.77	0.51	7.83	0.03	7.58	0.56	2.18	0.02	0.00	87.47
AARL	155L2-5	4	36.19	1.37	26.55	0.17	12.63	0.01	7.36	1.02	2.34	0.03	0.04	87.72
AARL	155L2-5	4	36.34	1.42	25.10	0.06	13.61	0.00	7.35	0.95	2.37	0.04	0.00	87.26
AARL	155L2-5	7	34.84	0.91	25.37	0.04	13.47	0.07	7.10	1.70	2.57	0.06	0.03	86.18
CG	203L2-1	1	37.42	0.38	31.16	0.02	6.68	0.03	9.12	0.70	2.23	0.02		87.76
CG	203L2-1	1	36.79	0.41	33.63	0.08	6.41	0.01	8.23	1.15	2.05	0.03		88.80
CG	203L2-1	9	36.30	2.04	26.65	0.00	11.18	0.02	8.45	1.60	2.01	0.07		88.33
CG	203L2-1	9	35.81	1.86	25.16	0.02	14.12	0.00	7.36	1.04	2.53	0.05		87.95
CG	203L2-2	1	37.24	0.22	34.98	0.00	5.41	0.01	8.07	0.95	2.20	0.03		89.10
CG	203L2-2	9	36.50	1.22	27.34	0.00	12.94	0.05	7.70	0.97	2.49	0.03		89.22
CG	219L2-1	1	36.76	0.34	30.98	0.04	6.94	0.00	9.00	0.51	2.21	0.03		86.81
CG	219L2-1	1	37.49	0.37	30.66	0.05	6.92	0.00	9.04	0.46	2.18	0.04		87.23
CG	219L2-1	9	35.92	1.12	27.07	0.00	13.79	0.01	6.72	1.01	2.36	0.01		88.02
CG	219L2-1	9	36.75	0.66	30.04	0.02	9.90	0.02	7.27	0.82	2.50	0.05		88.03

Digitised by the Department of Library Services in support of open access to information, University of Pretoria, 2021

Table V1 (contd) - Partial analyses of tourmaline - Page 4

Lab	Sample	Pos	SiO2	TiO2	Al2O3	Cr2O3	FeO	MnO	MgO	CaO	Na2O	K2O	F	Total
CG	219L2-2	1	37.11	0.44	29.85	0.12	10.97	0.03	7.31	0.34	2.67	0.04		88.89
CG	219L2-2	1	36.98	0.49	29.76	0.18	10.44	0.02	7.32	0.36	2.57	0.02		88.16
CG	219L2-2	9	36.55	0.87	28.58	0.02	12.00	0.00	7.13	0.88	2.50	0.04		88.58
CG	219L2-2	9	36.06	1.37	26.81	0.04	12.94	0.00	7.25	0.98	2.38	0.04		87.87
CG	246L2-1	1	36.48	0.47	26.84	0.02	13.15	0.00	7.34	0.30	2.84	0.06		87.50
CG	246L2-1	1	36.45	0.39	27.92	0.01	12.84	0.01	6.96	0.21	2.88	0.03		87.69
CG	246L2-1	9	36.24	1.95	26.14	0.04	13.44	0.02	7.02	0.59	2.81	0.08		88.34
CG	246L2-1	9	36.72	0.80	29.31	0.00	11.26	0.00	6.93	0.52	2.67	0.04		88.25
CG	265L2-1	1	36.67	1.15	29.81	0.32	9.46	0.01	7.73	1.23	2.07	0.05		88.52
CG	265L2-1	1	36.95	0.95	30.49	0.26	8.82	0.02	7.77	1.12	2.22	0.04		88.62
CG	265L2-1	9	37.52	0.17	33.03	0.00	7.51	0.00	7.54	0.34	2.78	0.03		88.91
CG	265L2-1	9	37.19	0.15	31.80	0.02	8.85	0.03	7.80	0.21	2.81	0.06		88.56
CG	265L2-2	1	37.56	0.07	32.50	0.03	9.14	0.01	6.59	0.11	2.85	0		88.86
CG	265L2-2	1	37.16	0.17	32.26	0.01	9.12	0.00	6.70	0.09	2.75	0.01		88.27
CG	265L2-2	9	37.58	0.66	32.58	0.01	8.81	0.00	6.76	0.28	2.92	0.04		89.64
CG	265L2-2	9	37.09	0.13	31.92	0.02	8.81	0.05	7.32	0.27	2.96	0.04		88.62
AARL	265L2-3	0	37.47	0.39	29.62	0.05	8.20	0.00	8.21	0.80	2.22	0.04	0.01	86.99
AARL	265L2-3	2	37.50	0.41	29.64	0.07	8.06	0.01	8.18	0.74	2.20	0.02	0.00	86.84
AARL	265L2-3	3	37.10	0.57	30.13	0.04	8.66	0.01	7.41	0.96	2.19	0.04	0.05	87.15
AARL	265L2-3	3	37.02	0.57	30.39	0.03	8.65	0.00	7.48	0.90	2.18	0.03	0.03	87.27
AARL	265L2-3	9	37.70	0.34	32.21	0.00	6.78	0.01	7.61	0.17	2.84	0.03	0.00	87.69
AARL	265L2-3	9	37.74	0.13	31.47	0.02	7.50	0.00	7.62	0.26	2.78	0.02	0.03	87.57
AARL	265L2-3	9	37.75	0.31	31.73	0.00	8.20	0.00	6.93	0.26	2.82	0.04	0.00	88.04
AARL	265L2-3	9	37.32	0.10	31.11	0.00	8.13	0.03	7.45	0.31	2.72	0.05	0.02	87.23
AARL	265L2-3	9	36.91	0.63	28.42	0.01	10.35	0.00	7.74	1.17	2.19	0.04	0.05	87.52
AARL	265L2-3	9	36.82	0.66	27.42	0.15	10.42	0.00	8.19	0.54	2.65	0.03	0.02	86.90
AARL	265L2-3	9	36.72	0.76	26.94	0.14	11.27	0.00	7.97	0.56	2.57	0.03	0.02	86.97
AARL	L105-1	1	35.98	0.28	29.76	0.01	15.76	0.01	3.06	0.68	2.22	0.03	0.23	88.01
AARL	L105-1	2	36.11	0.32	30.87	0.00	14.25	0.04	3.30	0.81	1.91	0.03	0.20	87.84
AARL	L105-1	3	36.43	0.57	30.93	0.01	13.40	0.03	3.72	0.82	1.93	0.03	0.21	88.08
AARL	L105-1	4	35.94	0.41	31.17	0.00	15.25	0.03	2.33	0.51	2.05	0.03	0.26	87.96
AARL	L105-1	5	35.67	0.33	30.82	0.01	14.60	0.02	3.18	0.58	2.17	0.03	0.19	87.59
AARL	L105-1	6	36.30	0.40	30.48	0.00	14.86	0.02	2.87	0.55	2.12	0.03	0.19	87.82
AARL	L105-1	7	35.84	0.46	31.00	0.02	14.64	0.00	3.01	0.50	2.14	0.02	0.20	87.83
AARL	L105-1	8	35.91	0.67	31.02	0.01	13.58	0.00	3.62	0.43	2.18	0.03	0.18	87.62
AARL	L105-1	9	35.26	0.58	31.30	0.03	14.02	0.02	2.94	0.44	2.01	0.02	0.20	86.82
AARL	L105-1	10	36.49	0.55	30.88	0.00	14.01	0.00	3.31	0.51	2.11	0.03	0.23	88.11
AARL	L105-1	11	35.90	0.58	29.94	0.02	17.08	0.03	2.04	0.68	2.03	0.03	0.18	88.50
AARL	L105-1	12	35.76	0.55	30.39	0.02	17.13	0.03	1.81	0.60	1.93	0.03	0.15	88.41
AARL	L105-1	13	35.55	0.43	32.57	0.00	14.23	0.05	2.01	0.33	1.83	0.01	0.19	87.21
AARL	L105-1	14	36.01	0.28	33.22	0.00	13.75	0.02	1.97	0.26	1.83	0.02	0.10	87.47
AARL	L105-1	15	36.15	0.15	34.19	0.01	13.70	0.03	1.68	0.22	1.79	0.02	0.09	88.05
AARL	L105-1	16	37.85	0.24	33.15	0.00	12.96	0.03	2.10	0.25	1.80	0.02	0.10	88.52
AARL	L105-1	17	36.10	0.43	30.93	0.00	16.16	0.01	1.90	0.42	2.03	0.03	0.13	88.14
AARL	L105-1	18	36.06	0.57	30.21	0.01	16.20	0.01	2.16	0.56	2.05	0.03	0.16	88.02
AARL	L105-1	19	36.02	0.41	31.46	0.00	13.78	0.04	3.07	0.30	2.10	0.03	0.15	87.36
AARL	L105-1	20	36.40	0.42	31.95	0.01	13.07	0.02	3.46	0.32	2.06	0.02	0.19	87.93
AARL	L105-1	21	36.63	0.22	31.12	0.00	14.77	0.03	2.72	0.36	2.10	0.05	0.17	88.16
AARL	L105-1	22	36.28	0.43	30.66	0.01	13.92	0.02	3.68	0.75	2.06	0.03	0.26	88.09
AARL	L105-1	23	49.20	0.21	24.82	0.02	12.62	0.04	2.34	0.51	1.63	0.04	0.16	91.58
AARL	L105-1	24	35.28	0.25	30.39	0.01	15.63	0.01	2.77	0.52	2.23	0.04	0.18	87.30

Digitised by the Department of Library Services in support of open access to information, University of Pretoria, 2021

Table VIa - Averaged partial analyses of Rooiberg tourmalines

Digitised by the Department of Library Services in support of open access to information, University of Pretoria, 2021

Table VIa - Averaged partial analyses of Rooiberg tourmaline

Tourmaline L1

Lab	Referenc	Pos	Sample	SiO2	TiO2	Al2O3	Cr2O3	FeO	MnO	MgO	CaO	Na2O	K2O	F	Total
CG	127L1-1	1	800	37.68	0.51	31.19	0.06	8.56	0.00	8.17	0.70	2.22	0.03		89.13
CG	127L1-1	4	801	37.47	0.52	32.86	0.02	8.01	0.00	7.55	0.87	2.20	0.04		89.53
CG	127L1-1	7	802	36.92	0.67	29.35	0.00	11.77	0.01	7.12	0.42	2.89	0.04		89.19
CG	127L1-1	9	803	36.96	0.48	30.64	0.01	10.16	0.00	7.25	0.43	2.99	0.04		88.97
CG	127L1-2	1	804	37.78	0.45	32.10	0.08	6.99	0.02	8.50	0.67	2.22	0.04		88.87
CG	127L1-2	6	805	36.99	0.88	31.43	0.04	9.27	0.01	7.01	1.20	2.02	0.04		88.88
CG	127L1-2	9	806	37.03	1.14	28.80	0.02	12.34	0.00	7.12	0.97	2.45	0.04		89.90
AARL	127L1-3	0	807	37.50	0.37	29.96	0.20	7.99	0.01	7.85	0.52	2.06	0.03	0.01	86.50
AARL	127L1-3	2	808	37.32	0.30	31.48	0.15	7.34	0.00	7.65	0.70	2.09	0.03	0.01	87.08
AARL	127L1-3	3	809	36.90	0.64	29.40	0.03	9.59	0.00	7.22	0.78	2.37	0.03	0.02	87.00
AARL	127L1-3	6	810	36.45	0.86	27.88	0.05	11.44	0.00	6.96	0.82	2.37	0.04	0.02	86.89
AARL	127L1-4	0	811	37.46	0.49	29.70	0.08	8.41	0.01	8.14	0.65	2.27	0.02	0.00	87.23
AARL	127L1-4	1	812	37.19	0.44	30.16	0.05	7.82	0.00	8.19	0.70	2.23	0.02	0.01	86.80
AARL	127L1-4	3	813	37.24	0.29	32.13	0.16	6.79	0.01	7.53	0.78	2.05	0.02	0.01	87.01
AARL	127L1-4	4	814	37.13	0.53	30.98	0.10	8.28	0.00	7.25	0.84	2.24	0.03	0.03	87.42
AARL	127L1-4	7	815	36.39	0.89	27.55	0.01	12.28	0.00	6.86	0.58	2.59	0.04	0.03	87.23
CG	205L1-1	1	816	37.06	0.23	29.82	0.00	10.29	0.00	7.10	0.23	2.86	0.03	0.00	87.63
CG	205L1-1	9	817	36.45	1.10	28.66	0.00	12.63	0.01	6.21	0.63	2.82	0.06	0.00	88.58
CG	205L1-2	1	818	37.18	0.50	30.43	0.03	10.22	0.01	7.57	0.76	2.57	0.04		89.33
CG	205L1-2	6	819	35.92	1.22	24.38	0.02	16.53	0.00	6.77	0.80	2.69	0.06		88.40
CG	205L1-2	9	820	35.87	0.46	28.42	0.00	14.29	0.01	6.19	0.40	2.93	0.04		88.62
CG	124L1-1	1	821	37.06	0.34	31.86	0.02	8.90	0.00	7.36	0.65	2.24	0.03		88.47
CG	124L1-1	4	822	37.23	0.43	32.19	0.08	8.49	0.00	7.49	0.75	2.52	0.02		89.21
CG	124L1-1	7	823	36.56	0.62	29.34	0.01	12.72	0.03	7.05	0.44	2.86	0.04		89.68
CG	124L1-1	9	824	36.96	0.27	31.65	0.00	9.53	0.01	7.24	0.16	3.06	0.07		88.95
CG	124L1-2	1	825	37.11	0.34	31.90	0.01	8.93	0.00	7.35	0.52	2.03	0.03		88.23
CG	124L1-2	6	826	36.08	1.83	26.99	0.01	13.63	0.00	7.06	1.15	2.34	0.04		89.13
CG	124L1-2	9	827	36.74	0.26	30.62	0.00	11.25	0.02	6.77	0.38	2.82	0.04		88.91
AARL	124L1-3	0	828	37.56	0.28	31.63	0.19	6.85	0.01	7.81	0.59	1.96	0.03	0.01	86.92
AARL	124L1-3	2	829	37.14	0.30	32.28	0.14	6.55	0.01	7.68	0.72	1.98	0.03	0.01	86.84
AARL	124L1-3	4	830	36.65	0.75	29.65	0.19	9.21	0.01	7.39	0.88	2.15	0.03	0.02	86.93
AARL	124L1-3	7	831	36.40	1.04	27.82	0.06	11.16	0.00	7.27	0.89	2.30	0.04	0.03	87.01
AARL	124L1-4	0	832	36.49	0.32	29.84	0.07	9.58	0.00	7.25	0.57	2.07	0.04	0.02	86.23
AARL	124L1-4	2	833	36.88	0.35	29.85	0.07	10.25	0.00	7.07	0.49	2.12	0.03	0.00	87.11
AARL	124L1-4	3	834	36.22	0.96	26.62	0.01	12.50	0.00	7.21	0.80	2.43	0.03	0.03	86.80
AARL	124L1-4	4	835	36.60	0.42	28.49	0.00	11.03	0.00	7.24	0.72	2.49	0.04	0.00	87.03
AARL	124L1-4	7	836	36.43	0.56	27.26	0.00	12.32	0.01	6.42	0.33	2.60	0.04	0.02	86.00
CG	227L1-1	1	837	37.33	0.36	31.37	0.03	7.93	0.00	7.87	0.37	2.58	0.03		87.87
CG	227L1-2	1	838	36.80	0.62	29.90	0.01	9.85	0.01	7.53	0.53	2.52	0.03	0.00	87.81
CG	227L1-2	9	839	36.57	0.92	27.84	0.00	12.14	0.02	7.26	0.94	2.54	0.05	0.00	88.29
AARL	227L1-3	0	840	37.08	0.34	29.41	0.01	9.44	0.00	7.40	0.34	2.46	0.03	0.01	86.53
AARL	227L1-3	1	841	36.96	0.38	29.51	0.00	9.25	0.00	7.43	0.35	2.41	0.03	0.01	86.33
AARL	227L1-3	2	842	37.30	0.33	29.63	0.01	9.18	0.00	7.53	0.38	2.43	0.03	0.01	86.83
AARL	227L1-3	6	843	36.54	0.75	27.43	0.01	11.78	0.01	7.16	0.90	2.38	0.05	0.04	87.02
AARL	227L1-4	0	844	37.32	0.31	31.35	0.02	7.20	0.03	7.70	0.74	2.23	0.04	0.02	86.95
AARL	227L1-4	2	845	35.88	0.84	27.88	0.01	11.27	0.01	7.26	0.86	2.37	0.05	0.00	86.41
AARL	227L1-4	3	846	36.40	1.05	26.68	0.02	12.39	0.01	7.16	0.98	2.34	0.05	0.03	87.10
AARL	227L1-4	6	847	36.28	1.10	26.35	0.01	12.73	0.01	7.18	0.94	2.32	0.05	0.04	87.01
AARL	227L1-4	9	848	36.64	0.40	27.89	0.01	11.61	0.00	7.09	0.78	2.40	0.05	0.03	86.89
CG	244L1-1	1	849	35.19	0.26	34.59	0.03	4.80	0.00	7.14	0.96	1.86	0.03	0.00	84.85
CG	244L1-1	9	850	36.44	1.36	26.86	0.01	13.30	0.01	7.40	1.15	2.44	0.05	0.00	89.02

Digitised by the Department of Library Services in support of open access to information, University of Pretoria, 2021

Table VIa (contd) - Averaged partial analyses of Rooiberg tourmaline
Tourmaline L2

Lab	Referenc	Pos	Sample	SiO2	TiO2	Al2O3	Cr2O3	FeO	MnO	MgO	CaO	Na2O	K2O	F	Total
CG	155L2-1	1	851	37.55	0.28	31.94	0.94	7.83	0.00	7.61	0.39	2.31	0.01	0.00	88.87
CG	155L2-1	9	852	36.63	0.58	28.97	0.00	12.19	0.02	6.88	0.20	2.79	0.07	0.00	88.32
CG	155L2-2	1	853	37.05	0.39	32.04	0.09	7.89	0.00	7.50	0.53	2.41	0.05	0.00	87.95
CG	155L2-2	9	854	36.45	1.10	28.43	0.11	12.22	0.00	6.78	0.57	2.70	0.06	0.00	88.42
AARL	155L2-3	0	855	37.35	0.30	29.91	0.91	7.96	0.00	7.55	0.39	2.17	0.02	0.03	86.59
AARL	155L2-3	1	856	37.56	0.36	30.36	0.66	8.04	0.01	7.50	0.55	2.26	0.03	0.01	87.34
AARL	155L2-3	2	857	37.10	0.63	29.17	0.12	9.88	0.03	7.28	0.74	2.38	0.04	0.02	87.39
AARL	155L2-3	3	858	37.11	0.70	29.35	0.00	10.34	0.03	7.08	0.65	2.45	0.04	0.01	87.74
AARL	155L2-3	6	859	36.04	1.13	27.26	0.10	11.07	0.02	7.20	1.00	2.32	0.05	0.03	86.21
AARL	155L2-3	8	860	36.51	0.08	29.17	0.00	10.94	0.01	6.83	0.07	2.69	0.04	0.05	86.38
AARL	155L2-3	10	861	36.30	0.64	27.66	0.01	12.50	0.01	6.36	0.58	2.66	0.03	0.06	86.82
AARL	155L2-4	2	862	37.63	0.29	31.16	0.06	7.38	0.01	7.68	0.50	2.13	0.02	0.03	86.90
AARL	155L2-4	4	863	36.37	1.50	25.41	0.12	12.90	0.02	7.24	1.00	2.30	0.06	0.02	86.94
AARL	155L2-4	5	864	36.28	1.68	25.90	0.14	12.60	0.01	7.36	1.06	2.34	0.06	0.01	87.42
AARL	155L2-4	7	865	36.56	1.58	25.98	0.23	12.66	0.01	7.08	1.05	2.34	0.04	0.00	87.51
AARL	155L2-4	7	866	36.39	1.47	26.72	0.17	11.93	0.02	7.17	1.02	2.27	0.04	0.03	87.24
AARL	155L2-4	8	867	36.98	0.07	29.57	0.00	10.69	0.02	6.63	0.38	2.72	0.03	0.03	87.11
AARL	155L2-4	9	868	36.49	0.07	29.68	0.00	10.70	0.02	6.74	0.38	2.70	0.03	0.03	86.83
AARL	155L2-4	10	869	36.88	0.32	30.23	0.00	9.54	0.00	6.62	0.22	2.85	0.02	0.03	86.71
AARL	155L2-5	1	870	37.09	0.59	29.01	0.08	10.18	0.02	7.20	0.78	2.42	0.04	0.01	87.42
AARL	155L2-5	3	871	37.38	0.29	30.94	0.62	7.58	0.01	7.60	0.49	2.15	0.02	0.01	87.10
AARL	155L2-5	4	872	36.27	1.39	25.83	0.12	13.12	0.00	7.35	0.99	2.36	0.04	0.02	87.49
AARL	155L2-5	7	873	34.84	0.91	25.37	0.04	13.47	0.07	7.10	1.70	2.57	0.06	0.03	86.18
CG	203L2-1	1	874	37.10	0.40	32.40	0.05	6.54	0.02	8.68	0.93	2.14	0.03	0.00	88.28
CG	203L2-1	9	875	36.05	1.95	25.90	0.01	12.65	0.01	7.90	1.32	2.27	0.06	0.00	88.14
CG	203L2-2	1	876	37.24	0.22	34.98	0.00	5.41	0.01	8.07	0.95	2.20	0.03		89.10
CG	203L2-2	9	877	36.50	1.22	27.34	0.00	12.94	0.05	7.70	0.97	2.49	0.03		89.22
CG	219L2-1	1	878	37.13	0.36	30.82	0.05	6.93	0.00	9.02	0.49	2.19	0.03	0.00	87.02
CG	219L2-1	9	879	36.33	0.89	28.56	0.01	11.85	0.02	6.99	0.92	2.43	0.03	0.00	88.02
CG	219L2-2	1	880	37.05	0.47	29.81	0.15	10.71	0.02	7.31	0.35	2.62	0.03	0.00	88.52
CG	219L2-2	9	881	36.30	1.12	27.70	0.03	12.47	0.00	7.19	0.93	2.44	0.04	0.00	88.22
CG	246L2-1	1	882	36.46	0.43	27.38	0.01	12.99	0.00	7.15	0.25	2.86	0.04	0.00	87.60
CG	246L2-1	9	883	36.48	1.38	27.72	0.02	12.35	0.01	6.97	0.56	2.74	0.06	0.00	88.29
CG	265L2-1	1	884	36.81	1.05	30.15	0.29	9.14	0.01	7.75	1.18	2.15	0.04	0.00	88.57
CG	265L2-1	9	885	37.35	0.16	32.42	0.01	8.18	0.02	7.67	0.27	2.80	0.04	0.00	88.74
CG	265L2-2	1	886	37.36	0.12	32.38	0.02	9.13	0.01	6.64	0.10	2.80	0.01	0.00	88.56
CG	265L2-2	9	887	37.34	0.40	32.25	0.02	8.81	0.02	7.04	0.28	2.94	0.04	0.00	89.13
AARL	265L2-3	0	888	37.47	0.39	29.62	0.05	8.20	0.00	8.21	0.80	2.22	0.04	0.01	86.99
AARL	265L2-3	2	889	37.50	0.41	29.64	0.07	8.06	0.01	8.18	0.74	2.20	0.02	0.00	86.84
AARL	265L2-3	3	890	37.06	0.57	30.26	0.03	8.66	0.00	7.45	0.93	2.18	0.03	0.04	87.21
AARL	265L2-3	9	891	37.28	0.42	29.90	0.05	8.95	0.01	7.64	0.47	2.65	0.03	0.02	87.42

Digitised by the Department of Library Services in support of open access to information, University of Pretoria, 2021

Table VIb - Atomic proportions and site allocations of Rooiberg tourmalines

Digitised by the Department of Library Services in support of open access to information, University of Pretoria, 2021

Table VIb - Atomic proportions and site allocations of Rooiberg tourmalines

Header data						Atomic proportions and site allocations															
						Si-site		Z-site					Y-site		X-site			Totals			
Sample	Ref	Pos	Rel Pos	Oxy	B	Si	Al(t)	Al(z)	Mg(z)	Al(y)	Ti	Cr	Fe(2)	Mg(y)	Ca	Na	K	X Tot	Y Tot	Z Tot	Si Tot
127L1-1	800	1	Core	29	3	6.01	0.00	5.87	0.14	0.00	0.06	0.01	1.14	1.80	0.12	0.69	0.01	0.81	3.02	6.00	6.01
127L1-1	801	4	Mantle	29	3	5.93	0.07	6.00	0.00	0.06	0.06	0.00	1.06	1.78	0.15	0.68	0.01	0.83	2.96	6.00	6.00
127L1-1	802	7	Mantle	29	3	6.01	0.00	5.63	0.37	0.00	0.08	0.00	1.60	1.36	0.07	0.91	0.01	1.00	3.05	6.00	6.01
127L1-1	803	9	Overgrowth	29	3	5.98	0.02	5.82	0.18	0.00	0.06	0.00	1.37	1.56	0.08	0.94	0.01	1.02	3.00	6.00	6.00
127L1-2	804	1	Core	29	3	5.99	0.01	5.99	0.01	0.00	0.05	0.01	0.93	2.00	0.11	0.68	0.01	0.81	2.99	6.00	6.00
127L1-2	805	6	Mantle	29	3	5.95	0.05	5.91	0.09	0.00	0.11	0.00	1.25	1.59	0.21	0.63	0.01	0.85	2.94	6.00	6.00
127L1-2	806	9	Overgrowth	29	3	6.01	0.00	5.51	0.49	0.00	0.14	0.00	1.67	1.23	0.17	0.77	0.01	0.95	3.04	6.00	6.01
127L1-3	807	0	Core	29	3	6.14	0.00	5.78	0.22	0.00	0.05	0.03	1.09	1.69	0.09	0.66	0.01	0.75	2.86	6.00	6.14
127L1-3	808	2	Core	29	3	6.04	0.00	6.00	0.00	0.01	0.04	0.02	0.99	1.85	0.12	0.66	0.01	0.79	2.91	6.00	6.04
127L1-3	809	3	Mantle	29	3	6.08	0.00	5.71	0.29	0.00	0.08	0.00	1.32	1.48	0.14	0.76	0.01	0.90	2.88	6.00	6.08
127L1-3	810	6	Mantle	29	3	6.09	0.00	5.49	0.51	0.00	0.11	0.01	1.60	1.22	0.15	0.77	0.01	0.92	2.93	6.00	6.09
127L1-4	811	0	Core	29	3	6.11	0.00	5.71	0.29	0.00	0.06	0.01	1.15	1.68	0.11	0.72	0.00	0.83	2.90	6.00	6.11
127L1-4	812	1	Core	29	3	6.07	0.00	5.80	0.20	0.00	0.05	0.01	1.07	1.80	0.12	0.71	0.00	0.83	2.92	6.00	6.07
127L1-4	813	3	Mantle	29	3	6.02	0.00	6.00	0.00	0.12	0.04	0.02	0.92	1.81	0.14	0.64	0.00	0.78	2.91	6.00	6.02
127L1-4	814	4	Mantle	29	3	6.03	0.00	5.93	0.07	0.00	0.07	0.01	1.13	1.69	0.15	0.71	0.01	0.86	2.89	6.00	6.03
127L1-4	815	7	Mantle	29	3	6.09	0.00	5.43	0.57	0.00	0.11	0.00	1.72	1.14	0.10	0.84	0.01	0.95	2.97	6.00	6.09
205L1-1	816	1	Core	29	3	6.08	0.00	5.76	0.24	0.00	0.03	0.00	1.41	1.50	0.04	0.91	0.01	0.96	2.94	6.00	6.08
205L1-1	817	9	Overgrowth	29	3	6.01	0.00	5.57	0.43	0.00	0.14	0.00	1.74	1.10	0.11	0.90	0.01	1.03	2.98	6.00	6.01
205L1-2	818	1	Core	29	3	5.99	0.01	5.77	0.23	0.00	0.06	0.00	1.38	1.58	0.13	0.80	0.01	0.94	3.02	6.00	6.00
205L1-2	819	6	Mantle	29	3	6.10	0.00	4.88	1.12	0.00	0.16	0.00	2.35	0.60	0.15	0.89	0.01	1.05	3.10	6.00	6.10
205L1-2	820	9	Overgrowth	29	3	5.97	0.03	5.55	0.45	0.00	0.06	0.00	1.99	1.09	0.07	0.95	0.01	1.03	3.13	6.00	6.00
124L1-1	821	1	Core	29	3	5.96	0.04	6.00	0.00	0.01	0.04	0.00	1.20	1.77	0.11	0.70	0.01	0.82	3.01	6.00	6.00
124L1-1	822	4	Mantle	29	3	5.94	0.06	5.99	0.01	0.00	0.05	0.01	1.13	1.77	0.13	0.78	0.00	0.91	2.96	6.00	6.00
124L1-1	823	7	Mantle	29	3	5.96	0.04	5.59	0.41	0.00	0.08	0.00	1.73	1.30	0.08	0.91	0.01	0.99	3.11	6.00	6.00
124L1-1	824	9	Overgrowth	29	3	5.95	0.05	5.95	0.05	0.00	0.03	0.00	1.28	1.69	0.03	0.96	0.01	1.00	3.00	6.00	6.00
124L1-2	825	1	Core	29	3	5.98	0.02	6.00	0.00	0.03	0.04	0.00	1.20	1.76	0.09	0.64	0.01	0.73	3.04	6.00	6.00
124L1-2	826	6	Mantle	29	3	5.97	0.03	5.23	0.77	0.00	0.23	0.00	1.89	0.97	0.20	0.75	0.01	0.96	3.09	6.00	6.00
124L1-2	827	9	Overgrowth	29	3	5.97	0.03	5.84	0.16	0.00	0.03	0.00	1.53	1.48	0.07	0.89	0.01	0.97	3.04	6.00	6.00
124L1-3	828	0	Core	29	3	6.07	0.00	6.00	0.00	0.03	0.03	0.02	0.93	1.88	0.10	0.62	0.01	0.72	2.89	6.00	6.07
124L1-3	829	2	Core	29	3	6.00	0.00	6.00	0.00	0.15	0.04	0.02	0.89	1.85	0.13	0.62	0.01	0.75	2.94	6.00	6.00
124L1-3	830	4	Mantle	29	3	6.03	0.00	5.75	0.25	0.00	0.09	0.03	1.27	1.57	0.16	0.69	0.01	0.85	2.95	6.00	6.03
124L1-3	831	7	Mantle	29	3	6.07	0.00	5.47	0.53	0.00	0.13	0.01	1.56	1.27	0.16	0.74	0.01	0.91	2.96	6.00	6.07
124L1-4	832	0	Core	29	3	6.05	0.00	5.83	0.17	0.00	0.04	0.01	1.33	1.62	0.10	0.67	0.01	0.78	3.00	6.00	6.05

Digitised by the Department of Library Services in support of open access to information, University of Pretoria, 2021

Table VIb (contd.) - Atomic proportions and site allocations of Rooiberg tourmalines

Header data				Atomic proportions and site allocations																	
						Si-site		Z-site					Y-site		X-site			Totals			
Sample	Ref	Pos	Rel Pos	Oxy	B	Si	Al(t)	Al(z)	Mg(z)	Al(y)	Ti	Cr	Fe(2)	Mg(y)	Ca	Na	K	X Tot	Y Tot	Z Tot	Si Tot
124L1-4	833	2	Core	29	3	6.07	0.00	5.79	0.21	0.00	0.04	0.01	1.41	1.53	0.09	0.68	0.01	0.77	2.99	6.00	6.07
124L1-4	834	3	Mantle	29	3	6.10	0.00	5.29	0.71	0.00	0.12	0.00	1.76	1.10	0.14	0.80	0.01	0.95	2.98	6.00	6.10
124L1-4	835	4	Mantle	29	3	6.08	0.00	5.58	0.42	0.00	0.05	0.00	1.53	1.37	0.13	0.80	0.01	0.94	2.96	6.00	6.08
124L1-4	836	7	Mantle	29	3	6.17	0.00	5.44	0.56	0.00	0.07	0.00	1.75	1.06	0.06	0.86	0.01	0.92	2.88	6.00	6.17
227L1-1	837	1	Core	29	3	6.02	0.00	5.96	0.04	0.00	0.04	0.00	1.07	1.85	0.06	0.81	0.01	0.88	2.97	6.00	6.02
227L1-2	838	1	Core	29	3	6.02	0.00	5.76	0.24	0.00	0.08	0.00	1.35	1.59	0.09	0.80	0.01	0.90	3.02	6.00	6.02
227L1-2	839	9	Overgrowth	29	3	6.04	0.00	5.43	0.58	0.00	0.11	0.00	1.68	1.21	0.17	0.82	0.01	0.99	3.00	6.00	6.04
227L1-3	840	0	Core	29	3	6.12	0.00	5.73	0.28	0.00	0.04	0.00	1.30	1.55	0.06	0.79	0.01	0.86	2.89	6.00	6.12
227L1-3	841	1	Core	29	3	6.11	0.00	5.75	0.25	0.00	0.05	0.00	1.28	1.58	0.06	0.77	0.01	0.84	2.91	6.00	6.11
227L1-3	842	2	Core	29	3	6.13	0.00	5.74	0.26	0.00	0.04	0.00	1.26	1.58	0.07	0.78	0.01	0.85	2.88	6.00	6.13
227L1-3	843	6	Mantle	29	3	6.11	0.00	5.41	0.59	0.00	0.09	0.00	1.65	1.19	0.16	0.77	0.01	0.95	2.93	6.00	6.11
227L1-4	844	0	Core	29	3	6.05	0.00	6.00	0.01	0.00	0.04	0.00	0.98	1.86	0.13	0.70	0.01	0.84	2.87	6.00	6.05
227L1-4	845	2	Core	29	3	6.03	0.00	5.52	0.48	0.00	0.11	0.00	1.58	1.34	0.16	0.77	0.01	0.94	3.03	6.00	6.03
227L1-4	846	3	Mantle	29	3	6.11	0.00	5.28	0.72	0.00	0.13	0.00	1.74	1.07	0.18	0.76	0.01	0.95	2.94	6.00	6.11
227L1-4	847	6	Mantle	29	3	6.11	0.00	5.23	0.77	0.00	0.14	0.00	1.79	1.03	0.17	0.76	0.01	0.94	2.97	6.00	6.11
227L1-4	848	9	Overgrowth	29	3	6.12	0.00	5.49	0.51	0.00	0.05	0.00	1.62	1.26	0.14	0.78	0.01	0.93	2.93	6.00	6.12
244L1-1	849	1	Core	29	3	5.77	0.23	6.00	0.00	0.45	0.03	0.00	0.66	1.74	0.17	0.59	0.01	0.77	2.89	6.00	6.00
244L1-1	850	9	Overgrowth	29	3	6.02	0.00	5.24	0.77	0.00	0.17	0.00	1.84	1.06	0.20	0.78	0.01	1.00	3.07	6.00	6.02
155L2-1	851	1	Core	29	3	5.99	0.01	5.99	0.01	0.00	0.03	0.12	1.04	1.80	0.07	0.72	0.00	0.78	2.99	6.00	6.00
155L2-1	852	9	Overgrowth	29	3	6.03	0.00	5.62	0.38	0.00	0.07	0.00	1.68	1.31	0.04	0.89	0.02	0.94	3.06	6.00	6.03
155L2-2	853	1	Core	29	3	5.97	0.04	6.00	0.00	0.05	0.05	0.01	1.06	1.80	0.09	0.75	0.01	0.86	2.97	6.00	6.00
155L2-2	854	9	Overgrowth	29	3	6.01	0.00	5.53	0.47	0.00	0.14	0.01	1.69	1.19	0.10	0.87	0.01	0.98	3.03	6.00	6.01
155L2-3	855	0	Core	29	3	6.12	0.00	5.78	0.22	0.00	0.04	0.12	1.09	1.62	0.07	0.69	0.00	0.76	2.87	6.00	6.12
155L2-3	856	1	Core	29	3	6.10	0.00	5.81	0.19	0.00	0.04	0.09	1.09	1.63	0.10	0.71	0.01	0.82	2.85	6.00	6.10
155L2-3	857	2	Core	29	3	6.10	0.00	5.65	0.35	0.00	0.08	0.02	1.36	1.43	0.13	0.76	0.01	0.90	2.88	6.00	6.10
155L2-3	858	3	Mantle	29	3	6.08	0.00	5.67	0.33	0.00	0.09	0.00	1.42	1.40	0.11	0.78	0.01	0.90	2.90	6.00	6.08
155L2-3	859	6	Mantle	29	3	6.07	0.00	5.41	0.59	0.00	0.14	0.01	1.56	1.22	0.18	0.76	0.01	0.95	2.93	6.00	6.07
155L2-3	860	8	Overgrowth	29	3	6.10	0.00	5.74	0.26	0.00	0.01	0.00	1.53	1.44	0.01	0.87	0.01	0.89	2.98	6.00	6.10
155L2-3	861	10	Overgrowth	29	3	6.11	0.00	5.49	0.51	0.00	0.08	0.00	1.76	1.08	0.11	0.87	0.01	0.98	2.92	6.00	6.11

Digitised by the Department of Library Services in support of open access to information, University of Pretoria, 2021

Table VIb (contd.) - Atomic proportions and site allocations of Rooiberg tourmalines

Header data						Atomic proportions and site allocations															
						Si-site		Z-site					Y-site		X-site			Totals			
Sample	Ref	Pos	Rel Pos	Oxy	B	Si	Al(t)	Al(z)	Mg(z)	Al(y)	Ti	Cr	Fe(2)	Mg(y)	Ca	Na	K	X Tot	Y Tot	Z Tot	Si Tot
155L2-4	862	2	Core	29	3	6.10	0.00	5.96	0.04	0.00	0.04	0.01	1.00	1.81	0.09	0.67	0.00	0.76	2.86	6.00	6.10
155L2-4	863	4	Mantle	29	3	6.15	0.00	5.06	0.94	0.00	0.19	0.02	1.82	0.88	0.18	0.76	0.01	0.95	2.91	6.00	6.15
155L2-4	864	5	Mantle	29	3	6.09	0.00	5.12	0.88	0.00	0.21	0.02	1.77	0.96	0.19	0.76	0.01	0.97	2.96	6.00	6.09
155L2-4	865	7	Mantle	29	3	6.12	0.00	5.13	0.87	0.00	0.20	0.03	1.77	0.90	0.19	0.76	0.01	0.96	2.90	6.00	6.12
155L2-4	866	7	Mantle	29	3	6.09	0.00	5.27	0.73	0.00	0.19	0.02	1.67	1.06	0.18	0.74	0.01	0.93	2.94	6.00	6.09
155L2-4	867	8	Overgrowth	29	3	6.11	0.00	5.76	0.24	0.00	0.01	0.00	1.48	1.39	0.07	0.87	0.01	0.95	2.88	6.00	6.11
155L2-4	868	9	Overgrowth	29	3	6.06	0.00	5.81	0.19	0.00	0.01	0.00	1.49	1.47	0.07	0.87	0.01	0.94	2.97	6.00	6.06
155L2-4	869	10	Overgrowth	29	3	6.08	0.00	5.88	0.12	0.00	0.04	0.00	1.32	1.50	0.04	0.91	0.00	0.95	2.86	6.00	6.08
155L2-5	870	1	Core	29	3	6.10	0.00	5.63	0.37	0.00	0.07	0.01	1.40	1.39	0.14	0.77	0.01	0.92	2.88	6.00	6.10
155L2-5	871	3	Mantle	29	3	6.07	0.00	5.92	0.08	0.00	0.04	0.08	1.03	1.76	0.09	0.68	0.00	0.76	2.90	6.00	6.07
155L2-5	872	4	Mantle	29	3	6.10	0.00	5.12	0.88	0.00	0.18	0.02	1.84	0.96	0.18	0.77	0.01	0.96	3.00	6.00	6.10
155L2-5	873	7	Mantle	29	3	6.00	0.00	5.15	0.85	0.00	0.12	0.00	1.94	0.98	0.31	0.86	0.01	1.19	3.04	6.00	6.00
203L2-1	874	1	Core	29	3	5.92	0.09	6.00	0.00	0.01	0.05	0.01	0.87	2.06	0.16	0.66	0.01	0.83	3.00	6.00	6.00
203L2-1	875	9	Overgrowth	29	3	6.02	0.00	5.09	0.91	0.00	0.25	0.00	1.77	1.06	0.24	0.74	0.01	0.98	3.07	6.00	6.02
203L2-2	876	1	Core	29	3	5.83	0.17	6.00	0.00	0.29	0.03	0.00	0.71	1.88	0.16	0.67	0.01	0.84	2.91	6.00	6.00
203L2-2	877	9	Overgrowth	29	3	6.00	0.00	5.30	0.70	0.00	0.15	0.00	1.78	1.19	0.17	0.80	0.01	0.97	3.12	6.00	6.00
219L2-1	878	1	Core	29	3	6.01	0.00	5.89	0.12	0.00	0.04	0.01	0.94	2.06	0.09	0.69	0.01	0.78	3.05	6.00	6.01
219L2-1	879	9	Overgrowth	29	3	6.01	0.00	5.57	0.43	0.00	0.11	0.00	1.64	1.29	0.16	0.78	0.01	0.95	3.04	6.00	6.01
219L2-2	880	1	Core	29	3	6.03	0.00	5.72	0.28	0.00	0.06	0.02	1.46	1.49	0.06	0.83	0.01	0.90	3.03	6.00	6.03
219L2-2	881	9	Overgrowth	29	3	6.02	0.00	5.41	0.59	0.00	0.14	0.00	1.73	1.19	0.17	0.79	0.01	0.96	3.06	6.00	6.02
246L2-1	882	1	Core	29	3	6.09	0.00	5.40	0.61	0.00	0.05	0.00	1.82	1.18	0.05	0.93	0.01	0.98	3.05	6.00	6.09
246L2-1	883	9	Overgrowth	29	3	6.04	0.00	5.41	0.59	0.00	0.17	0.00	1.71	1.13	0.10	0.88	0.01	0.99	3.01	6.00	6.04
265L2-1	884	1	Core	29	3	5.96	0.05	5.71	0.29	0.00	0.13	0.04	1.24	1.57	0.21	0.68	0.01	0.89	2.98	6.00	6.00
265L2-1	885	9	Overgrowth	29	3	5.96	0.04	6.00	0.00	0.06	0.02	0.00	1.09	1.82	0.05	0.87	0.01	0.92	2.99	6.00	6.00
265L2-2	886	1	Core	29	3	6.00	0.00	6.00	0.00	0.13	0.01	0.00	1.23	1.59	0.02	0.87	0.00	0.89	2.96	6.00	6.00
265L2-2	887	9	Overgrowth	29	3	5.97	0.03	6.00	0.00	0.04	0.05	0.00	1.18	1.68	0.05	0.91	0.01	0.97	2.94	6.00	6.00
265L2-3	888	0	Core	29	3	6.12	0.00	5.70	0.30	0.00	0.05	0.01	1.12	1.70	0.14	0.70	0.01	0.85	2.87	6.00	6.12
265L2-3	889	2	Core	29	3	6.13	0.00	5.71	0.29	0.00	0.05	0.01	1.10	1.70	0.13	0.70	0.00	0.83	2.86	6.00	6.13
265L2-3	890	3	Mantle	29	3	6.05	0.00	5.83	0.17	0.00	0.07	0.00	1.18	1.64	0.16	0.69	0.01	0.86	2.89	6.00	6.05
265L2-3	891	9	Overgrowth	29	3	6.09	0.00	5.75	0.25	0.00	0.05	0.01	1.22	1.61	0.08	0.84	0.01	0.93	2.89	6.00	6.09

Digitised by the Department of Library Services in support of open access to information, University of Pretoria, 2021

Table VII - Trace element content of cassiterite

Samples nnnL0, nnnL7 and nnnL8 are from Rooiberg.
Other samples are from:
L101-L103: Zaaiplaats
L104: Mutue-fides
L105: Erongo pegmatite, Namibia
L106: Pegmatite, Mmbabane, Swaziland
L108: Pegmatite, Omaruru, Namibia

Digitised by the Department of Library Services in support of open access to information, University of Pretoria, 2021

Table VII - Trace element content of cassiterite as determined by INAA

Lab No	Sample	Suspected tin phase*	Locality**	Fe %	Ca ppm	Na ppm	La ppm	Sm ppm	Eu ppm	Lu ppm	Co ppm	Gd ppm	Hf ppm	Sb ppm	Sc ppm	Ta ppm	Th ppm	U ppm	Zr ppm
R2	193L8	1	A-Q22-580	0.4	589	114	0.4	-	-	-	2.0	6	2	3	6	3	6	-	65
R6	216L8	1	A-M18-780	0.8	673	333	1.8	1.2	-	0.3	11.7	-	13	7	-	6	-	14	-
R13	152L8	1	A-Q22-565	0.3	806	134	-	-	0.2	-	2.0	-	6	3	11	4	9	-	166
R15	117L8	1	A-Q22-565	1.2	685	455	0.3	0.7	-	0.4	58.2	-	2	10	9	2	3	11	165
R21	436L8	1	A-Magazine-580	1.0	784	356	0.5	-	0.2	-	123.0	-	2	9	12	1	4	-	183
R22	221L8	1	A-M18-780	0.6	122	210	3.0	1.22	-	0.4	3.1	-	-	0.8	-	4	1	16	-
R9	251L7	2	A-JewelBox-680	0.4	682	1379	-	-	-	-	8.2	13	1	4	9	2	2	-	-
R10	447L0	2	A-19N-640	1.0	769	299	-	-	-	-	27.8	65	1	11	7	-	2	1	-
R16	272L7	2	A-U30-780	0.8	780	1075	0.7	0.54	0.2	-	51.8	-	2	0.4	8	4	2	14	-
R17	249L7	2	A-JewelBox-680	0.7	-	2697	-	-	-	-	-	-	438	-	9	-	-	-	-
R18	445L7	2	A-19N-640	0.9	697	247	0.5	-	-	-	13.2	35	1	8	26	1	-	-	-
R19	247L7	2	A-JewelBox-680	0.5	713	1038	-	-	0.5	-	2.1	-	4	5	7	471	2	-	-
R20	226L7	2	A-JewelBox-680	1.1	677	1484	1.8	-	0.2	-	8.6	12	1	6	18	4	1	-	-
R30	440L7	2	A-19N-640	2.1	-	-	-	-	-	-	241.0	-	-	-	7	-	-	-	-
R31	214L7	2	A-19N-640	1.0	-	1336	-	0.82	-	-	77.9	-	3	-	9	5	-	12	-
R7	293L0	-	NAD-C-1480	0.8	437	169	-	-	0.2	-	0.6	-	1	6	44	5	-	-	-
R1	363L0	-	C-Gap-1740	0.5	592	174	2.0	2.03	-	1.2	2.9	-	3	5	181	4	4	45	780
R8	419L0	-	C-A Upper-1870	1.1	804	322	-	-	-	-	2.5	-	-	8	141	24	-	-	-
R11	348L0	-	C-CA-1740	0.4	665	63	-	-	-	-	-	-	2	4	169	5	-	-	-
R14	349L0	-	C-CA-1740	0.4	-	141	1.4	1.28	-	-	-	-	-	-	176	4	-	27	-
R23	408L0	-	C-GLLoopO/D-1740	0.8	742	210	-	2.99	-	-	87.8	-	-	7	145	1	-	7	-
R24	398L0	-	C-GapLower-1870	0.8	807	180	2.0	-	0.4	-	2.2	-	-	5	99	2	-	-	506
R3	L103	-	Zaaiplts-#1 Pipe	0.3	701	-	1.8	-	3.6	2.6	7.3	-	135	0.5	122	5264	-	14	-
R34	L101	-	Zaaiplaats	0.7	-	635	1.9	0.68	-	0.3	-	-	3	-	19	7	-	12	-
R36	L102	-	Zaaiplaats	0.4	-	-	11.3	0.9	8.4	-	-	-	5	-	3	34	-	7	-
R4	L104	-	Mutue-fides	0.5	668	202	0.4	0.34	-	0.3	5.4	-	3	2	22	13	1	6	104
R5	L105	-	Erongo-pegmatite	0.6	653	42	-	0.7	-	0.2	0.9	-	2	0.4	3	11	-	8	72
R12	L106	-	Mmbabane	-	727	-	-	-	4.5	-	-	-	1	0.4	116	5925	-	-	-
R35	L108	-	Omaruru-pegmatite	-	-	-	-	-	-	3.5	-	-	120	-	20	9401	-	26	-
Lower limit of detection =				0.3	40	40	0.1	0.5	0.1	0.1	0.1	0.7	1	0.3	0.05	0.1	0.2	1	8

Suspected tin phase* : Samples of A Mine pockets only Locality** : Mine-lode/area-level

Digitised by the Department of Library Services in support of open access to information, University of Pretoria, 2021